ANALYSIS OF CHROMOSOMAL REARRANGEMENTS AFTER REPLICATION RESTART

SAED MOHEBI

SUBMITTED FOR THE DEGREE OF DOCTOR OF PHILOSOPHY
UNIVERSITY OF SUSSEX
AUGUST 2014

DECLARATION

I hereby declare that this thesis has not been and will not be, submitted in whole or in part to another University for the award of any other degree.

Signature:……

ACKNOWLEDGEMENTS

TO LIFE

I would like to express my deepest gratitude to my supervisor Jo Murray for the opportunity to undertake my PhD in her laboratory, and for her continuous and generous support, guidance, and patience throughout the process, without which the completion of this work would not be possible.

I would like to extend my appreciation to Tony Carr for his advice and support during my research.

I would also like to thank all the people who helped me in completion of this PhD, Ken'Ichi Mizuno, and Adam Watson for their contributions towards my research, and all of the members Murray and Carr laboratories.

Special thanks to my parents, my brother, Sara Mohebi, Lena Erchen, and Eric Cartman.

UNIVERSITY OF SUSSEX

SAED MOHEBI

A THESIS SUBMITTED FOR THE DEGREE OF DOCTOR OF PHILOSOPHY

ANALYSIS OF CHROMOSOMAL REARRANGEMENTS AFTER REPLICATION RESTART

Impediments to DNA replication are known to induce gross chromosomal rearrangements (GCRs) and copy-number variations (CNVs). GCRs and CNVs underlie human genomic disorders and are a feature of cancer. During cancer development, environmental factors and oncogene-driven proliferation promote replication stress. Resulting GCRs and CNVs are proposed to contribute to cancer development and therapy resistance.

Using an inducible system that arrests replication forks at a specific locus in fission yeast, chromosomal rearrangement was investigated. In this system, replication restart requires homologous recombination. However, it occurs at the expense of gross chromosomal rearrangements that occur by either faulty template usage at restart or after the correctly restarted fork U-turns at inverted repeats. Both these mechanisms of chromosomal rearrangement generate acentric and reciprocal dicentric chromosomes. The work in this thesis analyses the timing of replication restart and appearance of chromosomal rearrangements in a single cell cycle after induction of fork stalling. This research also identifies the recombination-dependent intermediates corresponding to the two pathways of rearrangements. Moreover, the DNA integrity checkpoint responses after replication fork arrest, homologous recombination dependent replication restart, and the accumulation of GCRs are investigated.

TABLE OF CONTENTS

LIST OF FIGURES

LIST OF TABLES

LIST OF ABREVIATIONS

2DGE	two-dimensional gel electrophoresis
AAA+	ATPase associated with various activities
AAD	ATR activating domain
APC/C	anaphase promoting complex/cyclosome
ARS	autonomous replicating sequence
AT	ataxia telangiectasia
BER	excision repair
BIR	break induced replication
bp	base-pair
CAK	CDK activating kinase
CDK	cyclin dependent kinase
CFS	common fragile sites
ChIP	chromatin immunoprecipitation
CMG	Cdc45-MCM-GINS
CNV	copy-number variation
DDK	Dbf4-dependent kinase
DDR	DNA damage response
dHJ	double Holliday junction
DNA	deoxyribonucleic acid
DSB	double strand break
DSBR	double strand break repair
dsDNA	double-stranded DNA
EM	electron microscopy

FXS	Fragile X syndrome
GCR	gross chromosomal rearrangements
HR	Homologous recombination
HU	Hydroxyurea
IR	ionizing radiation
LOH	loss of heterozygosity
M	mitosis
mb	mega-base
MCM	minichromosome maintenance proteins
MMR	mismatch repair
NAHR	non-allelic homologous recombination
NER	excision repair
NHEJ	non-homologous end joining
ORC	origin recognition complex
PCNA	proliferating cell nuclear antigen
PFGE	Pulsed field gel electrophoresis
PIKK	phosphoinositol 3’-kinase-like-kinase
PIP	PCNA interacting peptide
pre-RC	pre-replicative complexe
PRR	post-replication repair
RFB	replication fork barriers
RFC	replication factor C
RF	replication fork
RI	replication intermediate

RMCE	recombination-mediated cassette exchange
RNR	ribonucleotide reductase
RPA	replication protein A
RTS1	replication termination site one
S	DNA synthesis
SAC	spindle assembly checkpoint
SDSA	synthesis dependent strand annealing
SMC	structural maintenance of chromosome
SSA	single strand annealing
SSB	single stranded binding protein
ssDNA	single-stranded DNA
TBZ	thiabendazole
TLS	translesion synthesis

CHAPTER 1 – INTRODUCTION

The genetic material, deoxyribonucleic acid (DNA), encodes all the proteins essential to life. Therefore to pass on this genetic material to the next generation, each cell has to duplicate its DNA in a process known as DNA replication before segregating it into daughter cells. DNA replication is highly regulated and monitored during the cell cycle to ensure that the genetic material is passed on free of mistakes and genome integrity is kept intact. DNA replication can be compromised by a great variety of endogenous or exogenous factors such as oxidative products of cell metabolism or ionizing radiation (IR). To maintain genome integrity cells have developed signaling networks of DNA damage responses (DDR), which includes several aspects of DNA metabolism e.g. checkpoints, DNA repair, and transcriptional control (Bartek & Lukas, 2007; Branzei & Foiani, 2008).

In this introduction I will first give a brief over view of fission yeast as the model organism used in this study. Then I will go on to introduce cell cycle regulation, DNA replication, replication fork barriers that can cause replication fork arrest, the checkpoints that ensure the integrity of genomic material by preventing progression of cell cycle, and replication restart. I also will introduce site-specific protein-DNA barriers and systems to study replication restart. In this work, I will distinguish between proteins from different organisms by referring to proteins from *Schizosaccharomyces pombe* with *sp*, *Saccharomyces cerevisiae* with *sc*, and human with an *h.*

1.1 – *SCHIZOSACCHAROMYCES POMBE* AS A MODEL ORGANISM

Fission yeast *S. pombe* of *Schizosaccharomycetaceae* family is a rod shaped unicellular eukaryotic organism and the first of its genus, *Schizosaccharomyces* to be discovered. The last common ancestor between *S. pombe*, the budding yeast, *S. cerevisiae*, and metazoans diverged 420 to 330 million years ago (Sipiczki, 2000). This ancestral divergence between the two main yeast model organisms and metazoans has been of great importance to discovery of biological pathways conserved throughout the evolution. The 13.8Mb *S. pombe* genome was sequenced in 2002 and consists of 4940 genes on three chromosomes (Wood *et al.*, 2002). *S. pombe* is an haploid organism that spends the majority of its cell cycle, which takes between two to four hours in laboratory conditions, in G2. A very short G1 follows M phase and S phase coincides with the formation of the septum and cell division (Figure 1.1). Since the 1950's, *S. pombe* has been extensively studied and due to the ease of genetic manipulation and the relative small size of genome has served as one of the best model organisms to study cell cycle control, DNA replication, repair, and recombination (Wood *et al.*, 2002). Most *S. pombe* laboratory strains used are derived from the isolate that Urs Leupold used for his studies in the 1940's and 1950's (Leupold, 1993).

Figure 1.1

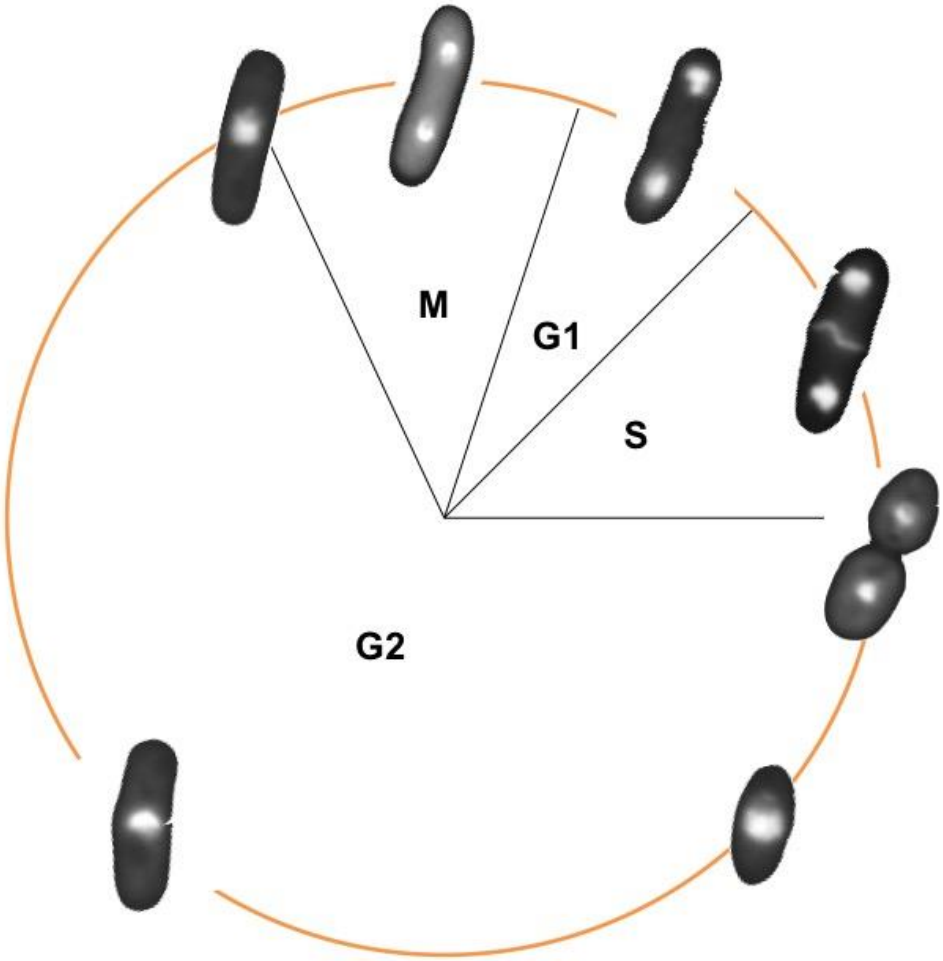

Figure 1.1 | *S. pombe* cell cycle. Diagram showing the stages of the *S. pombe* cell cycle. *S. pombe* cells where the DNA is stained with DAPI are superimposed on the diagram at the appropriate place in the cell cycle. G1 is very short and S phase is coincident with the formation of septum. Newly separated short early G2 cells grow lengthwise until they reach the critical size for cell division.

1.2 – CELL CYCLE AND ITS REGULATION

In order to proliferate, cells must undergo cell division once every cell cycle. For ease of study, the cell cycle is divided into four main phases: DNA synthesis (S), mitosis (M), and gaps phases separating the two known as G1 and G2. G1 phase is between M and S phase and during this time cells prepare for DNA replication. In S phase cells replicate their genetic material to sister chromatids. In G2, cells continue to grow and ensure that the replication of genetic material is complete and error free. In M cells equally divide the duplicated genetic material to the two opposite poles of the cell, after which cytokinesis takes place (Nurse, 1991).

In eukaryotes, progression through the cell cycle is regulated by serine/threonine cyclin dependent kinases (CDKs). This regulation ensures the precise replication and appropriate segregation of the genetic material. In the event of damage to the genetic material, cell cycle progression is halted to allow cells time to overcome the damage. In yeasts, the activity of a single CDK (*sp*Cdc2, *sc*Cdc28) drives cell cycle progression, whereas in metazoans different CDKs regulate the passage through different stages of the cell cycle. Depending on their level of activity, CDKs phosphorylate specific targets at specific times during the cell cycle and this confers the transition between the stages of the cell cycle. CDK activity oscillates through the cell cycle: in G1 there is little CDK activity but this gradually increases until the level at which S phase starts. CDK activity continues to increase through G2 to allow initiation of M. This activity drops in M to the levels seen in G1 restarting the cell cycle. Many aspects of DNA metabolism such as replication (discussed in section 1.3.2) and repair are directly affected by the CDK activity.

CDKs kinase activity is dependent on the binding to the regulatory subunits known as cyclins. There are two main categories of cyclins: G1 cyclins are required for G1-S transition and G2 cyclins facilitate G2-M progression. In *S. pombe* G1 cyclins include *sp*Cig1 and *sp*Puc1, and G2 cyclins *sp*Cig2 and *sp*Cdc13. G2 Cyclins show cell cycle stage specific patterns of expression, and this determines the activity of their partner CDKs at different stages of the cell cycle. G2 cyclins are also subject to anaphase promoting complex/cyclosome (APC/C)-dependent ubiquitination, which targets them to the protein degradation machinery during mitosis. Although essential, cyclin binding is not the only regulatory pathway of CDK activity. CDK activity is also determined by phosphorylation of various residues. For example, phosphorylation by CDK activating kinase (CAK) stimulates CDK activity. In contrast, CDK is also negatively regulated by tyrosine phosphorylation. An example is the inhibition of mitosis in fission yeast, which is mechanistically conserved in higher eukaryotes. *sp*Wee1/*sp*Mik1 phosphorylates Cdc2 on Tyr15, which inhibits the Cdc2-Cdc13 activity. The G2-M transition is brought about by dephosphorylation of Tyr15 by Cdc25, which allows full activation of Cdc2-Cdc13 (Branzei & Foiani, 2008; Diffley, 2004; Lees, 1995; Nurse, 1991; Nurse, 1997; Nurse, 2002; Rhind *et al.*, 1997). Inhibition of Cdc2-Cdc13 after DNA damage occurs through a double block mechanism whereby Wee1 is kept active and Cdc25 is kept inactive (Calonge & O'Connell, 2008).

1.3 – DNA REPLICATION

The fundamentals of the process of DNA replication are conserved through all three domains of life archaea, prokaryotes, and eukaryotes. Replication initiates at specific

sites, known as replication origins, and double-stranded DNA (dsDNA) is unwound bidirectionally by DNA helicases to give rise to single-stranded DNA (ssDNA). DNA polymerases, which move behind the helicases, catalyze base insertion and pairing hence the formation of the new DNA chain. DNA replication is semi-conservative and continuous on the leading strand but discontinuous on the lagging strand owing to the fact that DNA polymerases only incorporate nucleotides in the 5'→ 3' direction (Meselson & Stahl, 1958; Bessman et al. 1958; Okazaki *et al.*, 1968; D. Leipe *et al.*, 1998). In this section I will introduce a brief overview of prokaryotic and eukaryotic DNA replication.

1.3.1 – PROKARYOTIC DNA REPLICATION

In all bacterial chromosomes and plasmids examined to date, DNA replication initiates at a single origin of replication. This initiation event is followed by bidirectional replication by diverging replication machineries (Reyes-Lamothe *et al.* 2008). In *E. coli*, replication of the 4.7 mega-base (Mb) chromosome initiates at *oriC*, a 260 base-pair (bp) sequence distinguished by two sequence motifs: DnaA binding repeats, and an AT-rich DNA unwinding element which marks where the replication bubble forms (Bramhill & Kornberg, 1988; Kowalski & Eddy, 1989; Gille & Messer, 1991).

DnaA, a structurally conserved protein and related to eukaryotic Orc proteins is an AAA+ (ATPase associated with various activities) protein. DnaA is required for recognition of *oriC*, initiation of replication and initial melting of the DNA duplex at *oriC*, allowing the assembly of the replisome (Felczak & Kaguni, 2004; Duderstadt *et al.*, 2011). Prior to the onset of replication, ATP or ADP bound DnaA binds to the

DnaA binding motifs of *oriC*. As the replication initiates, additional copies of ATP-DnaA are recruited to *oriC* forming a helical complex that wraps duplex DNA around itself (Erzberger *et al.*, 2006; Grimwade *et al.*, 2007; Samitt *et al.*, 1989; Scholefield *et al.*, 2012). Binding of ATP-DnaA is essential to melt the DNA duplex at the DNA unwinding element of the *oriC*. ATP-DnaA can also directly bind the DNA unwinding element of *oriC* and actively unwind the duplex in an ATP-dependent manner (Bramhill & Kornberg, 1988; Ozaki et al., 2008; Speck & Messer, 2001). ADP-DnaA acts as a negative regulator of initiation. Despite the dependence of replication initiation on ATP-DnaA binding to *oriC*, DnaA remains tightly bound to ADP after initiation and this disfavours its assembly to *oriC*, thereby preventing reinitiation at *oriC* (Katayama *et al.*, 2010).

Once DnaA recognises and processes *oriC*, DnaB helicase is loaded onto the single stranded region of the DNA unwinding element of *oriC* by the cooperative action of the DnaA and DnaB loader, DnaC (Marszalek & Kaguni, 1994; Wang et al., 2008; Wickner & Hurwitz, 1975). Primase DnaG is then recruited to DnaB, expelling DnaC and synthesizing an RNA primer, which serves as the loading site for the clamp loader, γ complex. The γ complex is comprised of five different subunits ($\gamma_3\delta_1\delta'_1\chi_1\varphi_1$) and loads the β sliding clamp (the processivity factor for PolIII) onto the primed DNA in an ATP dependent manner. Once the β sliding clamp is loaded onto the primed DNA, the clamp loader dissociates from the complex, leaving the closed clamp on DNA (Hingorani & O'Donnell, 1998; Jeruzalmi *et al.*, 2001; Marians, 1992; Turner *et al.*, 1999).

Polymerase PolIII and the γ complex have been shown to bind to the same interface of the sliding clamp and compete for the clamp, however, the ATP hydrolysis-dependent dissociation of the clamp loader complex allows PolIII to bind to the β clamp

(López de Saro *et al.*, 2003; Naktinis *et al.*, 1996). Speed and processivity of PolIII increases by coupling to the β clamp compared to when un-coupled from the sliding clamp (Maki & Kornberg, 1985; Stukenberg *et al.*, 1991). In *E. coli*, PolIII drives both leading and lagging strand synthesis and is a trimeric complex of the α polymerase, ε proofreading exonuclease, and θ subunits (Studwell-Vaughan & O'Donnell,1991). In case of circular chromosomes, appropriate replication termination is important to prevention of over-replication and maintenance of genome integrity. In *E coli*. Ter sites direct the replication termination (discussed in section '1.4.5'). Tus protein binds to Ter sequences and blocks replication forks in a polar manner (Neylon *et al.*, 2005).

1.3.2 – EUKARYOTIC DNA REPLICATION

Unlike the situation in prokaryotes, in eukaryotes replication initiates at multiple origins of replication on each linear chromosome. Eukaryotic origins appear to be defined by the chromatin structure and local DNA topology rather than specific DNA sequences (Mechali, 2010). However budding yeast, *S. cerevisiae*, is known to have defined origins, also known as autonomous replicating sequences (ARSs), which are recognized and bound by the origin recognition complex (ORC) (Bell & Stillman, 1992; Stinchcomb *et al.*, 1979). In fission yeast, *S. pombe*, origins often have an AT-rich sequence to which Orc4 binds, but deletion of these stretches has minimal effects on origin firing (Chuang & Kelly, 1999; Heichinger *et al.*, 2006). In higher eukaryotes, origins of replication show even less sequence dependency but some reports indicate the presence of AT/CG rich sequences at some of the sites of ORC enrichment on chromosomes (Kong *et al.*, 2003; MacAlpine *et al.*, 2010).

Orc complex was first purified from budding yeast and the genes encoding the proteins identified (Bell & Stillman, 1992; Diffley & Cocker 1992; Bell *et al.*, 1993). During G1, six subunits of ORC (Orc1-6) in association with *sc*Cdc6/*sp*Cdc18 and Cdt1 recognize and bind the replication origins and facilitate the ATP-dependent loading of the minichromosome maintenance proteins (Mcm2-7), which act as the main replicative helicase (Cocker *et al.*, 1996; Liang *et al.*, 1995; Maiorano *et al.*, 2000; Nishitani *et al.*, 2000; Speck *et al.*, 2005). The MCM complex is assembled on DNA in an inactive double hexamer form that encircles the DNA duplex (Ervin *et al.*, 2009; Gambus *et al.*, 2011; Remus *et al.*, 2009). The assembly of inactive MCM onto the ORC bound origins to form pre-replicative complexes (pre-RCs) is referred to as origin licensing (Diffley, 2004). This and initiation of replication is summarized in Figure 1.2.

In S phase, two kinases, cyclin dependent kinase (CDK) and Cdc7-Dbf4 (Dbf4-dependent kinase (DDK)), govern the activation of inactive MCM and hence origin firing. Several subunits of MCM are phosphorylated by DDK. The inhibitory domain of Mcm4 is inactivated by DDK phosphorylation of the N-terminal domain of the protein (Sheu & Stillman, 2010). Moreover, DDK phosphorylation sites on Mcm4 and Mcm6, which require prior phosphorylation by other kinases such as Mec1 (*h*ATR), have been identified. Mutation of these DDK phosphorylation sites gives rise to a severe growth defect in the *mcm4/mcm6* double mutant (Randell *et al.*, 2010).

MCM activation involves recruitment of Cdc45 and GINS complexes to the MCM to form the CMG complex. Cdc45 and GINS proteins travel with replication forks and are essential for progression of the replication complex, also known as the replisome (Gambus *et al.*, 2006; Moyer *et al.*, 2006; Pacek *et al.*, 2006; Tercero *et al.*, 2000). It has been shown that the CMG complex exhibits significantly stronger helicase activity compared to that of MCM alone, suggesting that CMG is the functionally active

form of the helicase. Side by side comparison of activity of prurified *Drosophila* MCM and CMG showed that CMG is several hundred fold more active as a helicase than MCM (Ilves *et al.*, 2010). While the inactive MCM complex encircles the duplex DNA, MCM in the active form encircles the leading strand and displaces the lagging strand (Fu *et al.*, 2011).

Several additional factors including Sld2/hRecQ4L, Polε, Sld3/hTreslin, MCM10, and scDpb11/spRad4/hTopBP1, transiently associate with MCM/Cdc45/GINS to form the active CMG complex. In both fission and budding yeasts CDK phosphorylates Sld2 and Sld3 creating conformational changes, which provide a binding site for scDbp11/spRad4 (Fukuura *et al.*, 2011; Masumoto *et al.*, 2002; Tanaka *et al.*, 2007; Yabuuchi *et al.*, 2006; Zegerman & Diffley, 2007). Sld2 and a non-catalytic unit of Polε direct GINS recruitment and Sld3 and Sld7 promote Cdc45 assembly to MCM (Handa *et al.*, 2012; Muramatsu *et al.*, 2010; Nakajima & Masukata, 2002; Tanaka *et al.*, 2011). Human Treslin has been shown to be subject of phosphorylation by CDK and the residues are conserved in yeast Sld3. This phosphorylation is essential for replication (Boos *et al.*, 2001; Kumagai *et al.*, 2011). Once the CMG complex is assembled, it drives unwinding of the DNA at the origin exposing ssDNA, which is coated by ssDNA binding protein, replication protein A (RPA). The MCM complex and Cdc45 then facilitate loading of Polα/primase onto ssDNA at the origin and initiation of a short (~10 nucleotide) RNA primer synthesis by Pri1 subunit of Polα. The 3’ end of the nascent strand then translocates from the primase active site (Pri1) to the polymerase active site (Pol1). Pol1 subunit of Polα subsequently extends the RNA primer by approximately 20 nucleotides (Collins & Kelly, 1991; Frick & Richardson, 2001; Melendy & Stillman, 1993). This initiation event leads to loading of proliferating cell nuclear antigen (PCNA), the sliding clamp,

onto dsDNA by the clamp loader complex, replication factor C (RFC). PCNA was initially characterized as the processivity factor for Polδ (Prelich *et al.*, 1987; Tan *et al.*, 1986). PCNA, a homotrimeric ring shaped molecule, acts as a coordinator and binding platform for replicative and translesion polymerases as well as many other proteins involved in replication, repair, and cell cycle regulation (Moldovan *et al.*, 2007). The clamp loader consists of five subunits (RFC1-5) which are homologous to each other and to the γ and δ' subunits of *E. coli* γ complex (Cullman *et al.*, 1995; O'Donnell *et al.*, 1993). In short, the RFC complex loads PCNA onto the 3' primer-template junction in an ATP dependent manner (Podust *et al.*, 1998; Tsurimoto & Stillman, 1991). In *S. cerevisiae*, in a stepwise fashion, the RFC complex first binds two ATP molecules and then a third one when PCNA binds the complex. The complex then binds a fourth ATP when it binds the primer-template junction. DNA binding commits RFC to ATP hydrolysis, which then causes the RFC to eject leaving the closed PCNA ring encircling the dsDNA (Chen *et al.*, 2009; Gomes *et al.*, 2001). One of the replicative polymerases, Polε or Polδ is then recruited to PCNA, and binding to PCNA stimulates their activity (Chilkova *et al.*, 2007). Polε synthesizes the leading strand, and Polδ catalyzes lagging strand formation (Miyabe *et al.*, 2011; Miyabe *et al.*, in press; Nick McElhinny *et al.*, 2008; Pursell *et al.*, 2007).

In eukaryotic cells, since replication commonly initiates from multiple origins on multiple chromosomes (Sclafani & Holzen, 2007), an inappropriate re-initiation event from a single origin can lead to gene amplification and genetic rearrangements or cell death (Green *et al.*, 2010). Temporal separation of origin licensing and firing is the key to limiting DNA replication to exactly one round per cell cycle. CDKs and anaphase promoting complex/cyclin (APC/C) play direct roles in achieving this regulation. Licensing occurs only during the window between late M and G1 phase

where CDK activity is low and the APC/C is still active and Mcm2-7 assemble on ORC-bound origins. Origin licensing is inhibited outside G1 via three different mechanisms. Firstly, CDK phosphorylates multiple pre-RC subunits, which inhibits licensing via different mechanisms. CDK dependent phosphorylation of MCM components during S, G2, and M, promotes the nuclear export of the free Mcm2-7, therefore inhibiting re-licensing (Hennessy *et al.*, 1990; Labib *et al.*, 1999; Liku *et al.*, 2005; Nguyen *et al.*, 2000; Tanaka & Diffley 2002). Phosphorylation of Cdc6 by CDK targets the protein for degradation, thereby inhibiting licensing outside G1 (Drury et al., 1997; Elsasser *et al.*, 1999; Jang *et al.*, 2001; Perkins *et al.* 2001). CDK phosphorylation inhibits the interaction between Cdt1 and Orc6 to inhibit helicase loading (Chen & Bell, 2011). Secondly, in higher eukaryotes, Cdt1 is stoichiometrically inhibited by geminin outside G1, however, ubiquitination by the APC/C during G1 targets geminin for proteolysis, allowing licensing to occur only in G1 (De Marco *et al.*, 2009; Lee *et al.*, 2004; Wohlschlegel *et al.*, 2000). During S phase, Cdt1 is targeted to the protein degradation machinery by ubiquitination by the Cul4 ubiquitin ligase. PCNA is essential for Cul4 dependent degradation of Cdt1 (Arias & Walter, 2005; Arias & Walter, 2006). Lastly, as previously explained, origin firing and MCM activation requires CDK activity, which is cell cycle regulated.

Despite the fact that all potential origins are licensed before the start of the S phase, not all of the origins fire at the initiation of S phase, but rather fire in a coordinated and regulated manner. Some origins fire early in S phase and some are late firing (Blow & Dutta, 2005). Several factors contribute to enforcement of this regulation such as checkpoint signaling (which will be discussed in detail in the ‘checkpoint’ section), chromatin structure, nuclear positioning of chromatin in

mammals, and expression of certain proteins like those involved in origin firing e.g. Rif1 (Yamazaki *et al.*, 2013).

In budding yeast, Sir3, which interacts with Sir2 histone deacetylase, suppresses firing at subtelomeric origins (Stevenson & Gottschling, 1999). Hyper-acetylation of H3 caused by the lack of H3 deacetylase Rpd3 enhances genome-wide origin firing in a manner independent of checkpoint signaling (Aparicio *et al.*, 2004; Knott *et al.*, 2009; Vogelauer *et al.*, 2002). In fission yeast, telomeric repeats recruit Taz1, which inhibits Hsk1 dependent loading of Sld3 onto nearby origins. Paradoxically, heterochromatic centromere regions are replicated early in fission yeast due to Swi6/HP1 dependent recruitment of Hsk1 (Hayashi *et al.*, 2009; Tazumi *et al.*, 2012). These results emphasize the regulatory role of chromatin structure on origin firing.

Figure 1.2

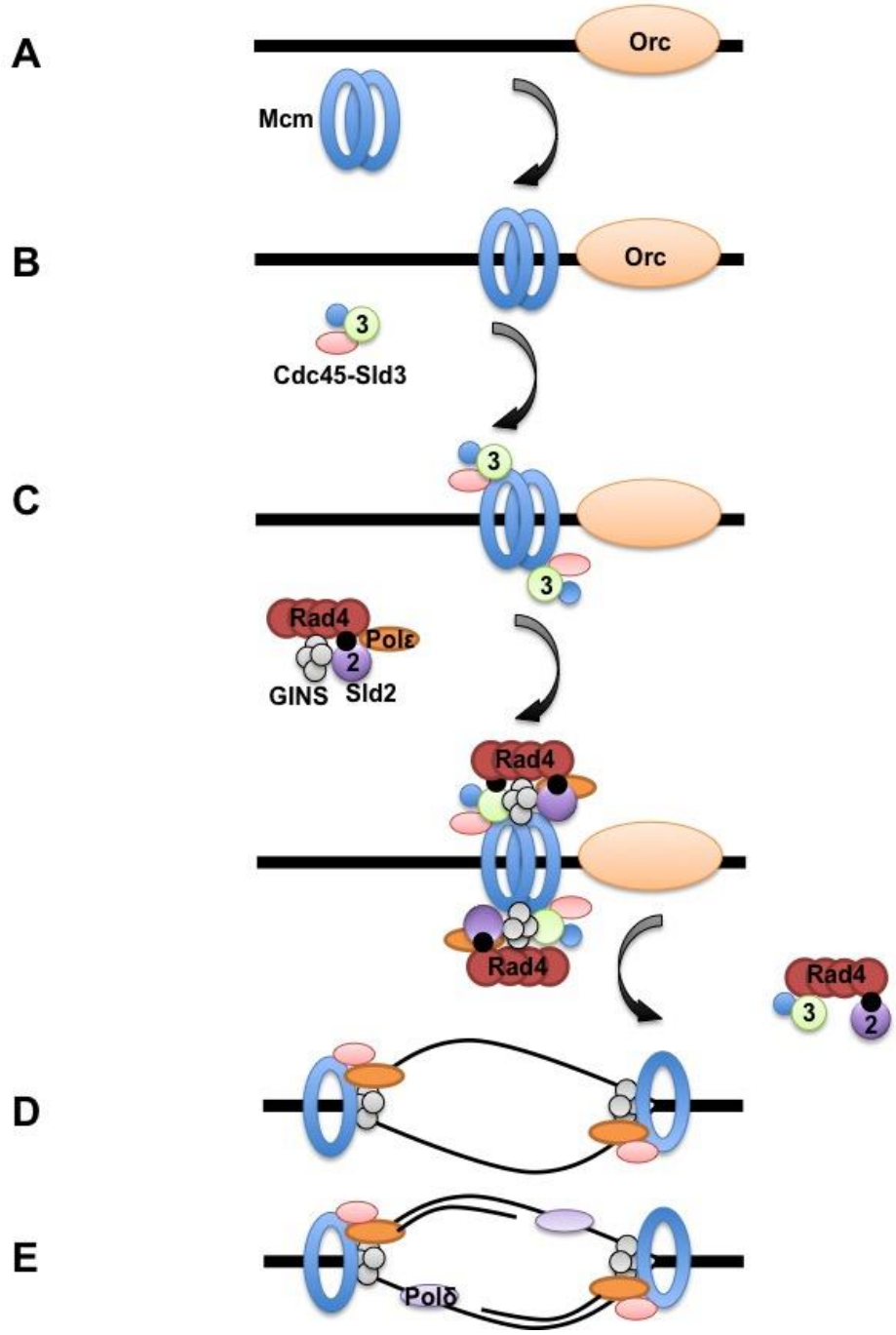

Figure 1.2 | Initiation of DNA replication. **A**- Origin licensing: ORC binds origin of replication and in concert with Cdc6 and Cdt1 loads MCM complex to form Pre-RC. **B & C**- DDK & CDK-dependent association of GINS and Cdc45 with Pre-RC. This reaction requires catalytic activity of Sld2, Sld3, Dpb11, and Polε. **D**- Origin melting by activated CMG complex. E- recruitment of Polα to unwound origin results in primer synthesis and this in turn recruits PCNA and replicative polymerases to initiate DNA synthesis.

Little is known about the mechanism of replication termination in eukaryotes but it is thought to occur either at random when two converging replication forks meet between origins or when replication fork reaches the telomeric sequences at the end of the chromosomes (Edenberg & Huberman, 1975). Replication termination also occurs at programmed replication fork barriers (discussed in section '1.4.5').

1.4 – REPLICATION FORK BARRIERS

Once replication is initiated, replication forks (RFs) can encounter obstacles that result in RF slow down or arrest. In the literature, two terms are used to define the conformation of the arrested RFs: "collapsed" fork is used for the situation in which the replication holoenzyme (replisome) is dis-assembled from the nascent DNA strand and "stalled" fork defines the situation where the RFs are stabilised and the replisome remains at the site of last incorporated base. It must be noted that a collapsed fork does not contain a break in the nascent DNA strand which is the case for a "broken" fork. A number of factors commonly referred to as replication fork barriers (RFB) can compromise DNA replication. These obstacles can be divided into template lesions, secondary DNA structures, alternative DNA metabolism, replication inhibitors, and non-histone protein-DNA complexes (Lambert & Carr, 2005). They could either affect the replicative helicase activity or DNA polymerase progression. Uncoupling of the replicative helicase and polymerase, and processing of arrested RFs results in formation of ssDNA ahead of or behind the RF.

The replication machinery can be blocked by a variety of template lesions that are introduced due to endogenous or exogenous damaging agents like oxidative metabolic products, UV light, ionising radiation, MMS, and CPT. These agents compromise replication by creating DNA damage such as abasic sites, pyrimidine dimers, inter strand crosslinks. Depending on the type of the lesion, the replication machinery action is compromised either through blocking the helicase activity or the polymerase itself (Barbour & Xiao, 2003; Lambert & Carr, 2005; Setlow *et al.*, 1963).

DNA sequences such as trinucleotide repeats (e.g. GGG or GAC), inverted and direct tandem repeats can undergo structural transitions and form secondary structures such as cruciforms, G quartets, hairpins, triplex DNA, left-handed Z-DNA. Again these can inhibit replication by compromising the action of either the replicative helicase or lagging or leading DNA polymerases (Pearson & Sinden, 1996 ; Trinh & Sinden, 1991; Sinden, 1994).

Since replication and transcription machineries share the same template, occasional collisions between the two are inevitable and these can interfere with fork progression (Brewer, 1988). Experimental evidence shows head-on collisions between DNA and RNA machineries to occur both in prokaryotes, and at the tRNA genes and rDNA loci of eukaryotes (Deshpande & Newlon, 1996; Takeuchi *et al.*, 2003). Other observed transcriptional related phenomenon that can cause fork stalling are stable R loops and transcription-dependent replication inhibition at poly G/C repeats. Stable R-loops form when mRNA displaces the non-template strand, giving rise to a loop structure (Santamaria *et al.*, 1998). In *E. coli* RNA mediated replication inhibition was reported at the site of G/C repeats, especially when the nascent RNA harbored G repeats (Krasilnikova *et al.*, 1998).

Hydroxyurea (HU) is the most widely used replication inhibitor and acts through inhibiting the ribonucleotide reductase (RNR), hence disturbing the nucleotide pool in the cell. HU treatment in checkpoint proficient cells results in stably stalled forks but in checkpoint deficient cells stalled forks are unstable and collapse forming chicken foot structures (Lopes *et al.*, 2001).

Non-histone protein-DNA complexes provide natural pause sites that are active in each cell cycle. In *E. coli* (as mentioned in section 1.2.1) replication terminates at Ter sequences. Similarly, in *Bacillus subtilis* a homodimer of RTP binds Ter sequences and arrests replication (Lewis *et al.*, 1989; Smith *et al.*, 1992). The *E. coli* genome harbours ten 23 bp Ter sites located in a region diametrically opposite to *oriC*. Ter sites act as polar fork barriers and are orientated in such way so as to allow the replication fork to pass through one cluster of Ter sites orientated in a non-active direction before meeting the Ter sites orientated in the non-permissive direction. This creates a 'trap' for replication forks enhancing the termination of the replication. Termination is achieved when the converging RF meets the arrested fork (Hill, 1992; Mulcair *et al.*, 2006). Tus has been shown to interact with DnaB helicase in a yeast two hybrid assay and a Tus mutant was shown to have lower affinity for DnaB binding and lower barrier activity despite its normal binding affinity to Ter (Mulugu *et al.*, 2001). Moreover, Tus has been shown to possess contra helicase activity specific to DnaB (Bedrosian & Bastia, 1991).

On the other hand, it has been shown that Tus interacts with a conserved cytosine residue in the Ter sequences which flips out and binds a pocket within Ter when RFs are passing in the non-permissive direction (Mulcair *et al.*, 2006). These data suggest that the activity of the barrier is achieved via both physical hindrance of the helicase movement, and the inhibition of the helicase activity of DnaB.

In eukaryotes, the rDNA polar RFBs prevent collisions between the replication and transcription machineries and are conserved throughout evolution (Tsang & Carr, 2008). The *S. cerevisiae* rDNA barriers were the first eukaryotic site-specific replication barriers to be discovered. Budding yeast rDNA consists of approximately 150 tandem repeats of 9.1kb, in one array on chromosome XII. Each repeat contains 5S and 35S ribosomal genes separated by two non-transcribed spacers, one of which contains RFBs 1-3 that overlap with HOT1 recombination hotspot and the other contains the aoutonomously replicating sequence (rARS). Replication initiates at rARS but the leftward moving fork is arrested at Fob1 dependent programmed polar barriers RFB1 and RFB2 (Brewer & Fangman, 1988; Kobayashi & Horiuchi, 1996; Tsang & Carr, 2008). The activity of Fob1 has been shown to depend on Tof1 (*sp*Swi1) (Hodgson *et al.*, 2007). In *S. pombe*, rDNA arrays reside at the two ends of the chromosome III. Similar to budding yeast rDNA, each repeat contains the 35S transcriptional unit and an ARS within the non-transcribed region. Four RFBs are found in each of the *S. pombe* rDNA repeats at 5' end of 35S transcriptional unit, the first is dependent on Swi1 and Swi3 members of replication fork protection complex (*Sc*Tof1/*h*Timeless & *Sc*Csm3/*h*Tipin respectively), and the second and third dependent on the *sc*Fob1 homologue *sp*Reb1, and Swi1 and Swi3, and the final pause site is dependent on transcription of ribosomal RNA (Krings & Bastia, 2004; Planta *et al.*, 1995). The fission yeast mating type switching locus also contains a polar fork barrier known as replication termination site one (*RTS1*). Replication stalling at *RTS1* requires Swi1, Swi3, Rtf1, and Rtf2 proteins and is discussed in detail in section 1.11 (Codlin & Dalgaard, 2003; Dalgaard & Klar, 2000).

1.5 – STABILISATION OF ARRESTED FORK

In eukaryotes, the replication checkpoint plays an important role in stabilizing arrested RFs and that in the absence of a proficient replication checkpoint replication forks undergo collapse at the site of the damage (Desany *et al.*, 1998; Tercero *et al.*, 2003). In both *S. cerevisiae* and *S. pombe* aberrant pathogenic structures accumulate and replication fails to resume in checkpoint deficient backgrounds in response to HU treatment (Lopes *et al.*, 2001; Meister *et al.*, 2005). Checkpoint defective budding yeast cells showed a considerable increase in the formation of X-shaped molecules corresponding to gapped regressed replication forks, when compared to a checkpoint proficient population (Cotta-Ramusino *et al.*, 2005; Sogo *et al.*, 2002). Moreover, the observation that checkpoint proficient replication mutants (such as *polα*) accumulate similar replication intermediates to that of HU treated checkpoint defective cells, suggests the replisome stabilizing function of the checkpoint proteins (Lopes *et al.*, 2001; Sogo *et al.*, 2002). Taken together, these studies exemplify the importance of the checkpoint response for survival of replication stress in both yeasts. Furthermore, studies have shown the high conservation of DDR in higher eukaryotes. Although the pathways are more elaborate in mammalian cells, the principles remain similar (Harper & Elledge, 2007). The intra-S (replication) checkpoint maintains the genome integrity by stabilization of replication forks, inhibition of late origin firing, and reducing the fork progression speed (Tercero *et al.*, 2001). In response to replication perturbation, checkpoint prevents entry into mitosis by inhibiting activation of CDK, ensuring the completion of replication before cell division (Enoch *et al.*, 1992, Lindsey *et al.*, 1998; O'Connell *et al.*, 2000). In addition, damage created due to problems in S phase, signals

through the G2/M DNA damage checkpoint, also known as the DNA integrity checkpoint to prevent entry into mitosis (Carr, 2002).

1.5.1 – DNA DAMAGE AND REPLICATION CHECKPOINTS

The DNA damage response is the signal transduction pathway that regulates different aspects of DNA metabolism with cell cycle progression. Checkpoints, elaborate network of proteins that sense and signal DNA perturbations, sit at the heart of this regulatory mechanism. While the observation that cells from ataxia telangiectasia (AT) patients did not delay the mitotic onset in response to radiation (and presence of DNA damage) predicted the existence of a DNA damage checkpoint (Painter & Young, 1980), the concept was not formalized until Weinert and Hartwell showed in *S. cerevisiae* that the *rad9* mutant unlike wild type cells did not delay mitosis in response to DNA damage (Weinert & Hartwell, 1988). In a key experiment they showed that the radiation-induced loss of viability in *rad9* mutant could be suppressed by allowing cells time to repair the DNA damage when mitosis was artificially blocked. Weinert and Hartwell then proposed the term ‘checkpoint’ to define regulatory pathways that delayed mitosis in response to DNA damage or replication stress (Weinert & Hartwell 1988; Weinert & Hartwell, 1989). Much of what is known about the checkpoint response was first discovered in yeasts but is highly conserved, here I summarise the mechanism of checkpoint activation.

Table 1.1

Human	***S. pombe***	***S. cerevisiae***
ATM	Tel1	Tel1
ATR	Rad3	Mec1
ATRIP	Rad26	Ddc2
RAD9	Rad9	Ddc1
HUS1	Hus1	Mec3
RAD1	Rad1	Rad17
RAD17	Rad17	Rad24
53BP1	Crb2	Rad9
MDC1	Brc1	Rtt107
Claspin	Mrc1	Mrc1
TopBP1	Rad4	Dbp11
Timeless	Swi1	Tof1
Tippin	Swi3	Csm3
Mre11	Mre11	Mre11
Rad50	Rad50	Rad50
Nbs1	Nbs1	Xrs2
CHK1	Cds1	Rad53
CHK2	Chk1	Rad53
EXO1	Exo1	Exo1
MUS81	Mus81	Mus81

Table 1.1 | Table of nomenclature. Table showing the names of human, *S. pombe*, and *S. cerevisiae* functionally analogous proteins. Note Cds1 is the orthologue of CHK2 and Rad53 but functionally the equivalent of hChk1.

Checkpoint proteins form complexes in the vicinity of the DNA lesion. Primary to both DNA damage and replication checkpoints are "sensors": the proteins that sense the DNA damage and replication stress. Mediator proteins facilitate recruitment of effector kinases to the sensor proteins. Sensors then activate the effector kinases, which in turn phosphorylate downstream targets resulting in inhibition of origin firing, replication fork stabilization, and cell cycle delay. Recruitment of particular mediators defines which effector kinase is used, thereby activating the damage or replication checkpoint. Simplistically, the DNA damage checkpoint detects DNA lesions whereas the DNA replication checkpoint is activated when fidelity of replication is compromised (Branzei & Foiani, 2009; Harper & Elledge, 2007; Kai & Wang, 2003; Lambert *et al.*, 2007). Central to checkpoint pathways are two members of phosphoinositol 3'-kinase-like-kinase (PIKK) family of proteins. ATM and ATR and their yeast orthologues Tel1 and *sp*Rad3/*sc*Mec1 respectively (see Table 1.1), along with their binding partners act as checkpoint sensors of DNA damage and initiate the checkpoint cascade. The main substrate for ATM is DSBs, therefore ATM is referred to as the sensor of the DNA damage checkpoint. The substrate for ATR is RPA-coated ssDNA exposed at arrested replication forks or processed DSBs, therefore ATR is referred to as the sensor of DNA replication checkpoint. In yeasts however, the role of Tel1 (ATM) in checkpoint activation is minimized and it is involved in maintenance of telomere stability. In contrast, *sp*Rad3 and *sc*Mec1, which were shown to be related to ATR, are critical for both the replication and DNA damage response. (Bentley *et al.*, 1996; Greenwell *et al.*, 1995; Morrow *et al.*, 1995).

In higher eukaryotes, ATM is found in cells in the form of inactive dimers. Upon DNA damage, ATM is recruited to the DSBs via interaction with Nbs1 of MRN complex which results in its autophosphorylation (on S367, S1981, and S1893),

monomerisation, and hence activation (Bakkenist & Kastan, 2003; Kozlov *et al.*, 2006; Uziel *et al.*, 2003). Activated ATM then phosphorylates H2AX on S139 to give rise to γH2AX, which in turn recruits MDC1 to the site of the damage (Burma *et al.*, 2001; Stewart *et al.*, 2003). ATM then phosphorylates MDC1, which results in recruitment of RNF8. RNF8 in turn ubiquitinates H2A, H2AX, and γH2AX resulting in recruitment of RNF168 and mediator proteins BRCA1 and 53BP1 (Doil *et al.*, 2009; Huen *et al.*, 2007; Mailand *et al.*, 2007). ATM then phosphorylates both BRCA1 and 53BP1, which results in recruitment of Chk2. ATM dependent phosphorylation of Chk2 results in its activation. Chk2 then phosphorylates CDC25A, which leads to its degradation and thereby prevention of cell cycle progression into mitosis (Cortez *et al.*, 1999; Matsuoka *et al.*, 2000; Xia *et al.*, 2001). As previously mentioned (section 1.2), CDC25 phosphatase activity is required for the G2-M transition.

ATR and its yeast homologues (*sp*Rad3/*sc*Mec1) are found in cells in a complex with their binding partners *h*ATRIP/*sp*Rad26/*sc*Ddc2 (Cortez *et al.*, 2001; Edwards *et al.*, 1999; Paciotti *et al.*, 2000). In the presence of stalled or broken RFs or DNA damage, ATRIP facilitates the binding of the complex to the exposed RPA-coated ssDNA at the site of the damage. Similarly in budding yeast Ddc2 is required for recruitment of Mec1-Ddc2 to RPA-ssDNA and *ddc2Δ smlΔ* shows similar phenotype to that of *mec1Δ smlΔ* (Cortez *et al.*, 2001; Paciotti *et al.*, 2000; Zou & Elledge, 2003). Mec1-Ddc2 recruitment to RPA is dependent on a conserved domain of Ddc2. However, mutations in the conserved FAT domain of Mec1 resulted in decreased interaction of Mec1-Ddc2 with RPA, suggesting enhancement of Mec1-Ddc2-RPA interaction by Mec1 (Ball *et al.*, 2005; Zou & Elledge, 2003). ATR-ATRIP recognition of ssDNA at the site of the damage is necessary for activation of the checkpoint but not sufficient. Once recruited to the site of the damage, ATR and its yeast homologues only

posses a basal kinase activity, which is not sufficient for full activation of a checkpoint cascade, and therefore ATR needs to be fully activated. Recruitment of a second sensing complex, the 9-1-1 complex, is essential for ATR checkpoint activation (Caspari *et al.*, 2000; Kai *et al.*, 2007; MacDougall *et al.*, 2007; Melo *et al.*, 2001). Independently of ATR, Rad17 (*sp*Rad17/*sc*Rad24) and four small subunits of replication factor C (RFC2-5) form the checkpoint clamp loader and recognize and bind to the 5' junction between ssDNA and dsDNA dependent on RPA at the site of DNA damage. The Rad17-RFC complex then deposits the 9-1-1 complex (*sp/h*Rad9-Hus1-Rad1, *sc*Ddc1-Mec3-Rad17), which shares structural similarities with PCNA, onto DNA (Doré *et al.*, 2009; Majka *et al.*, 2006A; Zou *et al.*, 2003). Mechanistically similar to PCNA loading by RFC(1-5), 9-1-1 loading onto ssDNA-dsDNA junctions requires ATP hydrolysis by Rad17 which results in opening of the 9-1-1 ring and its loading on DNA (Bermudez *et al.*, 2003; Bloom, 2009; Ellison & Stillman, 2003). In fission yeast Rad3 phosphorylates C-terminal of Rad9 on T412 and S423 and these phosphorylation are important for the DNA damage but not the replication checkpoint (Furuya *et al.*, 2004). In *S. cerevisiae*, the C-terminus of Ddc1 was shown to stimulate the kinase activity of Mec1 and activate the checkpoint, and artificial Ddc1-dependent recruitment of Mec1-Ddc2 to chromatin resulted in checkpoint activation (Bonilla *et al.*, 2008; Majka *et al.*, 2006B). In higher eukaryotes, Rad9 is also phosphorylated but independently of ATR. Rad9 phosphorylation results in recruitment of TopBP1/*sp*Rad4/*sc*Dbp11, which is important for ATR kinase activity (Kumagai *et al.*, 2006; Pfander & diffley, 2011; Puddu *et al.*, 2008; Takeishi *et al.*, 2010). ATR also phosphorylates ATRIP on S68 and S72 (Edwards *et al.*, 1999; Itakura *et al.*, 2004), and itself on various residues including T1989. This autophosphorylation site was shown to be important for activation of ATR kinase activity by TopBP1. Rad9 recruited TopBP1 binds phosphorylated T1989 of

ATR. The interaction between the ATR activating domain (AAD) of TopBP1 and ATR-ATRIP stimulates ATR kinase activity. ATR then phosphorylates TopBP1, which in turn further stimulates the kinase activity of ATR (Delacroix *et al.*, 2007; Kumagai *et al.*, 2006; Liu *et al.*, 2011). Moreover, in response to replication stress in budding yeast Dna2 nuclease-helicase has been shown to be able to activate Mec1 independent of its nuclease or helicase activities (Kumar & Burgers, 2013).

In response to replication stress, once ATR and its yeast homologs are recruited to the site of fork arrest and activated, they phosphorylate the mediator protein *h*Claspin and *sp*/*sc*Mrc1 (Errico *et al.*, 2007; Kumagai & Dunphy, 2000; Xu *et al.*, 2006; Zhao *et al.*, 2003). Claspin and Mrc1 then recruit *h*Chk1, *sp*Cds1, and *sc*Rad53, the effector kinase of the replication (intra-S) checkpoint (Alcasabas *et al.*, 2001; Kumagai & Dunphy, 2000; Kumagai *et al.*, 2004; Tanaka & Russell, 2001; Xu *et al.*, 2006; Zhao *et al.*, 2003). *sp*Cds1 and *sc*Rad53 are then phosphorylated by *sp*Rad3 and *sc*Mec1 respectively. This results in *sp*Cds1 dimerization and autophosphorylation, hence its full activation (Xu *et al.*, 2006; Yue *et al.*, 2011; Zhao *et al.*, 2003). Similarly, in higher eukaryotes Claspin is required for Chk1 activation indicating the conservation of this pathway (Kumagai *et al.*, 2004). However, the situation in metazoans is slightly different to yeasts, as during the course of evolution Chk2 (orthologue of *sp*Cds1/scRad53) has swapped roles with Chk1 and acts downstream of ATM (Labib & De Piccoli, 2010).

In response to DNA damage, ATR and its homologues *sp*Rad3 and *sc*Mec1 are also recruited to ssDNA at resected DSBs. In yeasts, this forms the major DNA damage response. As previously explained, once ATR and the 9-1-1 complex are recruited to the site of the lesion and activated, *h*TopBP1, *sp*Rad4 and *sc*Dbp11 are recruited by *h/sp*Rad9/*sc*Ddc1 and phosphorylated by ATR and its homologues, and this facilitates

the recruitment of the mediator proteins *h*53BP1, *sp*Crb2, and *sc*Rad9 (not a part of 9-1-1 checkpoint clamp) respectively (Du *et al.*, 2006; Mochida *et al.*, 2004; Pfander & Diffley, 2011). In both yeasts, the functional form of *sp*Crb2/*sc*Rad9 is a homodimer (Du *et al.*, 2004; Soulier & Lowndes; 1999) and in *S. pombe* Crb2 recruitment to Rad4 is dependent on a CDK-dependent phosphorylation and hence is cell cycle regulated (Du *et al.*, 2003). *sp*Crb2 and *sc*Rad9 are then phosphorylated by *sp*Rad3 and *sc*Mec1 respectively, and this results in recruitment of *sp*Chk1 and *sc*Rad53. *sp*Rad3 and *sc*Mec1 then phosphorylate *sp*Chk1 and *sc*Rad53 respectively (Emili, 1998; Lopez-Girona *et al.*, 2001; Qu *et al.*, 2012; Schwartz *et al.*, 2002; Vialard *et al.*, 1998). Similarly, in metazoans ATR phosphorylates Chk1 (Guo *et al.*, 2000). Chk1 phosphorylation results in its dimerization and full activation (Lee *et al.*, 2003; Schwartz *et al.*, 2003). Chk1 then targets Cdc25 and Wee1 to inhibit CDK and prevent entry to mitosis. It is worth noting that in budding yeast, Rad53 carries out most of the functions of Chk1 and Chk2, and acts as the main effector kinase of both the replication and damage checkpoints (Rhind & Russell, 2000). The *S. pombe* DNA integrity checkpoint pathways are summarized in Figure 1.3.

Figure 1.3

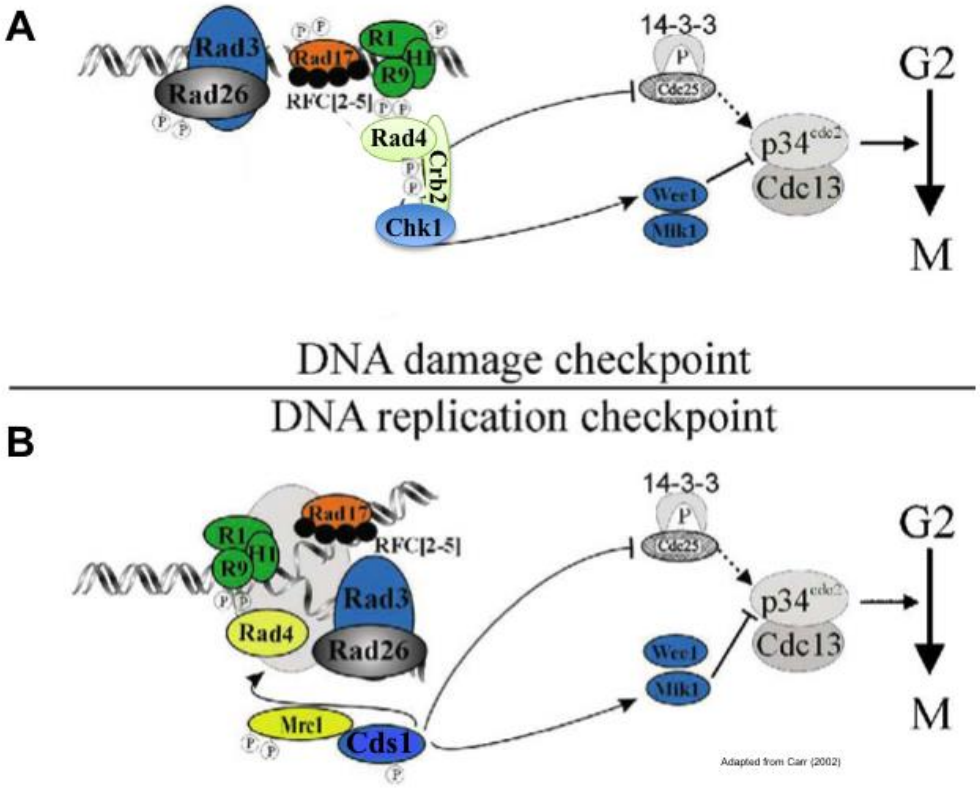

Figure 1.3 | DNA damage and replication checkpoints in *S. pombe*. A- model for the DNA damage and DNA replication checkpoints. In response to DNA damage, Rad3–Rad26 and Rag9–Rad1–Hus1 complexes bind to DNA independently of each other. Crb2 mediates the signalling to Chk1. Following phosphorylation, Chk1 subsequently regulates the kinases and phosphatases that determine the activity of Cdc2 resulting in cell cycle regulation. **B-** During DNA replication, the same core checkpoint proteins may associate with the replication complex. When replication stalls, Rad3 phosphorylates Cds1, a process mediated by Mrc1. Cds1 activity results in mitotic delay and also in the regulation of replication proteins.

1.5.2–CHECKPOINT RESPONSES TO DNA REPLICATION PURTURBATIONS

The replication checkpoint prevents firing of late origins and formation of new RFs in response to replication stress. In AT cells, unlike wild type, DNA synthesis is not inhibited in response ironizing radiation. This checkpoint defect was shown to be partly due to an inability to inhibit late origin firing (Larner *et al.*, 1999; Lee *et al.*, 1997; Zachos *et al.*, 2003). Similarly, in budding yeast in response to DNA damaging agents late origins fire only in checkpoint mutants (Shirahige *et al.*, 1998; Tercero & Diffley, 2001). Inhibition of late origin firing is brought about by inhibitory *sc*Rad53-dependent phosphorylation of Dbf4 and Sld3 in response to replication stress (Lopez-Mosqueda *et al.*, 2010; Zegerman & Diffley, 2010).

Several lines of evidence suggest that the DNA replication checkpoint protects arrested forks probably by affecting the phosphorylation state of replication fork proteins, and keeping the stably stalled replisome at the site of nucleotide incorporation. This prevents the fork collapse and the need for reloading the replisome (Cobb *et al*., 2005; Enoch *et al.*, 1992; Luca *et al*., 2004). When fission yeast cells are treated with HU, the DNA damage checkpoint is only activated in the absence of the replication checkpoint effector kinase, Cds1, suggesting that replication checkpoint protects arrested RFs in ‘stalled’ state and prevents formation of toxic DNA intermediates which activate the damage checkpoint (Lindsay *et al.*, 1998).

In contrast, in budding yeast where the Cds1 homologue, Rad53, is required for both the intra-S and DNA damage checkpoints, loss of Rad 53 leads to both replication fork collapse and loss of cell cycle delay. In *rad53* mutants, electron microscopy and two-dimensional (2D) electrophoresis showed the accumulation of aberrant DNA intermediates in response to HU treatment (Lopes *et al.*, 2001; Sogo *et al.*, 2002).

Moreover, chromatin immunoprecipitation (ChIP) showed that both leading and lagging strand DNA polymerases (polε and polδ) dissociate from the site of nucleotide incorporation in HU treated *mec1* mutants (Cobb *et al.*, 2003; Cobb *et al.*, 2005; Luca *et al.*, 2004). Similarly, it was recently shown in fission yeast that chicken foot structures accumulated in *cds1* null cells in response to HU (Hu *et al.*, 2012). Surprisingly, a more recent study in budding yeast showed the stable association of replisome with replication fork during replication stress in the absence of Rad53 or Mec1, and authors suggested the checkpoint regulation of replisome function rather than stability in response to replication stress (De Piccoli *et al.*, 2012).

Studies on a separation of function allele of Mec1, *mec1-100* which is unable to prevent late origin firing, showed that despite the defect in origin inhibition, forks are stably stalled in this mutant in response to replication stress, showing that the intra-S checkpoint influences fork stability independently of its role in the inhibition of late origin firing (Paciotti *et al.*, 2001; Tercero *et al.*, 2003). Replication fork-associated proteins that are not essential for replication but are necessary for maintaining the genome integrity include *sp*Swi1/*sc*Tof1/*h*Timless, *sp*Swi3/*sc*Csm3/*h*Tipin and *sp*/*sc*Mrc1/*h*Claspin. In both yeasts, Mrc1 and *sp*Swi1/*sc*Tof1 proteins have been shown to travel with the replication fork and prevent the uncoupling of the replicative apparatus from the site of nucleotide incorporation, which indicates a role for checkpoint proteins in DNA replication (Gambus *et al.*, 2006; Katou *et al.*, 2003; Noguchi *et al.*, 2003; Noguchi et *al.*, 2004). In budding yeast, Mrc1 loading to replication forks requires Tof1 and Csm3 (Calzada *et al.*, 2005). Stalling of arrested replication forks at programmed protein-DNA RFBs in both yeasts requires *sp*Swi1/Swi3 and *sc*Tof1/Csm3 (Calzada *et al.*, 2005; Shimmoto *et al.*, 2009). The observations that the HU sensitivity of fission yeast *mrc1Δ* mutants is suppressed by

mutations in *cdc45* and *mcm*, and that in budding yeast Mrc1 forms a complex with Cdc45 and MCM, could suggest that Mrc1 inhibits the Cdc45-MCM-GINS complex when the action of polymerase is compromised (Katou *et al.*, 2003; Nitani *et al.*, 2006). In fission yeast, regulation of cellular responses to replication arrest also requires the *sp*Hsk1-Dfp1 (*sc*Cdc7-Dbf4) kinase complex. Fission yeast Hsk1-Dfp1 has been shown to physically interact with the Swi1-Swi3 complex. In response to HU treatment, fission yeast Hsk1 and Dfp1 are phosphorylated by Cds1 and in budding yeast Rad53 phosphorylates Dbf4 (Lei *et al.*, 1997; Shimmoto *et al.*, 2009; Snaith *et al.*, 2000; Takeda *et al.*, 1999; Weinreich & Stillman, 1999).

Evidence suggests the checkpoint dependent down regulation of potentially dangerous recombinogenic events at stalled forks to prevent inappropriate fork processing. In fission yeast, Rad60, which is involved in the regulation of HR repair along with the Smc5/6 complex, is phosphorylated by Cds1in response to HU and this results in its nuclear delocalization. RF arrest confers lethality in a *rad60* mutant that inhibits regulation by Cds1 (Boddy *et al.*, 2003). However, Miyabe *et al.* showed that a non-phoshorylatable *rad60* mutant, which was located in the nucleus in HU, had no affect on viability (Miyabe *et al.*, 2009). In checkpoint proficient fission yeast cells, Cds1 also phosphorylates the TXXF motif of Mus81 in response to HU induced replication stress and this results in Mus81 delocalization from chromatin. Mutations in the TXXF motif result in a hyper recombinogenic phenotype (Kai *et al.*, 2005). Loss of Mus81 in *S. pombe* results in a reduction in rates of spontaneous deletions between direct repeats, consistent with RNAi depletion of Mus81 in human cells that resulted in a reduction in rates of recombination between direct repeats (Blais *et al.*, 2004; Doe *et al.*, 2004). In addition, Dna2 activity is regulated via Cds1phosphorylation, recruiting it to chromatin to prevent fork regression (Hu *et al.*, 2012). In response to HU treatment in

both budding yeast and human cells Exo1 is phosphorylated in a Mec1/ATR dependent manner and this results in its degradation and negative regulation (El-Shemerly *et al.*, 2008; Morin *et al.*, 2008). Similarly, in *S. pombe* Rad3 is important to restrain Exo1-dependent resection at collapsed replication forks (Tsang *et al.*, 2014). Together, these data suggest that the fork collapse seen in checkpoint defective cells in HU is due to the misregulation of multiple proteins.

It has also been shown that checkpoints up-regulate the dNTP pool in response to replication defects by modulating the activity of the RNR complex. In budding yeast, the RNR complex is inhibited by a small protein, Sml1, which is degraded upon entry to S phase and after DNA damage. Mec1 phosphorylates Dun1 kinase, which in turn phosphorylates Sml1. Dun1 dependent phosphorylation of Sml1 leads to Sml1 degradation and activation of RNR (Anderson *et al.*, 2010; Zhao *et al.*, 1998; Zhao *et al.*, 2001). Moreover, checkpoint activation results in phosphorylation of Dif1, which facilitates the nuclear import of the small subunit of RNR. Phosphorylation of Dif1 results in its degradation, which allows the cytoplasmic interaction of the small RNR subunit with the large, hence activation of RNR (Lee *et al.*, 2008; Wu & Huang, 2008). The evidence above demonstrates that replication checkpoint employs multiple pathways to ensure maintenance of perturbed RFs in a ‘stalled’ state that is competent to resume replication.

1.6 – RESTART OF ARRESTED REPLICATION FORKS

Replication fork barriers impose a great danger to replication progression and genome stability. Processing of arrested forks can result in genomic rearrangements. This

replication stress induced genome instability underlies a great proportion of the abnormalities in cancer cells (Branzei & Foiani, 2010). Cells have evolved multiple pathways to restart the arrested forks. Prokaryotic and eukaryotic replication restart pathways function in slightly different manners since firstly unlike the situation in eukaryotic cells, prokaryotic replication initiates from a single origin of replication and terminates at defined sites. Hence there is no converging fork to rescue the arrested forks. Secondly, prokaryotic cells lack the checkpoint functions that stabilize the arrested forks but instead readily reassemble collapsed RFs. In eukaryotes, the majority of arrested fork are held competent to resume replication by the action of the intra-S (replication) checkpoint and restart replication once the RFB is relieved (Lambert *et al.*, 2007).

Stalled forks formed due to covalent modifications of DNA can activate specific repair mechanisms known as post-replication repair (PRR) which facilitates the damage bypass to avoid prolonged stalling of RFs which could lead to aberrant processing and DSBs (Yeeles *et al.*, 2013). However, replication forks do collapse and in this case replication can be rescued by dormant origin firing and converging RFs. In the absence of a converging fork such as in subtelomeric regions, or in regions of poor origin density such as common fragile sites (CFSs) in humans, homologous recombination is required to set up a new replication fork (Carr & Lambert, 2013). In the following sections, I briefly summarize homologous recombination, prokaryotic replication restart, and eukaryotic processes involved in the restart of arrested forks including post-replication repair, and the role of recombination at collapsed replication forks in eukaryotic fork rescue is discussed.

1.7 – HOMOLOGOUS RECOMBINATION

Homologous recombination (HR) plays a central role in double strand break (DSB) repair, and the restart of stalled replication forks in all life forms. In eukaryotes, it is also important for the segregation of homologous chromosomes during meiosis, hence maintaining genome integrity. HR is induced in response to DSBs introduced endogenously, for example in the process of mating type switching in *S. cerevisiae* or during meiosis to facilitate chromosome segregation. It is also induced after exogenously-generated DSBs, for example as a result of exposure to mutagenic reagents or RF collapse. While HR is the main pathway for DSB repair in yeasts, in higher eukaryotes non-homologous end joining (NHEJ) is the preferred repair pathway in G1 and G2 but HR is essential in S phase (Kakarougkas & Jeggo, 2014).

HR relies on the presence of the homologous sister chromatid and is proposed to occur in several steps (Figure 1.4). In the first step, DNA ends at the site of DSB are processed in a polar manner (5'→3') to produce 3'overhangs. This step is known as 'end processing' or 'resection'. In the strand invasion stage, one of the 3' overhangs searches for the homologous sequence in the donor molecule and replaces the complementary strand. This results in the formation of an intermediate known as a 'D-loop'. In the synthesis dependent strand annealing (SDSA) model of repair, once the missing information has been copied by the invading strand by repair synthesis, the strand is displaced and reanneals with the original template (Figure 1.4). The complementary strand is then replicated resulting in a non-crossover repaired DNA molecule. In the Szostak model of double strand break repair (DSBR) after formation of D-loop the second end is captured and forms a structure known as a double Holliday junction (dHJ). Resolution of the dHJ results in formation of crossover and non-

crossover products. In contrast, dissolution of dHJs through the action of RecQ helicase and TopoisomeraseIII gives rise only to non-crossover products (Hartlerode & Scully, 2009; Paques & Haber, 1999; van den Bosch *et al.*, 2002; Wu & Hickson, 2003). The heart of the HR machinery is composed of the RAD52 epistasis group proteins (Rad50, Xrs2/Nbs1, Rad51, Rad52, Rad54, Rad55, Rad57). The genes encoding these proteins were first identified in budding yeast as IR or X-ray sensitive mutants that were HR defective. Homologues of these proteins have been identified in archaea, prokaryotes, and eukaryotes demonstrating the conservation of HR pathways throughout evolution (reviewed in Symington, 2002).

Figure 1.4

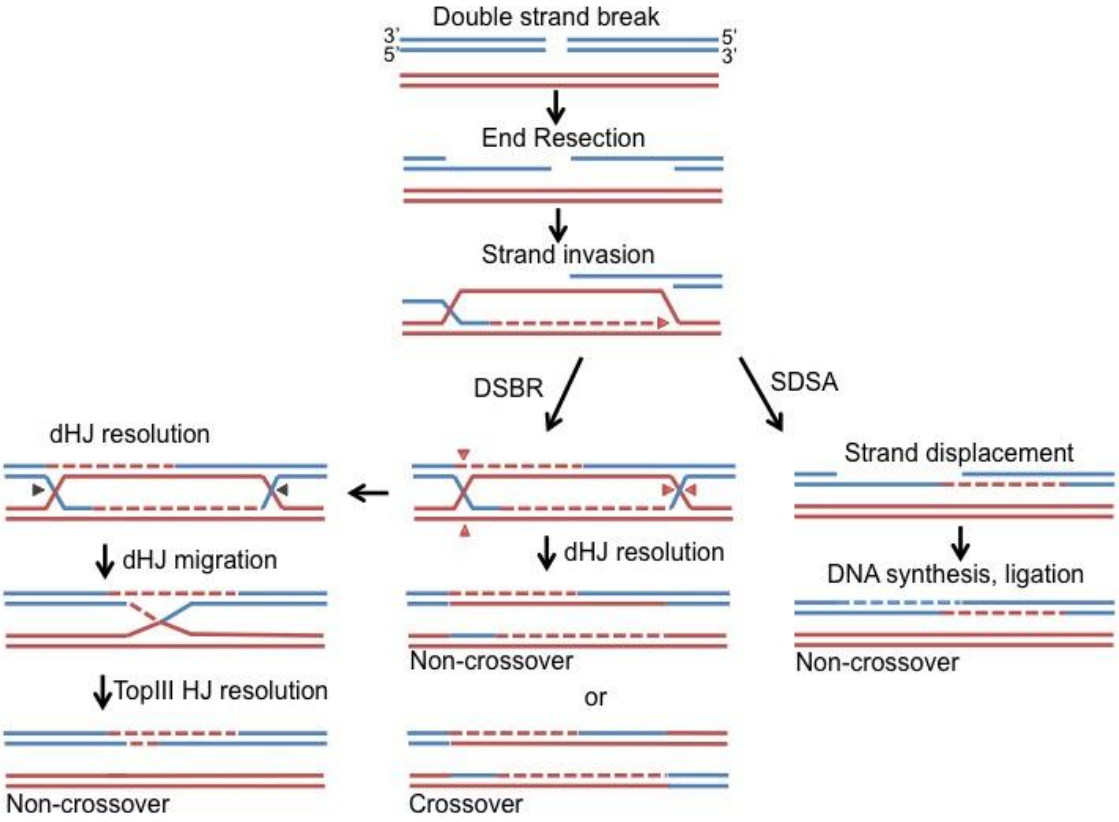

Figure 1.4 | Models of homologous recombination repair. DSB repair is initiated by 5'→3' resection of the broken ends creating 3' overhangs, which are initially coated with Rpa and subsequently Rad51. Rad51-dependent homology search and strand invasion creates the D-loop structure. In SDSA model of repair the invasive strand is displaced and repair synthesis occurs. In DSBR model of repair second end capture leads to formation of dHJ. Resolution of dHJ gives rise to crossover and non-crossovers as oppose to non-crossover production when dHJ is dissolved by helicase and topoisomerase.

1.7.1 – PROTEINS INVOLVED IN RESECTION

The MRN (Mre11, Rad50, Nbs1) complex (in *S. cerevisiae* MRX (Mre11, Rad50, Xrs1)) has distinct roles in telomere maintenance and DNA damage repair. In higher eukaryotes it is also required for checkpoint activation by recruiting ATM and consequently downstream signaling factors. MRN acts as the primary sensor of DSBs (Borde, 2007; Lavin, 2007; Petrini & Stracker, 2003). The Mre11 subunit has been shown to associate tightly with coiled coil region of Rad50 (Lammens *et al.*, 2011; Lim *et al.*, 2011; Williams *et al.*, 2011), to have a distinct affinity for DNA ends (de Jager *et al.*, 2001A), and possess 3'→5' exonuclease activity (Paull & Gellert, 1998). RAD50 consists of walker A and B ATP-binding cassettes that come together by antiparallel intervining coiled coil, and forms a homodimer that has structural homology to SMC (structural maintenance of chromosome) proteins (Hopfner *et al.*, 2000; Murray & Carr, 2008). It has been suggested that RAD50 in collaboration with Mre11 tethers the DNA ends together at the site of the DSB (de Jager *et al.*, 2001B). Nbs1, which harbors FHA, BRCT, and Mre11 and ATM interacting domains, has been shown to play a role in the translocation of the MRN complex to the nucleus and recruitment of DNA repair and damage checkpoint proteins to DSBs (Desai-Metha *et al.*, 2001; Lloyd *et al.*, 2009; Tsukamoto *et al.*, 2005).

It is believed that the MRN complex functions in HR by colaborating with *Sp*Ctp1/*Sc*Sae2/*h*CtIP to initiate end resection by endonucleatic cleavage of the 5' ends internal to DSB ends. Ctp1 is phosphorylated both in a cell cycle and DNA damage dependent manner (Akamatsu *et al.*, 2008; Chen *et al.*, 2008; Clerici *et al.*, 2005; Huertas *et al.*, 2008; Limbo et al., 2007; Sartori *et al.*, 2007; Symington, 2014). The MRX complex was reported to stimulate Sae2 activity in processing DNA hairpin

structures, and to collaborate with Sae2 to cleave covalently-bound Spo11 in meiotic recombination (Neale *et al.*, 2005; Lengsfeld *et al.*, 2007).

RecQ family helicases and Exo1 are implicated in the next stage of DNA processing in HR. Exo1 exhibits 5'→3'exonuclease activity and is also involved in mismatch repair, degradation of collapsed RFs, telomere maintenance, and control of crossovers during meiosis (Cotta-Ramusino *et al.*, 2005; Maringele & Lydall, 2002; Tran *et al.*, 2004). Studies show the role of Exo1 in extensive resection of DSBs (Gravel et al., 2008; Nimonkar *et al.*, 2008; Mimitou & Symington, 2008; Zhu *et al.*, 2008). The observation of residual recombinational activities in *exo1* mutants suggests that further parallel pathways were involved in end processing in HR. Human BLM and budding yeast Sgs1 (RecQ helicases) have been suggested to function in resection in concert with Dna2, which harbors 5'→3' exonuclease activity. The helicase unwinds the DNA duplex and Dna2 degrades the 5' strand (Nimonkar *et al.*, 2008; Mimitou & Symington, 2008; Zhu *et al.*, 2008). However, yeast cells lacking both Sgs1 and Exo1 show DNA break ends that are shorter than the initial cut fragment (Mimitou & Symington, 2008; Zhu *et al.*, 2008). These data suggest a model of resection where MRN in collaboration with Ctp1 carries out initial processing of DSB, and Exo1 and Sgs1-Dna2 carry out long-range resection.

It is worth noting that end resection is a crucial step that determines the balance of repair choice between HR and NHEJ pathways. In yeast, HR functions mainly in S and G2, when the sister chromatid is available as template strand, whereas NHEJ is the main repair mechanism through G1 (Aylon *et al.*, 2004; Ira *et al.*, 2004). In mammalian cells NHEJ is also the main repair pathway in G2 but HR is required for repair of DSBs in heterochromatin (Goodarzi & Jeggo, 2013) and is essential in S phase. Cyclin dependent kinases are suggested as regulatory factors affecting this choice of pathways

by periodically phosphorylating and dephosphorylating Ctp1 (Ctp1 is activated when phosphorylated). Several studies have made identical observations in budding yeast and human cells (Baroni *et al.*, 2004; You & Bailis, 2010). Conversely, excessive resection in HR can lead to gross chromosomal rearrangements (GCRs), therefore, the extent to which resection is carried out needs to be regulated. This regulation is achieved by activation of checkpoint proteins. Excess exposure of ssDNA as a result of resection recruits RPA (replication protein A), which initiates checkpoint signaling. This leads to activation of the downstream checkpoint kinase cascade. Exo1 activity is modulated by checkpoint proteins (El-Shemerly *et al.*, 2008; Morin *et al.*, 2008; Tsang *et al.*, 2014).

1.7.2 – PROTEINS INVOLVED IN STRAND INVASION

Recombinase Rad51, the homologue of bacterial RecA, is central to strand invasion and the homology search in mitotic HR. Rad51 exhibits ATPase activity and forms a right-handed nucleofilament on RPA-bound ssDNA, known as the presynaptic filament (Bianco *et al.*, 1998; Bleuit *et al.*, 2001; Shinohara *et al.*, 1992; Yu *et al.*, 2001). Despite the fact that RPA, the eukaryotic single stranded binding protein (SSB), that binds ssDNA, has been shown to stimulate RAD51 loading onto ssDNA by preventing formation of secondary structures, it has a higher affinity for ssDNA and is in abundance *in vivo*. This leads to a requirement for Rad52 and Rad55-Rad57 yeast mediator proteins to overcome the inhibitory effect of RPA and enhance Rad51 loading onto RPA-coated ssDNA (Gasior *et al.*, 1998; Krejci *et al.*, 2003; Bleuit *et al.*, 2001; Symington, 2002).

Rad52 binds RPA-coated ssDNA and also interacts with Rad51, and this interaction is required for Rad51 loading onto RPA-bound ssDNA (Krejci *et al.*, 2002; Seong *et al.*, 2008; Shinohara & Ogawa, 1998; Shinohara *et al.*, 1992). Substoichiometric amounts of Rad52 catalyze Rad51 nucleofilament formation by polymerization of nucleated Rad51 molecules (Song & Sung, 2000; Sugiyama et al., 1998; Sung et al., 2003). Rad52 also exhibits Rad51-independent strand annealing activity which mediates single strand annealing (SSA), a sub-pathway of HR, and promotes second end capture in post Rad51-dependent invasion steps (Ivanov *et al.*, 1996; McIlwraith & West, 2008; Sugiyama *et al.*, 2006). Similar to Rad52, the Rad55-Rad57 heterodimer directly interacts with Rad51 and can load Rad51 onto RPA-coated ssDNA. Although Rad55-Rad57 exhibits ATPase activity, it cannot catalyze the strand exchange (Hays et al., 1995; Johnson & Symington, 1995; Sung, 1997). Co-filamentation of Rad55-Rad57 with Rad51 stabilizes the presynaptic filament against Srs2 anti recombinase activity (Fung et al., 2009).

Strand invasion and homology search starts once Rad51 is successfully loaded on ssDNA. Rad51 with the assistance of two members of Snf2/Swi2 family of DNA-dependent ATPases, Rad54 and Rdh54, then catalyzes the formation of the D-loop structure (Petukhova *et al.*, 1998; Van Komen *et al.*, 2000). Rad54 and Rdh54 were also found to stabilize Rad51-coated ssDNA and promote branch migration in early stages of HR (Bugreev *et al.*, 2007; Mazin *et al.*, 2003; Mazin *et al.*, 2010; Solinger & Heyer, 2001). However, Rad54 acts as a negative regulator of Rad51 in late stages of HR by preventing inappropriate Rad51 binding and removing Rad51 from dsDNA to promote DNA synthesis (Chi *et al.*, 2006; Heyer *et al.*, 2006; Li & Heyer, 2009; Solinger *et al.*, 2002). Similarly, the Fbh1 and Srs2 helicases were found to have Rad51-antagonistic activity, which prevents Rad51 filament formation. Srs2 binds Rad51 and promotes

ATP hydrolysis within the presynaptic filament causing its weakening and dissembly of the Rad51 filament. This activity is of particular importance as inappropriate non-allelic or ectopic recombination increases loss of heterozygosity (LOH) and GCRs. These helicases channel break repair through the SDSA pathway, which reduces the production of crossovers (Antony *et al.*, 2009; Gangloff *et al.*, 2000; Lorenz *et al.*, 2009; Osman *et al.*, 2005).

An additional complex, Swi5-Sfr1, is required for HR in fission yeast and mammalian cells (Akamatsu & Jasin, 2010; Kurokawa *et al.*, 2008). The Swi5-Sfr1 complex interacts directly with Rad51 and stimulates strand exchange. The equivalent *S. cerevisiae* complex, Sae3-Mei5, is meiosis-specific, interacts with Dmc1 and promotes assembly of Dmc1 on meiotic chromosomes (Hayase *et al.*, 2004; Tsubouchi & Roeder, 2004).

1.7.3 – PROTEINS INVOLVED IN RESOLUTION

Once strand invasion has occurred HR can proceed via two alternative pathways, in SDSA invading strand in the D-loop structure is displaced. Alternatively second end capture sets the preference of DSBR. Little is known about factors affecting this preference. It has been proposed that filament displacement in SDSA is mediated by *sc*Srs2, *sp*Fml1 or *h*BLM & RTEL1. It is notable that these helicases favour the formation of non-crossover products (Barber *et al.*, 2008; Sun *et al.*, 2008; van Barbant *et al.*, 2000). In DSBR, the second end is captured to form a dHJ. Lao *et al.* (2008) showed that formation of dHJs is promoted by Rad52 in *S. cerevisiae*. Resolution or dissolution of dHJ in DSBR is the key step that predicts the production of non-

crossovers and crossovers based on symmetry of cleavage or helicase and topoisomerasIII activity respectively. In bacteria, the RuvC resolvase carries out the symmetrical resolution of HJs. Although no structural homologue of RuvC has been reported in eukaryotes, in human and *S. cerevisiae* symmetric resolution of dHJs is carried out by structure specific endonucleases *h*GEN1 and *sc*Yen1 (Ip *et al.*, 2008), and *h*MUS81-EME1 and *sc*Mus81-Mms4. GEN1 dimerises on HJs and resolves them by introducing dual nicks in the pair of non-crossing strands (Rass *et al.*, 2010) *S. pombe*, on the other hand, has no known homologue of GEN1/Yen1. However, the Mus81-Eme1 complex has been proposed to carry out the resolution of dHJs. The role of the heterodimeric Mus81-*Sp*Eme1/*Sc*Mms4 endonuclease complex in cellular growth and processing of perturbed replication forks has been the subject of various studies (Boddy *et al.*, 2000; Boddy *et al.*, 2001; Kai *et al.*, 2005; Kaliraman *et al.*, 2001; Interthal *et al.*, 2000). *In vitro* and *in vivo* studies have shown that the Mus81 complex has a substrate specificity for HJs, nicked HJs, D-loops, RFs with 5' ends at the junction point, and 3' flaps (Bastin-Shanower *et al.*, 2003; Fricke *et al.*, 2005; Osman *et al.*, 2003; Whitby *et al.*, 2003). Recently, Mus81-Eme1 has been shown to have resolvase activity in concert with Slx1-Sxl4 in mammalian cells (Castor *et al.*, 2013; Garner *et al.*, 2013; Wyatt *et al.*, 2013).

RecQ helicases (*Sp*Rqh1, *Sc*Sgs1, *h*BLM) in conjunction with Topoisomerase III are proposed to catalyse dHJ dissolution, which also lead to non-crossover products. In this process, two individual junctions of dHJ are migrated towards each other by the helicase to form a hemicatenane, which is then disentangled by TopIII to produce non-crossovers (Hope *et al.*, 2007; Oh *et al.*, 2007; Wu & Hickson, 2003). However, single HJs that arise during SDSA by branch migration of the initial D-loop cannot be dissolved and require resolution by structure specific endonucleases (Schwartz & Heyer

2011). *In vivo* analysis of meiotic and mitotic recombination intermediates has shown the presence of single and double HJs in both prokaryotes and eukaryotes (Bzymek *et al.*, 2010; Cromie *et al.*, 2006; Kobayashi & Ikeda, 1983; Schwacha & Kleckner, 1995).

It must be noted that while the same steps are involved in meiotic and mitotic HR, in some cases additional or different factors are required for meiotic recombination or vice versa and these are not discussed here (see Ehmsen & Heyer, 2010 for more details on meiotic recombination).

1.8 – PROKARYOTIC REPLICATION RESTART

oriC is the initiation point of replication in the 4.7Mb circular *E. coli* chromosome. Since the replication starts in a bidirectional manner, each fork needs to replicate a distance of 2.3Mb within which many obstacles can compromise the progression of the fork and completion of DNA replication. Multiple pathways have been shown to take part in prokaryotic fork rescue.

It has been well established that in prokaryotes recombinational events play a major role in reassembling a unidirectional RF when forks collapse (Sandler & Marians, 2000; Xu & Marians, 2003). PriA, which was originally discovered as an essential factor in the primosome required for conversion of circular single stranded DNA of φX174 phage to double stranded DNA, plays a central role in replication fork restart (Arai & Kornberg, 1981). The primosome is composed of PriA, PriB, PriC, DnaB helicase, DnaC, DnaT, and DnaG primase (McMacken *et al.*, 1977; McMacken & Kornberg, 1978). Please note that a different primosome is required for initiation of replication at *oriC* in *E. coli* (Bramhill & Kornberg, 1988). Studies of priA, priB, and

priC mutants suggest existence of at least two pathways for restarting the arrested replication forks in *E. coli*, PriA dependent and independent pathways. *priA* mutants are viable but have a very sick phenotype and are induced for the SOS response. *priB* and *priC* mutants are also viable and exhibit a more normal phenotype. *priB* and *priC* double mutants are still viable but show a sick phenotype. *priA* and *priC* or rep double knockouts are lethal. Collectively, these results suggest that the PriA dependent fork restart pathway requires PriB/PriC, whereas PriA independent pathway requires PriC and Rep, and that the PriA dependent pathway is the major fork rescue pathway considering the severe phenotype of priA mutants (Gregg *et al.*, 2002; Heller & Marians, 2005A; Nurse *et al.*, 1991; Sandler, 2000; Sandler *et al.*, 1999).

Experimental evidence did not uncover a direct role for PriA in cellular replication, however it was revealed that PriA has a high affinity for D-loops and arrested fork-like structures and binding to these stimulates its ATP hydrolysis activity in presence of single stranded binding protein (SSB). These data suggest that PriA can sense the stalled replication forks and promote reloading of the replisome through either recombination or non recombination-dependent events. SSB is proposed as the recruitment factor of PriA to the site of damage as PriA can bind SSB through its SSB interacting zinc motif (Cadman & McGlynn, 2004; McGlynn *et al.*, 1997; Mizukoshi *et al.*, 2003; Tanaka *et al.*, 2003). The role of PriA in replication restart has been suggested to function in two ways, first by creating a single stranded nick on the lagging strand, creating a platform for DnaB loading, and second by enhancing the origin-independent loading of the replisome at the site of arrested forks (Heller & Marians, 2006). In the PriA-dependent replication resumption pathway, PriA, PriB, and DnaT catalyze reloading of the replisome onto D-loop structures or recombination joint molecules

(Heller & Marians, 2005B). In the PriA independent pathway, PriC interaction with Rep coordinates the function of Rep and DnaB for fork restart (Heller & Marians, 2005A). In replication mutants (polIII or rep mutants), the fork reversal model of fork rescue has been proposed to restart the arrested forks. In this model, RecBCD prevents the RuvABC mediated chromosome linearization and an unidentified helicase enhances the fork reversal (RecA has been shown to mediate this reaction in *dnaB* mutants). The resulted 'chicken foot' structure is then recognized by PriA which promotes the reassembly of the replisome (Flores *et al.*, 2002; Grompone *et al.*, 2002; Gruss & Michel, 2001). In the UV induced fork arrest response, either RecFOR and RecA strand invasion activity mediates the bypass of the damage by nucleotide excision repair (NER), or the RecG catalyzed fork-reversal-mediated template strand switching assists the bypass of the damage, both of which requires PriA (Grompone *et al.*, 2004; Singleton *et al.*, 2001). However, in a gyrase mutant that accumulate positive supercoiling, no evidence of fork reversal has been observed, as RecBCD is not required for cell viability. The PriA dependent viability in this mutant suggests the direct PriA-dependent fork restart (Grompone *et al.*, 2003).

1.9 – EUKARYOTIC REPLICATION RESTART

While cells employ multiple pathways to account for errors in replication fidelity (mismatch repair/MMR) or template lesions, the continuous endogenous and exogenous insults lead to occasional damage on DNA. This damage is usually repaired by base excision repair (BER) or nucleotide excision repair (NER). However, if left unrepaired, the damage can compromise replication progression. When RFs meet template lesions,

BER and NER can no longer be utilized since the duplex is unwound and the complementary strand would not available to serve as a template for resynthesizing the excised region. While template lesions on the lagging strand are not thought to impact on replication progression due to the discontinuous nature of lagging strand replication, post replication repair pathways rescue replication stalls at leading strand template lesions. This is achieved through covalent modifications of PCNA (see Figure 1.4). In the translesion synthesis (TLS) pathway of PRR, monoubiquitination of PCNA recruits specialized translesion polymerases to bypass the damage. Polyubiquitination of PCNA leads to activation of error-free damage avoidance pathways to bypass the damage (Lehmann & Fuchs, 2006; Branzei & Foiani, 2010; Ulrich, 2011).

Hoege *et al.* first reported in *S. cerevisiae* ubiquitination of PCNA on K164 in response to DNA damage (Hoege *et al.*, 2002) and high conservation of K164 ubiquitination was shown in all eukaryotic species analyzed (Anderson *et al.*, 2008; Arakawa *et al.*, 2006; Frampton *et al.*, 2006; Leach and Michael 2005). Mono-ubiquitination of PCNA is mediated by E2 ubiquitin conjugating enzyme Rad6 and its E3 ubiquitin ligase partner Rad18 (Rad6/Rad18 complex) (Frampton *et al.*, 2006; Hoege *et al.*, 2002; Kannouche *et al.*, 2004; Watanabe *et al.*, 2004). This monoubiquitination of PCNA promotes activation of Y-family (Polη, Polι, Polκ, and REV1) DNA TLS polymerases (Stelter & Ulrich, 2003). These polymerases lack 3'→5' endonuclease proofreading ability, and have more open active site than replicative polymerases which enables them to accommodate and replicate irregular templates (Lehmann *et al.*, 2007; Prakash *et al.*, 2005). These characteristics enable TLS polymerases to replicate damaged templates but with low fidelity and increased mutagenesis. Therefore, TLS is also known as the error-prone pathway of damage tolerance (Ulrich & Takahashi, 2013). Y-family TLS polymerases harbor ubiquitin

binding motifs which can bind to ubiquitinated PCNA. Also, various TLS polymerases (Polη, Polι, Polκ) interact with PCNA via their PCNA interacting peptide (PIP) motifs. It has been shown that these motifs are important for PCNA binding and play a role in the regulation of function of TLS polymerases in response to DNA damage (Bienko *et al.*, 2005; Guo *et al.*, 2006; Parker *et al.*, 2007; Plosky *et al.*, 2006; Prakash *et al.*, 2005; Wood *et al.*, 2007). Zhuang *et al.* (2008) using a reconstituted yeast system showed that the switch between Polδ and Polη is dependent on K164-monoubiquitination of PCNA and fork stalling. Similarly, the ubiquitin dependent exchange of the replicative polymerase for a TLS polymerase was demonstrated in human cell extracts (Masuda *et al.*, 2010).

In response to fork stalling, poly-ubiquitination of PCNA is promoted by the heterodimeric E2 complex Ubc13/Mms2 and E3 ligase Rad5 (Figure 1.5). Ubiquitin chain formation is catalyzed on mono-ubiquitinated K164 via a non-canonical K63 linkage, which is distinct from K48-linked ubiquitin chain involved in proteasome-dependent protein degradation (Frampton *et al.*, 2006; Hoege *et al.*, 2002; Hofmann & Pickart, 1999; Ulrich & Jentsch, 2000). In metazoans, while RAD18 and UBC13 are essential for PCNA poly-ubiquitination, MMS2 is not required and embryonic stem cells from *mms2* knockout mice show PCNA poly-ubiquitination (Brun *et al.*, 2008). However, human homologues of Mms2, HLTF and SHPRH, have been shown to take part in polyubiquitination of PCNA (Motegi *et al.*, 2008; Unk *et al.*, 2008). In budding yeast, *rad5Δ*, *ubc13Δ*, or *mms2Δ* mutants show increased spontaneous or damaged induced mutagenesis, and *rev3* mutation confers a synergistic UV sensitivity in *rad5Δ* or *ubc13Δ* mutants (Broomfield *et al.*, 1998; Brusky *et al.*, 2000; Johnson *et al.*, 1992). In higher eukaryotes, reduction of expression of HLTF/SHPRH or inhibition of PCNA polyubiquitination results in UV induced mutagenesis (Chiu *et al.*, 2006; Motegi *et al.*,

2008). The evidence above indicates that PCNA polyubiquitination promotes an error-free pathway of PRR. Polyubiquitination is proposed to control error-free PRR via either a recombination-mediated template switching mechanism where the blocked strand invades the sister chromatid to form a D-loop or dHJ intermediates which facilitates the lesion bypass, or a fork reversal model where a regressed chicken foot intermediate forms allowing the fork to restart (Atkinson & McGlynn, 2009; Branzei & Foiani, 2010; Zhang & Lawrence, 2005). Although the exact molecular machinery governing the error-free pathway of PRR remains illusive, evidence suggests the involvement of members of FANCM family of helicases in this pathway. In budding yeast, *mph1* mutants show sensitivity to MMS, and increased spontaneous mutation rates that depend on TLS polymerases, suggesting the suppression of error-free PRR in the absence of Mph1. Interestingly while *mph1* mutants are HR proficient, a *rad51 mph1* double mutant shows the same rate of spontaneous mutations (Scheller *et al.*, 2000; Schürer *et al.*, 2004). Moreover, deletion of *mph1* suppresses the Rad51-dependent sister chromatid exchanges formed when cells are exposed to DNA damaging agents (Ede *et al.*, 2011). Together, this evidence suggests a role for Mph1 in HR dependent error-free pathway of PRR. Similarly in *S. pombe*, *fml1* (the FANCM homologue) mutants show sensitivity to crosslinking agents and Fml1 promotes recombination at stalled forks suggesting its role in error-free PRR (Sun *et al.*, 2008).

PCNA is sumoylated on K164 and to a lesser extent on K127 by the Sumo E2 ligase Ubc9 and Sumo E3 conjugator Siz1 in *S. cerevisiae* (Hoege *et al.*, 2002) and this modification has also been reported in higher eukaryotes (Arakawa *et al.*, 2006; Gali *et al.*, 2012; Gohler *et al.*, 2008; Leach & Michael 2005; Moldovan *et al.*, 2012). In budding yeast, PCNA sumoylation recruits Srs2 to the stalled fork. As previously described Srs2 is a helicase with anti-recombinogenic properties and acts via direct

disruption and prevention of formation of Rad51 filaments (Krejci *et al.*, 2003; Veaute *et al.*, 2003). Srs2 was found to physically interact with sumoylated PCNA via its C-terminal SIM motif, and elevated levels of recombination and crossover events were seen upon loss of PCNA sumoylation, suggesting an inability in recruitment of Srs2 to the site of damage and an anti-recombinase role of Srs2 in repair choice (Le Breton *et al.*, 2008; Papouli *et al.*, 2005; Pfander *et al.*, 2005; Robert *et al.*, 2006). The anti-recombinase activity of Srs2 suppresses inappropriate HR-dependent processing of stalled forks and favors the RAD6 repair pathway (Marini & Krejci, 2010).

Figure 1.5

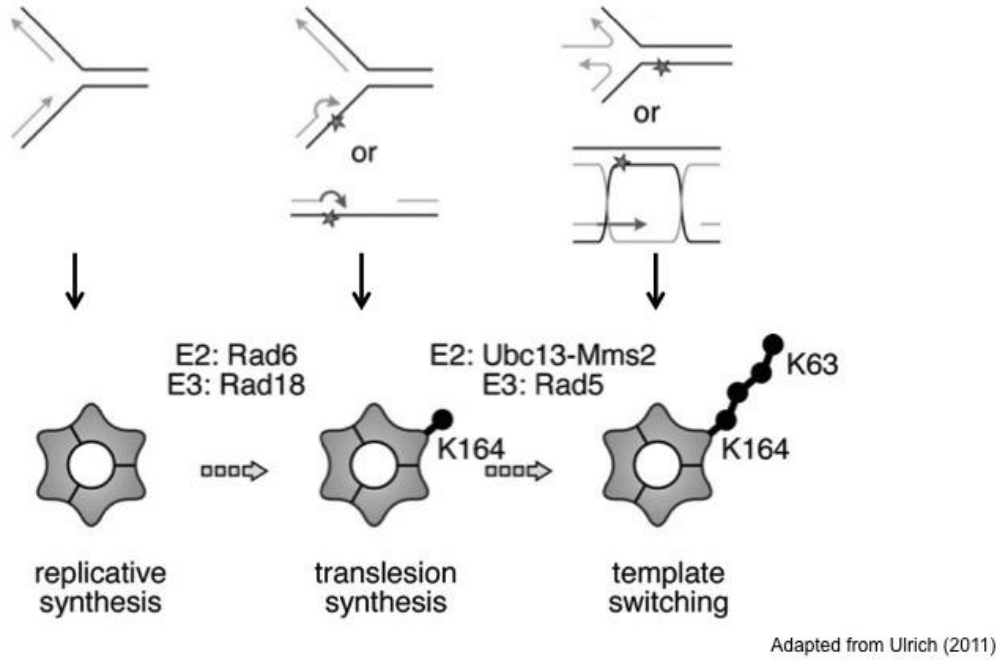

Figure 1.5 | Posttranslational modifications of PCNA govern translesion synthesis. During unstressed replication PCNA retains posttranslational neutral status. In response to template lesions, mono and poly ubiquitination of PCNA in response to replication stress or DNA damage lead to error-prone or error-free bypass of the damage respectively. Rad6/Rad18 mediate monoubiquitination and Ubc13-Mms2/Rad5 catalyse polyubiquitination of the sliding clamp.

1.10 – RECOMBINATION AT ARRESTED FORKS

In eukaryotes, in the absence of checkpoint functions or in situations where the checkpoint fails to stabilize the arrested replication forks when DNA polymerase function is compromised, forks collapse and HR is required for fork restart. Unlike bacteria, eukaryotic cells lack a PriA-like system to reload the replisomes on DNA when forks collapse. Viability in certain *S. cerevisiae* replication mutants (*mec1-srf, pol30* and *rad27*) has been shown to require recombination proteins (Merrill & Holm, 1998; Merrill & Holm, 1999; Symington, 1998). Rad52 and Mre11 form foci in response to HU treatment in checkpoint deficient cells, where the replisome dissociates from the nascent DNA strand (Lisby *et al.*, 2004). Similarly in *S. pombe* HR is required for viability in *rad2* (FEN1) null cells (Murray *et al.*, 1994) and Rad52 foci are seen in response to HU in *cds1* null cells, defective in the intra S phase checkpoint (Irmisch *et al.*, 2009). Checkpoint deficient *S. pombe* cells cannot complete the replication and accumulate aberrant structures at the site of fork collapse. The aberrant structures are suppressed in a *cds1 rad51* double knockout background but the viability is not restored consistent with homologous recombination being necessary for replication restart of collapsed forks (Meister *et al.*, 2005). In *Xenopus* extracts, GINS complex and Polε reloading at forks collapsed at ssDNA lesions depends on Rad51 and MRN complex (Hashimoto *et al.*, 2012). The exact pathways by which HR rescues the collapsed forks remain elusive. Break induced replication (BIR) has been suggested as a possible non-reciprocal recombination pathway to restart replication of one-ended broken forks. BIR depends on all the factors involved in passive replication with the exception of ORC and Cdc6 (Llorente *et al.*, 2008; Sakofsky *et al.*, 2012). BIR could also be induced via cleavage of a collapsed fork to form a one-ended DSB by nucleases such as Mus81 but

studies on HR-dependent replication restart at programmed polar RFBs have not found any evidence for such an intermediate (Lambert *et al.*, 2010: Mizuno *et al.*, 2013; Larsen *et al.*, 2014). However, these studies on programmed polar RFBs in both yeasts have revealed the influence of HR-dependent pathways on restoring collapsed replication forks and completing DNA replication.

Programmed polar RFBs in the budding yeast rDNA have been extensively studied to understand the fate of stalled forks during unperturbed replication. RFB repeats arrest replication forks in a unidirectional manner to avoid the collisions between replication and transcription machineries. Fork arrest requires Fob1 and arrested forks are then stabilized via a checkpoint independent function of Tof1 and Csm3 (Calzada *et al.*, 2005). A recombination hotspot (HOT1) is also located within the rDNA repeats and this overlaps with the RFBs. The regulation of recombination in the rDNA locus is exerted through the actions of Fob1, the transcription silencing protein Sir2 and cohesin (Kobayashi & Horiuchi, 1996; Tsang & Carr, 2008). Equal sister chromatid recombination events, which are dependent on Fob1 and transcription, are promoted by HOT1 to maintain the rDNA homeostasis.

HR also plays an important role in mating type switching of fission yeast. The mat locus consists of the transcriptionally active *mat1* and two silent donor cassettes *mat2P* and *mat3M*. The polar *RTS1* barrier optimizes the switching process by preventing the RFs moving through the locus in the telomere to centromere direction, which could interfere with efficient switching process at *mat1*. In switchable cells a Swi1/Swi3 and Swi7-dependent polar imprint is made on the lagging strand on the centromere side of *mat1* during the first round of replication. In the second round of replication this imprint on the leading strand in one of the daughter cells leads to formation of a one-ended DSB, the 3’ end of which invades the homologous region in

mat2 or *mat3* and initiates gene conversion. The second strand is then synthesized using the first strand as template. This results in formation of two daughter cells one of which has switched mating type (Klar, 2007). In the absence of the donor loci the one-ended DSB must be repaired using the sister chromatid and this is dependent on HR and Mus81 to restart the fork (Roseaulin *et al.*, 2008).

Recent studies in fission yeast have employed the mating type locus polar replication termination sequence (*RTS1*) to investigate the events involved in initiating replication restart when forks are arrested at a specific site in every cell cycle. When integrated at an ectopic locus, *RTS1* was shown to induce Rad52- and Rad51-dependent recombination between direct repeats by 50 fold. Whereas, in the presence of the RecQ helicase Rqh1 (WT), the observed recombination events were characterized as conversion events, deletion of Rqh1 resulted in deletion type events suggesting a DSB-free initiation of recombination at *RTS1* (Ahn *et al.*, 2005). In another fork stalling system developed in Carr's laboratory, two inverted repeats of *RTS1* flanking a marker at an ectopic locus caused rapid collapse of replication forks, survival of which was dependent on recombination proteins (Lambert *et al.*, 2005). This led the authors to propose that the replication rescue in this system occurs via HR without a DSB intermediate as in contrast to the one-ended DSB at the mating type locus (Roseaulin *et al.*, 2008) a DSB could not be seen even in backgrounds where such a break would not be repaired (Lambert *et al.*, 2005; Lambert *et al.*, 2010; Mizuno *et al.*, 2009). In the following sections I briefly summaries the results of these studies.

1.11 – *RTS1* FUNCTIONS

As previously explained, *RTS1* is necessary for efficient mating-type switching, and was the first replication fork barrier implicated to have a role in cellular differentiation (Dalgaard & Klar, 2001). *RTS1* contains two *cis*-acting elements known as region A and region B, which cooperate for efficient replication termination. Region A is a ~64-bp purine-rich region of %73 GA content, and region B contains four copies of a ~60-bp motif. Similar to fork pausing at rDNA RFBs, Swi1 and Swi3 are required for replication termination at *RTS1*. Fork stalling at *RTS1* also requires DNA binding proteins Rtf1 and Rtf2. Rtf2 binds the purine-rich region and enhances the efficiency of the barrier but is not necessary for its function, and the *rtf2Δ* phenotype can be suppressed by Rtf1 overexpression. Rtf1 binds the repeat motifs and this interaction is essential for the *RTS1* barrier activity (Codlin & Dalgaard, 2003). Rtf1 consist of two myb/SANT domains one of which interacts with both regions A and B of *RTS1*, whereas the second domain does not show great DNA binding affinity. The C-terminal tail of Rtf1 is required for replication arrest at *RTS1*, and mediates Rtf1 self-dimerization /polymerization. A model for replication termination at *RTS1* was proposed where four Rtf1 molecules bind the four repeats within the region B of *RTS1*. More Rtf1 is recruited to region A via Rtf1 C-terminal domain self polymerization activity resulting in an efficient polar fork stalling at *RTS1* (Eydmann *et al.*, 2008) (see Figure 1.6).

Figure 1.6

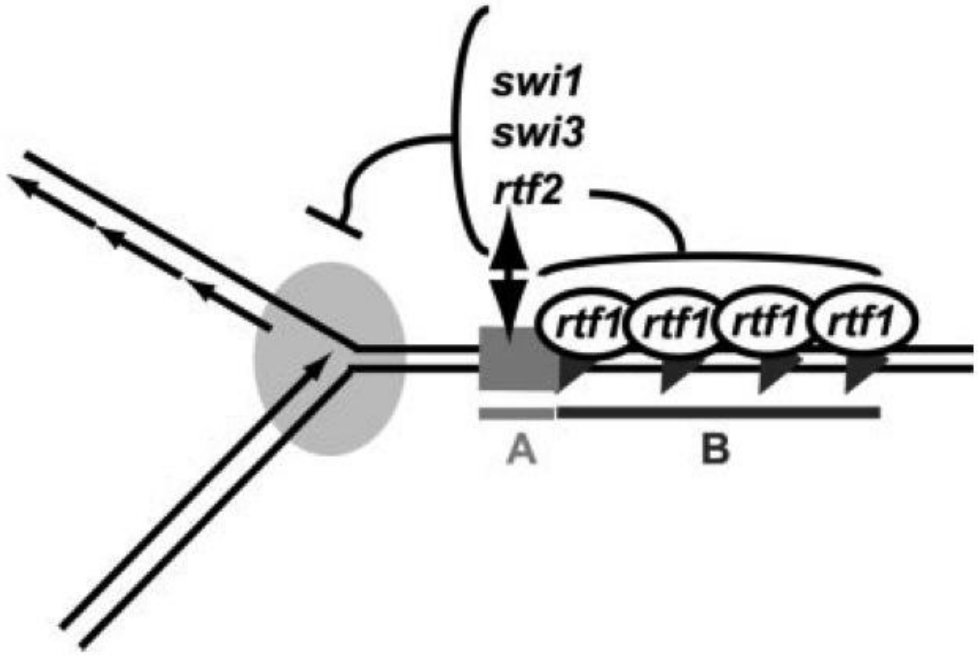

Figure 1.6 | Model for Rtf1 mediated replication fork arrest at *RTS1*. Four Rtf1 molecules bind the four repeats of the RTS1 (region B). C-terminal self polymerisation activity of Rtf1 results in recruitment and interaction of more Rtf1 with region A of the *RTS1*. This results in efficient polar fork stalling activity of the barrier. Rtf2, Swi1, and Swi3 also interact with the barrier.

1.12 – *RTS1*, FORK COLLAPSE AND RESTART

To create a difficult-to-replicate region and study RF restart, Lambert *et al.* (2005) created a system, named RuraR, by integrating inverted repeats of *RTS1* separated by a 1.8kb sequence containing the *ura4* gene at the *ura4* locus on ChrIII of fission yeast (Figure 1.7). The direction of replication is centromere to telomere at the *ura4* locus due to the presence of the efficient double origin ARS3004/3005 centromere proximal to the locus. To regulate fork stalling at *ura4* locus, the P*nmt41* inducible promoter was used to control Rtf1 expression (Lambert *et al.*, 2005). Induction of fork stalling in this system resulted in gene inversion, site-specific GCRs, and HR-protein dependent cell viability. Recombination proteins were recruited to the site of fork stalling and GCRs were recombination dependent. Moreover, GCRs were not dependent on checkpoint functions, suggesting the rapid collapse of the replisome at *RTS1*.

In a later variant of the stalling system developed by Mizuno *et al.* (2009), two inverted repeats of the *ura4* gene flanked by two *RTS1* inverted repeats (named RuiuR) were integrated at *ura4* locus creating a small palindrome. The palindrome was interrupted by insertion of a 14-bp spacer sequence (Figure 1.7). Induction of fork stalling in the palindrome system led to loss of viability due to HR-dependent formation of acentric and dicentric palindromic chromosomes. These were also observed at a lower frequency in the inverted repeat (RuraR) system. It should be noted that these palindromic chromosomes are sister chromatid fusions (see Figure 1.8) and, while the acentric fails to attach to the mitotic spindle, the dicentric alignes correctly but forms a chromosome bridge at anaphase.

In both systems no evidence of DSBs was detected even in strains defective for factors required for processing DSBs (Lambert et al., 2010; Mizuno *et al.*, 2009). This

evidence led to the model of a DSB independent mechanism of HR fork restart: a strand invasion event facilitated by recruitment of HR proteins to the nascent strand at the site of the collapsed fork. Strand invasion into the correct template initiates HR-dependent fork restart. However, inaccurate strand invasion into the wrong template leads to non-allelic HR (NAHR), which results in GCRs (Lambert *et al.*, 2010; Mizuno *et al.*, 2009) (This model is discussed in more detail in Chapter four. See Figure 4.7 for models). The increased frequency of GCRs in the palindrome (RuiuR) system was hypothesized to be due to branch migration of the invading strand in the palindrome to form a HJ at the center of the palindrome. This branch migration would not be possible in the inverted repeat (RuraR) system (Lambert *et al.*, 2010). To prevent the predicted branch migration, a series of constructs were made where a portion of the centromere-proximal *ura4* gene in the palindrome system was replaced with an exogenous sequence (named RPalR), and to prevent the non-allelic HR restart the telomere-proximal *RTS1* sequence of RPalR was replaced with Ter2/3 rDNA RFBs (named TPalR) (see Figure 1.7). The RPalR system was predicted to reduce the GCR levels and TPalR system to generate no GCRs. However, induction of fork stalling resulted in GCRs in both systems. This data suggested an alternative pathway of GCR production where the collapsed RF is restarted accurately by HR on the correct template but the restarted fork reverses the orientation of replication (U-turns) when replicating the palindrome center (Mizuno *et al.*, 2013). Thus two mechanisms leading to the generation of GCRs have been defined: firstly template exchange or non-allelic homologous recombination (NAHR) where the wrong template is used during restart, and secondly the restarted fork would restart correctly on the right template but this fork in non-canonical and error-prone with a high propensity to U-turn at inverted repeats (see Figure 4.7 for models). Both mechanisms generate intermediates that have to be resolved. NAHR dependent restart

generates HJs and the U-turn of the restarted fork generates HJ-like intermediates, the resolution of which results in formation of dicentric and acentric chromosomes. The error-prone nature of HR-restarted forks was confirmed by the Lambert lab in a separate study. Iraqui *et al.* (2012) showed that the restarted fork was prone to replication slippage events leading to small insertions and deletions. Therefore, although HR is required for replication restart and completion of replication, HR-dependent restart can lead to replication-induced genomic instability. Genomic instability is a hallmark of cancer, human hereditary diseases and many human syndromes (Aguilera & Garcia-Muse, 2013; Branzei & Foiani, 2010; Petermann & Helleday, 2010; Weinert *et al.*, 2009).

Figure 1.7

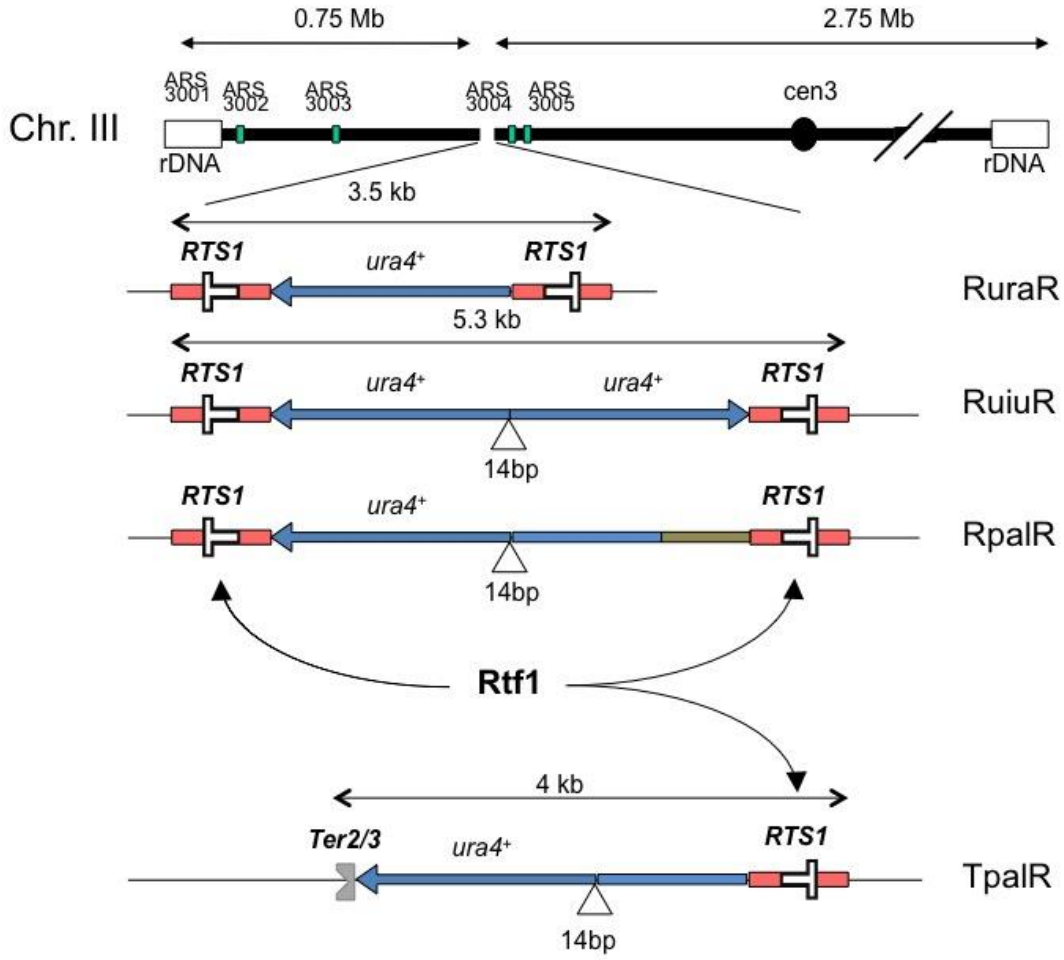

Figure 1.7 | RuraR and RuiuR fork stalling systems. Schematic of chromosome III (Chr.III) of *S. pombe*. Fork stalling systems are integrated into the *ura4* locus on Chr.III telomere proximal to efficient early firing ARS3004/3005. In RuraR inverted repeats of *RTS1* flank the *ura4* gene (blue arrows indicate the orientation). In RuiuR inverted repeats of the *ura4* gene are flanked by inverted repeats of the *RTS1* creating a small 5.3kb palindromic sequence. The centre of the palindrome is interrupted with 14bp of unrelated sequences. In RpalR the centromere proximal portion of *ura4* is replaced with unrelated sequences. In TpalR the telomere proximal *RTS1* is replaced with rDNA Ter2/3 polar RFBs. Induction of Rtf1 expression results in activation of *RTS1* barrier activity.

Figure 1.8

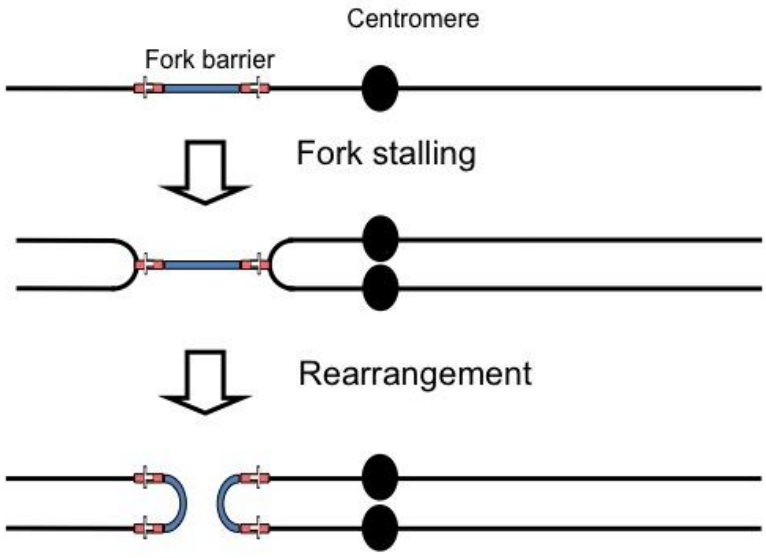

Figure 1.8 | HR-dependent replication restart in inverted repeats generates GCRs. Diagram showing the generation of GCRs after HR-dependent replication restart in inverted repeats. These are sister chromatid fusions resulting in reciprocal palindromic acentric and capped chromosomes. The acentric fails to attach to the mitotic spindle but the centromere on the dicentric (capped chromosome) alines correctly at mitosis due to the retention of sister chromatid cohesion but forms a bridge at anaphase.

1.13 – AIMS OF THE PROJECT

A limitation of the replication stalling systems used in Carr, Murray, and Lambert labs was that induction of replication stalling was controlled by Rtf1 expression from the *nmt* promoter and this takes 16-24 hours for full induction (Basi *et al.*, 1993). The *urg1* uracil-regulatable promoter originally reported by the Bahler lab (Watt, 2008) and subsequently optimised in the Carr lab (Watson *et al.*, 2011; Watson *et al.*, 2013) provides a budding yeast GAL-like system in fission yeast for rapid induction of genes of interest within a single cell cycle. Using this inducible system to control the expression of Rtf1 enables us to study the generation and consequences of fork arrest at a specific locus in a single cell cycle. The aim of this project is to monitor the generation of chromosome rearrangements upon induction of Rtf1 and fork arrest in synchronous cultures and to identify the intermediates formed by the restarted fork U-turn and to correlate the timing of events with checkpoint activation.

CHAPTER 2 – MATERIALS AND METHODS

2.1 – MEDIA USED IN THIS STUDY

2.1.1 – *S. POMBE* MEDIA

The media used were either of liquid or solid state. Supplements were added to the media as required at 100mg/l.

YE media:

0.5% w/v (5g/l) yeast extract 3.0% w/v (30g/l) glucose

YES media:

0.5% w/v (5g/l) yeast extract 3.0% w/v (30g/l) glucose

2.5g/l Difco Bacto Agar

Phloxin YES: 20mg/l Phloxin B (Sigma) was added to YES.

Edinburgh Minimal Media (EMM2)

50ml/l	20× EMM2 salts
25ml/l	20% NH4Cl
25ml/l	0.4M Na2HPO4
12.5ml/l	40% Glucose
1ml/l	1000× Vitamins
0.1ml/l	10000× Trace elements

20× EMM2 salts

61.20g/l	Potassium hydrogen phthallate
20.00g/l	KCl
21.40g/l	MgCl2.6H2O
0.20g/l	Na2 SO4
0.26g/l	CaCl2.2H2O

1000× Vitamins

1.0g/l	Pantothenic acid
10.0g/l	Nicotinic acid
10.0g/l	Inositol
0.01g/l	d-Biotin x

10000× Trace elements

5.0g/l	H3 BO3
4.0g/l	MnSO4
4.0g/l	ZnSO4.7H2O
2.0g/l	FeCl3.6H2O
1.5g/l	Na2 MoO4 1.0g/l KI
0.4g/l	CuSO4.5H2O
10.0g/l	Citric acid

Where necessary supplemented with: adenine, histidine, leucine, thiamine, uracil at final concentration of 100mg/l. The medium was filter sterilized after making.

2.1.2 – *E. COLI* MEDIA

Media used were either of solid or liquid state. Supplements were added to sterile liquid or molten agar prior to use.

L-Broth:

10g/l	NaCl
10g/l	tryptone
5g/l	yeast extract
1g/l	glucose
30mg/l	thymine

SOC medium:

20g/l	tryptone
5g/l	yeast extract
0.5g/l	NaCl

The medium was aoutoclaved and 10ml of filter-sterilised 1M $MgCl_2$, and 10ml of filter-sterilised 1M $MgSO_4$ was added to it prior to use.

2.2 – CHEMICALS USED FOR SELECTION

Table 2.1 | Chemicals used for selection in this study

Chemical	**Final Concentration**
Ampicillin	50mg/l

Geneticin disulphite	200mg/l
Hygromycin	200-400mg/l
Kanamycin	200mg/l

2.3 – LIST OF THE STRAINS USED IN THIS STUDY

Table 2.2 | List of the strains used in this study

Strain	Genotype
YSM012	*h⁻ ura4D-18 urg1::Purg1_NR::kan rtf1::nat*
YSM013	*h+ ura4D-18 urg1::Purg1_NRNR::kan rtf1::nat*
YSM015	*h⁻ RuraR urg1::Purg1_NR::kan rtf1::nat*
YSM016	*h+ RuraR urg1::Purg1_NR::kan rtf1::nat*
YSM072	*h+ ura4-D18 leu-32 urg1_NR::HPH rtf1::natMX6 nda3-KM311*
YSM073	*h+ ura4-D18 leu-32 urg1_NR::HPH rtf1::natMX6 nda3-KM311*
YSM074	*h+ RuiuR leu-32 urg1_NR::HPH rtf1::natMX6 nda3-KM311*
YSM075	*h+ RuiuR leu-32 urg1_NR::HPH rtf1::natMX6 nda3-KM311*
YSM076	*h+ RuiuR leu-32 urg1_NR::HPH rtf1::natMX6 nda3-KM311*
YSM077	*h- smt0 RuiuR leu-32 urg1_NR::HPH rtf1::natMX6 nda3-KM311*
YSM083	*h- smt0 RuiuR leu-32 urg1_NR::rtf1:eGFP:DSR rtf1::natMX6 nda3-KM311*
YSM084	*h- smt0 RuiuR leu-32 urg1_NR::rtf1:eGFP:DSR rtf1::natMX6 nda3-KM311*

YSM085	*h- smt0 RuiuR leu-32 urg1_NR::rtf1:eGFP:DSR rtf1::natMX6 nda3-KM311*
YSM086	*h- smt0 RuiuR leu-32 urg1_NR::rtf1:eGFP:DSR rtf1::natMX6 nda3-KM311*
YSM087	*h- smt0 RuiuR leu-32 urg1_NR::rtf1:eGFP:DSR rtf1::natMX6 nda3-KM311*
YSM088	*h- smt0 RuiuR leu-32 urg1_NR::rtf1:eGFP:DSR rtf1::natMX6 nda3-KM311*
YSM089	*h- smt0 RuiuR leu-32 urg1_NR::rtf1:eGFP:DSR rtf1::natMX6 nda3-KM311*
YSM090	*h- smt0 RuiuR leu-32 urg1_NR::rtf1:eGFP:DSR rtf1::natMX6 nda3-KM311*
YSM091	*h- smt0 RuiuR leu-32 urg1_NR::rtf1:DSR rtf1::natMX6 nda3-KM311*
YSM092	*h- smt0 RuiuR leu-32 urg1_NR::rtf1:DSR rtf1::natMX6 nda3-KM311*
YSM093	*h- smt0 RuiuR leu-32 urg1_NR::rtf1:DSR rtf1::natMX6 nda3-KM311*
YSM094	*h- smt0 RuiuR leu-32 urg1_NR::rtf1:DSR rtf1::natMX6 nda3-KM311*
YSM095	*h- smt0 RuiuR leu-32 urg1_NR::rtf1:DSR rtf1::natMX6 nda3-KM311*
YSM096	*h- smt0 RuiuR leu-32 urg1_NR::rtf1:DSR rtf1::natMX6 nda3-KM311*
YSM097	*h- smt0 RuiuR leu-32 urg1_NR::rtf1:DSR rtf1::natMX6 nda3-KM311*
YSM098	*h- smt0 RuiuR leu-32 urg1_NR::rtf1:DSR rtf1::natMX6 nda3-KM311*
YSM099	*ura4-D18 leu-32 ade6-704 urg1_NR::HPH rtf1::natMX6 Chk1-3HA nda3-KM311*
YSM100	*ura4-D18 leu-32 ade6-704 urg1_NR::HPH rtf1::natMX6 Chk1-3HA nda3-KM311*
YSM101	*h- smt0 RuiuR leu-32 ade6-704 urg1_NR::HPH rtf1::natMX6 Chk1-3HA*

	nda3-KM311
YSM102	*RuiuR leu-32 ade6-704 urg1_NR::HPH rtf1::natMX6 Chk1-3HA nda3-KM311*
YSM103	*RuiuR leu-32 urg1_NR::HPH rtf1::natMX6 Chk1-3HA nda3-KM311*
YSM107	*h- smt0 RuraR leu-32 urg1_NR::HPH rtf1::natMX6 nda3-KM311*
YSM108	*h- smt0 RuraR leu-32 urg1_NR::HPH rtf1::natMX6 nda3-KM311*
YSM109	*h- smt0 RuraR leu-32 urg1_NR::rtf1:eGFP:DSR rtf1::natMX6 nda3-KM311*
YSM110	*h- smt0 RuraR leu-32 urg1_NR::rtf1:eGFP:DSR rtf1::natMX6 nda3-KM311*
YSM111	*h- smt0 RuraR leu-32 urg1_NR::rtf1:eGFP:DSR rtf1::natMX6 nda3-KM311*
YSM112	*h- smt0 RuraR leu-32 urg1_NR::rtf1:eGFP:DSR rtf1::natMX6 nda3-KM311*
YSM113	*h- smt0 RuraR leu-32 urg1_NR::rtf1:eGFP:DSR rtf1::natMX6 nda3-KM311*
YSM114	*h- smt0 RuraR leu-32 urg1_NR::rtf1:eGFP:DSR rtf1::natMX6 nda3-KM311*
YSM115	*h- smt0 RuraR leu-32 urg1_NR::rtf1:DSR rtf1::natMX6 nda3-KM311*
YSM116	*h- smt0 RuraR leu-32 urg1_NR::rtf1:DSR rtf1::natMX6 nda3-KM311*
YSM117	*h- smt0 RuraR leu-32 urg1_NR::rtf1:DSR rtf1::natMX6 nda3-KM311*
YSM118	*h- smt0 RuraR leu-32 urg1_NR::rtf1:DSR rtf1::natMX6 nda3-KM311*
YSM119	*h- smt0 RuraR leu-32 urg1_NR::rtf1:DSR rtf1::natMX6 nda3-KM311*
YSM120	*h- smt0 RuraR leu-32 urg1_NR::rtf1:DSR rtf1::natMX6 nda3-KM311*
YSM121	*h- smt0 RuraR leu-32 urg1_NR::rtf1:DSR rtf1::natMX6 nda3-KM311*

YSM126	*h- smt0 A_P(2400)_A leu-32 urg1_NR::HPH rtf1::natMX6 nda3-KM311*
YSM127	*h- smt0 A_P(1214)_A leu-32 urg1_NR::HPH rtf1::natMX6 nda3-KM311*
YSM128	*h- smt0 A_P(0)noIR_A leu-32 urg1_NR::HPH rtf1::natMX6 nda3-KM311*
YSM129	*h- smt0 RuiuR leu-32 ade6-704 urg1_NR::rtf1:DSR rtf1::natMX6 Chk1-3HA nda3-KM311*
YSM130	*h- smt0 RuiuR leu-32 ade6-704 urg1_NR::rtf1:DSR rtf1::natMX6 Chk1-3HA nda3-KM311*
YSM131	*h- smt0 RuiuR leu-32 ade6-704 urg1_NR::rtf1:DSR rtf1::natMX6 Chk1-3HA nda3-KM311*
YSM132	*h- smt0 RuiuR leu-32 ade6-704 urg1_NR::rtf1:DSR rtf1::natMX6 Chk1-3HA nda3-KM311*
YSM133	*h- smt0 RuiuR leu-32 ade6-704 urg1_NR::rtf1:DSR rtf1::natMX6 Chk1-3HA nda3-KM311*
YSM134	*h- smt0 RuiuR leu-32 ade6-704 urg1_NR::rtf1:DSR rtf1::natMX6 Chk1-3HA nda3-KM311*
YSM141	*h- smt0 A_P(2400)_A leu-32 urg1_NR::rtf1:DSR rtf1::natMX6 nda3-KM311*
YSM142	*h- smt0 A_P(2400)_A leu-32 urg1_NR::rtf1:DSR rtf1::natMX6 nda3-KM311*
YSM143	*h- smt0 A_P(2400)_A leu-32 urg1_NR::rtf1:DSR rtf1::natMX6 nda3-KM311*
YSM144	*h- smt0 A_P(2400)_A leu-32 urg1_NR::rtf1:DSR rtf1::natMX6 nda3-KM311*
YSM145	*h- smt0 A_P(2400)_A leu-32 urg1_NR::rtf1:DSR rtf1::natMX6 nda3-KM311*

YSM146	*h- smt0 A_P(2400)_A leu-32 urg1_NR::rtf1:DSR rtf1::natMX6 nda3-KM311*
YSM147	*h- smt0 A_P(1214)_A leu-32 urg1_NR::rtf1:DSR rtf1::natMX6 nda3-KM311*
YSM148	*h- smt0 A_P(1214)_A leu-32 urg1_NR::rtf1:DSR rtf1::natMX6 nda3-KM311*
YSM149	*h- smt0 A_P(1214)_A leu-32 urg1_NR::rtf1:DSR rtf1::natMX6 nda3-KM311*
YSM150	*h- smt0 A_P(1214)_A leu-32 urg1_NR::rtf1:DSR rtf1::natMX6 nda3-KM311*
YSM151	*h- smt0 A_P(1214)_A leu-32 urg1_NR::rtf1:DSR rtf1::natMX6 nda3-KM311*
YSM152	*h- smt0 A_P(1214)_A leu-32 urg1_NR::rtf1:DSR rtf1::natMX6 nda3-KM311*
YSM153	*h- smt0 A_P(0)noIR_A leu-32 urg1_NR::rtf1:DSR rtf1::natMX6 nda3-KM311*
YSM154	*h- smt0 A_P(0)noIR_A leu-32 urg1_NR::rtf1:DSR rtf1::natMX6 nda3-KM311*
YSM155	*h- smt0 A_P(0)noIR_A leu-32 urg1_NR::rtf1:DSR rtf1::natMX6 nda3-KM311*
YSM156	*h- smt0 A_P(0)noIR_A leu-32 urg1_NR::rtf1:DSR rtf1::natMX6 nda3-KM311*
YSM157	*h- smt0 A_P(0)noIR_A leu-32 urg1_NR::rtf1:DSR rtf1::natMX6 nda3-KM311*
YSM158	*h- smt0 A_P(0)noIR_A leu-32 urg1_NR::rtf1:DSR rtf1::natMX6 nda3-*

	KM311
YKM812	*h^+ RuiuR rtf1::natMX6 urg1::P_{urg1}:1×CrypticStrart:$rtf1^+$:eGFP cdc25.22*
YKM813	*h^+ RuiuR rtf1::natMX6 urg1::P_{urg1}:1×CrypticStrart:$rtf1^+$:eGFP nda3-KM311 leu1-32*
YKM814	*h^+ RuiuR rtf1::natMX6 urg1::P_{urg1_NR}:1×CrypticStrartStop:$rtf1^+$:eGFP nda3-KM311 leu1-32*
YKM815	*h^+ RuiuR rtf1::natMX6 urg1::P_{urg1_NR}:1×CrypticStrartStop:$rtf1^+$:eGFP nda3-KM311*
YKM816	*h^- smt0 RuiuR rtf1::natMX6 urg1::P_{urg1_NR}:1×CrypticStrartStop:$rtf1^+$:eGFP nda3-KM311*
YKM865	*h^- smt0 RuiuR rtf1::natMX6 urg1::P_{urg1}:2×CrypticStrartStop:$rtf1^+$:eGFP leu1-32 nda3-KM311*
YKM866	*h^+ RuiuR rtf1::natMX6 urg1::P_{urg1}:2×CrypticStrartStop:$rtf1^+$:eGFP leu1-32 nda3-KM311*
YKM872	*h^- smt0 RuiuR rtf1::natMX6 urg1::P_{urg1}:2×CrypticStrartStop:$rtf1^+$:eGFP cdc25.22*
YKM873	*h^- smt0 RuiuR rtf1::natMX6 urg1::P_{urg1}:2×CrypticStrartStop:$rtf1^+$:eGFP cdc25.22*
YKM874	*h^- smt0 RuiuR rtf1::natMX6 urg1::P_{urg1}:2×CrypticStrartStop:$rtf1^+$:eGFP cdc25.22*
YKM875	*h^- smt0 RuiuR rtf1::natMX6 urg1::P_{urg1}:2×CrypticStrartStop:$rtf1^+$:eGFP cdc25.22*

2.4 – *S. POMBE* TECHNIQUES

2.4.1 – RANDOM SPORE ANALYSIS OF *S. POMBE* CROSSES

To cross the strains, freshly grown cells of appropriate strains were mixed together on ELN plates and incubated at appropriate temperature (based on the cross) for two to three days. The ascus formation was monitored under the microscope and a full loop of cells was resuspended in 1ml of water containing 1µl/ml Helix Pomatia Juice (BioSepra #213472). The mixture was incubated over night at room temperature. ~500 spores were then plated on YEA plates.

2.4.2 – YEAST TRANSFORMATION

Cells were grown in YE over night to a density of 5×10^6/ml. 2×10^8 cells were collected for each transformation and washed in 50ml water. Cells were then washed in 5ml of LiAc-TE (0.1M lithium acetate [*pH* 7.5], 10mM Tris-HCl [*pH* 7.5], 1mM EDTA). Cells were resuspended in LiAc-TE at 2×10^9 cells/ml. 10µl of DNA or 1µl plasmid DNA and 2µl of salmon sperm DNA were added to 100µl of the cell suspension. Mixture was incubated for 10 minutes at room temperature. 260µl of 40% PEG/LiAc-TE (PEG4000 was dissolved in LiAc-TE) was added to the mixture. Cells were incubated for 30-60 at 30°C then 43µl of DMSO was added. Cells were heat-shocked at 42°C for 5 minutes and then washed in 1ml of sterile water. Samples were resuspended in 100µl of sterile water and plated onto appropriate selection plates.

2.4.3 – RECOMBINATION MEDIATED CASSETTE EXCHANGE

The appropriate PAW8 plasmid was transformed into the desired *S. pombe* base strain constructed as described in Watson *et al.* (2008). Trasformant were selected for (leu^+ cells). Transformants were then grown in EMM2 containing leucine (so that cells lose the plasmid) and other necessary supplements. About 500 cells were then plated onto minimal plates containing leucine and other necessary supplements. The resulting colonies were then replica plated onto –leu plates to check for the absence of the plasmid and YEA plates containing the appropriate antibiotic selection to check for the loss of the antibiotic resistance gene in the base strain hence the success of the cassette exchange

2.4.4 – GENOMIC DNA EXTRACTION

Cells were grown in 50ml YE to an OD of 1.0 and were resuspended in 1ml of SP1 buffer (1.2M sorbitol, 50mM citric acid, 50mM Na2HPO4, 40mM EDTA [*pH* 5.6]) containing 1mg/ml Lyticase. Cells were incubated at 37°C until the cell wall was digested (10-30 minutes). Cells were spun at 3000rpm and the pellet was resuspended in 450µl of 5× TE (0.05M Tris-HCl, 0.005M EDTA [*pH* 7.5]). 50µl of 10% SDS was added and the mixture was incubated for 5 minutes at room temperature. 150µl of 5M KAc was added and samples were incubated on ice for 10 minutes. Samples were spun at 13000rpm for 10 minutes and the supernatant was transferred to a fresh tube. 1 volume isopropanol was added to the supernatant and the mixture was spun at 14000 for 10 minutes at 4°C. The supernatant was aspirated and the pellet was washed with 0.5ml of 70% ethanol. The mixture was spun and the pellet was resuspended in 250µl of 5x

TE. 10µl of 10mg/ml RNase in 5× TE was added and samples were incubated for 20 minutes at 37°C. 4µl of 10% SDS and 20µl of 10m5/ml proteinase K were added to the mixture and samples were incubated at 55°C for an hour. For DNA extraction 500µl chloroform: isoamyl alchohol was added, samples were spun at 13000rpm for 5 minutes at room temperature, and the upper phase was transferred to a new tube. This step was repeated once more. Then 1/10 volume 3M sodium acetate and 1 volume isopropanol was added and samples were incubated on ice for 10 minutes. Samples were then spun at 14000rpm for 15 minutes at 4°C and washed twice with 500µl of 70% ethanol. The pellet was then resuspended in 100µl of 1× TE.

2.4.5 – PREPARATION OF AGAROSE-EMBEDDED DNA

Cells were grown to mid-log-phase and 1.5×10^8 cells were harvested and treated with 1% volume sodium azide and 10% volume 0.5M EDTA [*pH* 8] and kept on ice for ten minutes. Cells were then spun at 3.5k rpm and washed with 50ml of sterile water. Samples were then resuspended in 1ml of CSE buffer (20mM citrate/phosphate [*pH* 5.6], 40mM EDTA, 1.2M sorbitol). 250µl of 3000unit/ml lyticase solution in CSE was added to samples which were then incubated at 37°C for 10-30 minutes. Once samples were digested, they were spun at 1000g and resuspended in 150µl of TSE buffer (10mM Tris-HCl [*pH* 7.5], 45mM EDTA, 0.9M sorbitol). Samples were incubated at 37°C for three minutes. 200µl of pre-warmed 0.8% agarose (Lonza InCert® Agarose) in TSE was added to samples and then the samples were loaded into plug molds. The plug molds were incubated on ice for 5 minutes. Then the agarose plugs were extruded into 5ml of lysis buffer 1 (50mM Tris-HCl [*pH* 7.5], 250mM EDTA, 1% SDS) and incubated at 50°C for 90 minutes. Then the agarose plugs were removed into lysis

buffer 2 (1% lauryl sarcosine, 500mM EDTA [*pH* 9.5]), 125µl of 20mg/ml proteinase K was added, and samples were incubated at 55°C for 24 hours. Then another 125µl of 20mg/ml proteinase K was added and samples were incubates at 55°C for 24 hours. Samples were stored at 4°C.

2.4.6 – DIGESTION OF AGAROSE-EMBEDDED DNA

1/3 of DNA plugs were washed with ice-cold TE for 30 minutes. This was repeated twice more. Samples were then incubated on ice in 1ml of appropriate digestion buffer. After removal of the buffer, 400µl of the buffer and 100 units of the appropriate enzyme were added and samples were incubated at 37°C for four hours.

2.4.7 – ELECTROPHORESIS OF DIGESTED AGAROSE-EMBEDDED DNA

A solution of agarose in 1× TBE of appropriate concentration was prepared and kept at 55°C for 30 mins. Meanwhile, the digested agarose-embedded DNA was washed three times in 1× TBE for 10 minutes. The agarose plugs were then placed on a come and fixed on the come using few drops of melted agarose. In the cold room, melted agarose was poured in a tray and the comb (containing the agarose plugs) was carefully placed on the tray. The agarose was left to set for 30 minutes. The gel was then run at 50V for appropriate length of time (depending on the size of the fragment to be analysed) at room temperature. The samples were then transferred onto a nylon membrane.

2.4.8 – PULSED-FIELD GEL ELECTROPHORESIS (PFGE)

0.8% agarose (Biorad Certified Megabase Agarose) was melted in 1× TAE buffer and kept at 55°C. Half of a DNA plug was equilibrated three times with 1× TAE for 10 minutes. The agarose plugs were then placed on a come and fixed on the come using few drops of melted agarose. The melted agarose was poured in the appropriate gel tray and the come was placed. Once the gel was set, it was placed on the Biorad CHEF-DRIII tank and run using below settings:

Cooling module	14°C
Power supply [Biorad CHEF-DRIII]	
Initial switch time	1.8t (1800 seconds)
Final switch time	1.8t (1800 seconds)
Run Time	48 hours
Angle	100 degrees
Voltage	2 V/cm

2.4.9 – TWO DIMENSIONAL DNA GEL ELECTROPHORESIS (2DGE)

Cells were grown to mid-log-phase and 1.25×10^9 cells were harvested and treated with 1% volume sodium azide and 10% volume 0.5M EDTA [*pH* 8] and kept on ice. Cell were pelleted and washed with 20ml of ice-cold water and transferred into a 50ml falcon tube. Cells were pelleted at 3.5K rpm at 4°C for three minutes and the supernatant was completely removed. Liquid nitrogen was used to snap freeze the samples. The frozen sample was thawed on ice and resuspended in 2.5ml of CSE (20mM Citrate/Phosphate [*pH* 5.6], 40mM EDTA, 1.2M Sorbitol). 500µl of

300units/ml lyticase in CSE was added to the samples. The cell suspension was incubed at 37°C for 10-15 minutes. Samples were transferred on ice and pelleted at 1000g at 4°C. The supernatant was aspirated and the pellet was resuspended in 300µl of CSE. The suspension was incubated at 37°C for three minutes. 400µl of pre-warmed 1% agarose in CSE was mixed with each sample. The mixture was then loaded into a plug mould. The plug molds were then incubated on ice for 10 minutes. The DNA plugs were then extruded into 10ml of PK buffer (1% lauryl sarcosine, 25mM EDTA [*pH* 8]) containing 0.5ml of 20mg/ml Proteinase K solution and incubated at 50°C for 30 minutes. This step was repeated twice more after removal of the old PK buffer each time. The buffer was then removed. Another 10ml of buffer PK containing 0.5 ml of 20mg/ml Proteinase K was added and the samples were incubated at 50°C over night. Five plugs per sample were incubated in 50ml of ice-cold 50× TE (10mM Tris-HCl [*pH* 7.5], 50mM EDTA) for three hours. The buffer was then changed for fresh ice-cold 50× TE and samples were incubated at 4°C over night. The plugs were then washed three times in 50ml of ice-cold 1× TE (10mM Tris-HCl [*pH* 7.5], 1mM EDTA). Plugs were transferred into 2ml test tubes and incubated with 1ml of 2× appropriate NEB digestion buffer for 30 minutes on ice. The buffer was then changed to 1ml of 1× NEB buffer and samples were incubated another 30 minutes on ice. The buffer was then replaced with 0.4ml of fresh 1× NEB buffer and 100 units of the desired restriction enzyme were added to the tube. The samples were incubated at 37°C for two hours. Samples were incubated at 70°C for 10 minutes and then at 37°C for five minutes. Another 100 units of the restriction enzyme was added and samples were incubated at 37°C for one hour. 10µl of 10mg/ml RNAse and 10µl of beta-Agarase I were added and the samples were incubated at 37°C for one hour. Samples were then spun at 13K rpm at 4°C for one minute. The supernatant was collected and 90µl of 3M sodium acetate and 1ml of

isopropanol were added. Samples were kept at 4°C overnight. Samples were pelleted and washed with ice-cold 70% ethanol. Pellets were dried at room temperature for 10 minutes and then resuspended in 20µl of TE. 5µl of 20× loading dye (0.83% Bromophenol Blue, 0.83% Xylene Cyanol FF, 50% Glycerol) was added and samples were loaded on an agarose gel prepared with 0.35% agarose in 1× TBE. The gel was run at 50V for an appropriate length of time depending on the size of the DNA fragment to be analyzed. The gel was then stained using 22.5µl of ethidium bromide in 750ml of the used running buffer. The first dimension run was then cut out of the gel and placed in the second dimension gel tray. Pre-melted 0.9% agarose in 1× TBE containing 10.5µl of 10mg/ml ethidium bromide was then poured and incubated at 4°C until the gel was set. The gel was then run at 200V in 2l of 1× TBE containg 70µl of 10mg/ml ethidium bromide. The DNA was then transferred onto a nylon membrane by capillary transfer (see Southern blot section) and stored at 4°C.

2.4.10 – SOUTHERN BLOT

The genomic DNA was then digested using the appropriate enzyme. To do this, the appropriate amount of each sample was digested in 5% volume of the appropriate digestion enzyme and 10% volume appropriate 10x enzyme buffer at 37°C for 60 minutes. The samples were then run on a long agarose gel of appropriate concentration (depending on the size of the fragment) in 1× TBE at 50V.

The gel was then incubated for 20 minutes in depurinating solution (0.25M HCl) in a shaker. Then the gel was washed in denaturing solution (1.5M NaCl and 0.5M NaOH) for 30 minutes on a shaker. Then gel was washed in neutralizing solution (1M Tris and 1.5M NaCl). The gel was then transferred to a membrane employing 10× SSC buffer

(1.5M NaCl, 0.15M sodium citrate [*pH* 7]) and capillarity force over night. The membrane was then washed in 2× SSC buffer for 5 minutes on a shaker. The membrane was air dried on a piece of filter paper and then the DNA was cross-linked to the membrane using UV light at 1200J/m2. The membrane was stored at 4°C.

For Hybridising probe to the membrane, first the membrane was washed in dH2O for 5 minutes. Then 80ml of preheated 65°C hybridising solution I (6× SSC, 1x Denhardt [100x: 2% Ficoll 400, 300mM NaCl, 2% polyvinylpyrrolidone, 2% BSA], 1% sarcosyl, 0.1% BSA) was added to the hydrated membrane in a tube. The tube then was placed in hybridising oven for one hour at 65°C. Meanwhile, 1µl of 50ng/µl probe was added to 44µl dH2O. The solution was boiled in a water bath for 5 minutes and then placed on ice. In the radioactivity room, the labelling mix and 5µl of 35P-αdCTP were added to the DNA and the mixture was incubated at 37°C for 15 minutes. The labeled probe was then spun in a pre-spun G50 column at 3000rpm for 1 minute and incubated at 100°C for 5 minutes. Then the mixture was kept on ice. Then the probe was added to 20ml preheated 65°C hybridising solution II (6× SSC, 1x Denhardt, 1% sarcosyl, 200µl 10mg/ml salmon sperm DNA). Then hybridising solution I was replaced with hybridising solution II and the tube was put back in the oven at 65°C over night. Then the membrane was washed with 50ml preheated 65°C buffer I (2× SCC, 1% SDS) in the oven for 10 minutes and then with 450ml of buffer I on a shaker for 15 minutes. In the following step the membrane was washed twice, each time with 500ml of 42°C buffer II (0.1× SSC, 0.1% SDS) on a shaker for 15 minutes. The membrane was then air dried on tissue and wrapped in cling film and placed in a phosphoimager cassette over night. The membrane was scanned to obtain the Southern blotting results.

2.4.11 – TCA WHOLE CELL PROTEIN EXTRACTION

5×10^7 cells of logarithmically growing cells were pelleted and washed with 50ml of dH_2O. Cells were then resuspended in 200µl of 20% trichloroacetic acid (TCA) solution. Acid washed glass beads were added to the samples. Cells were lysed using a ryboliser (FastPrep24, MP) at 6.5 m/s for 30 seconds. This step was repeated 2-3 times. The samples were then collected by puncturing the tubes and centrifugation into new tubes. Samples were pelleted at 14K at 4°C for 10 minutes and the supernatant was removed. Samples were resuspended in 200µl of 1× TCA sample buffer, boiled for five minutes, and stored at -20°C.

1× TCA Sample Buffer:

1 volume	4× SDS sample buffer
1 volume	1 M Tris, pH 8
2 volume	dH2O
2.5%	β-mercaptoethanol

4× SDS Sample Buffer

250mM	Tris-base [*pH* 6.8]
20%	Glycerol
0.004 g/ml (w/v)	Bromphenol blue
0.08 g/ml (w/v)	SDS

2.4.12 – WESTERN BLOT

Appropriate amounts of resolving and stacking polyacrylamide (ProtoGel 30%, 37.5:1 Acrylamide to Bisacrylamide) solutions were made as described in Sambrook *et al.* (1989) and gels were prepared. Samples were run through the stacking gel at 80V and through the resolving gel at 100V using 1x running buffer (0.025M Tris base, 0.25M Glycine, 0.1% SDS). Samples were then transferred onto a nitrocellulose membrane in transfer buffer (20mM Tris, 20% Methanol, 750mM Glycine) at room temperature for 90 minutes. The membrane was then blocked using 3% milk solution (Marvel dried skimmed milk in PBS (Phosphate buffered saline)) at 4°C over night. The appropriate dilution of the primary antibody was added to PBS solution contacting 3% milk and 0.1% Tween20. The membrane was incubated at room temperature for one hour. The membrane was washed 3x in 0.1% Tween20 in PBS for ten minutes. The appropriate dilution of the secondary antibody was added to membrane submerged in PBS containing 3% milk and 0.1% Tween20 and incubated for one hour at room temperature. The membrane was washed 3× in 0.1% Tween20 in PBS for ten minutes. The membrane was then dried using a paper tissue. ECL plus western blot detection reagents were added to the membrane and the reaction was detected using an X-ray film in the dark room. The film was developed with a Xograph Imaging Systems Compact X4.

2.4.13 – WESTERN BLOT USING PHOS-TAG

To detect the Cds1 phosphoshift, Phos-tag was used in the gel mixture as described below:

7.5% resolving gel mix was prepared containing final concentration of 20μM Phostag, and 40μmM $MnCl_2$. Stacking gel was prepared as described in previous section. The gel was run at 15mA. Wet-transfer onto a cellulose membrane was performed at 300mA for two hours. The membrane was blocked using 3% milk in PBS, 0.1% tween mixture for one hour at room temperature. The membrane was incubated in 0.5% milk in PBS containing 1:2000 dilution of the Cds1-antibody at room temperature over night. The membrane was washed three times in PBS solution containing 1% tween for 20 minutes. The membrane was incubated in 1:2500 dilution of the secondary antibody in 0.5% milk in PBS solution for one hour. The membrane was then washed another three times in PBS solution containing 1% tween for 20 minutes. ECL plus western blot detection reagents were added to the membrane and the reaction was detected using an X-ray film in the dark room. The film was developed with a Xograph Imaging Systems Compact X4.

Table 2.3 | Antibodies used in this study

Antibody	**Type**	**Supplier**	Dilution
Anti-HA	Mouse monoclonal	Santa Cruz, F7 sc- 7392	1:5000
Anti-Cdc2	Rabbit monoclonal	Santa Cruz, sc-53	1:5000
Anti-H2A(pS129)	Rabbit ploYclonal	Abcam, ab17353	1:5000
Anti-Cds1	Rabbit polyclonal	Provided by Y. Daikagou	1:2000
Rabbit anti-mouse HRP	Rabbit polyclonal	Dakocytomation, P0260	1:2500
Swine anti-rabbit HRP	Rabbit polyclonal	Dakocytomation, P0217	1:2500

2.4.14 – FACS ANALYSIS

5ml of cells of density of 1×10^7 were added to 500µl of pre-chilled 200mM EDTA [*pH* 8]and 50µl of 10% sodium azide was added to samples. Samples were spun at 3K rpm for three minutes. Cells were resuspended in 1ml of dH2O and spun at 13K for one minute. Samples were then resuspended in 1ml of 70% ethanol and stored at 4°C. 500µl of each sample was then spun at 13K for one minute. Samples were then washed with 500µl of 50mM sodium citrate [*pH* 7] and resuspended in 500µl of sodium citrate. 50µl of 10mg/ml RNAse was added and samples were incubated at 37°C for three hours. 10µl of 500µg/ml propidium iodide was added to FACS tubes and 200µl of each sample was added. 1ml of FACS buffer was added to each sample which was then vortexed and applied to the FACS machine.

2.5 – *E. COLI* TECHNIQUES

2.5.1 – DH5α COMPETENT *E. COLI* TRANSFORMATION

Cells were thawed on ice for 20 minutes. 100ng of DNA was added to 100µl aliquot of DH5α cells. Samples were then incubated on ice for 20 minutes. Cells were heat-shocked at 42°C for 30 seconds. Then 1ml of LB was added to the cells and samples were incubated at 37°C for an hour shaking at 250rpm. The cells were pelleted at 5500rpm for 1 minute and plated on LB agar containing the appropriate antibiotic.

2.5.2 – PLASMID MAXIPREPS AND MINIPREPS

For maxipreps and minipreps cells were grown at 37°C over night in 100ml or 10ml of LB containing the appropriate antibody respectively. Cells then were harvested by centrifugation at 6000rpm for 5 minutes at 4°C. The DNA was then extracted following QIAGEN maxi and mini plasmid purification handbook. The concentration of the plasmid obtained was then measured against a marker and samples were stored at -20°C.

2.6 – GENERAL TECHNIQUES

2.6.1 – ETHANOL PRECIPITATION

2.5 volume of 100% ethanol and 1/10 volume of 3M NaOAc were added to the DNA samples and the mixture was vortexed and placed on ice for 10 minutes. Samples were then centrifuged at 14000rpm for 15 minutes. The supernatant was aspirated and the samples were washed twice using 0.5ml 70% ethanol (centrifuged at 14000rpm for 5 minutes). The pellet was then air dried and then resuspended in the appropriate volume of 1× TE.

2.6.2 – DNA ELECTROPHORESIS

Gels were poured at 0.8% agarose in 0.5x TE containing 0.5µg/mg ethidium bromide. Samples were mixed with loading dye and were loaded on the gel. The gel was run in 0.5× TE for 45 minutes at 100V. The DNA was then visualised under UV light.

2.6.3 – DNA GEL PURIFICATION

Samples were loaded on 8% low melting point agarose (Invitrogen # 16520**)** in 0.5× TE gel. The gel was run and then was visualized in exposure to 350nm UV light. The appropriate band was cut out and the DNA was extracted following Qiagen gel extraction protocol.

2.6.4 – RESTRICTION ENZYME DIGEST

To carry out the digestions, 5% volume of desired restriction enzyme and 10% volume of the appropriate 10× restriction enzyme buffer were added to the DNA sample. The mixture then was incubated at 37°C for 30-60 minutes. The success of the digestion was then checked by running the sample on a gel.

2.6.5 – DNA LIGATION

To set up DNA ligation mixtures, DNA concentrations of the insert and vector was measured using NanoDrop™ 1000.

A three to one ratio of insert ends to vector ends were (50-100ng of vector DNA depending on the size) added to below general reaction mixture to make a final volume of 10µl. T4 DNA ligase (NEB #M0202S) was used for ligation reactions.

10× T4 Buffer:	1µl
ATP:	1µl
DTT:	1µl
T4 Ligase:	1µl

2.6.6 – REMOVAL OF THE 3' OVERHANGS FROM DNA ENDS

T4 DNA polymerase (NEB #M0203S) was used to remove the 3' overhangs from the ends of DNA and form blunt ends. 1 unit of T4 DNA polymerase per each microgram of DNA was added to DNA solution in 1× NEB buffer II and presence of dNTPs. Samples were then incubated at 12°C for 15 minutes. To stop the reaction, excess of EDTA (>10mM) was added and samples were incubated at 75°C for 20 minutes.

2.6.7 – REMOVAL OF THE 5' PHOSPHATE GROUP FROM DNA ENDS

Antarctic Phosphatase (NEB #M0289S) was used to remove the 5'-P group from DNA ends. To do this, 10% volume Antarctic Phosphatase buffer and 5% volume Antarctic Phosphatase were added and samples were incubated at 37°C for 30-60 minutes. The reaction was then stopped by incubating the samples at 65°C for 10 minutes.

CHAPTER 3 – OPTIMISATION OF FORK STALLING INDUCTION AND CELL CYCLE SYNCHRONISATION

3.1 – INTRODUCTION

Replication fork stalling at inverted repeats of the replication termination site, *RTS1*, placed in an inverted orientation at a unique locus in the fission yeast genome induces HR-dependent generation of GCRs and the accumulation of dicentric and acentric chromosomes (Lambert *et al.*, 2005; Lambert *et al.*, 2010; Mizuno *et al.*, 2009; Mizuno *et al.*, 2013). Replication stalling is dependent on Rtf1, which binds *RTS1* and in these studies Rtf1 expression was under the control of the thiamine repressible *nmt* promoter, which takes 16 hours to fully induce (Basi *et al.*, 1993). Since the *S. pombe* cell cycle is completed within two to three hours, it can be estimated that the reported level of rearrangements in the previous studies was a steady state level accumulated over three generations (samples were analyzed after 24 hours of induction P_{nmt} to allow maximum induction levels of Rtf1, since Rf1 levels reach maximum within 16hrs of induction, it can be estimated that rearrangements accumulate over three generations (~8hrs)). The induction time of *nmt* promoter is a significant disadvantage when the aim is to investigate the timing of rearrangements in a single cell cycle considering the time required for the *nmt* induction and *S. pombe* cell cycle. Therefore an alternative method of rapidly inducing Rtf1 using the *urg1* promoter was optimized as described below.

Watt *et al.* (2008) characterized the promoter of the $urg1^+$ gene and showed that the transcript levels peak approximately 30 minutes after addition of uracil to medium.

Work in the Carr laboratory showed that while induction kinetics were not maintained if the *urg1* promoter was moved from its native locus, the replacement of the native *urg1* open reading frame (ORF) with ectopic ORFs results in similar induction kinetics of these ectopic ORFs to that of *urg1* (Watson *et al.*, 2011). This led to the development of a Cre recombinase and lox recombination based recombination-mediated cassette exchange (RMCE) system (Watson *et al.*, 2008) at the *urg1* locus to facilitate rapid exchange of ORFs at this locus (Watson *et al.*, 2011). This provided an inducible system enabling rapid induction of Rtf1 to initiate the fork stalling in a single cell cycle. The initial inducible system to regulate Rtf1 is shown in Figure 3.1 (adapted from Watson *et al.* (2011) and further optimization described in this chapter).

Synchronous cell cultures facilitate the biochemical assessment of the timing of the rearrangements and checkpoint responses to fork stalling. Fission yeast cells can be synchronized by making use of temperature sensitive cell cycle mutants, drugs, or selection based on cell size. While synchronizing by size selection (i.e. centrifugal elutriation, lactose gradients) remain the most physiological, centrifugal elutriation can only be carried out on a single strain at a time and lactose gradients do not yield adequate number of cells required for biochemical assessments. Use of temperature sensitive cell cycle mutants facilitates the side by side comparison of multiple strains. The *cdc25-22* allele arrests the cell cycle at G2-M boundary at temperatures above 35°C, and the *cdc10-M17* allele can be used to arrest the cell cycle in G1. However, temperatures above 35°C induce heat shock response in *S. pombe*, cells are very sick at 37°C and die at 38°C (Forsburg & Rhind, 2006).

Figure 3.1

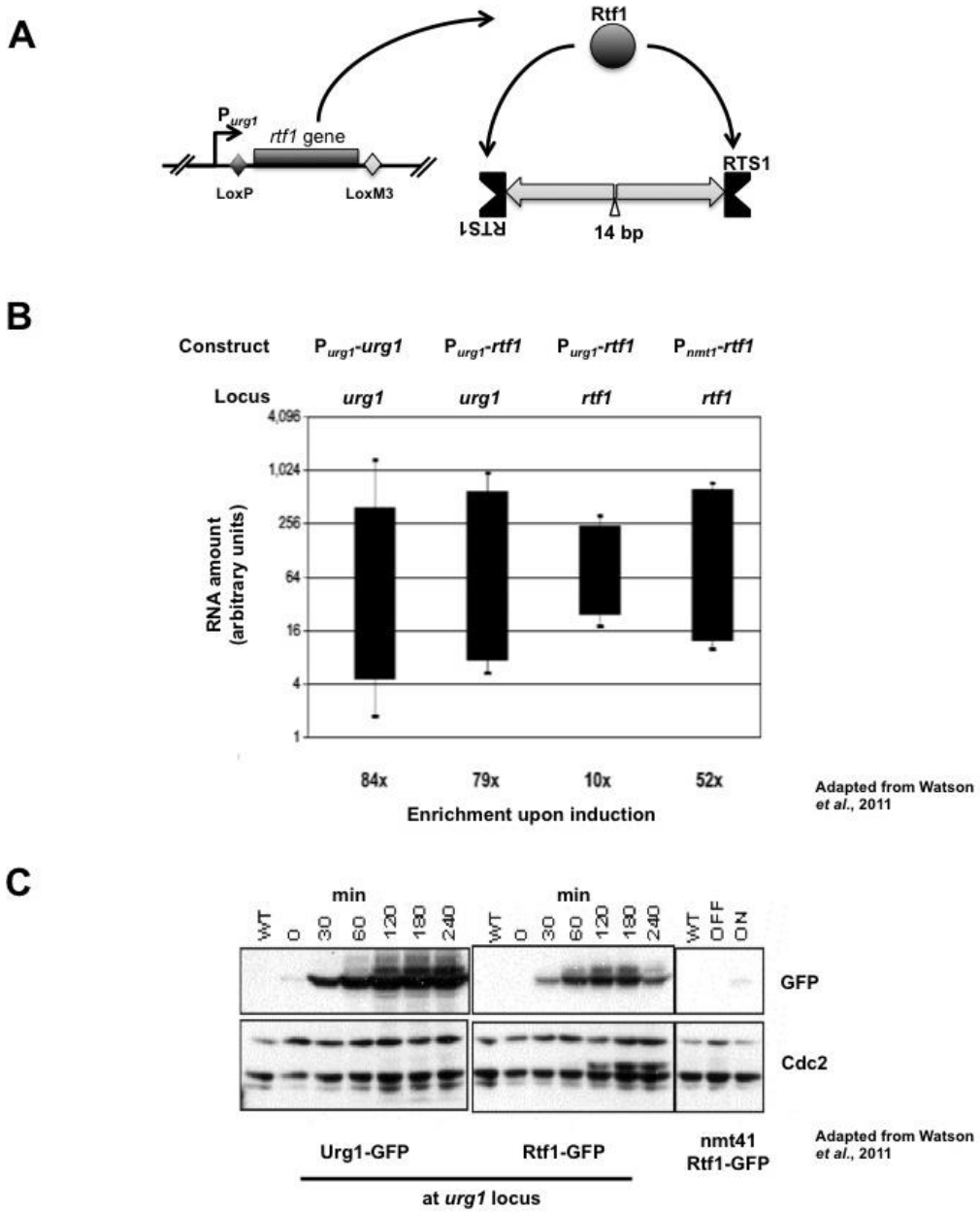

Figure 3.1 | Kinetics of P_{urg1} driven induction of Rtf1. A- Diagram showing the control of expression of Rtf1 from the *urg1* promoter and subsequent activation of fork stalling. **B-** mRNA levels of P_{urg1} driven expression of *urg1* and *rtf1* expressed from the *urg1* and *rtf1* loci upon addition of uracil to medium. **C-** Western blot showing Urg1, and Rtf1 protein levels after expression under the control of P_{urg1} at the *urg1* locus. Note that the levels of Rtf1 protein are much higher when expressed from the *urg1* locus compared to *nmt1* induction at the native locus, even though the mRNAs are expressed with a similar range. Please note that all data presented in this figure are provided by A. Watson.

The Yanagida laboratory first characterized the nuclear division arrest (*nda*) genes in a screen for cell division cycle mutants (Toda *et al.*, 1983; Umesono *et al.*, 1983), and subsequently showed that *nda3*$^{+}$ gene encodes β-tubulin (Hiraoka *et al.*, 1984). At restrictive temperatures (<20°C), *nda3-KM311* cells fail to form functional β-tubulin and the mitotic spindle, and uniformly arrest nuclear division in prometaphase with condensed chromosomes. However, this nuclear division arrest is highly reversible upon temperature shift to permissive temperatures (>30°C) and the mutant cells resume the rest of the mitosis synchronously (Hiraoka *et al.*, 1984). Nuclear division arrest in *nda3-KM311* is brought about by the action of the spindle assembly checkpoint (SAC), which prevents the initiation of anaphase until all the kinetochores are stably captured by the spindle. In the presence of unattached kinetochores the SAC is 'on' and anaphase is inhibited. This inhibition is alleviated and the SAC is satisfied once all the kinetochores are stably attached to microtubules (Nezi & Musacchio, 2009).

In this chapter I describe the development of a rapidly inducible fork stalling system in synchronous *S. pombe* cultures. This system was then used to characterize the kinetics of RF restart-dependent GCRs as detailed in subsequent chapters.

I therefore utilized a cold sensitive mutant, *nda3-KM311*, to arrest the cell cycle in mitosis. The other advantage of using *nda3-KM311* to synchronize cells is that, unlike *cdc25-22* and *cdc10-M17* mutants, the profile of the origin firing in the subsequent S phase is similar to that of an unperturbed S phase (Y. Daigaku, personal communication).

Figure 3.2

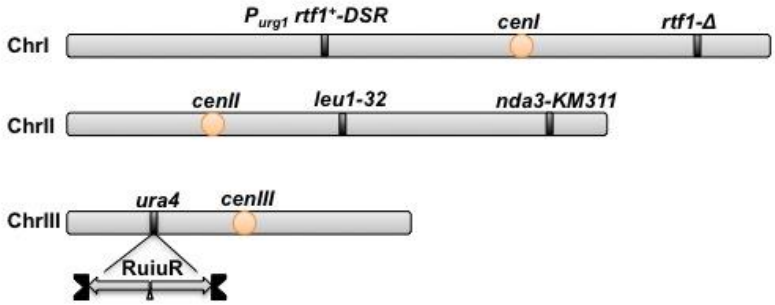

Figure 3.2 | Strains constructed for this study. Diagram showing the basic genetic make up of the strains used in this study. Please note that additional alleles were used in strains when appropriate (e.g. *chk1-3HA* to investigate the checkpoint response).

3.2 – REGULATION OF *NDA3-KM311* BLOCK AND RELEASE

Hiraoka *et al.* (1984) obtained the optimal synchrony using *nda3-KM311* to block cell cycle in prometaphase by shifting the temperature down to 20°C for ten hours, and shifting the temperature up to 36°C to release the cells from the cell cycle block. They also showed that cultures of densities higher that 5 x 10^6 cells ml^{-1} do not achieve the same efficiency of synchrony after the block and release (Hiraoka *et al.*, 1984). In order to reduce the time required to achieve good synchrony, a series experimental conditions were tested to identify the condition conferring an optimal synchronization.

Furthermore, to avoid the induction of a heat response, a releasing temperature of 30°C was chosen. The strain *h⁻ smt0 ade6-704 nda3-KM311* (nda3 control) was grown to early log-phase (3×10^6 cells ml^{-1}) and arrested at either 20°C or 16°C for four, five, or six hours. To release from the block, the temperature was shifted up to 30°C and cell cycle progression was monitored by septation index. To score cell cycle progression, cells were fixed in methanol at 15 minute intervals after release, stained with DAPI and Calcofluor to detect DNA and septum respectively, and scored based on having either, one nucleus (G2), two separated nuclei (mitotic), and two nuclei with septum (septated). Cells showing chromosome mis-segregation, chromosome bridges, or where the septum bisected the nucleus were scored as 'cut' phenotype (Figure 3.3). As discussed by Hiraoka *et al.* (1984), cells blocked at 20°C with blocking times under ten hours did not show desired synchrony (only data from a five-hour arrest are shown as an example, Figure 3.6 A). However, cells blocked at 16°C for six hours showed highly synchronous cell cycle progression with a septation peak of ~80% at 60 minutes after the release. In *S. pombe* S phase coincides with the formation of the septum (Figure 1.1). Extended analysis of the cell cycle progression after release of *nda3-*

KM311 cells blocked at 16°C for six hours showed the synchronous cell cycle progression with septation peaking at 60 minute in the first cell cycle and at 240 minute in the second (Figure 3.3B).

Figure 3.3 (following page) | *nda3-KM311* cells show synchronous cell cycle progression after block and release. A- Graphs showing the cell cycle progression of *nda3-KM311* cells arrested at different restrictive temperatures and released at 30^{o}C. To examine the optimal cell cycle synchrony conditions, cells of *h^{-} smt0 ade6-704 nda3-KM311* were grown to a concentration of 3x10^{6} cells ml^{-1} at 30^{o}C and arrested at either 16^{o}C or 20^{o}C. Cells were released from the block by temperature shift to 30^{o}C, and cell cycle progression was monitored by analysing septation index. DNA was stained with DAPI and calcofluor was used to visualize the septum. Mitotic cells are binucleate and S phase coincides with the formation of septum. Aberrant mitotic 'cut' cells show chromosome bridges and lagging chromosomes. Optimal cell cycle synchrony is achieved when cells are arrested at 16^{o}C for six hours (bottom left). Analysis of septation index shows a peak of septation of 80% under these conditions. **B-** Cell cycle progression of *nda3-KM311* after 6-hour block at 16^{o}C and release at 30^{o}C. The peak of first S phase takes place 60 minutes after the release and the second S phase at 240 minutes.

Figure 3.3

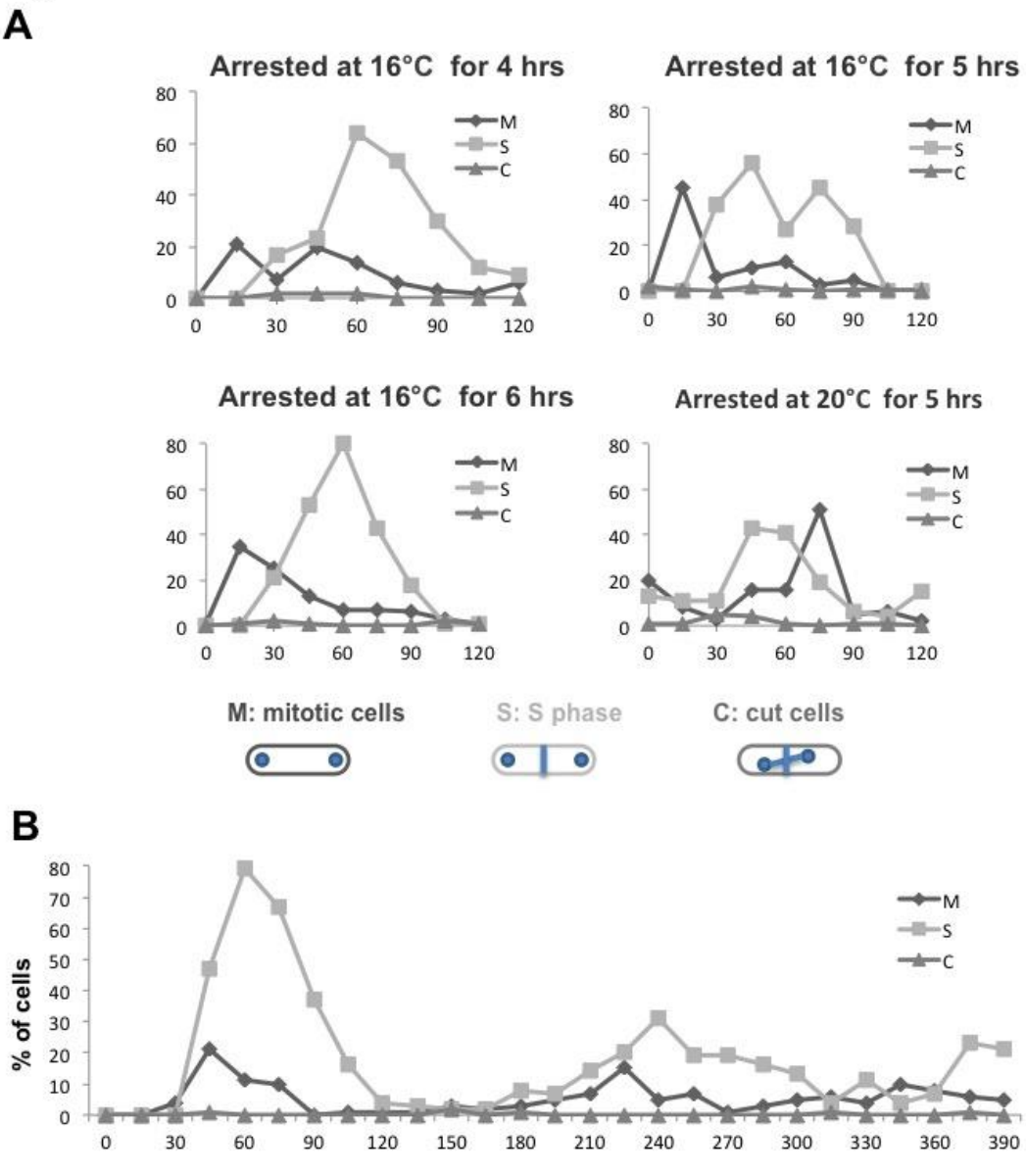
A
Arrested at 16°C for 4 hrs
Arrested at 16°C for 5 hrs
Arrested at 16°C for 6 hrs
Arrested at 20°C for 5 hrs
M
S
C
M: mitotic cells
S: S phase
C: cut cells
B
% of cells

3.3 – REGULATION OF P_{URG1} DRIVEN EXPRESSION OF RTF1

3.3.1 – CYPTIC START-STOP CODONS

Previous work in the Carr laboratory indicated that control of Rtf1 expression by the *urg1* promoter was somewhat leaky (Watson *et al.*, 2008). This resulted in the induction of fork stalling even in the 'Off' state. In an attempt to reduce the 'Off' state levels of rearrangements when using the *urg1* promoter to drive Rtf1 expression, mutations were made that introduced an AUG codon in the 5'-UTR of the mRNA to reduce the translational efficiency (Kozak, 2002), and strains containing either one or two cryptic start-stop (CSS) codons upstream of the Rtf1 ORF were created. The levels of rearrangements were assessed in a replication stall system where inverted *RTS1* stall sites flank inverted repeats of *ura4*$^+$ and form part of a palindrome (Figure 3.4A). This system, termed RuiuR, generates the maximum rearrangements, with 20% of cells dying after Rtf1 induction using the *nmt1* promoter (Mizuno *et al.*, 2009). The RuiuR strain was crossed into the *urg1* base strain (*h- smt0 ura4-D18 leu-32 urg1_NR::HPH rtf1::natMX6 nda3-KM311*) and the *rtf1* cassette with the cryptic start-stop codons integrated by recombination mediated cassette exchange (RMCE) (see Figure 3.2 for schematic of resulting strain). Restriction fragment length analysis was performed to determine the background level of rearrangements without induction. Cells were grown to mid-log phase and harvested. DNA was extracted in agarose plugs and restriction enzyme digestion carried out using *Bgl*II. DNA species were separated using gel electrophoresis and detected by Southern blot analysis.

Figure 3.4

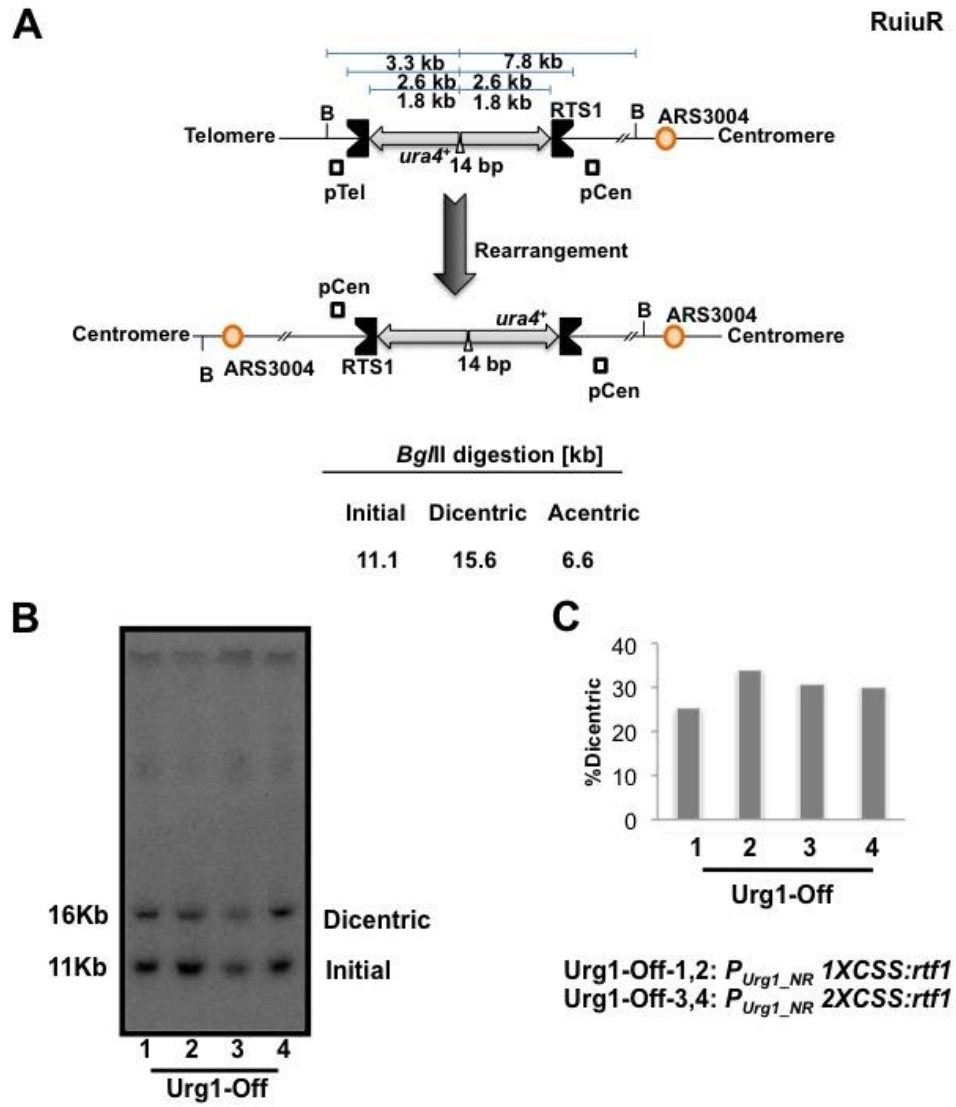

Figure 3.4 | Rearrangements in P_{urg1} 'Off' cultures. **A-** Diagram showing the *Bgl*II fragments and expected sizes before and after rearrangements at the RuiuR locus. Probe 'Cen' and 'Tel' detect the initial locus and dicentric and acentric fragments, respectively, after rearrangements. **B-** Representative Southern blot showing the rearrangement levels in two independent isolates of *RuiuR* P_{urg1_NR} *1XCSS:rtf1 nda3-KM311* or *RuiuR* P_{urg1_NR} *2XCSS:rtf1 nda3-KM311*when P_{urg1} is **NOT** induced. Genomic DNA was prepared in plugs and digested with *Bgl*II and restriction products were separated by gel electrophoresis. Probe Cen was used to detect the dicentric fragment. **C-** Quantification of the data in **B** shows 30±5% of the DNA in the rearranged form. For quantification of the dicentric signal, the average intensity of the dicentric band calculated by ImageQuant™ was calculated as a percentage of the total intensities of the dicentric and original signals.

In the absence of rearrangements a ~11kb 'original' band was detected, and after rearrangement a ~16kb dicentric band (Figure 3.4A), and a ~6kb acentric band are expected. Quantification of these bands provides a measure of the "Off" rates of expression. Probe Cen, homologous to sequences centromere proximal to RuiuR was used to detect the dicentric fragment in the Southern blots. Figure 3.4B and C shows the results of this experiment and the quantification of the Southern blot signals. Use of 5' UTR CSS sites did not result in any reduction in the 'Off' levels of Rtf1 (Figure 3.4). The background level of rearrangements was >20% in all *RuiuR* P_{urg1_NR} *1XCSS/2XCSS:rtf1 nda3-KM311* strains analyzed. This level of rearrangements at the 'Off' state was too high to be of use in further analysis.

3.3.2 – DESTABILISATION OF TRANSCRIPT USING DSR ELEMENTS

In an attempt to reduce the stability of the transcript I next tested the use of DSR elements. Harigaya *et al.* (2006) characterized a mechanism for selective removal of meiosis specific mRNAs in vegetatively growing *S. pombe* cells. In this process, the YTH domain protein Mmi1 directs meiosis specific transcripts, characterized by the presence of 3'-end determinant of selective removal (DSR) sequences, to nuclear exosomes for degradation. The 157bp DSR element of *spo5* was identified (Harigaya *et al.*, 2006) and it was shown that the DSR elements contain tandem repeats of U(U/C)AAAC motif (Chen *et al.*, 2011; Yamashita *et al.*, 2012). To reduce the 'Off' levels of Rtf1 expression the *spo5* DSR element was cloned into the 3'UTR of *rtf1* in the previously described PAW8E*Nde*I plasmid (Watson *et al.*, 2008) harboring GFP-tagged *rtf1:eGFP*. The resulting *rtf1:eGFP-DSR* was used to create the *RuiuR*

P_{urg1_NR}::rtf1:eGFP-DSR nda3-KM311 strain by RMCE. In parallel, to test the possible effects of the GFP tag on rates of Rtf1 stability and degradation, an untagged rtf1-DSR cassette was used to create *RuiuR P_{urg1_NR}::rtf1-DSR nda3-KM311*. Restriction fragment length analysis was utilized to examine the induced and background levels of rearrangements. Cells of the resulting strains were prepared in two rounds of liquid pre-cultures in EMM2 minimal medium lacking uracil and then grown to early log-phase. Uracil at 0.25mg/ml was added to induce the 'On' cultures and cells were harvested after 180 minutes (~one cell cycle in EMM2 minimal medium). DNA was extracted in agarose plugs and digested with *Bgl*II. DNA gel electrophoresis was performed and dicentric fragments were detected using probe Cen in Southern blots (Figure 3.5). DNA samples extracted from the original *RuiuR nmt41::rtf1* strain (described in Mizuno *et al.* (2009)) were used as controls. The cells of both *RuiuR P_{urg1_NR}::rtf1:eGFP-DSR* (Figure 3.5A) and *RuiuR P_{urg1_NR}::rtf1-DSR* (Figure 3.5B) showed significant reductions in the background levels of rearrangements (0.4%-1%) in the 'Off' state, and the levels of rearrangements were comparable to that of *RuiuR P_{nmt41}::rtf1* cells when the *nmt* promoter was repressed. Induction of the *urg1* promoter resulted in a 5-10% accumulation of dicentrics after three hours in both *RuiuR P_{urg1_NR}::rtf1:eGFP-DSR* Figure 3.5A) and *RuiuR P_{urg1_NR}::rtf1-DSR* cultures (Figure 3.5B). This showed that the GFP tag did not affect the Rtf1 protein levels in either of the induced or un-induced situations. These data show that utilizing DSR elements to regulate *urg1* promoter transcripts, results in a reduction of protein levels in both induced and un-induced states. This was published (Watson AT, Daigaku Y, Mohebi S, Etheridge TJ, Chahwan C, Murray JM, Carr AM. PlosOne, 2013).

Figure 3.5 (following page) | DSR element reduces Rtf1-dependent chromosomal rearrangements. A- Induction of Rtf1 using *urg1* promoter in the RuiuR system results in the formation of dicentric chromosomes. Lanes labelled as 'nmt rtf1' are the original *nmt41* driven *rtf1 RuiuR* strains used as controls. urg1 rtf1-GFP-DSR 1-7 are seven independent isolates of *h- smt0 RuiuR leu-32* P_{urg1_NR}*::rtf1:eGFP-DSR rtf1::natMX6 nda3-KM311*. ON is 3hrs after the addition of uracil to induce *Purg1* and OFF are the equivalent uninduced cultures. Genomic DNA was extracted in plugs and digested with *Bgl*II. Probe Cen was used to detect the dicentric fragment. **B-** Quantification of the data in **A** shows that using the DSR element reduces P_{urg1} background levels to a similar level to that of P_{nmt41} driven expression of Rtf1. Induction of Purg1 resulted in ~10 fold accumulation of dicentrics after 3hrs. **C-** Induction of P_{urg1} results in formation of dicentrics in strains where *rtf1* does not have the GFP tag. Lanes labelled as 'nmt rtf1' are the original *nmt41* driven *rtf1 RuiuR* strains as controls. urg1 rtf1-DSR 1-7 are seven independent isolates of *h- smt0 RuiuR leu-32* P_{urg1_NR}*::rtf1:DSR rtf1::natMX6 nda3-KM311*. **D-** Quantification of data in C shows that similarly to the GFP tagged *rtf1* strains using DSR sequences reduces the 'OFF' levels of rearrangements in P_{urg1} strains to a level comparable to that of the *nmt1* promoter.

Figure 3.5

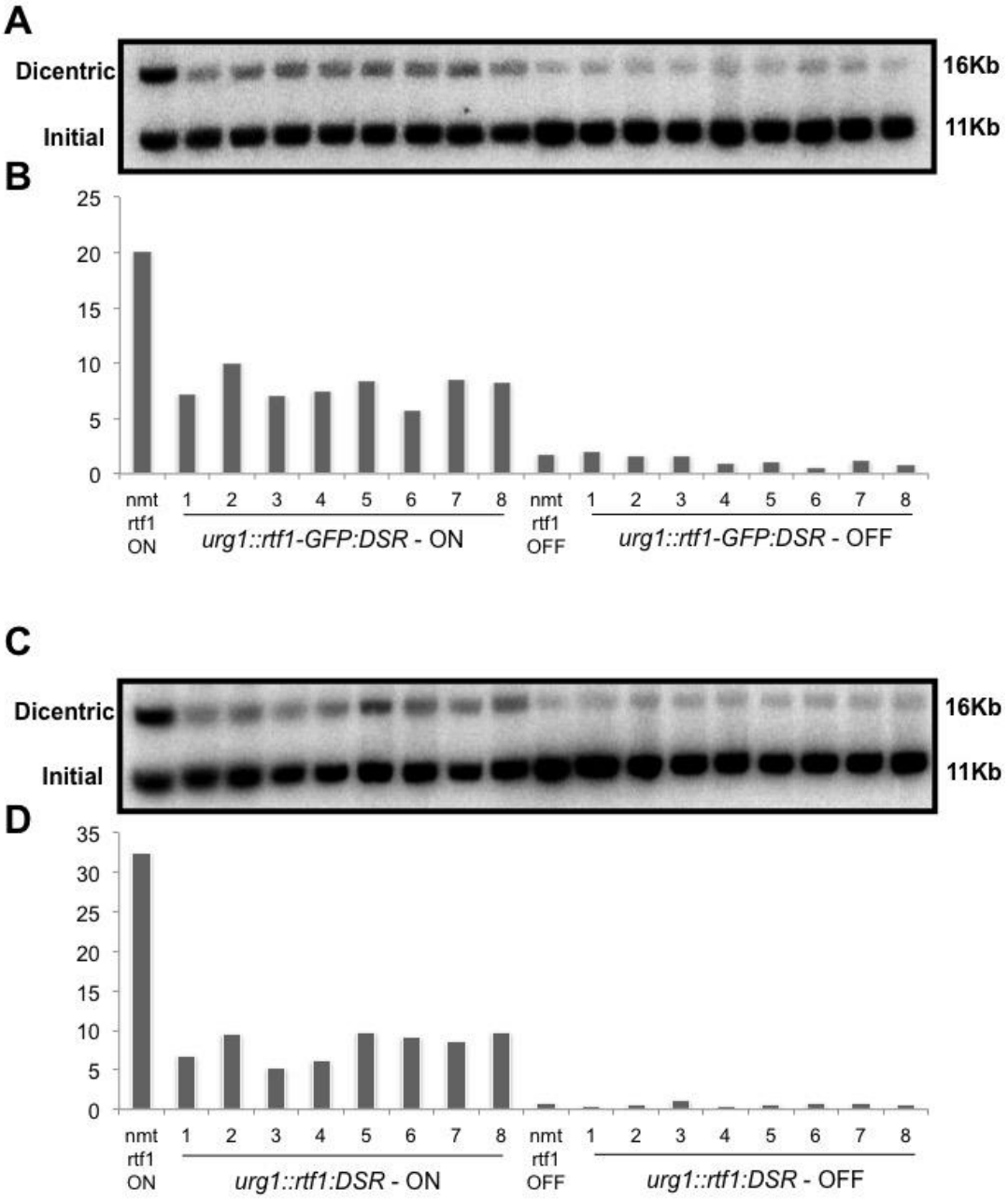
A
Dicentric
Initial
16Kb
11Kb
B
25
20
15
10
5
0
nmt rtf1 ON
1 2 3 4 5 6 7 8
urg1::rtf1-GFP:DSR - ON
nmt rtf1 OFF
1 2 3 4 5 6 7 8
urg1::rtf1-GFP:DSR - OFF
C
Dicentric
Initial
16Kb
11Kb
D
35
30
25
20
15
10
5
0
nmt rtf1 ON
1 2 3 4 5 6 7 8
urg1::rtf1:DSR - ON
nmt rtf1 OFF
1 2 3 4 5 6 7 8
urg1::rtf1:DSR - OFF

3.3.3 – CHARACTERISATION OF GCRS FORMED AFTER INDUCTION OF P_{URG1}

In order to confirm that the use of the DSR element to regulate Rtf1 levels results in efficient fork stalling at *RTS1*, the level of GCRs was determined after induction for three hours. Since one cell cycle takes approximately three hours in minimal media at 30°C and the majority of *S. pombe* cells in a logarithmically growing culture are in G2, most cells should have gone through a single S phase under these conditions. Pulsed field gel electrophoresis (PFGE) was used to investigate formation of acentric species upon induction of *urg1* promoter for one cell cycle. To examine the accumulation of intact acentric chromosomes, independent isolates of *RuiuR* P_{urg1_NR}*::rtf1-DSR nda3-KM311* were grown to early log phase and induced for three hours. To rule out an effect of the *nda3-KM311* background rearrangements were also characterized in an *nda3+* background (*RuiuR* P_{urg1_NR}*::rtf1-DSR*). Levels of acentric formation were compared to those after induction of *nmt41* driven Rtf1 after 24 hours (*RuiuR* P_{nmt41}*::rtf1*) (Figure 3.6). Cells were harvested and DNA was extracted in agarose plugs. Probe 'Tel' homologous to telomeric sequences was used to detect the acentics. Analysis of the PFGE data showed that induction of the *urg1* promoter results in accumulation of the acentric species after three hours (Figure 3.6). The 'off' levels of rearrangements in P*urg1* strains were similar to the P_{nmt} control strain. Moreover, the *nda3-KM311* allele did not affect the rates of induction and background levels of rearrangements as shown by comparison to the *urg1* strain with wild type $nda3^{+}$ (second and eleventh lanes). These results implied that Rtf1 expression under the *urg1* promoter is efficient and results in accumulation of acentric chromosomes.

Figure 3.6

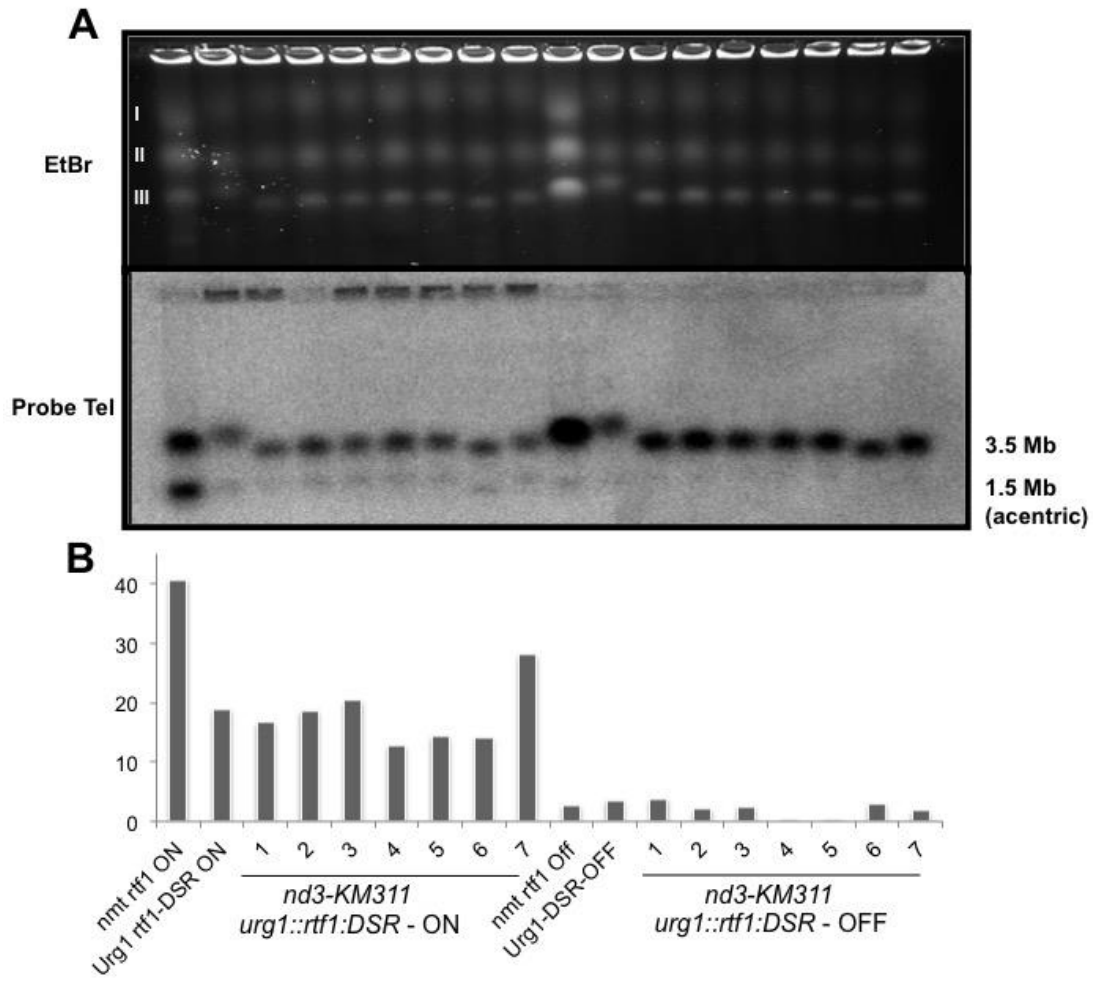

Figure 3.6 | Acentric chromosomes accumulate upon induction of P_{urg1}. A- EtBr stained pulsed field gel (top) and corresponding Southern blot (bottom) showing the chromosomal rearrangements in the RuiuR system after induction of P*urg1*::*rtf1-DSR* for 3hrs. I,II, and III on the Etbr stained gel indicate the three chromosomes. Chromosome III is detected at ~3.5Mb and the acentric chromosome at ~1.5Mb using Probe Tel. Lanes labelled as nmt-rtf1 (original P_{nmt41} strain) and urg1-DSR are used as controls. nda3-Urg1-DSR 1-7 are the same strains as used in Figure **3.5 (C)**. Note the sizes of chromosome III and the acentric chromosome vary with rDNA repeat copy number as the rDNA occupies two regions at either end of chromosome III.
B- Quantification of data in **A** shows accumulation of acentric 3hrs after the addition of uracil. The 'OFF' levels remain similar to that of *nmt* promoter. *nda3-KM311* allele does not affect the kinetics of P_{urg1} induction.

3.3.4 – CHARACTERISATION OF REPLICATION INTERMEDIATES FORMED AFTER P_{URG1} DRIVEN EXPRESSION OF RTF1

To further confirm the efficiency of the fork stalling at *RTS1* using the *urg1* promoter, two-dimensional gel electrophoresis (2DGE) was carried out after induction of Rtf1. Branched DNA molecules are known to migrate anomalously in agarose gels compared to linear fragments of equal mass (Bell & Byers, 1983). In 2DGE, DNA species are separated according to restriction fragment size in the first dimension, and based on their shape in the second dimension. To achieve this, the first dimension is run at low voltage in low percentage agarose. This allows the low mobility branched molecules (RIs) to run close to their true molecular weight, and this separates DNA molecules according to mass. The second dimension is run at high voltage using a gel of high agarose concentration and in the presence of ethidium bromide. These conditions exaggerate the difference between the mobility of molecules of different shapes (i.e. linear vs branched). This results in separation based on shape, which enables the analysis of branched replication intermediates such as bubbles or Y arcs (Bell & Byers, 1983; Brewer & Fangman, 1987). Experimental evidence obtained from replication of the 2μM plasmid revealed the patterns produced by RIs (Figure 3.7B) in two-dimensional gels (Brewer & Fangman, 1987). Retardation of passively replicated Y shaped molecules forms a Y arc, due to the differences in deviation of their three dimensional shape from the linear molecules. A small Y migrates close to the monomer and a large Y further away on the downward section of the arc. A half replicated molecule is made of three equal branches and this deviates the most from the linear and therefore is retarded the most in the second dimension to form the apex of the Y arc. Replication bubbles are produced by the movement of two diverging RFs initiated

within the fragment. These open structures migrate most slowly. Double Ys are produced by the approach of two converging forks initiated outside the fragment and run in a line closer to the linear than Y-shaped molecules. Spots on an arc result from the accumulation of similar shape and sized molecules, as when replication is paused at a specific site. Finally, X-shaped molecules such as HJs run as a spike upward from the end of the Y arc to the end of the double Y arc.

To visualize replication arrest in asynchronous cultures, cells of *h- smt0 RuiuR leu-32* P_{urg1_NR}*::rtf1-DSR rtf1::natMX6 nda3-KM311* were grown to early log phase and the 'On' cultures were induced. Cells were harvested at the 'Off' state, and three, four and six hours after induction. DNA was extracted from the cells in agarose plugs, digested with *Ase*I (Figure 3.7A) and 2DGE carried out. A probe with homology to sequences centromeric to RuiuR (Cen) was then used to identify replication intermediates in the Southern blot. 2DGE analysis of the 'Off' state (figure 3.7E) showed formation of a Y arc signal indicating the passive progression of replication in the region. The faint spot on the Y arc showed an accumulation of replication intermediates of a particular size (8-9kb) consistent with a slight degree of pausing at *RTS1* due to the leakiness of *urg1* promoter.

Figure 3.7 (following page) | Fork stalling is efficient when P_{urg1} drives Rtf1 expression. **A**- cartoon showing the original and dicentric *Ase*I fragments at RuiuR and the expected sizes. **B-** Schematic illustrating the different intermediates separated by 2DGE. **C, D-** Diagrams showing the expected replication intermediates at RuiuR in 'OFF' and 'ON' cultures respectively. **E-** Southern blots showing the 2DGE analysis of replication intermediates of asynchronous RuiuR cultures. Cells were grown to early log phase and uracil was added to induce *Purg1*. Cells were harvested at 0 minutes ('OFF', top left), 3hrs (top right), 4hrs (bottom left), and 6hrs (bottom right) after the addition of uracil. When fork stalling is 'OFF' signals corresponding to the 7kb monomer spot (blue arrow) and passively replicating 'Y' arc (black arrow) are visible. A signal corresponding to a slight degree of pausing is at the expected size of 8-9kb on the 'Y' arc (red arrow). Three hours after induction, two signals at 8-9.5kb on the 'Y' arc (blue arrow) and 9.5kb on the double 'Y' arc (red arrow) corresponding to a single pause at *RTS1* and double arrest respectively are detected. Recombination dependent intermediates are visible at 11-13kb (green arrow). Four hours after induction a clear pause signal, the nature of which will be discussed in the next chapter, is detectable (orange arrow). Six hours after induction the intensity of the 7.4kb monomer spot increases due to the accumulation of the dicentric (blue arrow). **F-** lower exposure of 6 hr blot to show dicentric monomer spot (blue arrow).

Figure 3.7

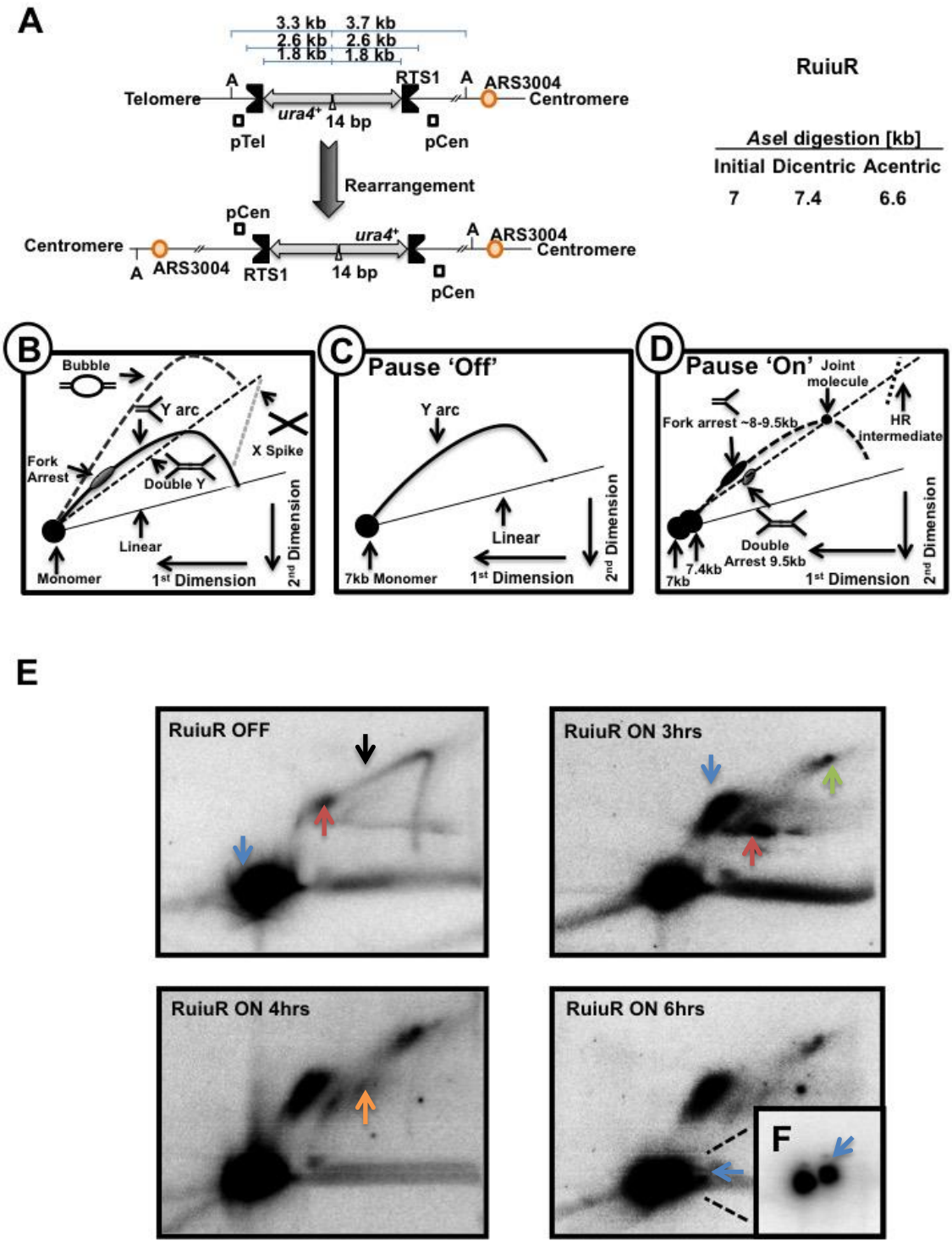
A
3.3 kb
3.7 kb
2.6 kb
2.6 kb
1.8 kb
1.8 kb
Telomere
A
RTS1
A
ARS3004
Centromere
ura4+
14 bp
pTel
pCen
Rearrangement
pCen
Centromere
ura4+
A
ARS3004
Centromere
A
ARS3004
RTS1
14 bp
pCen
RuiuR
AseI digestion [kb]
Initial Dicentric Acentric
7 7.4 6.6
B
Bubble
Y arc
X Spike
Fork Arrest
Double Y
Linear
Monomer
1st Dimension
2nd Dimension
C
Pause 'Off'
Y arc
Linear
7kb Monomer
1st Dimension
2nd Dimension
D
Pause 'On'
Joint molecule
Fork arrest ~8-9.5kb
HR intermediate
Double Arrest 9.5kb
7.4kb
7kb
1st Dimension
2nd Dimension
E
RuiuR OFF
RuiuR ON 3hrs
RuiuR ON 4hrs
RuiuR ON 6hrs
F

However, when P*urg1* was induced, after three hours of induction the 'Y' arc signal was not detectable and a signal corresponding to the size expected for single fork arrests at *RTS1* sites was observed. The double pause at both *RTS1* sites was detected as a ~9kb spot on the double Y arc. A signal migrated at ~11-13kb corresponding to recombination intermediates (Lambert *et al.*, 2010) formed at the apex of the Y arc. Moreover, the intensity of the 7.4kb monomer spot signal increased, which indicates the accumulation of rearranged dicentric species. Four hours after induction of Rtf1 an additional signal was detectable at 10-11kb. The nature of the molecules producing this signal is discussed in the next chapter. Six hours after induction of Rtf1 a further increase in the rearranged monomer signal was observed indicating the accumulation of dicentric products over time. The intensity of the observed 'pausing' signal (~90%) was comparable to previously published data (Lambert *et al.*, 2010), demonstrating the efficient expression of Rtf1 and stalling when *urg1* promoter and DSR element are used to control Rtf1 expression.

3.3.5 – CHARACTERISATION OF KINETICS OF FORK STALLING

To test whether the DSR element affected the kinetics of induction of fork stalling, 2DGE was carried out in synchronous cultures of P_{urg1_NR}*::rtf1-DSR nda3-KM311* and as control (No DSR) strain P_{urg1_NR}*::rtf1 nda3-KM311* (Figure 3.8) . Cells of both strains were grown to early log phase and synchronised as described in 3.1. P_{urg1} was induced before the release and samples were harvested at 0, 60, 75, and 90 minutes after the release. DNA was extracted, digested with *Ase*I, and 2DGE was performed. Probe 'Cen' was used to identify the replication intermediates.

Figure 3.8

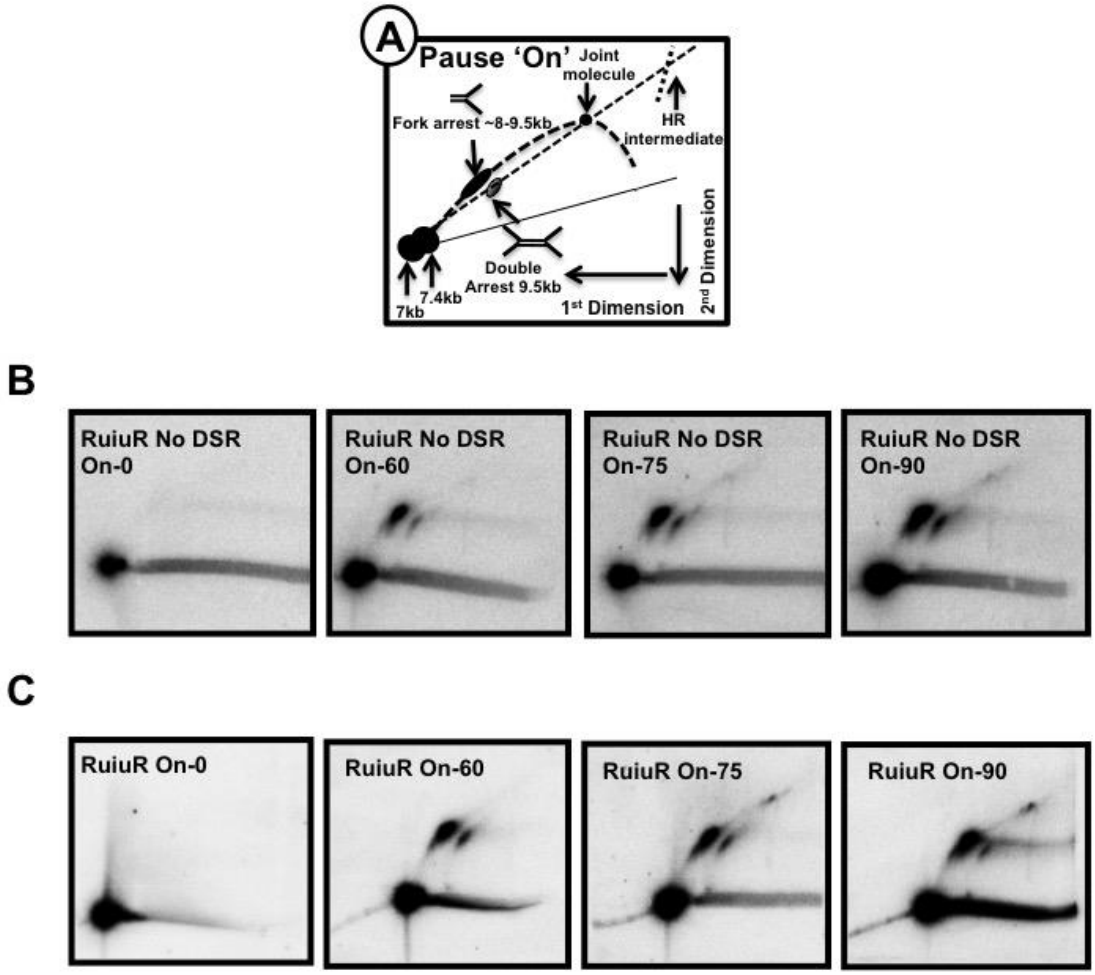

Figure 3.8 | Use of the DSR element does not affect the fork stalling efficiency. Southern blots showing the 2DGE analysis of replication intermediates in synchronised RuiuR cells. Cells were grown to early log phase and synchronised. Uracil was added before releasing the cells and samples were taken at time points 0, 60, 75, and 90 minutes. **A-** Diagrams showing the expected replication intermediates at RuiuR when fork stalling is induced. B- Southern blots showing the replication intermediates of the control strain without the DSR element. At t=0, synchronised cells are still in mitosis, therefore only a monomer signal is detected. At 60 minutes after the release, S phase is initiated and single and double pause signals at *RTS1* sites are visible. A faint trace of 'Y' arc is also detectable. At 75 minutes recombination intermediates are detected consistent with HR restart. These intermediates persist and are still detectable at 90 minutes, as is the faint 'Y' arc. **C-** Southern blots showing the replication intermediates of the DSR strain used in **Fig 3.7**. The results show the detection of similar intermediates to that of the control strain at each time point. The quantification of the pause signals at t=60 showed similar intensity of pause spots between the control (**A**) and the DSR (**B**) strains (87% and 90% respectively).

The analysis of the replication intermediates observed in synchronous cultures of both the control strain (no DSR element to reduce the background Rtf1 levels) and the DSR strain used in previous experiments showed detection of only the monomere signal at timepoint 0 after the release. This is expected as the *nda3-KM311* cells arrest the cell cycle in prometaphase at restrictive temperature and resume the rest of mitosis upon shifting the temperature to the permissive temperature. One hour after the release, signals corresponding to the single and double pause at *RTS1* sites, and a faint 'Y' arc are detectable in both the control and the strain harboring the DSR sequence at intensities of 87% and 90% respectively. In order to quantify the arrest efficiency, the intensity of the pausing signals was presented as a percentage of the total intensities of replication intermediates observed. By 75 minutes after the release, both control and the DSR strain showed a signal corresponding to recombination-dependent replication intermediates correlating with the initiation of HR-dependent fork restart at *RTS1* sites. Moreover the faint trace of the 'Y' arc was detectable in both strains. Analysis of the intermediates observed at 90 minutes after the release showed the accumulation of similar intermediates to that of 75 minutes. These results indicated that the efficiency of the fork stalling at *RTS1* was not affected when the DSR element is employed to control the Rtf1 levels, and the overall reduction of Rtf1 levels did not affect the kinetics of barrier activity at *RTS1* when compared to the strain without the DSR element.

3.4 – DISCUSSION

Development of an inducible replication stalling systems such as RuiuR provided a unique opportunity to investigate the role of HR in the restart of collapsed replication

forks. The results of genetic and biochemical studies in our laboratories demonstrated the importance of HR in the restart of replication at *RTS1*. However, studies of the timing of HR-restart were not technically achievable due to the extended time required for full induction of the medium strength *nmt41* promoter. Identification of the uracil inducible *urg1* promoter offered a plausible inducible system similar to P_{GAL} of *S. cerevisiae*. Although P_{urg1} showed similar dynamic range of 'On' and 'Off' states of protein levels to that of *nmt1* promoter, its basal level of transcription was relatively high and Rtf1 protein levels at 'Off' state were too high and resulted in GCRs in the RuiuR system before induction. In this chapter I showed that regulation of *rtf1* RNA stability using the *spo5* DSR element results in a reduction of the basal transcription levels controlled by the *urg1* promoter to a level similar to that of P_{nmt1}. Despite the fact that using the DSR element results in a general reduction of protein levels in both 'On' and 'Off' states of the promoter (Watson *et al.*, 2013), induction resulted in expression of enough Rtf1 molecules to drive efficient fork stalling at *RTS1* and, importantly, with similar kinetics to that of the strain with no DSR element (demonstrated by PFGE and 2DGE in synchronous and asynchronous cultures).

Several conditions of block and release of *nda3-KM311* allele were examined in the aim of identifying the best synchronization conditions. I reported the optimal synchrony conditions and demonstrated the synchronous cell cycle progression by following septation index. Optimization of rapid induction of Rtf1 from *urg1* promoter, and *nda3-KM311* cell cycle synchrony provided a versatile tool to investigate the timing of events leading to GCRs in fork stalling systems, and cell cycle regulation in response to these events.

CHAPTER 4 – CHARACTERISATION OF HR-DEPENDENT REPLICATION RESTART IN A SINGLE CELL CYCLE

4.1 – INTRODUCTION

Replication restart in a palindrome has been shown to generate GCRs at a high frequency (Mizuno *et al.*, 2009). Two DSB free mechanisms have been identified for the generation of acentrics and dicentics after HR-dependent replication restart at *RTS1*. In the NAHR-dependent model of rearrangements strand invasion of the nacent 3' strand at the stite of the collapsed fork into the wrong template leads to GCRs. Strand invasion into the correct strand restarts replication at *RTS1* but the restarted fork is non-cannonical and U-turns at the centre of the palindrome and this results in GCRs (Lambert *et al.*, 2010; Mizuno *et al.*, 2013). The data leading to these hypotheses were the result of steady state of rearrangements over three generations, as the *nmt* promoter was used to control Rtf1 expression and cultures were analysed three generations after full induction of the *nmt* promoter. In order to support the models that rearrangements occur upon replication restart, and to identify the replication intermediates corresponding to the two mechanisms of generation of GCRs, the timing of rearrangements and replication intermediates were investigated in a single cell cycle using the rapid induction of the fork stalling system (RuiuR) that I optimized in synchronous cultures (as described in Chapter three).

4.2 – CHARACTERISATION OF CELL CYCLE PROGRESSION UPON INDUCTON OF FORK STALLING

To characterize cell cycle progression upon induction of fork stalling in the RuiuR system, the strain *RuiuR* P_{urg1_NR}*::rtf1-DSR nda3-KM311* was grown to early log phase. The cell cycle was blocked in mitosis by incubating at 16°C, and uracil was added to induce replication pausing at *RTS1* sites in the 'On' culture one hour before the release by shifting the temperature up to 30°C. Figure 4.1A shows a graphic explaining the experimental set up. Samples for septation index and flow cytometry (FACS) analysis were harvested every 15 minutes after the release. Septation index was scored as explained in section 3.1 and FACS analysis was performed. Flow cytometry is a powerful tool for measuring DNA content and monitoring cell cycle distribution. In FACS analysis, haploid G1 cells show a 1C DNA content, whereas G2 cells are of 2C DNA content. In *S. pombe* G2 phase compromises 70% of the cell cycle. Cells complete M, G1 and enter S phase prior to cell division. Therefore, mitotic and G1 cells are also of 2C DNA content. This causes a predominantly a 2C DNA content in an asynchronous culture. S phase is characterised by the area under an intermediate peak between 2C and 4C DNA content as the two daughter cells, which are still joined together and so counted as a single unit, move transiently to a 4C content and back to 2C as they separate (Sabatinos & Forsburg, 2009).

Scoring septation index showed that in both 'Off' and 'On' cultures the first peak of septation occurs at 60 minutes after the release. Both cultures proceeded to mitosis at ~215 minutes after the release with the second peak of septation occurring ~240 minutes after the release. Since S phase in fission yeast is coincident with formation of septum, this indicated that S phase occurred at 60 and 240 min after

release and that the second S phase was not delayed in the induced culture. Consistent with this, the analysis of FACS data in both induced and uninduced RuiuR cultures (Figure 4.1C) revealed that there was no significant difference in progression of cell cycle between the induced and uninduced cultures (judged by shift of the 2C peak towards a 4C peak) with the first S phase initiated at 60 minutes and completed by 120±15 minutes after the release, and the second occurring at 240 minutes.

Cell cycle progression in both induced and uninduced cultures was similar to that of the *nda3-KM311* control strain (no palindrome, see Figure 3.3B). This indicated no delay into mitosis after induction of fork stalling in the induced culture compared to the 'Off' and no palindrome controls. However a population of 'cut' cells where observed during the second M phase after the release in the 'On' culture (Figure 4.1B lower panel) and chromosome bridges were observed during mitosis, showing that GCRs had occurred (Figure 4.1D). These data showed that the generation of chromosomal rearrangements after HR-dependent restart at *RTS1* does not lead to a mitotic delay, nor to a delay to S phase in the next cell cycle.

Figure 4.1 (following page) | HR-dependent restart does not lead to mitotic delay. A- cartoon illustrating the experimental set up. Cells were synchronized in mitosis by *nda3-KM311* block and samples were taken at intervals after the release for appropriate experimentation. **B-** Septation and mitotic indices showing the cell cycle progression profile of 'Off' (top) and 'On' cultures. Coloured bar indicates the different stages of the cell cycle. DNA was stained with DAPI and calcofluor was used to visualize the septum. Mitotic cells are binucleate and S phase coincides with the formation of septum. Aberrant mitotic cells with chromosome bridges and lagging chromosomes or where the septum bisects the DNA were scored as 'cut'. **C-** Flow cytometry profiles of DNA content of the 'Off' (top) and 'On (bottom). Asterisks indicate the shift corresponding to S phase. **D-** Examples of chromosome bridges observed during the second mitosis after the release.

Figure 4.1

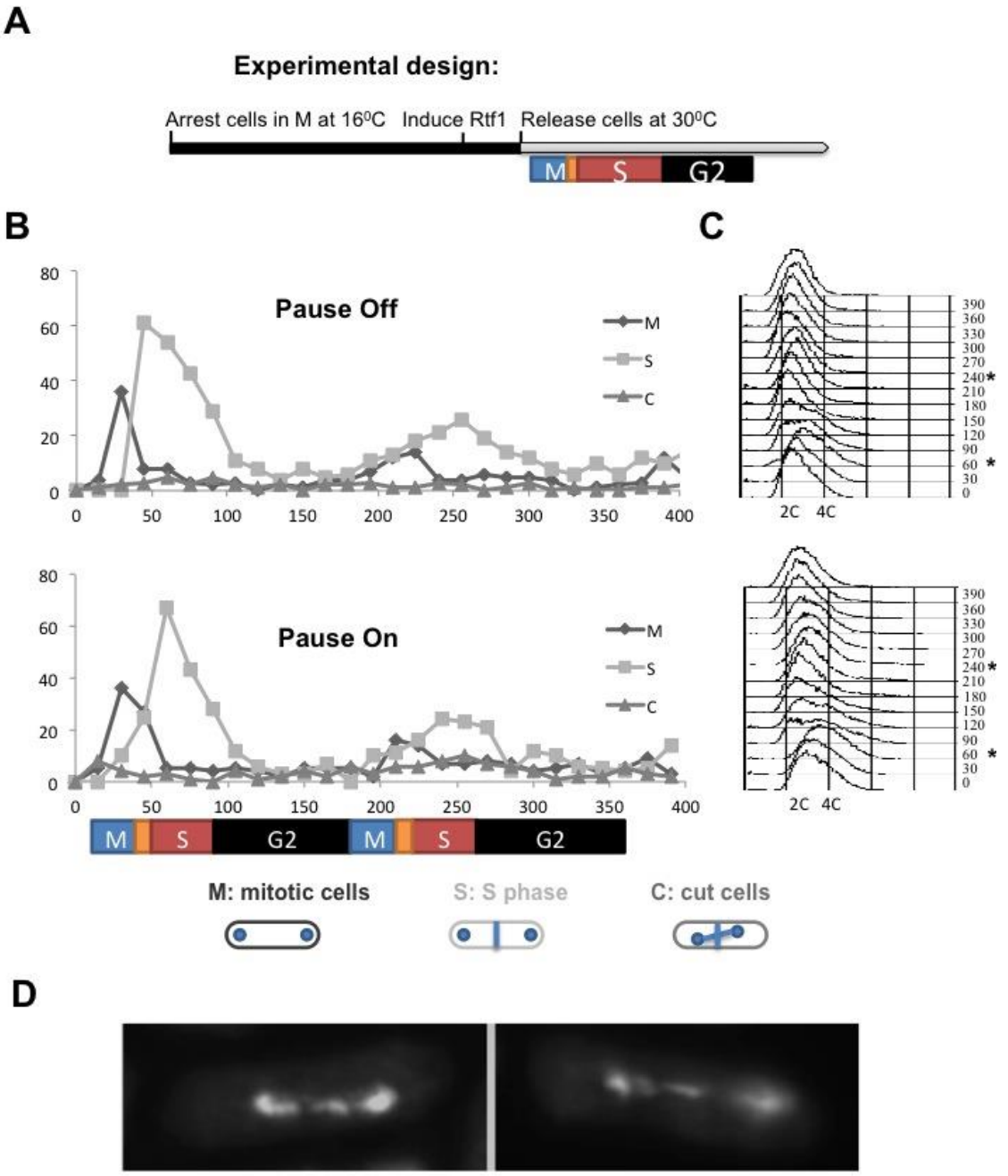
A
Experimental design:
Arrest cells in M at 16⁰C
Induce Rtf1
Release cells at 30⁰C
M
S
G2
B
C
Pause Off
Pause On
M
S
C
2C
4C
M: mitotic cells
S: S phase
C: cut cells
D

4.3 – DICENTRIC CHROMOSOMES ACCUMULATE IN G2

To characterize the timing of chromosomal rearrangements after the restart, restriction fragment analysis was performed on DNA samples obtained at intervals from either induced, or uninduced synchronous cultures of *RuiuR* P_{urg1_NR}*::rtf1-DSR nda3-KM311*. An *rtf1Δ* (no stall) strain (*RuiuR* P_{urg1_NR}*::hphMX6 nda3-KM311 rtf1::*natMX6) was used as control. Samples from an uninduced culture were used to determine the background level of rearrangements due to slight leakiness of P_{urg1}. Strains were grown to early log phase and the cell cycle was blocked in mitosis by shifting the temperature to 16°C for six hours. Uracil was added to the 'On' culture prior to the release and cells were released by shifting the temperature to 30°C. Samples were taken at intervals and genomic DNA was extracted in agarose plugs. DNA was then digested with *Ase*I (see Figure 3.7 for a schematic of *Ase*I restriction sites in RuiuR after rearrangement) and gel electrophoresis was performed. A 7kb band is expected in the absence of rearrangements, the dicentric fragment migrates at 7.4kb, and the acentric fragment at 6.6kb band. Probe 'Cen' homologous to sequences centromere proximal to RuiuR was used to detect the initial and dicentric fragments in the Southern blot analysis. Figure 4.2A shows the result of this experiment and quantification of the bands observed in the Southern blot.

Figure 4.2 (following page) | Dicentric chromosomes accumulate in G2. A- (left hand side)- Representative Southern blot showing the timing of formation of rearrangements in the cell cycle. In all 'On', 'Off', and 'no stall', cells were grown to early log phase and synchronized. The time course started as cells were released and samples were collected at indicated intervals. DNA was prepared in agarose plugs and restriction fragment length analysis was performed using *Ase*I. **A- (right hand side)-** Quantification of the bands observed in the Southern blot. **B- (left hand side)-** Representative Southern blot showing the restriction fragment length analysis using *Bgl*II. The experiment was repeated as in **A** and DNA samples were digested using *Bgl*II. **B (right hand side)-** Quantification of the data in Southern blot. To quantify the signals observed in the Southern blots, the intensity of each band calculated using ImageQuant™ was presented as a percentage of the total intensity of signals of each individual lane. Cartoons illustrating *Bgl*II and *Ase*I restriction sites and rearrangements at RuiuR are presented above the blots. In both time courses the intensity of the dicentric fragment increases from 150 min (early G2) but slow migrating RI are seen in S and decline in G2.

Figure 4.2

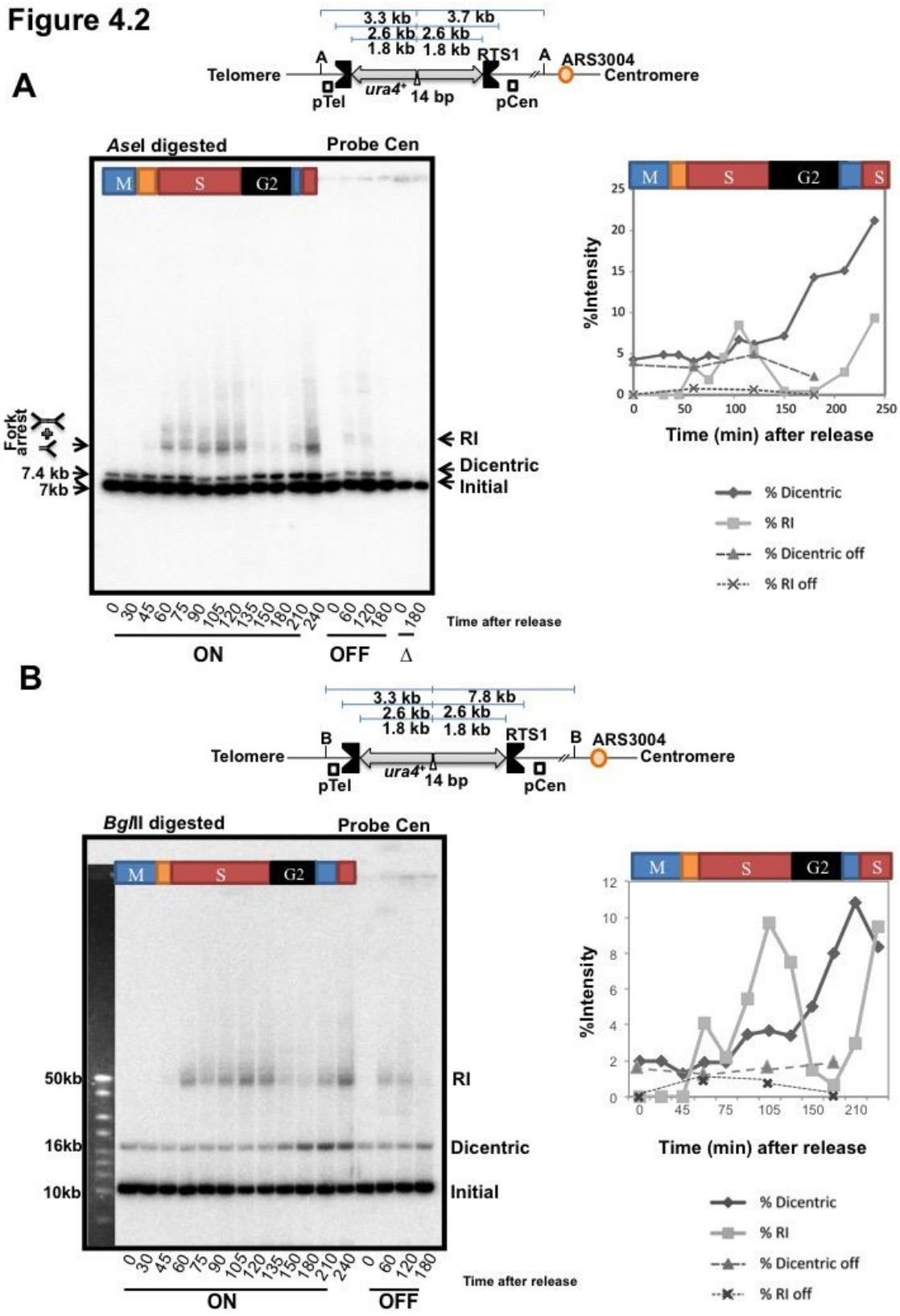
A
3.3 kb
3.7 kb
2.6 kb
2.6 kb
1.8 kb
1.8 kb
RTS1
A
ARS3004
Telomere
Centromere
pTel
ura4+
14 bp
pCen
AseI digested
Probe Cen
M
S
G2
Fork arrest
7.4 kb
7kb
RI
Dicentric
Initial
0 30 45 60 75 90 105 120 135 150 180 210 240 0 60 120 180 0 180
Time after release
ON
OFF
Δ
%Intensity
Time (min) after release
% Dicentric
% RI
% Dicentric off
% RI off
B
3.3 kb
7.8 kb
2.6 kb
2.6 kb
1.8 kb
1.8 kb
RTS1
B
ARS3004
Telomere
Centromere
pTel
ura4+
14 bp
pCen
BglII digested
Probe Cen
50kb
16kb
10kb
RI
Dicentric
Initial
0 30 45 60 75 90 105 120 135 150 180 210 240 0 60 120 180
Time after release
ON
OFF
%Intensity
Time (min) after release
% Dicentric
% RI
% Dicentric off
% RI off

As expected, in the *rtf1Δ* samples only the 7kb original *Ase*I fragment was observed consistent with GCRs being dependent on HR restart of arrested fork at *RTS1*. The analysis of 'Off' samples taken at 60 minutes intervals over the first cell cycle showed both the 7kb original band and the 7.4kb dicentric band, which remained constant throughout the time course experiment. This indicated the background levels of rearrangements due to leakiness of the *urg1* promoter. In the 'On' samples, where the stalling was induced, the 7kb original and the 7.4kb dicentric bands are present throughout the time course. However, quantification of the dicentric signal showed that the dicentric fragment increased from early G2 (150 minutes after the release) leading to 15.8% of rearrangements by late G2. Moreover, a signal of slow migrating replication/recombination intermediates was detected at the start of S phase (60 minutes after the release). The intensity of this signal peaked at 105 minutes after the release and dropped upon the completion of S phase (~135 minutes after the release). The RI species peaked during the S phase and were resolved as the dicentric signal accumulated, consistent with the conversion of one form to the other.

This experiment was repeated on both 'On' and 'Off' cultures (Figure 4.2B) and restriction fragment length analysis was performed as explained above using *Bgl*II for better separation of original and rearranged bands (cartoon and expected sizes of RuiuR showing *Bgl*II restriction sites is presented in Figure 4.2B and 3.4). Consistent with the previous experiment, quantification of the signals seen in the Southern blot showed similar kinetics of formation and disappearance of bands. Dicentic chromosomes accumulated in G2 as the slow migrating intermediates were resolved and the 'Off' levels of rearrangements remained constant throughout the time course experiment.

4.4 – HOMOLOGOUS RECOMBINATION DEPENDENT RESTART OCCURS IN S PHASE

To characterise the slow migrating intermediates formed during the S phase (Figure 4.2), 2DGE was employed. Cells of *RuiuR* P_{urg1_NR}*::rtf1-DSR nda3-KM311* and the no stall control strain *RuiuR* P_{urg1_NR}*::hphMX6 nda3-KM311 rtf1::natMX6* were grown to early log phase and synchronised in M. Fork stalling was induced, or not, one hour before the release and the cells released from the block. Samples were collected for 2DGE analysis at one hour intervals for 'Off' and 'no stall' controls and in the induced culture at 15 minute intervals during the first S phase and 30 minutes intervals over G2 covering up to the second S phase after the release (Figure 4.3). DNA was extracted, digested with *Ase*I, and 2DGE was performed. Probe 'Cen' homologous to sequences centromere proximal to RuiuR was used to detect RIs. In the *rtf1Δ* 'no stall' control culture (Figure 4.3A) at time point 0 after the release, where cells were in mitosis, only the monomer spot is detected. Analysis of samples from the rest of the time course showed passive replication of the RuiuR fragment as judged by the formation of a native Y arc at 60 minutes. The Y arc is hardly detectable by 180 minutes after the release (G2). Similarly, in the 'Off' culture (Figure 4.3B) only the monomer is detectable at time point 0. Analysis of later samples showed the formation of the Y arc at 60 minutes and this signal declined by 180 minutes after the release (G2). In addition, a pause signal on the Y arc corresponding to the accumulation of Y structures at *RTS1* was detected at time points 60 and 120 minutes, consistent with the slight degree of leakiness of $P_{urg}1$.

Figure 4.3 (following page) | Homologous recombination restarts replication in S phase. 2DGE analysis of RuiuR replication intermediates detected by a probe homologous to sequences centromere proximal to RuiuR. Cells were grown to early log phase and synchronized. Fork stalling was induced, or not, 60 minutes before the release and the time course was started as cells were released. Samples were collected at indicated intervals. DNA was prepared and digested with *Ase*I. **A-** Schematic illustrating different intermediates separated by 2DGE. **B & C-** Diagrams showing the expected replication intermediates in RuiuR system in 'OFF' and 'ON' states respectively. **D-** 2DGE analysis of 'no stall' control. The black arrow indicates the Y arc and the light blue arrow indicates the monomer spot. **E-** 2DGE analysis of the 'Off' state of fork stalling. The red arrow indicates the arrest at *RTS1*. **F-** 2DGE analysis of the 'On' culture at intervals through a single cell cycle. The red arrow indicates the pause at *RTS1* and the dark blue indicates the double pause at *RTS1* sites. The green and yellow arrows indicate the HR-dependent intermediates and the purple arrow indicates a novel spot in the second cell cycle.

Figure 4.3

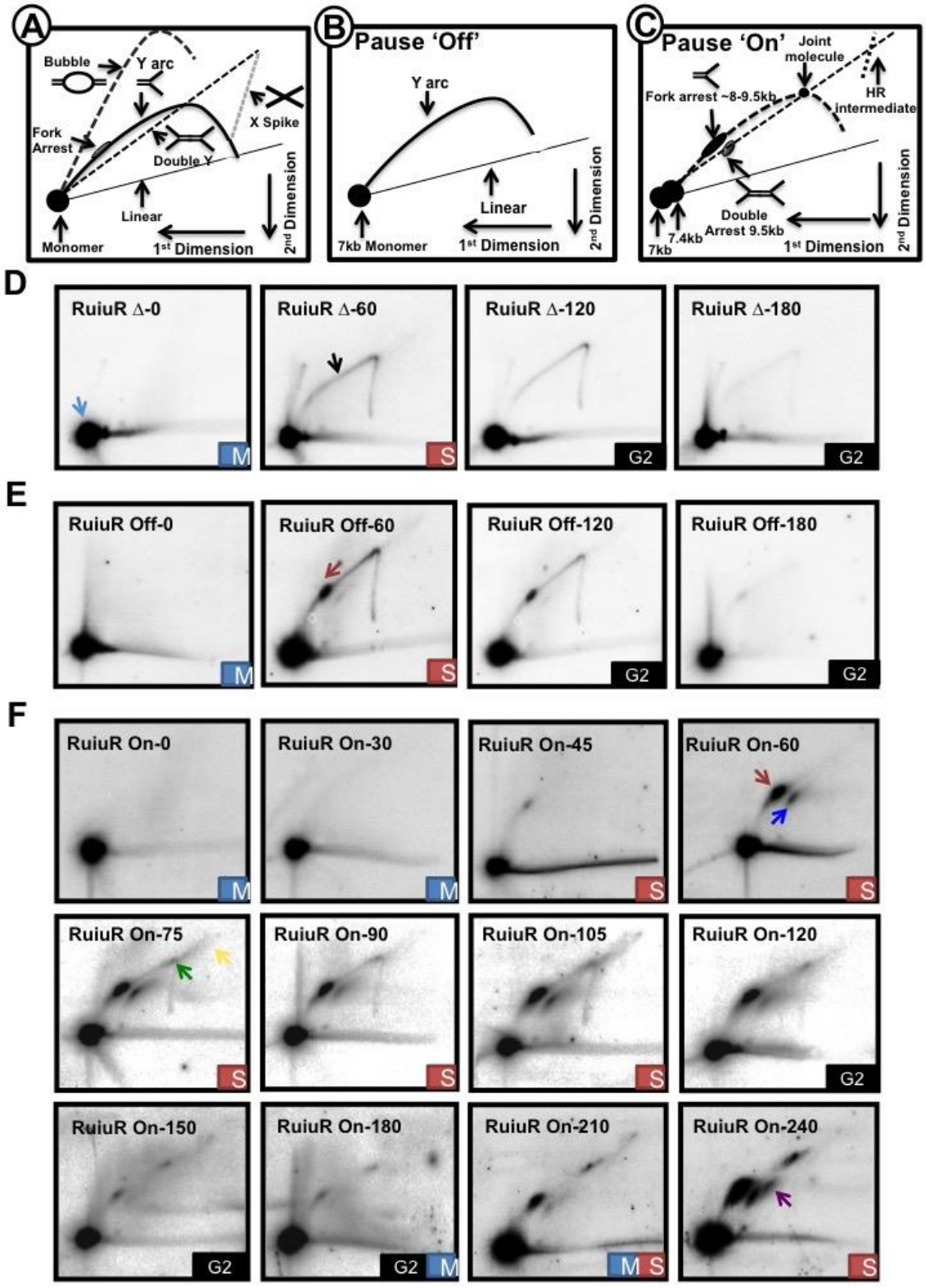
A
Bubble
Y arc
X Spike
Fork Arrest
Double Y
Linear
Monomer
1st Dimension
2nd Dimension
B
Pause 'Off'
Y arc
Linear
7kb Monomer
1st Dimension
2nd Dimension
C
Pause 'On'
Joint molecule
Fork arrest ~8-9.5kb
HR intermediate
Double Arrest 9.5kb
7kb
7.4kb
1st Dimension
2nd Dimension
D
RuiuR Δ-0
RuiuR Δ-60
RuiuR Δ-120
RuiuR Δ-180
E
RuiuR Off-0
RuiuR Off-60
RuiuR Off-120
RuiuR Off-180
F
RuiuR On-0
RuiuR On-30
RuiuR On-45
RuiuR On-60
RuiuR On-75
RuiuR On-90
RuiuR On-105
RuiuR On-120
RuiuR On-150
RuiuR On-180
RuiuR On-210
RuiuR On-240
M
S
G2

In the ‘On’ culture, initiation of S phase is evident 45 minutes after the release, as judged by a faint short Y arc signal and the accumulation of Y structures at a pause spot migrating at a size consistent with arrest at centromere proximal *RTS1* pause site. As discussed in Chapter one, active replication origins ars3004/5 are 3kb centromere proximal to RuiuR, whereas the telomere proximal origin, ars3003, is 40kb away. The pause signal on the Y arc reaches maximum intensity 60 minutes after the release (see Figure 3.7 and 3.8 for comparison) with the double pause at both centromere and telomere *RTS1* sites visible on the double Y arc. At 75 minutes after the release, two additional signals were detected, one at the apex of the Y arc, and one on the X spike. These intermediates have been shown by Lambert *et al.* to be dependent on HR and thus are consistent with HR-dependent replication restart (Lambert *et al.*, 2010). These HR dependent intermediates persist throughout the S phase and decrease in intensity in G2 (from t=150 minute). Replication intermediates observed in G2 and M (time point 180 when 80-90% of cells were in late G2) were comparable to that of the ‘Off’ culture: the intensity of the arrest signal and the HR-dependent intermediates dropped to a minimum. However in the S phase of the second cell cycle (240 minute after the release) the spots corresponding to the pause at *RTS1* sites and HR restart reappear. An additional spot specific to the second cell cycle was also detected, the nature of which is discussed in the next section. These results indicated that HR-dependent restart of the fork occurred in S phase 15 minutes after replication stalling, and this led to formation of HR intermediates that were detected for approximately 45 minutes until declining in G2.

4.5 – DICENTRIC CHROMOSOMES REPLICATE IN THE SECOND CELL CYCLE

In order to visualize and differentiate between any potential acentric and dicentric specific replication intermediates, the membranes that contained the samples shown in (Figure 4.3) were reprobed with a probe (Probe Tel) homologous to sequences telomere proximal to RuiuR. Figure 4.4 shows the expected sizes of *Ase*I fragment of RuiuR when rearranged to acentric and dicentric chromosomes and a cartoon to show intermediates detected by both probes after 2DGE. The major direction of replication through the locus is centromere to telomere as most forks will arrive first from the nearby centromere-proximal origin (ars3004/5). Both probes detect the telomere and centromere proximal single arrested forks. However, the intensity of these pause signals will depend on the probe. As detailed in Figure 4.4 C and D when using Probe Tel the intensity of the telomere proximal arrest is expected to be greater than that of the centromere proximal arrest as it will hybridise to two regions of homology on the Y-shaped telomere-proximal arrest molecule compared to one region of homology on a centromere-proximal arrest molecule.

Figure 4.4

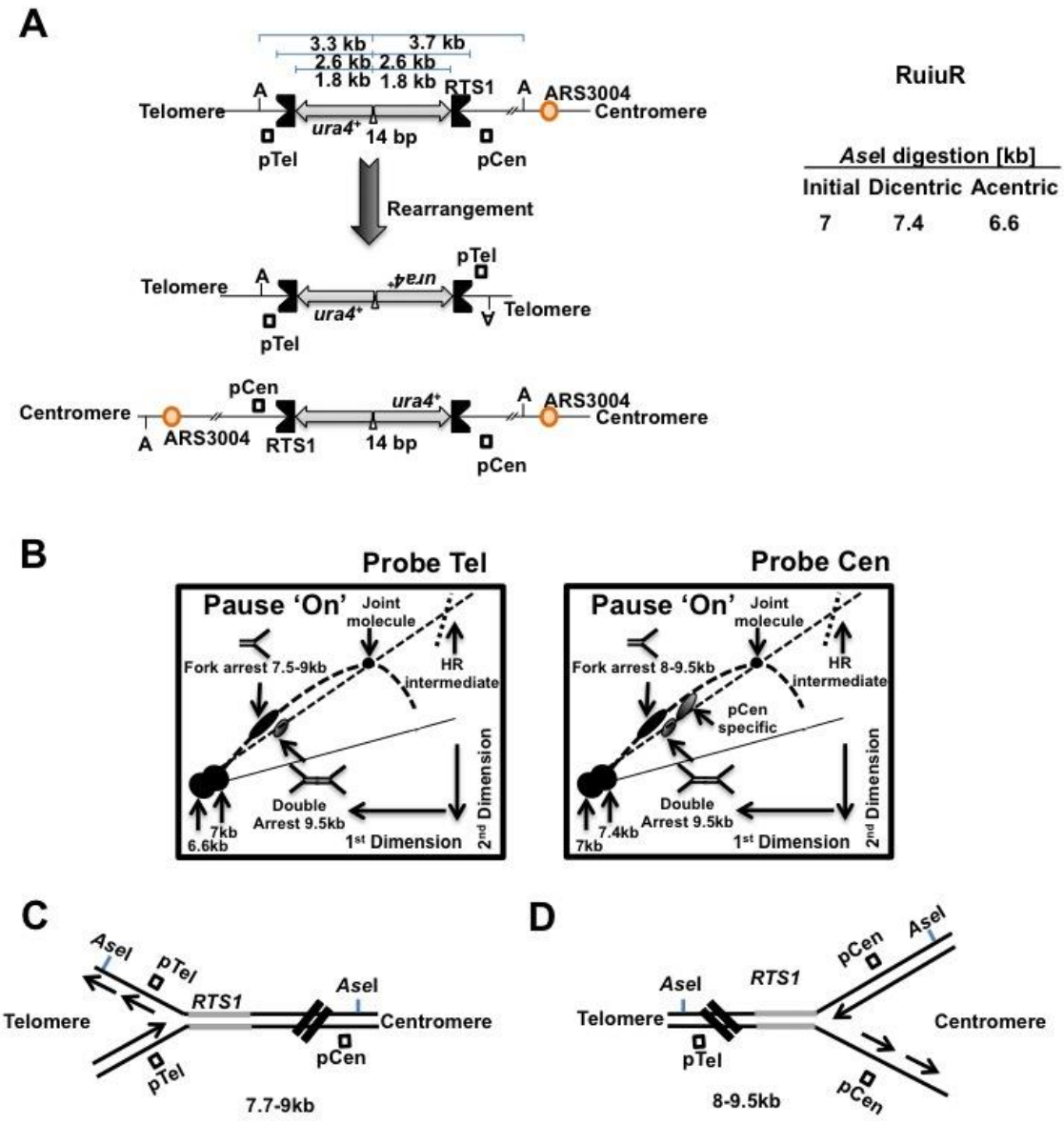

Figure 4.4 | *Ase*I fragment of RuiuR. A- Cartoon showing the *Ase*I fragment RuiuR and expected sizes when rearranged to acentric and dicentric chromosome. **B-** Schematic of replication intermediates of *Ase*I RuiuR detected with Probe Tel (left) homologous to sequences telomere proximal to RuiuR, and Probe Cen (right) homologous to sequences centromere proximal to RuiuR. **C-** Cartoon illustrating single replication arrest at telomere proximal *RTS1* in RuiuR. **D-** Cartoon illustrating single replication arrest at centromere proximal *RTS1* in RuiuR. Note that both Probe Cen and Tel detect the both telomere and centromere proximal single arrested forks. However when using Probe Tel the intensity of the telomere proximal arrest is expected to be greater than that of the centromere proximal arrest and vice versa. The major direction of replication through the locus is centromere to telomere as most forks will arrive first from the nearby centromere proximal origin.

Figure 4.5A shows the results of re-probing the membranes presented in Figure 4.3 with the telomeric probe (Probe Tel). At t=0 the monomer spot signal detected with Probe Tel corresponds to the 7kb original *Ase*I fragment with an additional minor spot of 6.6kb corresponding to the rearranged acentric fragment, consistent with the background level of rearrangements (Figure 4.5A). Due to re-probing the membrane the signal intensities were weaker but at 75 minutes after release single and double pause sites and HR-dependent intermediates, indicative of fork arrest and restart were detected. These intermediates decline in G2 similarly to Figure 4.3, and reappeared again in the second cell cycle (time point 240).

To differentiate between acentric and dicentric specific intermediates, the images obtained from the experiment shown in Figure 4.3 (probed with Probe Cen) were recolored in magenta and the images obtained from probing with Probe Tel were recolored in green. The resulting images were merged (Figure 4.5B). Replication intermediates in common between both probes were detectable in white, P Tel specific (corresponding to acentric) in green, and P Cen specific (corresponding to dicentric) in magenta. As expected from the size, the 6.6kb monomer spot was detected only by Probe Tel. In addition, the monomer proximal tail of the single pause at *RTS1* on the Y arc was detected in green corresponding to the pausing at telomere proximal *RTS1* (time point 75-120). While this pause is also be detected by P Cen it is more intense with the P Tel probe as this would hybridize to two regions on the Y arc (see Figure 4.4 C and D).

The double pause at both *RTS1* sites was detectable in white. However the second cell cycle specific signal detected in time point 240 of Figure 4.3C was detected in magenta. While this could be due to the weak Probe Tel signal, it is likely that this is specific to Probe Cen as a similar Probe Cen-specific spot is seen after P_{nmt41} induction

of Rtf1 arrest (K. Mizuno, personal communication). The size of this replication intermediate is ~9-10kb consistent with the expected size of the arrest at *RTS1* on the dicentric chromosome (monomer size: 7.4kb), therefore this signal likely was formed due to the replication pausing at *RTS1* site during replication of the dicentric chromosome in the second cell cycle after the release.

Figure 4.5 (following page) | The dicentric replicates in the second S phase. A- 2DGE analysis of RuiuR replication intermediates detected by a probe (Probe Tel) telomere proximal to RuiuR. The membranes from experiment shown in Figure 4.3 were reprobed with Probe Tel. **B-** Overlays of acentric and dicentric specific signals. Images obtained from figure 4.3 were recoloured in magenta (dicentric) and pictures from 4.5A in green (acentric), and merged. The spots common between acentric and dicentric light up in white, Probe Tel specific (acentric) in green, and Probe Cen specific (dicentric) in magenta. The white arrow in time point 240 indicates the second cell cycle dicentric-specific novel spot corresponding to replication of the dicentric in the second S phase.

Figure 4.5

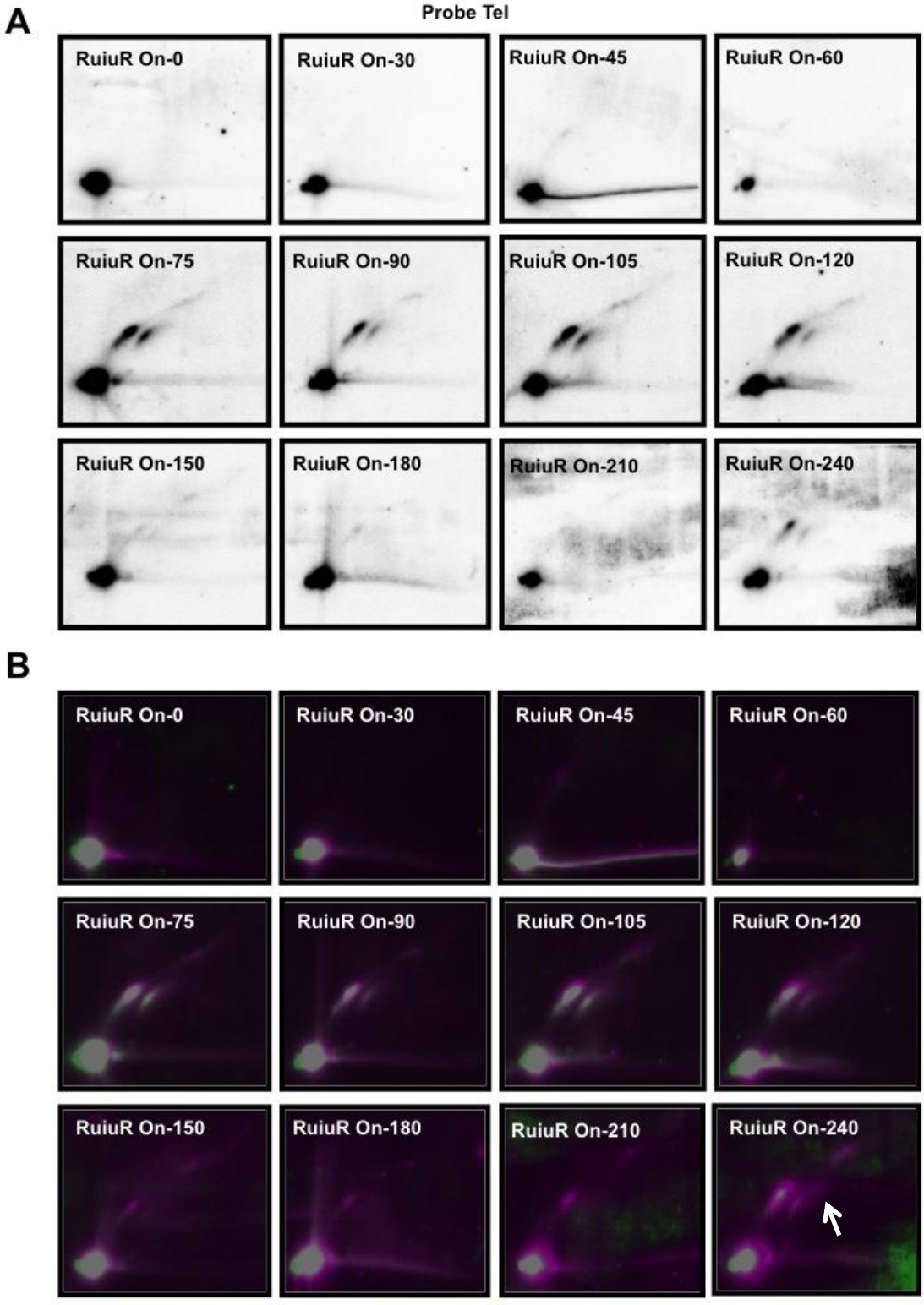
A
Probe Tel
RuiuR On-0
RuiuR On-30
RuiuR On-45
RuiuR On-60
RuiuR On-75
RuiuR On-90
RuiuR On-105
RuiuR On-120
RuiuR On-150
RuiuR On-180
RuiuR On-210
RuiuR On-240
B
RuiuR On-0
RuiuR On-30
RuiuR On-45
RuiuR On-60
RuiuR On-75
RuiuR On-90
RuiuR On-105
RuiuR On-120
RuiuR On-150
RuiuR On-180
RuiuR On-210
RuiuR On-240

4.6 – KINETICS OF HR-DEPENDENT RESTART DURING S PHASE

To further characterize the timing of replication restart at *RTS1*, a time course with samples taken five-minute intervals during the S phase was performed. The strain *RuiuR* P_{urg1_NR}*::rtf1-DSR nda3-KM311* was grown to early log phase and the cell cycle was arrested at 16°C for six hours. Rtf1 expression was induced one hour before the release. Cells were released by shifting the temperature to 30°C and samples were collected at five-minute intervals. DNA was extracted and digested with *Ase*I. 2DGE was performed and Probe Cen homologous to centromere proximal sequences to RuiuR was used to detect replication intermediates in the Southern blots (Figure 4.6). Consistent with the result of the experiment shown in section 4.4, only the monomer spot was detected in mitosis (time point 0). Similarly to the previous time course, initiation of S phase was marked by faint pausing at *RTS1* 45 minutes after the release and the intensity of the arrest signal at *RTS1* reaches maximum intensity by 60 minutes after the release. Note that the intermediates detectable are equivalent at the same time points in Figure 4.3 (e.g. compare 75, 90 and 105 minutes) showing the reproducibility of cell cycle progression between experiments. At t=65, the HR-dependent spot at the apex of the Y arc was detected but the larger HR-dependent molecules seen on the X spike were not detected until 75 minutes after the release. These replication intermediates persist throughout the S phase with decreasing intensity in G2.

Figure 4.6

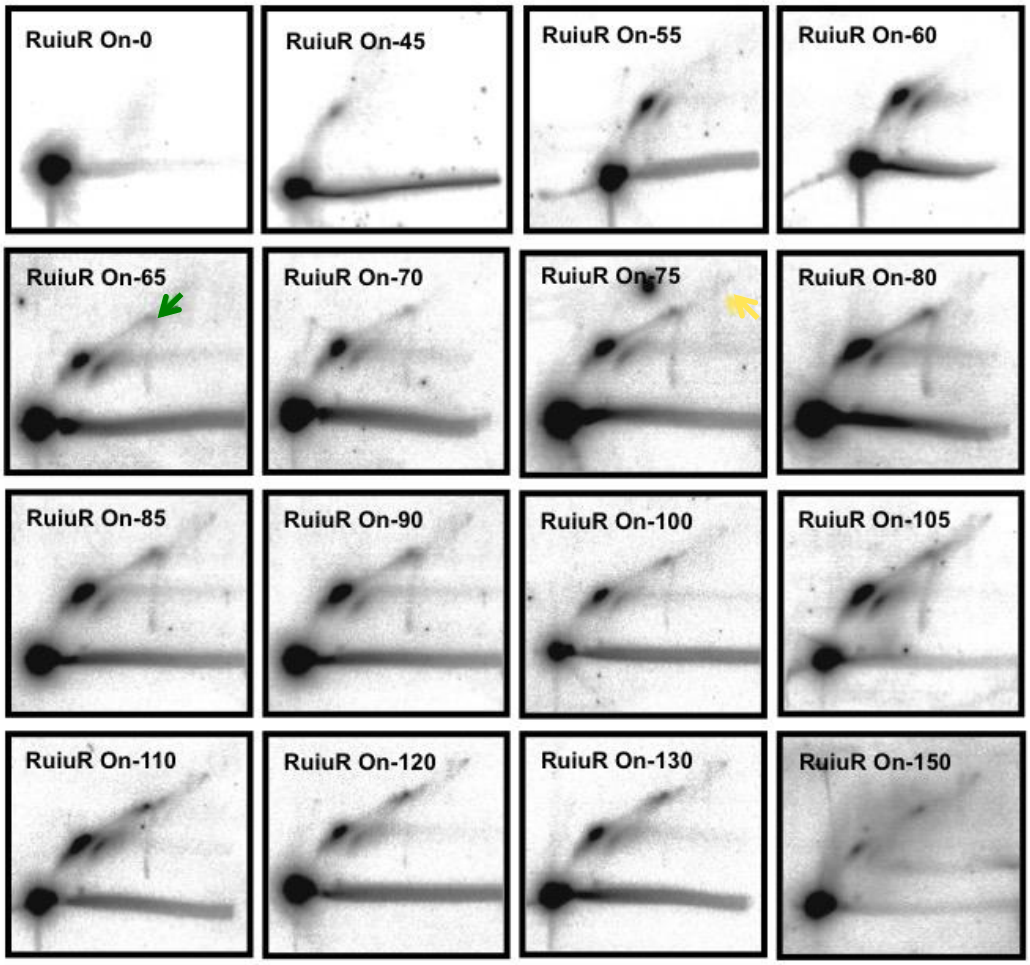

Figure 4.6 | Kinetics of HR-dependent restart in S phase. 2DGE analysis of replication intermediates at RuiuR. Probe Cen was used to detect signals in Southern blots. Cells were grown to early log phase and synchronised in mitosis. Fork stalling was induced 60 mins before the release and the time course started as the cells were released. Samples were collected at indicated time points. The green arrow (t=65) indicates the HR-dependent intermediates at the apex of the Y arc. The yellow arrow (t=75) indicates the HR-dependent intermediates on the X spike.

4.7 – DISCUSSION

In this chapter, the timing of HR-dependent restart of collapsed replication forks at *RTS1* in the RuiuR system was investigated. The analysis of cell cycle progression showed that both 'On' where replication arrest is induced at RuiuR and control 'Off' cultures progress through the cell cycle with similar kinetics with no delay into the entry to mitosis or S phase in the next cell cycle. However, chromosome mis-segregation was seen in at mitosis in the induced culture due to the formation of dicentric chromosomes. Investigation into the timing of HR-restart-dependent chromosomal rearrangements showed the accumulation of the dicentric species in ~15-20% of the cells in G2 when the replication barrier was active. This accumulation coincided with a decrease in the intensity of slow migrating intermediates. Analysis of these slow migrating forms showed that these corresponded to replication arrest and HR-dependent restart intermediates. Strikingly, restart occurred in S phase within 15 minutes of replication arrest, and the resulting HR intermediates were dealt with before mitosis.

Two mechanisms leading to GCRs in the fork stalling system were previously identified: non-allelic homologous recombination (NAHR), and the U-turn of the restarted fork (Lambert *et al.*, 2010; Mizuno *et al.*, 2013). NAHR occurs when the Rad51-coated 3' nascent strand behind the collapsed fork invades into the wrong homologous template leading to formation of a D-loop and the subsequent HJ(s) (Figure 4.7A). Depending on the orientation of the resolution of the HJ(s) either the parental chromosome is restored (non-cross over) or dicentric and acentic chromosomes are formed (cross over). The U-turn of the restarted fork, however, occurs when replication restarts via strand invasion on the correct template but the restarted fork is non-canonical and error-prone, and U-turns at the center of the palindrome resulting in

formation of the acentric and dicentric chromosomes (Figure 4.7B). Lambert *et al.* (2010) identified the HR-dependent replication intermediates resulting from NAHR by 2DGE in the RuraR fork stalling system, where rearrangements are only NAHR-dependent. Thus ectopic recombination events provide a marker for replication restart and it should be noted that replication restart on the correct template is not detectable by 2DGE. Lambert *et al.* defined two HR-dependent intermediates: a joint molecule spot was detected at the apex of the Y arc, which by semi-quantitative PCR only contained one junction between the *RTS1* repeats and thus corresponds to a D-loop, and the signal observed on the X spike which contained HJs. In the palindrome system RuiuR, however, rearrangements are dependent on both NAHR and U-turn of the restarted fork Mizuno *et al.*, 2013). The U-turn would be predicted to form a closed fork structure that would be converted to an HJ-like structure by the converging fork. After *Ase*I digestion the expected sizes for D-loop and U-turn intermediates are 10.5kb, and 10.3-10.7kb respectively. Therefore, both intermediates are predicted to run at the apex of the Y arc and are not distinguishable.

Analysis of replication intermediates after replication fork arrest at RuiuR showed the HR-dependent restart of the replication at *RTS1* 15 minutes after the fork collapse, judged by detection of the HR-dependent replication intermediates at both the apex of the Y arc and on the X spike. However, closer investigation of the timing of restart revealed a temporal separation between the time that the signal at the apex of the Y arc and the signal on the X spike were detected.

Figure 4.7

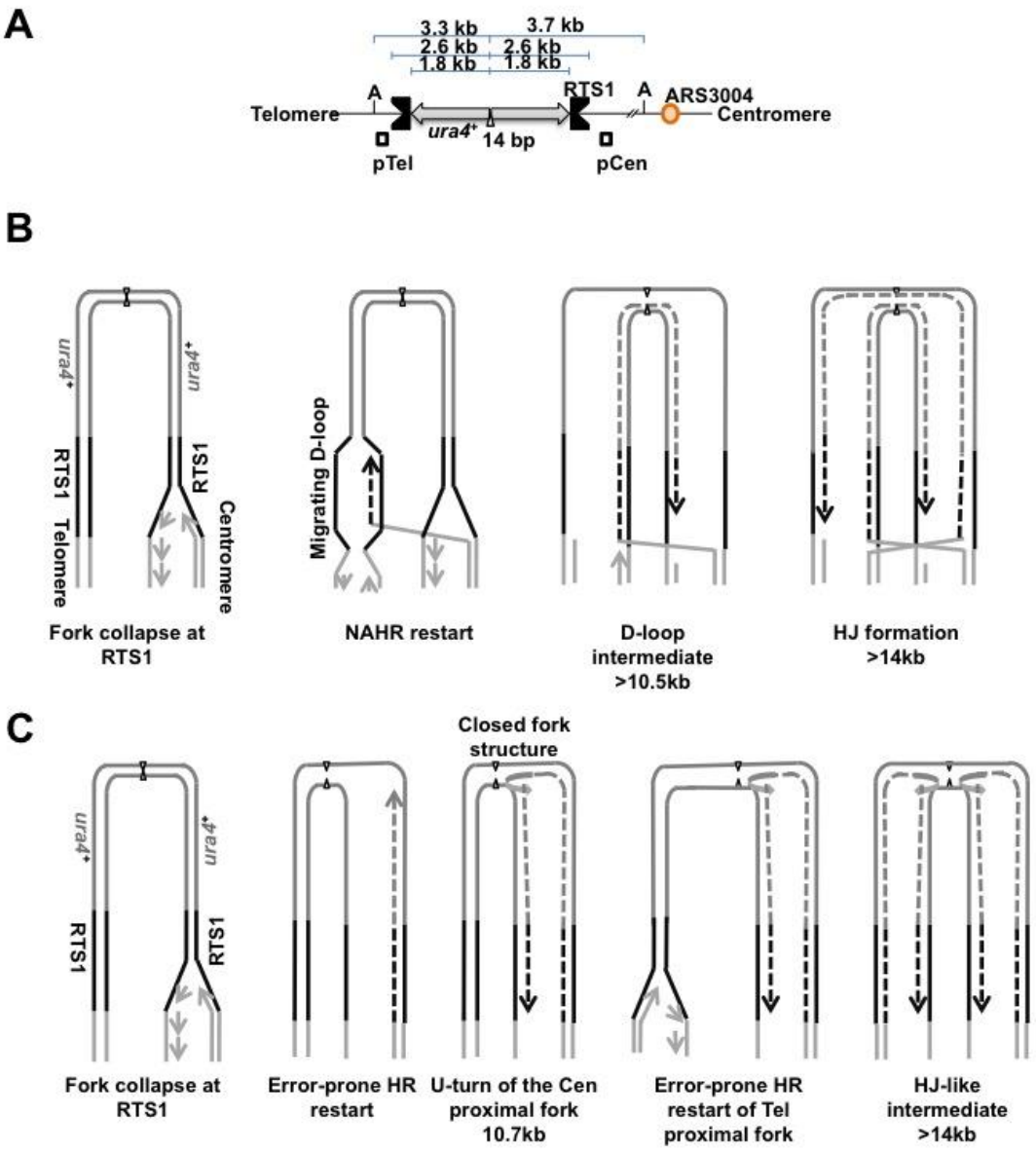

Figure 4.7 | HR dependent mechanisms of replication restart at *RTS1*. A- Cartoon showing the *Ase*I fragment of RuiuR. **B-** Model demonstrating the NAHR restart of the replication. After fork arrest, association of HR proteins forms a recombinogenic 3' end, which can invade either at the correct or incorrect locus. An invasion into the incorrect locus leads to formation of D-loop (10.5kb) and subsequent HJ formation (>14kb). Please note that a second end capture is also possible leading to formation of two HJs (not shown). Dashed lines indicate HR-restarted replication. **C-** Model for HR-dependent error-prone restart of replication. A recombinogenic 3' end formed at the arrest site at *RTS1* invades at the correct locus. The restarted fork is non-canonical and error-prone, and executes a U-turn (10.7kb) at the centre of the palindrome leading to GCRs. The dashed lines indicate the HR-dependent restart. Expected sizes of replication intermediates are noted below the corresponding cartoons.

This could suggest that conversion of a D-loop or a closed fork structure to HJ-like intermediates depends on the time required for the replication arrest and restart of the second fork. Alternatively, the delay between detection of closed fork/D-loop structures and the X shaped molecules could be an indicative of a temporal separation between the two pathways of the HR-dependent rearrangement. In both mechanisms of restart HJs or HJ like structures are formed, resolution of which results in GCRs. In the next chapter the relative contribution of the two pathways to the RI seen on replication restart is investigated.

In summary, these data determined the timing in a single cell cycle of replication arrest, HR-dependent replication restart and formation of GCRs upon induction of fork stalling. The timing of restart as measured by the detection of HR-dependent intermediates is consistent with the timing of replication of the intervening *ura4* sequences as measured by DNA copy number change (I. Miyabe, personal communication).

CHAPTER 5 – CHARACTERISATION OF REPLICATION INTERMEDIATES CORRESPONDING TO RESTART MECHANISMS

5.1 – INTRODUCTION

Two mechanisms have been identified for HR-dependent formation of acentric and dicentric chromosomes, NAHR template switch and the U-turn of the restarted fork (Lambert *et al.*, 2010; Mizuno *et al.*, 2013) (See figure 4.7). NAHR-dependent GCRs were generated in the RuraR fork stalling system where two inverted repeats of the *RTS1* are separated by 1.8kb *ura4*$^{+}$ gene. Introduction of an inverted repeat of the *ura4*$^{+}$ gene to create a 5.3kb palindrome containing inverted repeats of the *RTS1* sequence (RuiuR) resulted in a significant increase in the rates of GCR generation. This was originally thought to be due to the branch migration of the invading strand to create an HJ at the center of palindrome in the RuiuR system. However, GCRs were observed in TpalR system where ~500bp of the centromere proximal *ura4*$^{+}$ in RuiuR was truncated to eliminate branch migration, and the telomere proximal *RTS1* was replaced with *TER2/3* rDNA fork barriers to eliminate the possibility of faulty restart by NAHR (see Figure 1.7). It must be noted that fork restart at the rDNA barrier is not dependent on either Rtf1 or HR proteins and simply pauses the converging fork allowing more time for HR-dependent restart of collapsed fork at *RTS1* (Kings *et al.*, 2004; Mizuno *et al.*, 2013). Thus the GCRs generated in the TpalR system must be due the error-prone

nature of the restarted fork, which U-turns at the center of the inverted repeat. With the aim of identifying the timing of GCRs and replication intermediates corresponding to the U-turn event, experiments were set out to carry out over one cell cycle in TpalR system, as in this system which lacks a second *RTS1* NAHR is abolished. The RuraR system in which a U-turn event is not possible and rearrangements are due to NAHR was used to differentiate between the two HR-dependent chromosomal rearrangement mechanisms.

5.2 – TIMING OF RESTART DEPENDENT REARRANGEMENTS IN THE CELL CYCLE IN TPALR SYSTEM

In order to characterize the timing of chromosomal rearrangements in the TpalR fork stalling system, the strain *TpalR* P_{urg1_NR}*::rtf1-DSR nda3-KM311* was grown to early log phase. Cell cycle was arrested at 16°C for six hours and fork stalling was induced by addition of uracil to medium one hour before the release. Cell cycle was release by shifting the temperature to 30°C and samples for time course experiment were taken at intervals. DNA was extracted in agarose plugs and restriction fragment length analysis was performed using *Bgl*II. This was expected to give rise to a ~10kb initial band, a ~14kb band when DNA is rearranged to the dicentric form, and a ~5kb band corresponding to the acentric fragment (see Figure 5.1A for map and expected sizes of the *Bgl*II fragments at TpalR). Probe Cen homologous to sequences centromere proximal to TpalR was used to detect dicentric chromosomes in the Southern blots (Figure 5.1B). Consistent with the observations in the RuiuR construct, the 10kb original and the 14kb dicentric bands were observed and the intensity of the dicentric

band increased with a similar timing in G2 indicating the accumulation of dicentric chromosomes. Slow migrating replication intermediates were detectable by the start of the S phase (t=60), and declined in early G2 as dicentric chromosomes started to accumulate. Replication intermediates reappeared upon entry into the S phase of the second cell cycle after the release (time point 210-240). This data confirmed that the chromosomal rearrangements caused by the U-turn of the non-canonical restarted fork occur within a single cell cycle, and that the replication intermediates formed due to HR-dependent replication restart are dealt with before entry to mitosis.

Figure 5.1 (following page) | HR-dependent restart induces GCRs in TpalR in a single cell cycle. A- diagram showing the *Bgl*II sites at TpalR (left) and table showing the expected fragment sizes (right). **B-** Graph showing the mitotic and septation indices of the induced TpalR culture. Samples were collected at 15 minute intervals after the release and cells were fixed in methanol. DNA was stained with DAPI and septum with calcofluor. Cells with two separate nuclei were scored as mitotic (M), cells with two nuclei and septum as septated (S), and cells showing chromosome mis-segregation, bisection of DNA by septum, or lagging chromosomes as 'cut' (C). **C-** Southern blot from a representative time course showing the timing of the chromosomal rearrangements over a single cell cycle. Cells were grown to early log phase and synchronised in mitosis. Fork stalling was induced one hour before release and the time course started upon the release at 30^{o}C. Fragment length analysis was performed using *Bgl*II and probe Cen homologous to sequences centromere proximal to TpalR was used to detect the locus.

Figure 5.1

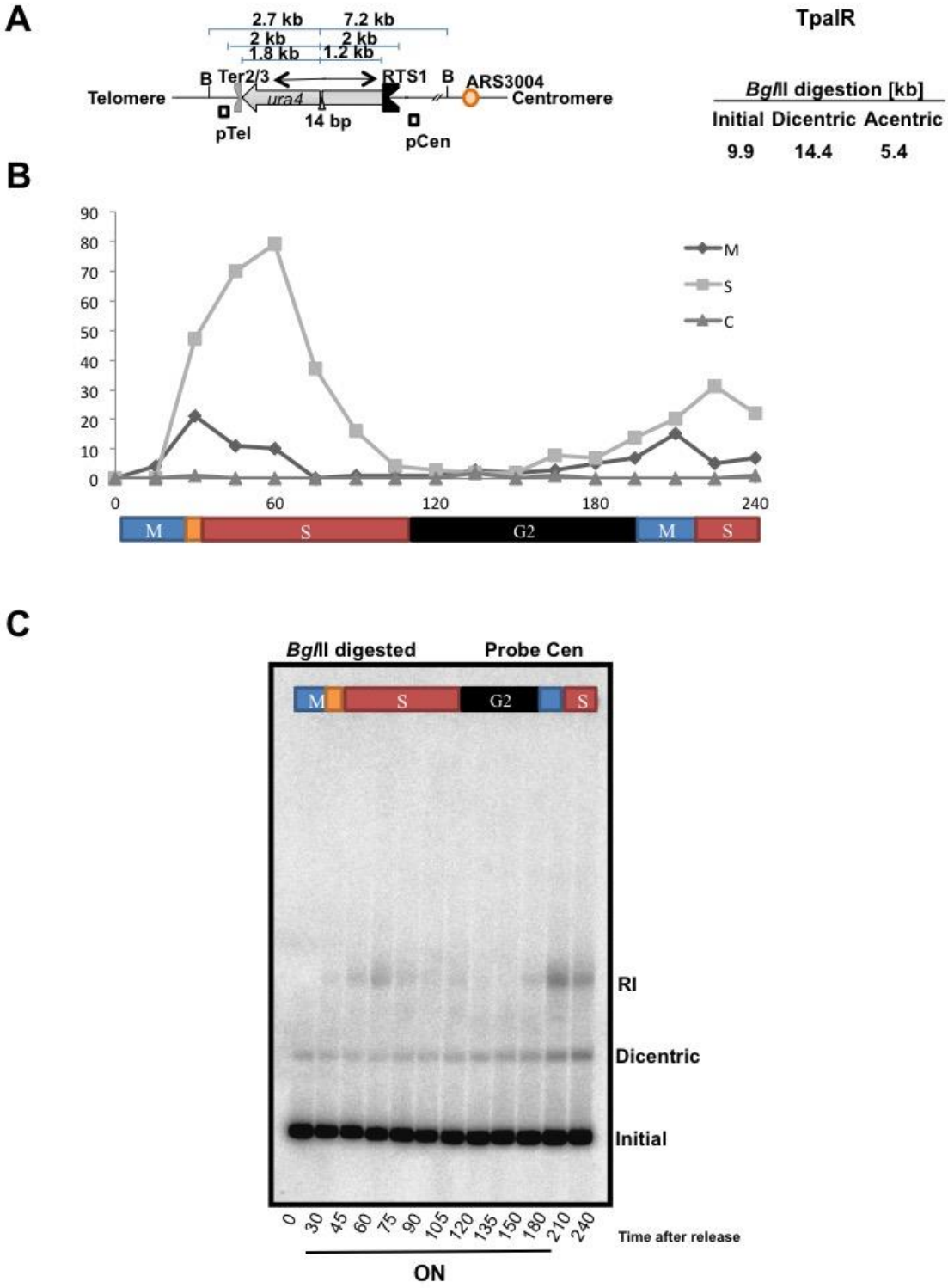
A
2.7 kb
7.2 kb
2 kb
2 kb
1.8 kb
1.2 kb
B
Ter2/3
RTS1
B
ARS3004
Telomere
ura4
Centromere
14 bp
pTel
pCen
TpaIR
BglII digestion [kb]
Initial Dicentric Acentric
9.9 14.4 5.4
B
90
80
70
60
50
40
30
20
10
0
0
60
120
180
240
M
S
C
M
S
G2
M
S
C
BglII digested
Probe Cen
M
S
G2
S
RI
Dicentric
Initial
0 30 45 60 75 90 105 120 135 150 180 210 240
Time after release
ON

5.3 – ANALYSIS OF REPLICATION INTERMEDIATES OF TPALR

In order to characterise the replication intermediates seen during the S phase in Figure 5.1, 2DGE was carried out in synchronous cell cultures. *TpalR* P_{urg1_NR}*::rtf1-DSR nda3-KM311* cells were grown to early log phase and synchronised in mitosis. Fork stalling was induced, or not, one hour before the release and the time course started as cells were released. Samples were taken at one-hour intervals in the uninduced culture and at 15-minute intervals over the S phase and 30-minute intervals over G2, covering up to the second cell cycle after the release in the induced culture. DNA was extracted in agarose plugs and digested with *Ase*I (see Figure 5.2A for *Ase*I sites in TpalR). 2DGE was performed and Probe Cen homologous to sequences centromere proximal to TpalR was used to detect replication intermediates in Southern blots. Figure 5.2B shows the result of this experiment in the 'Off' culture. At t=0 where cells were still in mitosis, only the 5.8kb monomer was detected. Passive replication indicated by formation of the Y arc was seen at time points 60 and 120 and this signal was gone at time point 180 after the release. A faint signal corresponding to arrest at *RTS1* was detected consistent with a slight degree of leakiness of P_{urg1}. Similarly to the experiments described in the previous chapter, in the induced culture (Figure 5.2C), at t=0 only the monomer was detected and initiation of the S phase was seen at 45 minutes after the release judged by detection of the Y arc and faint pausing at *RTS1* (~7kb). 60 minutes after the release, fork pausing at *TER2/3* was detected at ~6.5kb and full arrest at *RTS1* at ~7-8kb, indicating that replication fork arrest occurs with similar kinetics to the RuiuR system. Double arrest signal at both *RTS1* and *TER2/3* was detected on the double Y line at ~7.5-8.5kb. A signal was detected at the apex of Y arc corresponding to the predicted size of a U-turn intermediate (~8.9kb). Moreover, an extended double Y signal

reaching sizes bigger than 12kb was detected. This could be due to convergence of forks restarting at the *Ter2/3* barriers with the U-turn at the centre of the palindrome. In time points 75-135 the intensity of the fork arrest signals drops significantly indicating that most of the cells in the culture restart replication in this region. However a signal was observed on the X spike corresponding to accumulation of X structures and this signal was gone by 150 minutes after the release. At late G2/m (t=180) the replication intermediates were comparable to that observed in the 'Off' cultures, indicating that the replication intermediates formed upon HR-dependent restart at *RTS1* are dealt with before entry to the next cell cycle. In the S phase of the second cell cycle (t=240) the signals corresponding to the fork arrests and U-turn and HJ like intermediates reappeared. These data indicated that intermediates consistent with the U-turn of the restarted replication fork arise in the S phase, with similar timing to intermediates in the RuiuR system. X shaped molecules then accumulated, which disappeared in G2 prior to entry into the next cell cycle. This strongly suggests that the U turn of the restarted fork gives rise to a closed fork structure that is detectable as a defined spot on the Y arc. This is converted to double Y and X structures by the incoming fork. These intermediates are resolved in G2 into acentric and dicentric chromosomes, consistent with the resolution of HJ-like structures.

Figure 5.2 (following page) | HR-dependent restart occurs in S phase. 2DGE analysis of TpalR replication intermediates detected by a probe homologous to sequences centromere proximal to TpalR. Cells were grown to early log phase and synchronized. Fork stalling was induced, or not, 60 minutes before the release and the time course was started as cells were released. Samples were collected at indicated intervals. DNA was prepared in agarose plugs and digested using *Ase*I. **A-** Cartoon showing TpalR and *Ase*I restriction sites (left) and table showing the expected sizes (right) **B-** 2DGE analysis of the 'Off' state. The black arrow indicates the Y arc and the blue arrow indicates the monomer spot. **C-** 2DGE analysis of the 'On' culture. The red arrow indicates the arrest at *RTS1*, the green arrow shows the pause at *TER2/3*, and the orange indicates the double pause at *RTS1* and *TER2/3* sites. The purple arrow indicates the U-turn intermediate and the yellow arrow indicates the signal corresponding to accumulation of X shaped molecules.

Figure 5.2

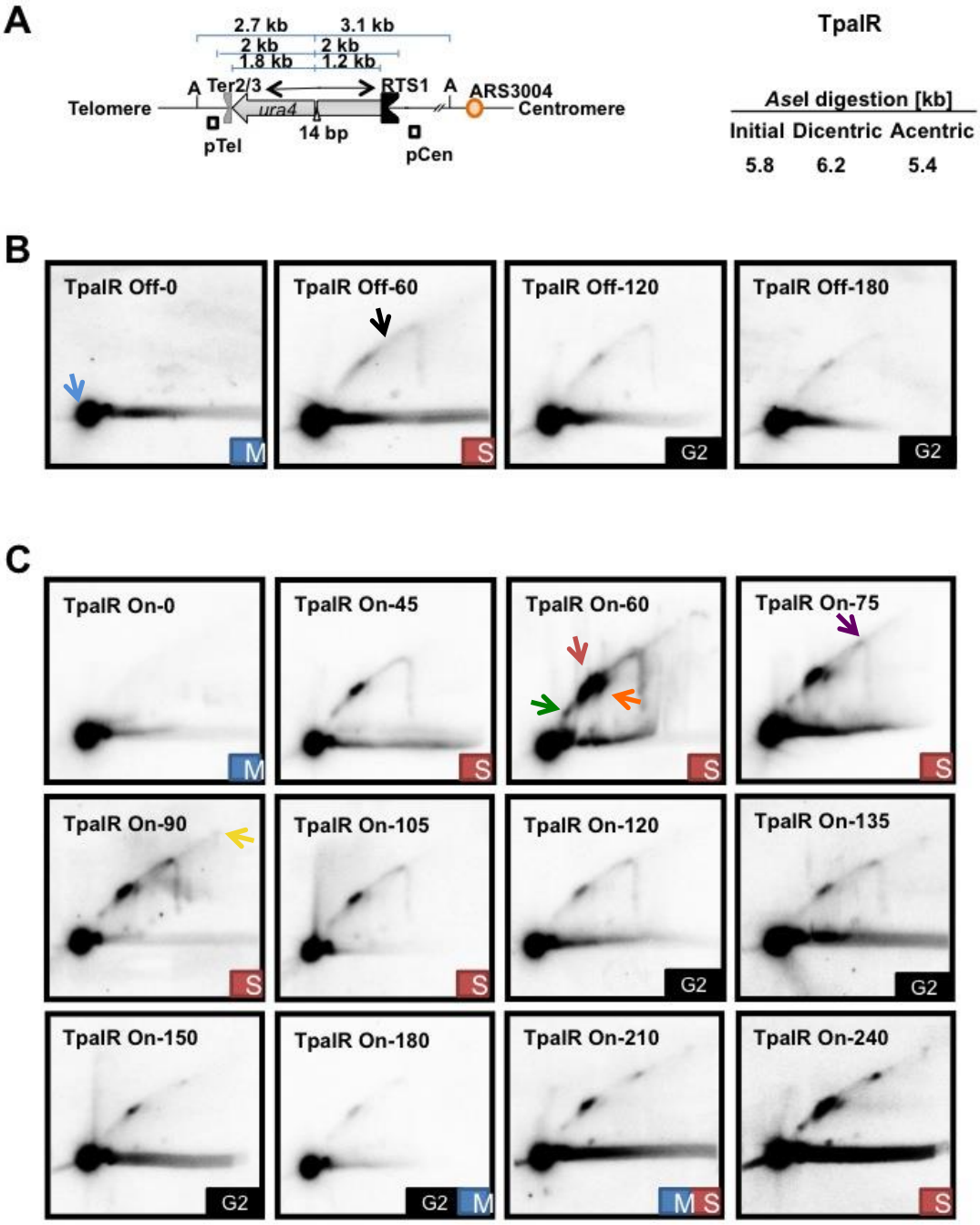
A
2.7 kb
3.1 kb
2 kb
2 kb
1.8 kb
1.2 kb
A Ter2/3
RTS1
A
ARS3004
Telomere
ura4
Centromere
14 bp
pTel
pCen
TpaIR
AseI digestion [kb]
Initial Dicentric Acentric
5.8 6.2 5.4
B
TpaIR Off-0
TpaIR Off-60
TpaIR Off-120
TpaIR Off-180
M
S
G2
G2
C
TpaIR On-0
TpaIR On-45
TpaIR On-60
TpaIR On-75
TpaIR On-90
TpaIR On-105
TpaIR On-120
TpaIR On-135
TpaIR On-150
TpaIR On-180
TpaIR On-210
TpaIR On-240
M
S
S
S
S
S
G2
G2
G2
G2
M
M S
S

5.4 – ANALYSIS OF REPLICATION INTERMEDIATES OF RURAR

In order to visualize the replication intermediates formed upon induction of fork stalling in the RuraR construct where a U-turn event is not possible, 2DGE was performed on samples obtained form synchronous cultures. Strain *RuraR* P_{urg1_NR}*::rtf1-DSR nda3-KM311* was grown to early log phase and cell cycle was synchronised. Fork stalling was induced, or not, one hour before the release and samples were taken at intervals upon the release. DNA was extracted in agarose plugs and digested with *Ase*I (see Figure 5.3A for a map of RuraR and *Ase*I sites). 2DGE was performed and Probe Cen homologous to sequences centromere proximal to RuraR was used to detect replication intermediates in the Southern blots (Figure 5.3). Analysis of replication intermediates of the 'Off' state (Figure 5.3B) indicated passive progression of replication throughout the cell cycle and a slight degree of fork arrest at centromere proximal *RTS1* showing the leakiness of *urg1* promoter. In the induced culture (Figure 5.3C), at t=0 after the release, where cells were completing mitosis, only the ~5.2kb monomer spot was detected. With similar timing to the previous systems initiation of S phase was evident at 45 minutes judged by the formation of Y arc and a faint arrest signal at centromere proximal *RTS1* at ~6.5-7kb, and detection of Y arc. 60 minutes after the release signals corresponding to telomere proximal (~6kb), centromere proximal, and double arrest (~7.5-8kb) at both *RTS1* sequences of RuraR were detected. While a signal corresponding to the D-loop intermediate was not detectable a faint X spike signal corresponding to HR-dependent intermediates was detected, and these intermediates accumulated by 90 minutes but were resolved by 150 minutes after the release (G2). In late G2 (t=180) only the monomer and a faint trace of arrest at centromere proximal RTS1 were detected. In the S phase of the second cell cycle (t=240) signals corresponding to fork arrests and HJ

intermediates reappeared. These data indicated that NAHR occurred in S phase and resolution of the resulting HR intermediates in G2, with a similar timing to resolution of intermediates due to the U turn of the restarted fork, before entry into the next cell cycle.

Figure 5.3 (following page) | Replication intermediates due to NAHR at RuraR. 2DGE analysis of RuraR replication intermediates detected by a probe homologous to centromere proximal sequences to RuraR. Cells were grown to early log phase and synchronized. Fork stalling was induced, or not, 60 minutes before the release and the time course was started as cells were released. Samples were collected at indicated intervals. DNA was prepared in agarose plugs and digested using *Ase*I. **A-** Cartoon showing RuraR and *Ase*I restriction sites (left) and table showing the expected sizes of rearrangements (right) **B-** 2DGE analysis of the 'Off' state. The black arrow indicates the Y arc and the blue arrow indicates the monomer spot. **C-** 2DGE analysis of the 'On' culture. The red arrow indicates the arrest at centromere proximal *RTS1*, the green arrow shows the arrest at telomere proximal *RTS1*, and the orange indicates the double pause at both *RTS1* sequences of RuraR. The purple arrow indicates the signal corresponding to HR intermediates.

Figure 5.3

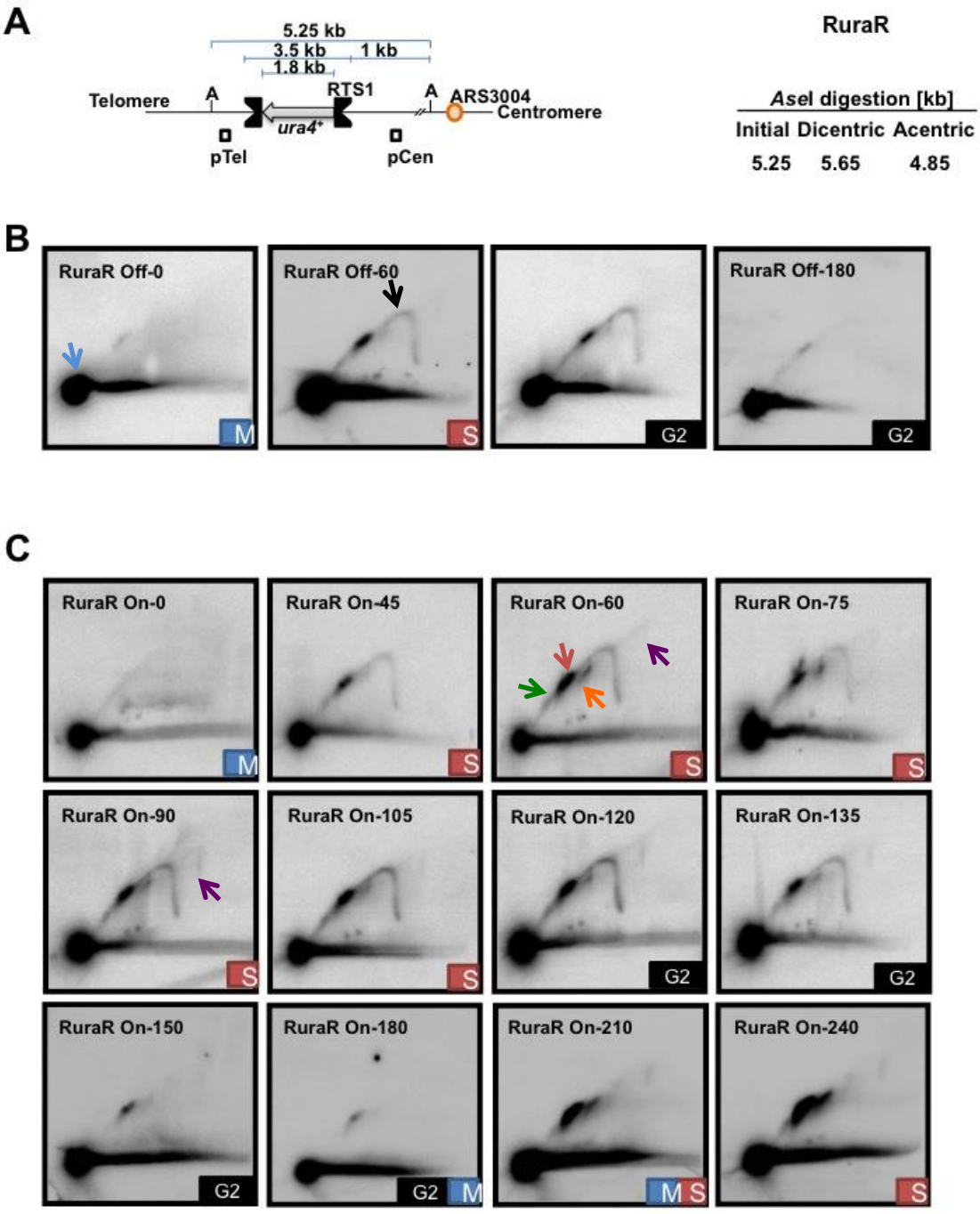
A
5.25 kb
3.5 kb
1 kb
1.8 kb
Telomere
A
RTS1
A
ARS3004
Centromere
ura4+
pTel
pCen
RuraR
AseI digestion [kb]
Initial Dicentric Acentric
5.25 5.65 4.85
B
RuraR Off-0
M
RuraR Off-60
S
G2
RuraR Off-180
G2
C
RuraR On-0
M
RuraR On-45
S
RuraR On-60
S
RuraR On-75
S
RuraR On-90
S
RuraR On-105
S
RuraR On-120
G2
RuraR On-135
G2
RuraR On-150
G2
RuraR On-180
G2 M
RuraR On-210
M S
RuraR On-240
S

5.5 – FURTHER CHARACTERIZATION OF PUTATIVE U-TURN INTERMEDIATE

The U-turn model of chromosome rearrangement at RTS1 predicts the formation of a closed fork like structure, which would migrate on the Y arc dependent on the restriction enzyme digest. In order to test that the signal observed at the apex of the Y arc in the TPalR system corresponds to the U-turn 2DGE was performed on DNA fragment digested with a different restriction enzyme (*Bam*HI). It was predicted that this would result in migration of the U turn signal on the downward large Y arc according to the restriction fragment length (Figure 5.4).

Cells were grown to early log phase and synchronized in mitosis. Fork stalling was induced, or not, 60 minutes before the release and samples were collected 90 minutes after the release. DNA was extracted and digested using *Bam*HI. Fork stalling at *RTS1* is predicted to form ~12kb pause spot on the small Y arc. The U-turn intermediate should run at ~14kb on the large Y arc. The analysis is complicated due to technical problems associated with running such large fragments on 2DGE. It was found that migration of the non-linear molecules was retarded and molecules did not run according to their true size. This can be seen by comparison of the dicentric monomer (blue arrow) and the pause signal (red arrow) which are both expected to run at ~12kb on the linear and Y arc respectively. However, if it is assumed that all non-linear molecules are retarded to similar extent and the faint spot detected on the large Y arc only in the 'On' culture (green arrow) would correspond to the U-turn intermediate. This supports the prediction that a closed fork structure would migrate on the Y arc according to size. To optimize and confirm this analysis both agarose gel concentration and running voltage of the first and second dimensions need to be reduced.

Figure 5.4

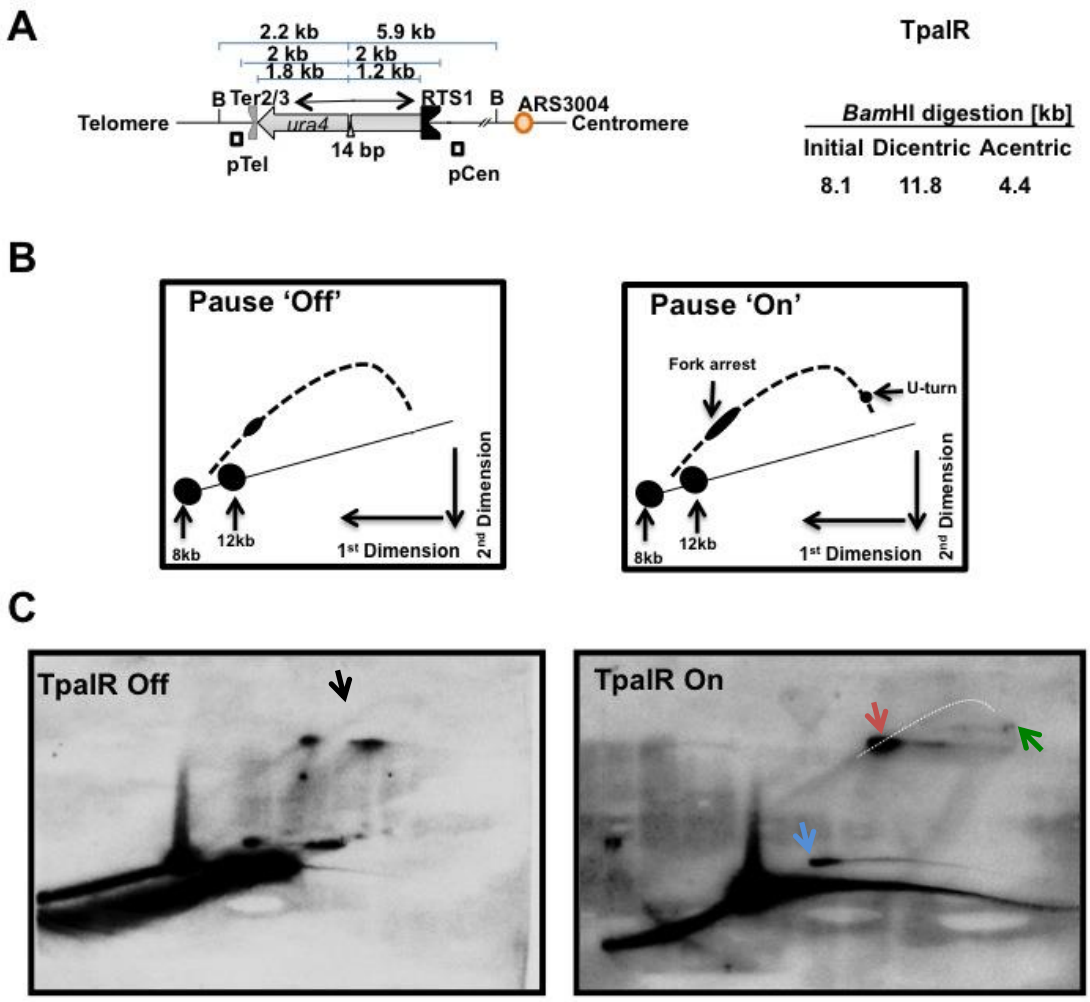

Figure 5.4 | Further characterization of putative U-turn intermediate. 2DGE analysis of TpalR replication intermediates detected by a probe homologous to centromere proximal sequences of TpalR. Cells were grown to early log phase and synchronized in mitosis. Fork stalling was induced, or not, 60 minutes before the release and samples were collected 90 minutes after the release. DNA was extracted in agarose plugs and digested using *Bam*HI. **A-** Cartoon showing TpalR and *Bam*HI restriction sites (left) and table showing the expected sizes of rearrangements (right) **B-** diagrams showing the predicted replication intermediates of TpalR when pausing is 'Off" (left) and 'On' (right). Rearranged dicentric chromosomes are expected at ~12kb on the linear. Fork stalling signal at *RTS1* is expected at ~12kb on the small Y arc. A U-turn intermediate is expected at ~14kb on the large Y arc. **C-** 2DGE analysis of the 'Off' state (left). The black arrow indicates the Y arc. 2DGE analysis of the 'On' culture (right). The red arrow indicates the arrest at *RTS1*, blue arrow indicates the dicentric monomer spot, and the green arrow indicates a spot corresponding to a U-turn intermediate on the large Y arc. The white dashed line traces the Y arc. Although the rearranged dicentric chromosomes and the pause signal are both expected to run at ~12kb on the linear and Y arc respectively, the migration of the non-linear molecules was retarded and not according to their true size. However, it can be assumed that all non-linear molecules are retarded to a similar extent and thus the spot detected on the large Y arc corresponds to the U-turn intermediate.

5.6 – DISCUSSION

Similarly to the findings in the RuiuR fork stalling system reported in previous chapter, here I show that in the TpalR fork stalling system, where restart by NAHR is not possible due to the absence of a homologous telomere proximal *RTS1* sequence, dicentric chromosomes start to accumulate in G2 phase of the cell cycle (1D gel). This accumulation occurred simultaneously with disappearance of slow migrating replication intermediates. Analysis of these intermediates showed HR-dependent restart of the collapsed fork in S phase, resulting in accumulation of HR intermediates that were resolved in G2 before entry into the next cell cycle. A replication intermediate corresponding to the expected size of a U-turn event was identified at the apex of Y arc. The U-turn model of chromosomal rearrangement at *RTS1* predicts formation of a closed fork like structure, which would migrate on the Y arc dependent on the restriction enzyme digest. Preliminary experiments using an alternative restriction digest support this but further experiments are required to optimize the 2DGE conditions and confirm these results.

Analysis of the replication intermediates in the RuraR system, where rearrangements occurs via the NAHR mechanism, showed the occurrence of the NAHR in the S phase, with the resulting HR intermediates being resolved in G2 prior to entry into the next cell cycle. A signal corresponding to a D-loop intermediate could not be detected. This may be due to the expected size of an D-loop intermediate (~6.2kb) as this would run with the signal corresponding to the fork arrest at centromere proximal *RTS1*. In addition, Lambert *et al.* (2010) used cross-linking agents to stabilize replication intermediates, and Benzoylated Naphthoylated DEAE–Cellulose (BND) to enrich for replication intermediates from steady state cultures. BND binds ssDNA in

high salt conditions. When DNA was prepared without crosslinking the D-loop signal was not detectable, suggesting the transient and labile nature of this intermediate. In contrast, the data presented in this chapter showed the detection of an intermediate corresponding to a U-turn event in the TpalR system, consistent with the closed fork-like structure being a more stable intermediate.

In both the TpalR and RuraR systems and the palindrome system RuiuR (see previous chapter) double Y or X shaped intermediates were detectable from 90 min. In TpalR these predominantly ran on the double Y arc, in RuraR were predominantly on the X spike and consistent with both types of rearrangements occurring in RuiuR on both arcs in this system. In all cases these intermediates decreased in G2 consistent with resolution of all intermediates occurring before mitosis. These data confirmed the occurrence of the HR-dependent restart in S phase and resolution of the resulting intermediates in G2 resulting in an accumulation of dicentric chromosomes. Moreover, considering the labile nature of a D-loop intermediate in this system and the more stable nature of a U-turn intermediate, it can be concluded that the intermediate detected at the apex of Y arc in RuiuR system (Chapter 4) likely corresponds to a U-turn event.

CHAPTER 6 – ANALYSIS OF CHECKPOINT RESPONSES TO GROSS CHROMOSOMAL REARRANGEMENTS

6.1 – INTRODUCTION

In previous chapters I determined the timing of replication restart of the collapsed fork and showed the generation of gross chromosomal rearrangements. Similar to the RuraR and TpalR fork stalling systems, in the RuiuR fork stalling system HR-dependent restart of the collapsed fork occurs in S phase, and this results in the generation of HR intermediates. These HR intermediates accumulated in S phase and were resolved in G2 (approximately 55 minutes later), coinciding with an increase in gross chromosomal rearrangements and accumulation of dicentric and acentric chromosomes. However, analysis of cell cycle progression showed no cell cycle delay and cells progressed into mitosis where chromosome bridges were formed at anaphase. This implied that the HR intermediates and subsequent GCRs were not detected by checkpoint machineries. Therefore I set out to directly investigate the checkpoint responses to replication restart dependent HR intermediates and GCRs. Given that in the RuiuR system GCRs were seen in ~15% of the population and since cross overs leading to acentric and dicentric chromosomes result from 50% of HJs, dependent on the plane of the resolution, it can be estimated that ~30% of cells in the population contains recombination intermediates that are resolved in G2. Thus this provides an ideal system to investigate whether HR intermediates at a single locus are detectable by the DNA integrity checkpoints.

As described in Chapter one, in fission yeast the ATR homologue Rad3 is activated in response to both replication stress and DNA damage, whereas the role of ATM homologue Tel1 is minimal in the checkpoint response. However, Rad3 dependent phosphorylation of effector kinases Cds1 and Chk1 can be used as a marker for activation of DNA replication checkpoint and DNA damage checkpoint respectively.

6.2 – A SINGLE ARRESTED FORK IS NOT SUFFICIENT FOR GLOBAL ACTIVATION OF DNA REPLICATION CHECKPOINT

To investigate the DNA replication checkpoint response to collapsed forks at an specific locus in the *S. pombe* genome, *RuiuR* P_{urg1_NR}*::rtf1-DSR nda3-KM311* cells were grown to early log phase and synchronised in mitosis. Fork stalling was induced before the release and time course samples were harvested at 15-minute intervals after release covering up to the end of the second cell cycle. In *S pombe*, depleting the nucleotide pool by HU treatment leads to global replication stress and activation of the replication checkpoint. As controls an asynchronous culture and cells exposed to HU for three hours were used. Whole cell protein was extracted and western blot analysis used to detect phosphorylation of Cds1 (Figure 6.1).

To test the sensitivity of the western blot assay, the phosphorylation shift of Cds1 was investigated in dilutions of protein extract obtained from the asynchronous cells treated with 10mM HU for three hours (+HU), with the -HU control from untreated asynchronous cells (Figure 6.1A). The phsophorylation shift of the Cds1 was detectable in all dilutions of the +HU samples (down to 1% +HU). To detect the possible activation of DNA replication checkpoint to forks collapsed at a specific locous

whithin the genome, phosphorylation shift of Cds1 was investigated in protein extracts obtained from cells harvested at indicated time points in Figure6.1B. In the HU treated control the mobility shift of pCds1 was detected indicating the activation of the DNA replication checkpoint (Figure 6.1B). However, no pCds1 shift was detected in either the first or the second S phase after the induction of fork stalling. As the majority (>90%) of replication forks arrest at *RTS1* in RuiuR (Lambert *et al.*, 2010), it can be concluded that a fork arrest at a single locus does not lead to global activation of the DNA replication checkpoint.

Figure 6.1

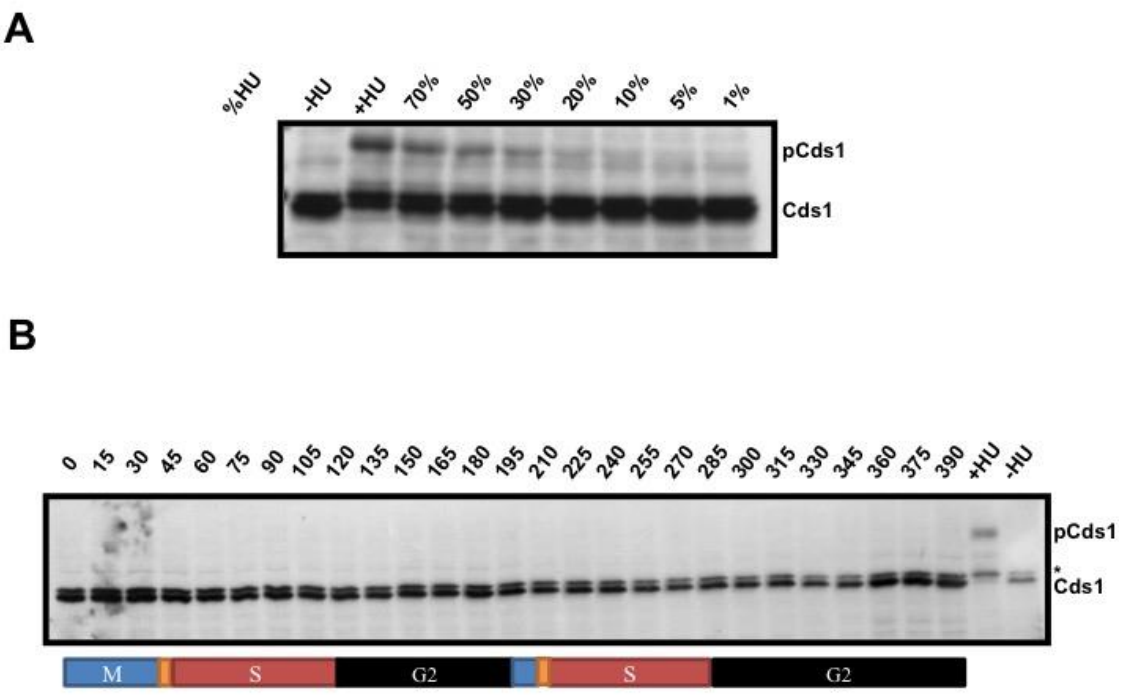

Figure 6.1 | Replication restart at single locus does not globally activate the DNA replication checkpoint. A- Western blot showing the detection of pCds1 shift in HU treated cells (+HU) and serial dilutions of HU treated extracts with the untreated asynchronous sample (-HU) indicated as percentage of the HU treated control in the diluted sample. pCds1 is detectable in dilutions down to 1% of the HU treated sample. **B-** Representative western blot showing the pCds1 shift after Rtf1 induction. The lane labeled **+HU** indicates asynchronous control cells treated with 10mM HU for three hours. Cds1 was detected by anti-Cds1 antibody. Asterisk indicates a none-specific band that acts as a loading control. The colored bar indicated the different stages of the cell cycle.

6.3 – DNA DAMAGE CHECKPOINT IS ACTIVATED IN THE SECOND CELL CYCLE AFTER FORK STALLING

To analyse the DNA damage checkpoint response to HR intermediates and GCRs, *RuiuR* P_{urg1_NR}*::rtf1-DSR chk1:3HA nda3-KM311* cells were grown to early log phase. Cell cycle synchronised in mitosis and Rtf1 induction was induced, or not, one hour before the release. The cell cycle block was alleviated and samples were harvested at 15-minute intervals for two cell cycles. Whole cell protein extracts were prepared and analysed by western blotting (Figure 6.2). The time course was also carried out on a 'no stall' *rtf1Δ* strain (*RuiuR* $P_{urg1\_NR::}$*HPH chk1:3HA nda3-KM311 rtf1::natMX6*). Asynchronous cells and cells treated with 200 Gy were used as controls to detect the phosphoshift of pChk1. Chk1 phosphorylation was detectable in neither the 'no stall' nor the 'Off' cultures when compared to pCk1 shift of ionising radiation treated control. In the induced culture, no pChk1 was detected in the first cell cycle but the mobility shift of pChk1 was visible in G2 of the second cell cycle (time point 285 onwards). This indicates that replication fork collapse at *RTS1*, HR restart dependent events that lead to formation of HR intermediates and subsequent accumulation of GCRs in the G2 after fork stalling do not activate the DNA damage checkpoint in the first cell cycle. However, the checkpoint was activated in the second G2 implying the dependency of this activation on passage through mitosis and cell division.

Figure 6.2

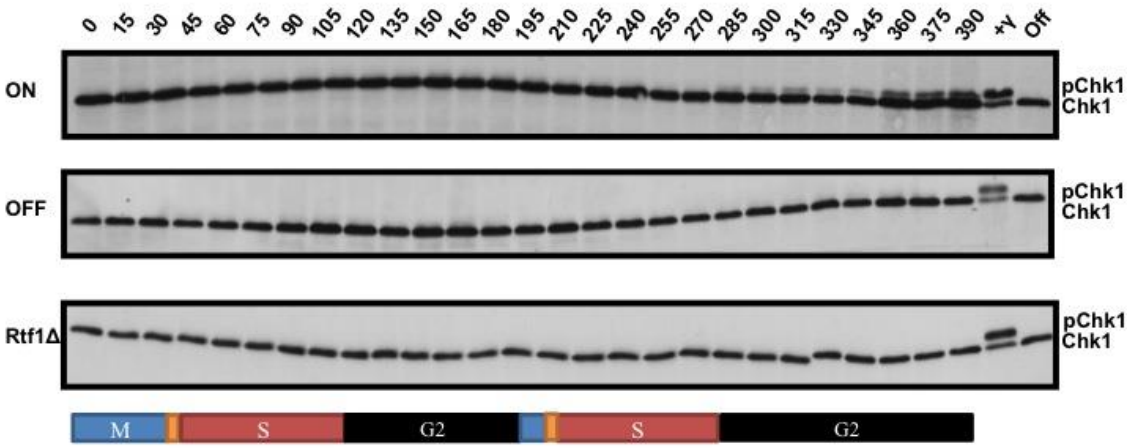

Figure 6.2 | DNA damage checkpoint is activated in the second cell cycle after induction of Rtf1. Representative western blot showing the pChk1 shift after Rtf1 induction in induced (top panel), uninduced (middle panel), and 'no stall' (bottom panel) cultures. The lane labeled **+γ** indicates asynchronous control cells treated with 200 Gy. (Cdc2 loading control is presented in Figure 6.4). Chk1-HA was detected by anti-HA antibody. The coloured bar indicates the different stages of the cell cycle.

6.4 – DNA DAMAGE CHECKPOINT ACTIVATION IS DEPENDENT ON PASSAGE THROUGH MITOSIS

HR- dependent restart of collapsed forks at *RTS1*, and the resulting acentric and dicentric chromosomes did not trigger a checkpoint response in the first cell cycle. The DNA damage checkpoint, however, was activated in the G2 of second cell cycle after induction of fork stalling. This implied checkpoint activation was due to the generation of DNA damage after segregation of the dicentric chromosome at mitosis. This chromosome would aline correctly at metaphase but form a chromosome bridge at anaphase. Breakage of the bridge by molecular forces or by septum formation at cytokinesis would generate a one-ended DSB in the next cell cycle. To test whether checkpoint activation was dependent on passage through mitosis, the second mitosis was disrupted using thiabenzadole (TBZ), a microtubule depolymerising drug. Cells from strain *RuiuR* P_{urg1_NR}*::rtf1-DSR chk1:3HA nda3-KM311* were grown to early log phase and synchronised in mitosis. Fork stalling was induced, or not, one hour before the release and samples were collected at 15-minute intervals after the release. TBZ was added to half of the induced culture 120 minutes after the release (G2). Whole cell protein extracts were prepared and western blot analysis was carried out. Asynchronous cells irradiated with 200 Gy were used as control to detect mobility shift of pChk1. Cell cycle progression was monitored by scoring mitotic and septation indices (Figure 6.3). Analysis of cell cycle progression showed normal progression of the cell cycle in the induced culture but partial inhibition of the second cell cycle in the induced culture treated with TBZ (Figure 6.3A). Note that TBZ treatment does not block progression of all cells into the next cell cycle. Investigation of Chk1 phosphorylation (Figure 6.3B) showed the absence of pChk1 shift in the uninduced culture but in the induced culture

without TBZ, the Chk1 phosphorylation shift was detected as expected in the second G2. However, the induced culture treated with TBZ failed to trigger a full checkpoint response (Quantified in Figure 6.3C). These data showed that while HR intermediates and GCRs did not trigger the DNA integrity checkpoints in the first cell cycle, the checkpoint is activated dependent on passage through mitosis. These data is consistent with the induction of DNA damage during mitosis and/or cytokinesis triggering a checkpoint response in the second cell cycle.

Figure 6.3

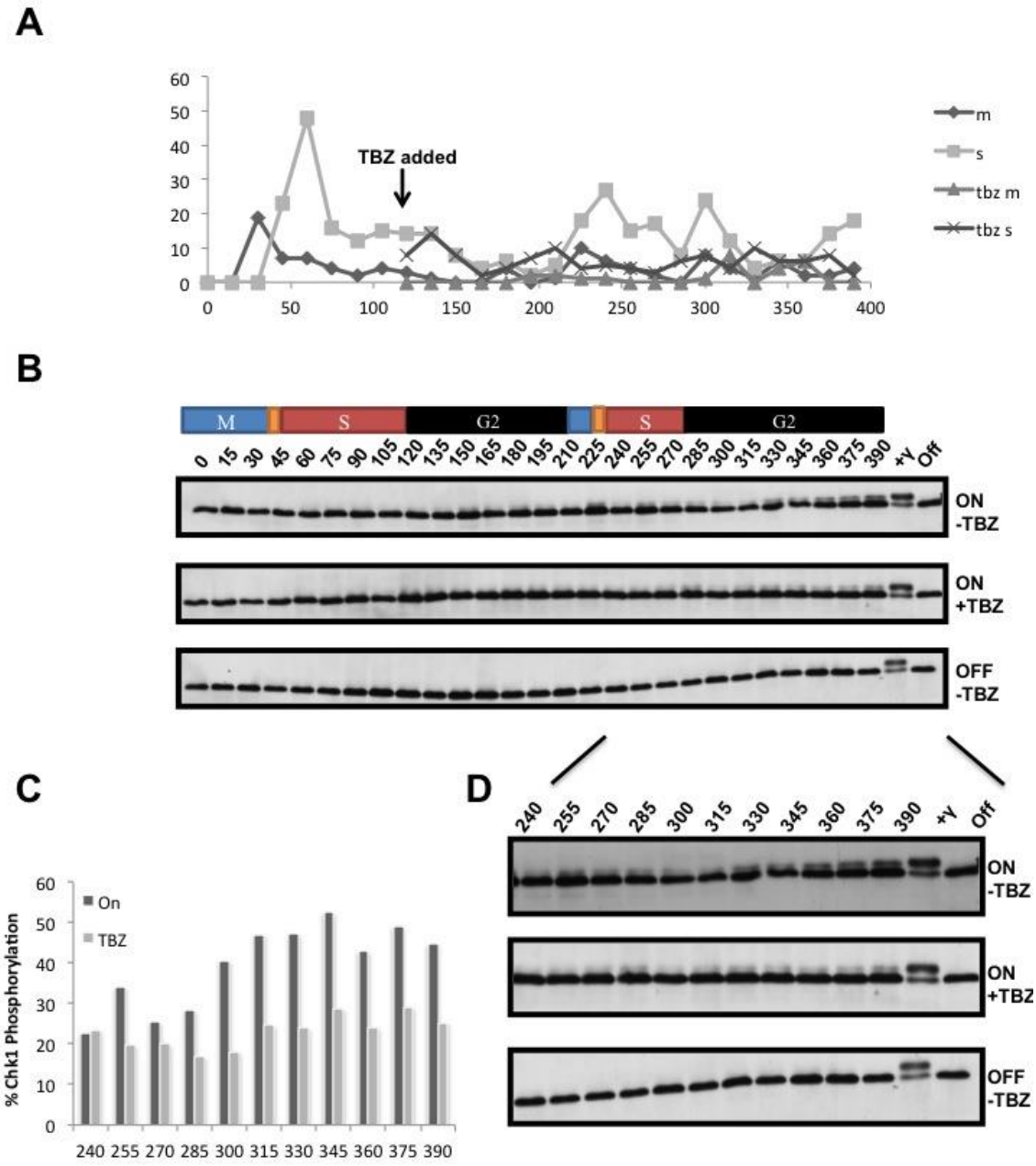

Figure 6.3 | Checkpoint activation is dependent on passage through mitosis. **A-** Graph showing the cell cycle progression of TBZ treated and untreated induced cultures. **m** and **s** denote the percentage of mitotic and septated cells after release from the mitotic block. **B-** Western blot analysis showing the mobility shift of pChk1 in induced –TBZ (top panel), induced +TBZ (middle panel), and uninduced -TBZ cultures. Coloured bar indicates different stages of the cell cycle. **C-** Quantification of Chk1 phosphorylation at indicated time points. **D-** Enlargement of indicated time points from **B**.

6.5 – DNA DAMAGE RESPONSE DOES NOT LEAD TO H2A PHOSPHORYLATION

As discussed in Chapter one, in response to DNA damage histone H2A is phosphorylated in an ATM/ATR dependent manner, and this assists recruitment of various downstream checkpoint proteins and checkpoint signal amplification. To examine the phosphorylation state of H2A after induction of fork stalling, *RuiuR* P_{urg1_NR}*::rtf1-DSR chk1:3HA nda3-KM311* cells were grown to early log phase and synchronised in mitosis. Rtf1 was induced, or not, 60 minutes before the release and samples were collected at intervals after the release. In parallel, the time course experiment was performed on an *rtf1Δ* 'no stall' strain. Whole cell protein extracts were prepared and western blot analysis was performed. Anti-pH2A antibody was used to detect pH2A (Figure 6.4). IR treated asynchronous cells were used as a control to detect H2A phosphorylation, and Cdc2 was used as a loading control. In neither 'On', 'Off', nor 'no stall' cultures was pH2A detectable in the first or the second cell cycles after the release. Therefore, a single site of DNA damage is not sufficient to induce global phosphorylation of H2A detectable by western blot analysis.

Figure 6.4

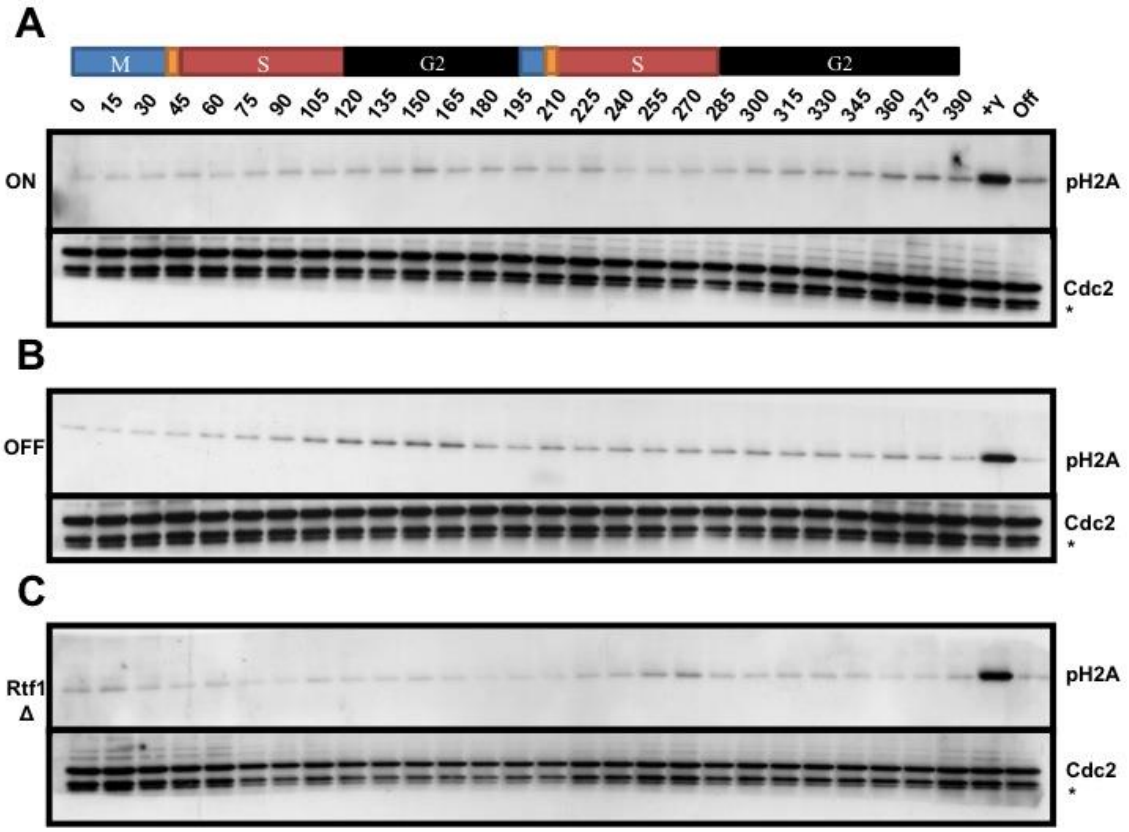

Figure 6.4 | A single DNA break does not lead to detectable levels of phosphorylation of H2A. Western blots showing the phosphorylation state of H2A (top panel) and Cdc2 loading control (bottom panel) in 'On' **A**, 'Off' **B**, and 'no stall' **C** cultures. The lane labeled with +γ indicates the IR (200 Gy) treated asynchronous control. The colored bar indicates different stages of the cell cycle. Asterisk indicates non-specific band. pH2A was detected with anti-pH2A antibody. Cdc2 was detected with anti-Cdc2 antibody.

6.6 – DISCUSSION

In this chapter the checkpoint response to events following restart of an arrested replication fork at a specific site in genome was investigated. In previous chapters I showed that induction of fork stalling in RuiuR system leads to fork arrest in S phase. Replication is restarted shortly after pausing and requires homologous recombination (Lambert *et al.*, 2005), but this restart occurs at the expense of generating in appropriate recombination intermediates that are resolved to form acentric and dicentric chromosomes in G2. However analysis of cell cycle progression showed no mitotic delay in response to HR intermediates or GCRs. Since the dicentric is a sister chromatid fusion with a single functional centromere, it is predicted that the centromere would align correctly at mitosis satisfying the SAC, but generate a chromosome bridge at anaphase. Breakage of the bridge by either spindle forces or breakage by the septum would lead to the daughter cells inheriting a single ended DSB.

GCR levels are not affected by loss of checkpoint proteins Rad3, Cds1, and Chk1 in the RuraR system (Tsang et al., 2014) or in the RuiuR palindrome system (K. Mizuno, personal communication). However, a slight loss of viability was seen in *rad3Δ* mutants consistent with a requirement for Rad3 to limit resection behind the collapsed fork (Tsang *et al.*, 2014). To establish the status of checkpoint activation in response to fork collapse and HR restart, the phosphorylation state of effector kinases of both intra-S (Cds1) and DNA damage (Chk1) checkpoint was investigated. Induction of fork stalling did not lead to activation of the replication checkpoint in either the first, or the second cell cycle after Rtf1 induction. This indicated that a single collapsed fork in not sufficient to globally activate the intra-S checkpoint. The lack of checkpoint activation in the second S phase after release could be due to the timing of breakage as

septum formation is coincident with second S phase. This would imply that breakage occurs as a result of cytokinesis rather than mechanical forces. Alternatively, the DSBs formed by mechanical breakage or cytokinesis are not processed to expose ssDNA during S phase. The DNA damage checkpoint was not activated in the first cell cycle after fork stalling induction but was activated in the second G2 dependent on passage through mitosis. This is consistent with processing at the DSB in G2 being dependent on CDK levels. No global phosphorylation of H2A was detected demonstrating that one DSB is not sufficient to detect H2A phosphorylation by western blot analysis. It should be noted that up to 15% of cells in the second cell cycle would contain a DSB but >90% of cells in the first cell cycle arrest and restart replication leading to ~30% containing HR intermediates which resolve into acentric and dicentric chromosomes in 15% of cells. Thus, the DNA damage checkpoint activation in the second cell cycle provides a control for the lack of activation in the first cell cycle.

CHAPTER 7 – DISCUSSION AND CONCLUSIONS

7.1 – OVERVIEW

Preserving genome integrity is of vital importance to cellular life. The genetic material is under constant insult from indigenous and exogenous agents resulting in replication arrest. Therefore, eukaryotic cells have evolved failsafe mechanisms, known as checkpoints, to ensure the detection and appropriate response to replication stress. The replication checkpoint helps to ensure the faithful completion of replication after replication stress by activating dormant origin firing, delaying cell cycle progression, maintaining arrested RFs in replication competent state, and preventing processing of arrested RFs, which can lead to genomic instability (Branzei & Foianai, 2005; Lambert *et al.*, 2007). Arrested replication forks can be rescued by dormant origin firing and converging replication forks, however in regions with low origin density or regions of unidirectional replication, replication restart mechanisms become essential for the completion of replication. Homologous recombination plays an important role in restart of arrested replication forks but at the expense of non-allelic homologous recombination (NAHR) resulting in loss of heterozygosity, gross chromosomal rearrangements (GCRs) and chromosomal instability (Carr & Lambert, 2013). Several lines of evidence have demonstrated the link between replication stress and human hereditary diseases, tumourigenesis and cancer (Magdalou *et al.*, 2014; Mirkin, 2007). Burrell *et al.* (2013) showed that replication stress was the main cause of chromosome instability in colorectal cancer. In human early embryonic development, replication arrest and restart

at small CGG repeats of FMR1 locus causes an alteration in the direction of replication leading to repeat expansion. This results in the absence of FMR1-encoded protein and leads to Fragile X syndrome (FXS), the most common form of hereditary mental disability in males (Gerhardt *et al.*, 2014).

The stochastic nature of replication stress has posed an obstacle to defining the role of checkpoints in response to individual replication problems and HR restart of replication forks. In this study I investigated the timing of HR-dependent replication restart and the checkpoints response to events following replication fork collapse at a specific locus in the genome of fission yeast.

To study site-specific replication restart a polar replication fork barrier enforced by Rtf1 binding to RTS1 sequences was employed. Induction of Rtf1 results in fork collapse at *RTS1* in S phase. HR is required for restart (Lambert *et al.*, 2005) but this is error prone and generates GCRs due to to NAHR (Lambert *et al.*, 2010) and the U-turn of the restarted started fork between small inverted repeats (Mizuno *et al.*, 2013). In this study I developed a system to analyse events in a single defined cell cycle following replication collapse and restart. Cell cycle synchrony using the cold sensitive beta tubulin mutant, *nda3KM311,* and rapid induction of Rtf1 expression using *urg1* promoter were optimised. Using this system, I showed that replication arrest at *RTS1* occurred in S phase. Collapsed replication forks were restarted by HR in S phase, at the expense of formation of HR intermediates that required resolving in 30% of the population. The nature of the intermediates resulting from the two alternative mechanisms generating GCRs was investigated. In both cases HR intermediates were resolved in G2 before entry into mitosis, coinciding with the accumulation of GCRs in ~15% of the population. Investigation into the activation of the DNA integrity checkpoints showed that replication arrest, HR-dependent restart, and accumulation of

GCRs do not globally activate either the DNA replication or DNA damage checkpoints in the first cell cycle. However, the DNA damage checkpoint was activated in G2 of the second cell cycle.

7.2 – REPLICATION INTERMEDIATES

In the fork stalling systems, forks collapse at *RTS1* and subsequent HR-dependent restart drives accumulation of HR joint molecules, which I showed to peak in S phase and decline in G2. Previous work in the Carr, Lambert, and Murray laboratories identified two mechanisms of formation of GCRs in the *RTS1* fork stalling systems, NAHR and U-turn of the restarted fork (Lambert *et al.*, 2010; Mizuno *et al.*, 2013). The HJ-like intermediates observed in approximately ~30% of the population (estimated based on the level of cross-over products observed) in RuiuR are the result of both mechanisms. Mizuno *et al.* (2013) showed that in the RuiuR system the majority of dicentic formation is due to error-prone nature of the restarted fork executing a U-turn at the centre of the palindrome.

In NAHR the first detectable HR intermediate is the D-loop (Lambert et al, 2010) (see Figure 4.3). In the alternative mechanism the non-canonical and error-prone restarted replication fork U-turns at an inverted repeat. This is predicted to form a closed fork structure. Since both D-loop and U turn are predicted to run at the same place in the RuiuR system I used two separate systems to distinguish U-turn and NAHR events: TpalR, where NAHR is abolished, and the original Lambert system RuraR, where there is no palindrome and only NAHR is possible. While the D-loop was not detectable (likely due to the fact that crosslinking was not employed to prevent branch

migration), I identified a stable replication intermediate corresponding to the U-turn event on both RuiuR and TpalR (Chapters four & five). This migrated on the Y arc dependent on size consistent with it being a closed Y structure. This is the first characterisation of this structure. Future work would be to optimise the amount of this intermediate with a view to visualisation by EM.

7.3 – HOLLIDAY JUNCTIONS

Restart by NAHR is predicted to give rise to intermediates containing a single HJ or in the case of a second end capture double HJs (dHJs). (The model for the generation of single HJs is given in Figure 4.7. For the dHJ model see Lambert *et al.*, 2010). These HJ intermediates were visible in the RuraR system as a descending X spike and were present from S to early G2 (75-135 minutes).

The error-prone model of replication restart at *RTS1* (U-turn) also predicts the formation of HJ-like intermediates upon convergence of the second restarted fork (Mizuno *et al.*, 2013). The exact nature of this structure is unknown but it was visible in both RuiuR and TpalR systems as an extension to the double Y structure terminating at the top of the X spike (consistent with it being an HJ-like structure). Given the constraints of sister chromatid cohesion it could be argued that, unlike the HJs formed by NAHR, this structure might not be recognised and resolved until under tension in mitosis (see Figure 7.1) but these intermediates declined in G2with a similar kinetics to the HJs seen in the RuraR system. These data indicated that the U-turn of the restarted fork results in the formation of HJ-like intermediates, which are processed in G2.

Figure 7.1

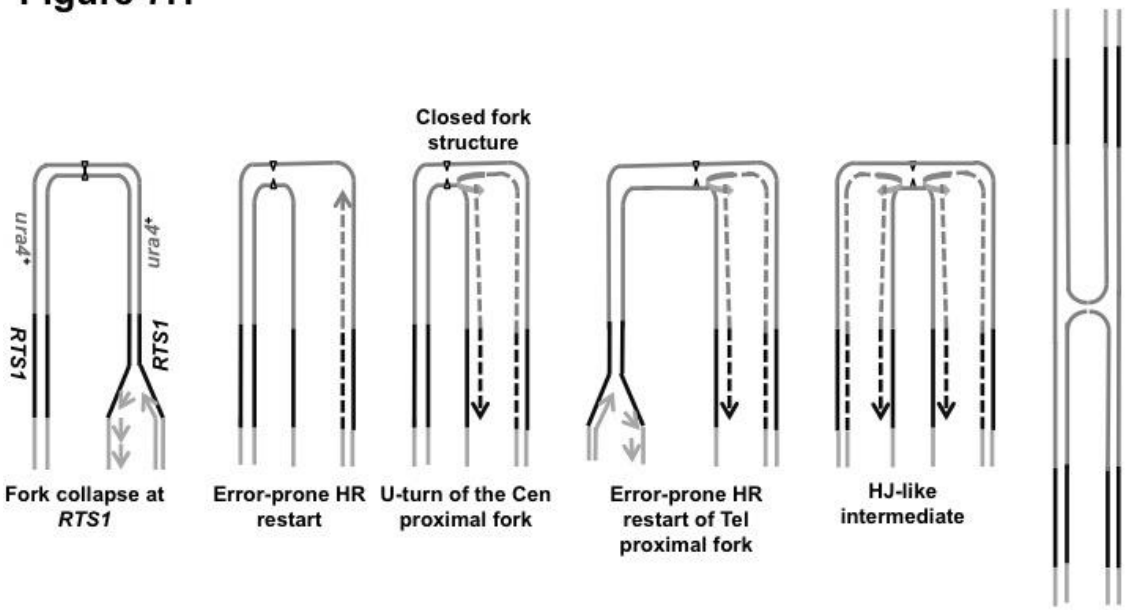

Figure 7.1 | U-turn of the HR-restarted fork. Model illustrating the error-prone HR-dependent restart of the collapsed fork at *RTS1*. This model predicts formation of a closed fork structure, which is converted into a HJ-like structure.

7.4 – RESOLUTION OF INTERMEDIATES

Restart by NAHR is predicted to give rise to intermediates containing a single HJ or in the case of a second end capture double HJs (dHJs). The error-prone model of replication restart at *RTS1* (U-turn) also leads to intermediates that resemble a single HJ (Mizuno *et al.*, 2013). All these intermediates require further processing by dissolvase or resolvase complexes.

dHJs can be dissolved through the action of the RecQ helicase in concert with Top3 (Wu & Hickson, 2003). In *S. pombe* this activity is carried out by Rqh1 in collaboration with topoisomeraseIII. However, Lambert *et al.* (2010) argued that Rqh1 was dispensable for processing of dHR intermediates formed by NAHR due to their inability to branch migrate in the RuraR system. Consistent with this both the level of HR intermediates and viability were not affected in a *rqh1* null background (Lambert *et al.*, 2010). Single HJs are not dissolvable and must be resolved. This is the case for single HJs resulting from NAHR and for U-turn intermediates that are postulated to resemble a single HJ-like structure.

In bacteria, RuvC has been shown to have selective resolvase activity for double stranded four-way HR joint molecules (Benson & West, 1994; Takahagi *et al.*, 1994). A RuvC homologue has not been identified in eukaryotic cells but structure specific nucleases have been proposed to resolve HR intermediates (Shwartz & Heyer, 2011). Three resolvase complexes have been identified in eukaryotes, *Sp*/*Sc*Slx1-Slx4, *h*SLX1-SLX4, *Sc*Yen1/*h*GEN1, and *Sp*Mus81-EME1, *Sc*Mus81-Mms4, *h*MUS81-EME1. Unlike budding yeast and higher eukaryotes, no Yen1/GEN1 homologue has been identified in fission yeast. The structure-specific nuclease activity of Slx1-Slx4 has been demonstrated on an array of branched molecules owing to Slx1 enzymatic activity

(Coulon *et al.*, 2004; Fekairi *et al.*, 2009; Fricke & Brill, 2003; Munoz *et al.*, 2009; Svendsen *et al.*, 2009), but deletion of core Rad52 proteins does not restore viability of *sgs1Δ, sgs1Δ slx1/slx4Δ* backgrounds indicating that Slx1-Slx4 does not act on processing of HR intermediates (Bastin-Shanower *et al.*, 2003). Rather the complex is required for maintenance of rDNA homeostasis (Coulon *et al.*, 2006; Kaliraman & Brill 2002).

Unlike Slx1-Slx4, loss of viability of *rqh1Δ mus81Δ* is restored by deletion of HR genes (Boddy *et al.*, 2000) indicating the role of Mus81 in processing of HR intermediates in the absence of dissolvase in fission yeast. To eliminate the inappropriate processing of stalled replication forks, the nuclease activity of Mus81-Eme1 complex is cell cycle regulated. In budding yeast Mus81-Mms4 is activated in G2 by Cdc5-dependent phosphorylation of Mms4 (Gallo-Fernández *et al.*, 2012; Matos *et al.*, 2011). In fission yeast, Eme1 is phosphorylated in a cell cycle-dependent manner by Cdc2 (CDK), and this primes Eme1 for Rad3-dependent super phosphorylation which results in activation of the complex (Dehe *et al.*, 2013). Moreover in *S. pombe*, in response to replication stress, Mus81 is negatively regulated by Cds1 and excluded from chromatin (Boddy *et al.*, 2000; Froget *et al.*, 2008; Kai *et al.*, 2005). The cell cycle dependent regulation of Mus81-Eme1 complex could explain the persistent nature of the HR intermediates observed after replication restart in fork stalling systems until G2. HR-dependent restart leads to formation of the HR joint molecules that are resolved in G2 when Mus81-Eme1 complex is activated. This could be tested either by creation of a Mus81 ‘shut off’ strain, in which Mus81 expression is controlled by *nmt4*1 repressible promoter, or using auxin inducible degron (AID) system, which involves a plant specific protein degradation mechanism depending on response to auxin, and a conserved poly ubiquitination pathway (Kanke *et al.*, 2011).

In higher eukaryotes, the MUS81-EME1 complex exists throughout the cell cycle but requires interaction with SLX1-SLX4 complex for its HJ resolution activity. This interaction is cell cycle regulated and occurs predominantly at prometaphase. This is proposed to be due to a preference for HJ dissolution by BLM, and to prevent inappropriate processing of HJs by MUS81 in early stages of the cell cycle (Castor *et al.*, 2013; Garner *et al.*, 2013; Wyatt *et al.*, 2013). In *S. pombe*, Mus81-Eme1 activity is also cell cycle regulated through CDK-dependent phosphorylation of Eme1. However this phosphorylation peaks after S phase and the complex is most active in G2. This is thought to minimise inappropriate Mus81 processing to prevent genomic instability in S phase, and to ensure resolution of intermediates that eluded Rqh1 processing before mitosis. This also highlights the dependency of fission yeast on Mus81 for HJ processing, likely due to the lack of a Yen1/GEN1 homologue (Boddy et al., 2001; Dehe et al., 2013).

7.5 – CHECKPOINT ACTIVATION

Investigation of the checkpoint responses (Chapter six) to replication stalling and HR-dependent restart, showed no checkpoint activation in the first cell cycle after fork stalling when HR intermediates were formed and resolved into isochromosomes, but the DNA damage checkpoint was activated in the second cell cycle. The checkpoint sensors ATM and ATR respond to extended regions of stretches of RPA coated ssDNA. ssDNA is formed during S phase due to uncoupling of replicative helicase and polymerase at stalled forks and in G2 by processing of DSBs. Replication arrest at the *RTS1* DNA protein barrier is thought to act via blocking the replicative helicase

(Eydmann *et al.*, 2008) and thus ssDNA is not exposed by uncoupling of replicative holoenzyme. Rather fork collapse leads to fork regression generating a 3' end, which coated by Rad51, can invade into the original template independently of a DSB (Lambert *et al.*, 2010; Mizuno *et al.*, 2009). Tsang *et al.* (2014) showed that Rad3 (ATR) checkpoint sensor limited the resection behind the collapsed fork at *RTS1* but did not affect the HR-dependent restart or GCRs. Consistent with lack of ssDNA formation during the block and restart at *RTS1* I showed that the intra S checkpoint was not globally activated in the first cell cycle after the release as judged by Cds1 phosphorylation. Thus the intra S phase checkpoint acts locally to restart replication at the site of damage rather than globally to inhibit mitosis.

I showed the dependency of DNA damage checkpoint activation on passage through mitosis in the second cell cycle after induction of fork stalling. This suggests occurrence of a DSB during mitosis or cytokinesis. In human cells this would activate a checkpoint in G1 (Giunta *et al.*, 2010) but in the *S. pombe* system used here cells proceeded into S phase without delay. This may be due to the fact that S phase is coincident with septation and therefore a break at cytokinesis may not occur before the cells are in S phase. The DNA replication checkpoint prevents end resection during the S phase (Boddy et al., 2000; Hu *et al.*, 2012; Sogo *et al.*, 2002; Tsang *et al.*, 2014). DNA end resection of DSBs has been shown to be CDK dependent and therefore limited in G1 and S. Collaboration of the MRN complex with Ctp1 (*Sc*Sae2/*h*CtPI) is required for initiation of resection at DSBs (Garcia *et al.*, 2011; Symington & Gautier, 2011). CDK-dependent phosphorylation of Sae2/CtPI has been shown to promote resection at DSBs (Huertas *et al.*, 2008; Huertas & Jackson, 2009). In fission yeast, Ctp1 expression is cell cycle regulated with no to low abundance in G1-S and highest expression in G2 (Limbo *et al.*, 2007). It has been shown in budding yeast that once

resection is initiated by MRN-CtpI, Exo1 in concert with Sgs1-Dna2 carries out long-range resection (Gravel *et al.*, 2008; Mimitou & Symington, 2008). Exo1 is phosphorylated by CDK in S/G2 and this promotes its end resecting ability (Tomimatsu *et al.*, 2014). Also, CDK-dependent phosphorylation of Dna2 has been shown to promote its recruitment to the site of DSB, and resection (Chen *et al.*, 2011). In the system used here activation of the DNA damage checkpoint in G2 implies that the cell cycle-dependent regulation of resection of the DSB formed by dicentric breakage delays processing until G2 of the second cell cycle after fork stalling induction, exposing ssDNA and subsequently activating the DNA damage checkpoint.

7.6 – MODEL

The data presented in this study leads to the following model (Figure 7.2) in which replication collapse at *RTS1* is restarted by HR mechanisms in S phase leading to accumulation of HR intermediates. The absence of ssDNA in these structures results in no signalling to the intra S or DNA damage checkpoints. The accumulated HR intermediates are resolved in G2, consistent with when Mus81/Eme1 becomes active, leading to the accumulation of GCRs. Dicentric chromosomes align correctly on spindle satisfying the spindle assembly checkpoint and anaphase is triggered. This results in formation of chromosome bridges that break producing a DSB during mitosis and/or cytokinesis and leading to the daughter cells inheriting a one-ended DSB. Resection is prevented by the intra S checkpoint but the DSB is subject to processing in G2 when CDK levels rise resulting in the accumulation of RPA coated ssDNA. The exposed ssDNA activates the DNA damage checkpoint in the second cell cycle.

Figure 7.2 (following page) | Model of checkpoint activation in response to replication fork collapse and restart. Activation of fork barrier activity leads to fork collapse at *RTS1*. Replication is restarted in a DSB-free homologous recombination dependent manner in S phase, without activating the intra S checkpoint due to lack of ssDNA. However, this restart event is error prone and leads to accumulation of HR intermediates in S phase. These HR intermediates are resolved in G2 giving rise to acentric and dicentric formation. Rearranged dicentric chromosomes are captured by spindle and broken by formation of septum (cytokinesis, coincident with second S phase). The intra S checkpoint prevents resection of this DSB in the second S phase. However, high CDK activity leads to DSB resection in G2, exposing ssDNA. This in turn, activates the DNA damage checkpoint (Chk1) in the second cell cycle after induction of fork stalling.

Figure 7.2

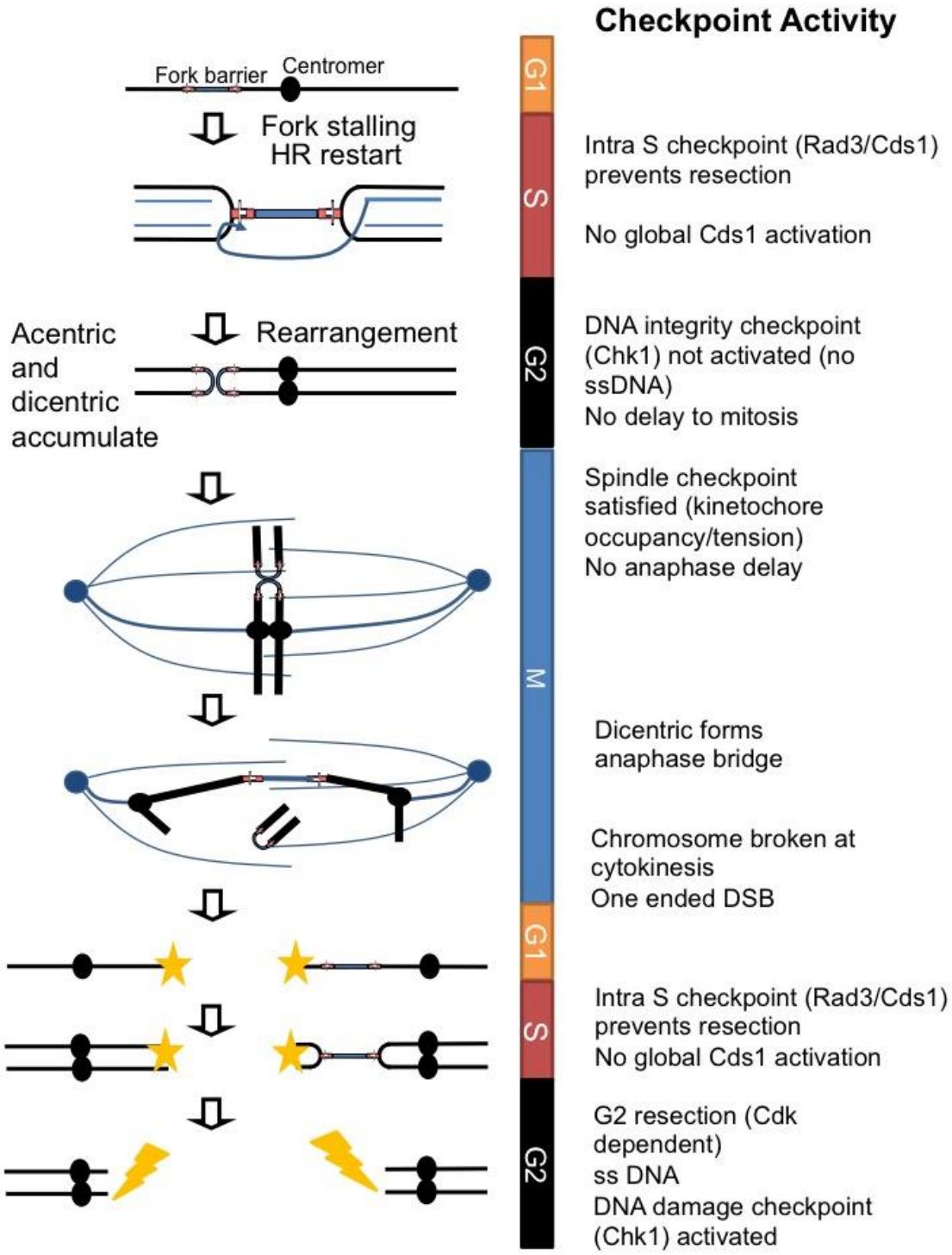
Checkpoint Activity
Fork barrier
Centromer
Fork stalling
HR restart
Intra S checkpoint (Rad3/Cds1) prevents resection
No global Cds1 activation
G1
S
G2
Acentric and dicentric accumulate
Rearrangement
DNA integrity checkpoint (Chk1) not activated (no ssDNA)
No delay to mitosis
Spindle checkpoint satisfied (kinetochore occupancy/tension)
No anaphase delay
M
Dicentric forms anaphase bridge
Chromosome broken at cytokinesis
One ended DSB
G1
Intra S checkpoint (Rad3/Cds1) prevents resection
No global Cds1 activation
S
G2 resection (Cdk dependent)
ss DNA
DNA damage checkpoint (Chk1) activated
G2

7.7 – CONCLUDING REMARKS

These results are of importance as defects in DNA replication have been shown to greatly increase chromosomal instability, and chromosomal instability is hallmark of cancer development (Branzei & Foiani, 2007). Common fragile sites (CFSs), first described as gaps induced in human metaphase chromosomes under mild replication stress, are known to have difficult to replicate sequences prone to form secondary structures, harbour large genes, and exhibit low origin density (Franchitto, 2013).

Several studies have shown replication stress dependent expression of CFSs, leading to chromosomal instability and cancer development (Le Beau *et al.*, 1998; Hellman *et al.*, 2000; Mitsui *et al.*, 2010; Ozeri-Galai *et al.*, 2011; Palakodeti *et al.*, 2004; Palakodeti *et al.*, 2010; Ried *et al.*, 2000; Wang *et al.*, 1999). Our fork stalling system offers a versatile tool to study replication restart, resembeling the characteristics of CFSs by creating a difficult to replicate region, and providing further evidence of role of replication stress in expression of CFSs. The data presented in this study supports a model of genomic instability where inappropriate HR events initiated by fork collapse and restart generate intermediates which are not detected by checkpoints, and this leads to gross chromosomal rearrangements. Passage of these GCRs through mitosis leads to chromosome bridges and acentric chromosomes, generating DSBs and driving further chromosomal instability.

REFERENCES

-Aguilera A., García-Muse T. 2013. Causes of genome instability. Annu Rev Genet. 47, 1–32.

-Ahn J.S., Osman F., Whitby M.C. 2005. Replication fork blockage by RTS1 at an ectopic site promotes recombination in fission yeast, EMBO J. 24:2011–2023.

-Akamatsu Y, Murayama Y, Yamada T, Nakazaki T, Tsutsui Y, Ohta K, et al. 2008. Molecular characterization of the role of the Schizosaccharomyces pombe nip1+/ctp1+ gene in DNA doublestrand break repair in association with the Mre11-Rad50-Nbs1 complex. Mol Cell Biol. 28:3639–51.

-Akamatsu Y1, Jasin M. 2010. Role for the mammalian Swi5-Sfr1 complex in DNA strand break repair through homologous recombination. PLoS Genet. Oct 14;6(10):e1001160.

-Alcasabas AA, Osborn AJ, Bachant J, Hu F, Werler PJ, Bousset K, Furuya K, Diffley JF, Carr AM, Elledge SJ. 2001. Mrc1 transduces signals of DNA replication stress to activate Rad53. Nat Cell Biol. 3(11):958-65.

-Anderson HJ, Vonarx EJ, Pastushok L, Nakagawa M, Katafuchi A, Gruz P, Di Rubbo A, Grice DM, Osmond MJ, Sakamoto AN, Nohmi T, Xiao W, Kunz BA. 2008. Arabidopsis thaliana Y- family DNA polymerase eta catalyses translesion synthesis and interacts functionally with PCNA2. Plant J 55:895–908.

-Antony, E., Tomko, E.J., Xiao, Q., Krejci, L., Lohman, T.M., Ellenberger, T. 2009. Srs2 disassembles Rad51 filaments by aprotein-protein interaction triggering ATP turnover and dissociation of Rad51 from DNA. Mol. Cell, 35, 105–115.

-Aparicio, J.G. et al. 2004. The Rpd3-Sin3 histone deacetylase regulates replication timing and enables intra-S origin control in Saccharomyces cerevisiae. Mol. Cell. Biol. 24, 4769–4780.

-Arai K, Kornberg A. 1981. Unique primed start of phage fX174 DNA replication and mobility of the primosome in a direction opposite chain synthesis. Proc Natl Acad Sci USA 78: 69–73.

-Arakawa H, Moldovan GL, Saribasak H, Saribasak NN, Jentsch S, Buerstedde JM. 2006. A role for PCNA ubiquitination in immu- noglobulin hypermutation. PLoS Biol 4:e366.

-Arias EE, Walter JC. 2005. Replication-dependent destruction of Cdt1 limits DNA replication to a single round per cell cycle in Xenopus egg extracts. Genes Dev. 19(1):114–26.

-Arias EE, Walter JC. 2006. PCNA functions as a molecular platform to trigger Cdt1 destruction and prevent re-replication. Nat. Cell Biol. 8(1):84–90.

-Atkinson, J., McGlynn, P. 2009. Replication fork reversal and the maintenance of genome stability. Nucleic Acids Research, 37(11), 3475–3492.

-Aylon, Y. et al. 2004. The CDK regulates repair of double-strand breaks by homologous recombination during the cell cycle. EMBO J. 23, 4868–4875.

-Bakkenist, C. J., Kastan, M. B. 2003. DNA damage activates ATM through intermolecular autophosphorylation and dimer dissociation. Nature, 421(6922), 499–506.

-Ball, H. L., Myers, J. S., Cortez, D. 2005. ATRIP binding to replication protein A-single-stranded DNA promotes ATR-ATRIP localization but is dispensable for Chk1 phosphorylation. Molecular Biology of the Cell, 16(5), 2372–2381.

-Barber, L.J. et al. 2008. RTEL1 maintains genomic stability by suppressing homologous recombination. Cell 135, 261–271.

-Barbour L., Xiao W. 2003. Regulation of alternative replication bypass pathways at stalled replication forks and its effects on genome stability: a yeast model. Mutation Research 532:137–155.

-Baroni, E. et al. 2004. The functions of budding yeast Sae2 in the DNA damage response require Mec1- and Tel1-dependent phosphorylation. Mol. Cell. Biol. 24, 4151–4165.

-Bartek J, Lukas J. 2007. DNA damage checkpoints: from initiation to recoveryor adaptation. Curr Opin Cell Biol 19:238–45.

-Basi, G., Schmid, E., Maundrell, K. 1993. TATA box mutations in the Schizosaccharomyces pombe nmt1 promoter affect transcription efficiency but not the transcription start point or thiamine repressibility. Gene, 123(1), 131–136.

-Bedrosian, C. L., Bastia, D. 1991. Escherichia coli replication terminator protein impedes simian virus 40 (SV40) DNA replication fork movement and SV40 large tumor antigen helicase activity in vitro at a prokaryotic terminus sequence . Proc. Natl. Acad. Sci.USA 88 , 2618 – 2622.

-Bell SP, Kobayashi R, Stillman B. 1993. Yeast origin recognition complex functions in transcription silencing and DNA replication. Science 17;262(5141):1844-9.

-Bell SP, Stillman B. 1992. ATP-dependent recognition of eukaryotic origins of DNA replication by a multiprotein complex. Nature 357(6374):128–34.

-Bell, L., Byers, B. 1983. Separation of branched from linear DNA by two-dimensional gel electrophoresis. Analytical Biochemistry, 130(2), 527–535.

-Benson FE, West SC. 1994. Substrate specificity of the Escherichia coli RuvC protein. Resolution of three- and four-stranded recombination intermediates. J Biol Chem 269:5195–5201.

-Bentley, N. J., Holtzman, D. A., Flaggs, G., Keegan, K. S., DeMaggio, A., Ford, J. C., Hoekstra, M, Carr, A M. 1996. The Schizosaccharomyces pombe rad3 checkpoint gene. The EMBO Journal, 15(23), 6641–6651.

-Bermudez, V. P., Lindsey-Boltz, L. A., Cesare, A. J., Maniwa, Y., Griffith, J. D., Hurwitz, J., Sancar, A. 2003. Loading of the human 9-1-1 checkpoint complex onto DNA by the checkpoint clamp loader hRad17-replication factor C complex in vitro. Proceedings of the National Academy of Sciences of the United States of America, 100(4), 1633–1638.

-Bessman MJ, Lehman IR, Simms ES, Kornberg A. 1958. Enzymatic synthesis of deoxyribonucleic acid. II. General properties of the reaction. J Biol Chem. 233:171–177.

-Bianco PR, Tracy RB, Kowalczykowski SC. 1998. DNA strand exchange proteins: A biochemical and physical comparison. Front Biosci. 3:570–603.

-Bienko M, Green CM, Crosetto N, Rudolf F, Zapart G, Coull B, Kannouche P, Wider G, Peter M, Lehmann AR, Hofmann K, Dikic I. 2005. Ubiquitin-binding domains in Y-family polymerases regulate translesion synthesis. Science 310:1821-1824.

-Bloom, L. B. 2009. Loading clamps for DNA replication and repair. DNA Repair, 8(5), 570–578.

-Blow J, Dutta A. 2005. Preventing re-replication of chromosomal DNA. Nat Rev Mol Cell Biol 6(6), 476–486.

-Boddy, M. N., Gaillard, P. H., McDonald, W. H., Shanahan, P., Yates, J. R., Russell, P. 2001. Mus81-Eme1 are essential components of a Holliday junction resolvase. Cell, 107(4), 537–548.

-Boddy, M. N., Lopez-Girona, A., Shanahan, P., Interthal, H., Heyer, W. D., Russell, P. 2000. Damage tolerance protein Mus81 associates with the FHA1 domain of checkpoint kinase Cds1. Molecular and Cellular Biology, 20(23), 8758–8766.

-Boddy, M. N., Shanahan, P., McDonald, W. H., Lopez-Girona, A., Noguchi, E., Yates, J. R., III, Russell, P. 2003. Replication checkpoint kinase Cds1 regulates recombinational repair protein Rad60. Molecular and Cellular Biology, 23(16), 5939–5946.

-Bonilla, C. Y., Melo, J. A., Toczyski, D. P. 2008. Colocalization of sensors is sufficient to activate the DNA damage checkpoint in the absence of damage. Molecular Cell, 30(3), 267–276.

-Boos D, Sanchez-Pulido L, Rappas M, Pearl LH, Oliver AW, Ponting CP, Diffley JFX. 2011. Regulation of DNA replication through Sld3-Dpb11 interaction is conserved from yeast to humans. Curr Biol, 21:1152-1157.

-Borde V. 2007. The multiple roles of the Mre11 complex for meiotic recombination. Chromosome Res.15(5):551-63.

-Bramhill D, Kornberg A. 1988. Duplex opening by DnaA protein at novel sequences in initiation of replication at the origin of the E. coli chromosome. Cell 52(5):743–55.

-Branzei D, Foiani M. 2008. Regulation of DNA repair throughout the cell cycle. Nat Rev Mol Cell Biol 9:297–308.

-Branzei, D., Foiani, M. 2005. The DNA damage response during DNA replication. Current Opinion in Cell Biology, 17(6), 568–575.

-Branzei, D., Foiani, M. 2007. Interplay of replication checkpoints and repair proteins at stalled replication forks. DNA Repair, 6(7), 994–1003.

-Branzei, D., Foiani, M. 2010. Maintaining genome stability at the replication fork. Nature Reviews. Molecular Cell Biology, 11(3), 208–219.

-Brewer, B. J. 1988. When polymerases collide: replication and the transcriptional organization of the E. coli chromosome. Cell 53:679–686.

-Brewer, B. J., and W. L. Fangman. 1988. A replication fork barrier at the 3’ end of yeast ribosomal RNA genes. Cell 55:637–643.

-Brewer, B. J., Fangman, W. L. 1987. The localization of replication origins on ARS plasmids in S. cerevisiae. Cell, 51(3), 463–471.

-Broomfield S, Chow BL, Xiao W. 1998. MMS2, encoding a ubiquitin-conjugating-enzyme-like protein, is a member of the yeast error-free postreplication repair pathway. Proc Natl Acad Sci USA; 95:5678–5683.

-Brun J, Chiu R, Lockhart K, Xiao W, Wouters BG, Gray DA. 2008. hMMS2 serves a redundant role in human PCNA polyubiquitination. BMC Mol Biol; 9:24.

-Brusky J, Zhu Y, Xiao W. 2000. UBC13, a DNA-damage-inducible gene, is a member of the error-free postreplication repair pathway in Saccharomyces cerevisiae. Curr Genet; 37:168–174.

-Bugreev DV, Hanaoka F, Mazin AV. 2007. Rad54 dissociates homologous recombination intermediates by branch migration. Nature Struct. Mol. Biol. 14:746–753.

-Burma, S., Chen, B. P., Murphy, M., Kurimasa, A., Chen, D. J. 2001. ATM phosphorylates histone H2AX in response to DNA double-strand breaks. The Journal of Biological Chemistry, 276(45), 42462–42467.

-Burrell, R. A., McClelland, S. E., Endesfelder, D., Groth, P., Weller, M.-C., Shaikh, N., et al. 2013. Replication stress links structural and numerical cancer chromosomal instability. Nature, 494(7438), 492–496.

-Cadman CJ, McGlynn P. 2004. PriA helicase and SSB interact physically and functionally. Nucleic Acids Res 32: 6378–87.

-Calonge, T. M., O'Connell, M. J. 2008. Turning off the G2 DNA damage checkpoint. DNA Repair, 7(2), 136–140.

-Calzada A, Hodgson B, Kanemaki M, Bueno A, Labib K. 2005. Molecular anatomy and regulation of a stable replisome at a paused eukaryotic DNA replication fork. Genes Dev. 19(16):1905-19.

-Calzada A, Hodgson B, Kanemaki M, Bueno A, Labib K. 2005. Molecular anatomy and regulation of a stable replisome at a paused eukaryotic DNA replication fork. Genes Dev. 19(16):1905-19.

-Carr, A. M., Lambert, S. 2013. Replication Stress-Induced Genome Instability: The Dark Side of Replication Maintenance by Homologous Recombination. Journal of Molecular Biology. doi:10.1016/j.jmb.2013.04.023.

-Caspari T, Murray JM, Carr AM. 2002. Cdc2-cyclin B kinase activity links Crb2 and Rqh1-topoisomerase III. Genes Dev. 16(10):1195-208.

-Caspari, T., Dahlen, M., Kanter-Smoler, G., Lindsay, H. D., Hofmann, K., Papadimitriou, K., et al. 2000. Characterization of Schizosaccharomyces pombe Hus1: a PCNA-related protein that associates with Rad1 and Rad9. Molecular and Cellular Biology, 20(4), 1254–1262.

-Castor, D., Nair, N., Déclais, A.-C., Lachaud, C., Toth, R., Macartney, T. J., et al. 2013. Cooperative Control of Holliday Junction Resolution and DNA Repair by the SLX1 and MUS81-EME1 Nucleases. Molecular Cell, 52(2), 221–233.

-Chen L, Nievera CJ, Lee AY, Wu X. 2008. Cell cycle-dependent complex formation of BRCA1.CtIP.MRN is important for DNA double-strand break repair. J Biol Chem. 283:7713–20.

-Chen, S., Bell, S. P. 2011. CDK prevents Mcm2-7 helicase loading by inhibiting Cdt1 interaction with Orc6. Genes & Development, 25(4), 363–372.

-Chen, S., Levin, M. K., Sakato, M., Zhou, Y., Hingorani, M. M. 2009. Mechanism of ATP-driven PCNA clamp loading by S. cerevisiae RFC. Journal of Molecular Biology, 388(3), 431–442.

-Chen, X., Niu, H., Chung, W.H., Zhu, Z., Papusha, A., Shim, E. Y., et al. 2011. Cell cycle regulation of DNA double-strand break end resection by Cdk1-dependent Dna2 phosphorylation. Nat. Struct. Mol. Biol. 18, 1015–1019.

-Chi, P., Kwon, Y., Seong, C., Epshtein, A., Lam, I., Sung, P., Klein, H.L. 2006. Yeast recombination factor Rdh54 functionally interacts with the Rad51 recombinase and catalyzes Rad51 removal from DNA. J. Biol. Chem., 281, 26268–26279.

-Chiu RK, Brun J, Ramaekers C, Theys J, Weng L, Lambin P, Gray DA, Wouters BG. 2006. Lysine 63- polyubiquitination guards against translesion synthesis-induced mutations. PLoS Genet; 2:e116.

-Chuang RY, Kelly TJ. 1999. The fission yeast homologue of Orc4p binds to replication origin DNA via multiple AT-hooks. Proc. Natl. Acad. Sci. USA 96(6):2656–61.

-Clerici, M., Mantiero, D., Lucchini, G., Longhese, M. P. 2005. The Saccharomyces cerevisiae Sae2 protein promotes resection and bridging of double strand break ends. The Journal of Biological Chemistry, 280(46), 38631–38638.

-Cobb J.A., Schleker T., Rojas V., Bjergbaek L., Tercero J.A., Gasser S.M. 2005. Replisome instability, fork collapse, and gross chromosomal rearrangements arise

synergistically from Mec1 kinase and RecQ helicase mutations, Genes Dev. 19:3055–3069.

-Cobb JA, Bjergbaek L, Shimada K, Frei C, Gasser SM. 2003. DNA polymerase stabilization at stalledreplication forks requires Mec1 and the RecQ helicase Sgs1. EMBO J. 22:4325–36.

-Cocker JH, Piatti S, Santocanale C, Nasmyth K, Diffley JF. 1996. An essential role for the Cdc6 protein in forming the pre-replicative complexes of budding yeast. Nature 379(6561):180–82.

-Codlin, S., and J. Z. Dalgaard. 2003. Complex mechanism of site-specific DNA replication termination in fission yeast. EMBO J. 22:3431–3440.

-Collins, K. L., Kelly, T. J. 1991. Effects of T antigen and replication protein A on the initiation of DNA synthesis by DNA polymerase alpha-primase. Molecular and Cellular Biology, 11(4), 2108–2115.

-Cornacchia, D. et al. 2012. Mouse Rif1 is a key regulator of the replication-timing programme in mammalian cells. EMBO J. 31, 3678–3690.

-Cortez D, Guntuku S, Qin J, Elledge S J. 2001. ATR and ATRIP: partners in checkpoint signaling. 294(5547), 1713–1716.

-Cortez D, Wang Y, Qin J, Elledge S J. 1999. Requirement of ATM-dependent phosphorylation of brca1 in the DNA damage response to double-strand breaks. Science, 286(5442), 1162–1166.

-Cotta-Ramusino C., Fachinetti D., Lucca C., Doksani Y., Lopes M., Sogo J., Foiani M. 2005. Exo1 processes stalled replication forks and counteracts fork reversal in checkpoint-defective cells. Mol. Cell 17:153–159.

-Coulon S, Gaillard P-HL, Chahwan C. et al. 2004. Slx1–Slx4 are subunits of a structure-specific endonuclease that maintains ribosomal DNA in fission yeast. Mol Biol Cell 15:71–80.

-Coulon S, Noguchi E, Noguchi C. et al. 2006. Rad22Rad52-dependent repair of ribosomal DNA repeats cleaved by Slx1–Slx4 endonucle- ase. Mol Biol Cell 17:2081–2090.

-Cullmann G, Fien K, Kobayashi R, Stillman B. 1995. Characterization of the five replication factor C genes of Saccharomyces cerevisiae. Mol Cell Biol 15: 4661– 4671.

-Dalgaard, J. Z., and A. J. Klar. 2000. swi1 and swi3 perform imprinting, pausing, and termination of DNA replication in S. pombe. Cell 102:745–751.

-Dalgaard, J. Z., Klar, A. J. 2001. A DNA replication-arrest site RTS1 regulates imprinting by determining the direction of replication at mat1 in S. pombe. Genes & Development, 15(16), 2060–2068.

-de Jager, M., Dronkert, M.L., Modesti, M., Beerens, C.E., Kanaar, R. and van Gent, D.C. 2001A. DNA-binding and strand-annealing activities of human Mre11: implications for its roles in DNA double-strand break repair pathways. Nucleic Acids Res. 29, 1317–1325.

-de Jager, M., van Noort, J., van Gent, D.C., Dekker, C., Kanaar, R. and Wyman, C. 2001B. Human Rad50/Mre11 is a flexible complex that can tether DNA ends. Mol. Cell 8, 1129–1135.

-De Marco V, Gillespie PJ, Li A, Karantzelis N, Christodoulou E, et al. 2009. Quaternary structure of the human Cdt1-Geminin complex regulates DNA replication licensing. Proc. Natl. Acad. Sci. USA 106(47):19807–12.

-De Piccoli, G., Katou, Y., Itoh, T., Nakato, R., Shirahige, K., Labib, K. 2012. Replisome stability at defective DNA replication forks is independent of S phase checkpoint kinases. Molecular Cell, 45(5), 696–704.

-Dehé, P.-M., Coulon, S., Scaglione, S., Shanahan, P., Takedachi, A., Wohlschlegel, J. A., et al. 2013. Regulation of Mus81-Eme1 Holliday junction resolvase in response to DNA damage. Nature Structural & Molecular Biology, 20(5), 598–603.

-Delacroix, S., Wagner, J. M., Kobayashi, M., Yamamoto, K.-I., Karnitz, L. M. 2007. The Rad9-Hus1-Rad1 (9-1-1) clamp activates checkpoint signaling via TopBP1. Genes & Development, 21(12), 1472–1477.

-Desai-Mehta, A., Cerosaletti, K.M. and Concannon, P. 2001. Distinct functional domains of nibrin mediate Mre11 binding, focus formation, and nuclear localization. Mol. Cell Biol. 21, 2184–2191.

-Deshpande, A. M., and C. S. Newlon. 1996. DNA replication fork pause sites dependent on transcription. Science 272:1030–1033.

-Detlef D. Leipe, L. Aravind1 and Eugene V. Koonin. 1999. Nucl. Acids Res. 27 (17): 3389-3401.

-Diffley JF, Cocker JH. 1992. Protein-DNA interactions at a yeast replication origin. Nature 357(6374):169–72.

-Doil, C., Mailand, N., Bekker-Jensen, S., Menard, P., Larsen, D. H., Pepperkok, R., et al. 2009. RNF168 binds and amplifies ubiquitin conjugates on damaged chromosomes to allow accumulation of repair proteins. Cell, 136(3), 435–446.

-Doré, A. S., Kilkenny, M. L., Rzechorzek, N. J., Pearl, L. H. 2009. Crystal structure of the rad9-rad1-hus1 DNA damage checkpoint complex--implications for clamp loading and regulation. Molecular Cell, 34(6), 735–745.

-Drury LS, Perkins G, Diffley JFX. 1997. The Cdc4/34/53 pathway targets Cdc6p for proteolysis in budding yeast. EMBO J 16: 5966–5976.

-Du, L.-L., Moser, B. A., Russell, P. 2004. Homo-oligomerization is the essential function of the tandem BRCT domains in the checkpoint protein Crb2. The Journal of Biological Chemistry, 279(37), 38409–38414.

-Du, L.-L., Nakamura, T. M., Moser, B. A., Russell, P. 2003. Retention but not recruitment of Crb2 at double-strand breaks requires Rad1 and Rad3 complexes. Molecular and Cellular Biology, 23(17), 6150–6158.

-Du, L.-L., Nakamura, T. M., Russell, P. 2006. Histone modification-dependent and independent pathways for recruitment of checkpoint protein Crb2 to double-strand breaks. Genes & Development, 20(12), 1583–1596.

-Duderstadt KE, Chuang K, Berger JM. 2011. DNA stretching by bacterial initiators promotes replication origin opening. Nature 478(7368):209–13.

-Ede, C., Rudolph, C. J., Lehmann, S., Schürer, K. A., Kramer, W. 2011. Budding yeast Mph1 promotes sister chromatid interactions by a mechanism involving strand invasion. DNA Repair, 10(1), 45–55.

-Edenberg, H.J., Huberman, J.A. 1975. Eukaryotic chromosome replication. Annu. Rev. Genet. 9, 245–284.

-Edwards, R. J., Bentley, N. J., Carr, A. M. 1999. A Rad3-Rad26 complex responds to DNA damage independently of other checkpoint proteins. Nature Cell Biology, 1(7), 393–398.

-El-Shemerly, M., Hess, D., Pyakurel, A. K., Moselhy, S. & Ferrari, S. 2008. ATR-dependent pathways control hEXO1 stability in response to stalled forks. Nucleic Acids Res. 36, 511 – 519.

-Ellison, V., Stillman, B. 2003. Biochemical characterization of DNA damage checkpoint complexes: clamp loader and clamp complexes with specificity for 5' recessed DNA. PLoS Biology, 1(2), E33.

-Elsasser S, Chi Y, Yang P, Campbell JL. 1999. Phosphorylation controls timing of Cdc6p destruction: A biochemical analysis. Mol Biol Cell 10: 3263–3277.

-Emili, A. 1998. MEC1-dependent phosphorylation of Rad9p in response to DNA damage. Molcel, 2(2), 183–189.

-Enoch T., Carr A.M., Nurse P. 1992. Fission yeast genes involved in coupling mitosis to completion of DNA replication, Genes Dev. 6,2035–2046.

-Errico, A., Costanzo, V., Hunt, T. 2007. Tipin is required for stalled replication forks to resume DNA replication after removal of aphidicolin in Xenopus egg extracts. Proceedings of the National Academy of Sciences of the United States of America, 104(38), 14929–14934.

-Erzberger JP, Mott ML, Berger JM. 2006. Structural basis for ATP-dependent DnaA assembly and replication-origin remodeling. Nat. Struct. Mol. Biol. 13(8):676–83.

-Evrin C, Clarke P, Zech J, Lurz R, Sun J, Uhle S, Li H, Stillman B, Speck C. 2009. A double-hexameric MCM2-7 complex is loaded onto origin DNA during licensing of eukaryotic DNA replication. Proc Natl Acad Sci USA 2009, 106:20240-20245.

-Eydmann, T., Sommariva, E., Inagawa, T., Mian, S., Klar, A. J. S., Dalgaard, J. Z. 2008. Rtf1-mediated eukaryotic site-specific replication termination. Genetics, 180(1), 27–39.

-Fekairi S, Scaglione S, Chahwan C. et al. 2009. Human SLX4 is a Holliday junction resolvase subunit that binds multiple DNA repair/recombination endonucleases. Cell 138:78–89.

-Felczak MM, Kaguni JM. 2004. The box VII motif of Escherichia coli DnaA protein is required for DnaA oligomerization at the E. coli replication origin. J. Biol. Chem. 279(49):51156–62

-Flores, M. J., Ehrlich, S. D. Michel, B. 2002. Primosome assembly requirement for replication restart in the Escherichia coli holDG10 replication mutant. Mol. Microbiol. 44, 783–792.

-Forsburg, S. L., Rhind, N. 2006. Basic methods for fission yeast. Yeast (Chichester, England), 23(3), 173–183.

-Frampton J, Irmisch A, Green CM, Neiss A, Trickey M, Ulrich HD, Furuya K, Watts FZ, Carr AM, Lehmann AR. 2006. Postreplication repair and PCNA modification in Schizosaccharomyces pombe. Mol Biol Cell 17:2976–2985.

-Franchitto, A. 2013. Genome Instability at Common Fragile Sites: Searching for the Cause of Their Instability. BioMed Research International, 2013, 730714.

-Frick D N., Richardson C C. 2001. DNA primases. Annu Rev Biochem, 70, 39–80.

-Fricke WM, Brill SJ. 2003. Slx1–Slx4 is a second structure-specific endonuclease functionally redundant with Sgs1–Top3. Genes Dev 17:1768–1778.

-Froget B, Blaisonneau J, Lambert S, Baldacci G. 2008. Cleavage of stalled forks by fission yeast Mus81/Eme1 in absence of DNA replication checkpoint. Mol Biol Cell 19:445–456.

-Fu YV, Yardimci H, Long DT, Guainazzi A, Bermudez VP, Hurwitz J van Oijen A, Scharer OD, Walter JC. 2011. Selective bypass of a lagging strand roadblock by the eukaryotic replicative DNA helicase. Cell. 146:931-941.

-Fukuura M, Nagao K, Obuse C, Takahashi TS, Nakagawa T, Masukata H. 2011. CDK promotes interactions of Sld3 and Drc1 with Cut5 for initiation of DNA replication in fission yeast. Mol Biol Cell. 22:2620-2633.

-Fung, C.W., Mozlin, A.M., Symington, L.S. 2009. Suppression of the double-strand-break-repair defect of the Saccharomyces cerevisiae rad57 mutant. Genetics, 181, 1195–1206.

-Furnari B, Rhind N, Russell P. 1997. Cdc25 mitotic inducer targeted by chk1 DNA damage checkpoint kinase. Science 277(5331), 1495–1497.

-Furuya, K., Poitelea, M., Guo, L., Caspari, T., Carr, A. M. 2004. Chk1 activation requires Rad9 S/TQ-site phosphorylation to promote association with C-terminal BRCT domains of Rad4TOPBP1. Genes & Development, 18(10), 1154–1164.

-Gali, H., Juhasz, S., Morocz, M., Hajdu, I., Fatyol, K., Szukacsov, V., et al. 2012. Role of SUMO modification of human PCNA at stalled replication fork. Nucleic Acids Research, 40(13), 6049–6059.

-Gallo-Fernández M, Saugar I, Ortiz-Bazán MÁ. et al. 2012. Cell cycle-dependent regulation of the nuclease activity of Mus81–Eme1/ Mms4. Nucleic Acids Res 40:8325–8335.

-Gambus A, Jones RC, Sanchez-Diaz A, Kanemaki M, van Deursen F, Edmondson RD, Labib K. 2006. GINS maintains association of Cdc45 with MCM in replisome progression complexes at eukaryotic DNA replication forks. Nat Cell Biol. 8:358-366.

-Gambus A, Jones RC, Sanchez-Diaz A, Kanemaki M, van Deursen F, Edmondson RD, Labib K. 2006. GINS maintains association of Cdc45 with MCM in replisome progression complexes at eukaryotic DNA replication forks. Nat Cell Biol. 8(4):358-66.

-Gambus A, Khoudoli GA, Jones RC, Blow JJ. 2011. MCM2-7 form double hexamers at licensed origins in Xenopus egg extract. J Biol Chem. 286:11855-11864.

-Gangloff, S., Soustelle, C. & Fabre, F. 2000. Homologous recombination is responsible for cell death in the absence of the Sgs1 and Srs2 helicases. Nature. Genet. 25, 192–194.

-Garcia, V., Phelps, S. E. L., Gray, S., Neale, M. J. 2011. Bidirectional resection of DNA double-strand breaks by Mre11 and Exo1. Nature 479, 241–244.

-Garner, E., Kim, Y., Lach, F. P., Kottemann, M. C., Smogorzewska, A. 2013. Human GEN1 and the SLX4-associated nucleases MUS81 and SLX1 are essential for the resolution of replication-induced Holliday junctions. Cell Reports, 5(1), 207–215.

-Gasior SL, Wong AK, Kora Y, Shinohara A, Bishop DK. 1998. Rad52 associates with RPA and functions with Rad55 and Rad57 to assemble meiotic recombination complexes. Genes Dev. 12:2208–2221.

-Gerhardt, J., Tomishima, M. J., Zaninovic, N., Colak, D., Yan, Z., Zhan, Q., et al. 2014. The DNA replication program is altered at the FMR1 locus in fragile X embryonic stem cells. Molecular Cell, 53(1), 19–31.

-Gille H., Messer W. 1991. Localized DNA meltingand structural pertubationsin the origin of replication oriC, of Escherichia coli in vitro and in vivo. EMBO J. 10(6):1579–84.

-Giunta, S., Belotserkovskaya, R., Jackson, S. P. 2010. DNA damage signaling in response to double-strand breaks during mitosis. The Journal of Cell Biology, 190(2), 197–207.

-Göhler, T., Munoz, I. M., Rouse, J., Blow, J. J. 2008. PTIP/Swift is required for efficient PCNA ubiquitination in response to DNA damage. DNA Repair, 7(5), 775–787.

-Gomes, X. V., Schmidt, S. L., Burgers, P. M. 2001. ATP utilization by yeast replication factor C: II. Multiple stepwise ATP binding events are required to load proliferating cell nuclear antigen onto primed DNA. J. Biol. Chem. 276, 34776–34783.

-Goodarzi, A. A., Jeggo, P. A. 2013. The repair and signaling responses to DNA double-strand breaks. Advances in Genetics, 82, 1–45.

-Gravel, S., Chapman, J. R., Magill, C., Jackson, S. P. 2008. DNA helicases Sgs1 and BLM promote DNA double-strand break resection. Genes Dev. 22, 2767–2772.

-Green BM, Finn KJ, Li JJ. 2010. Loss of DNA replication control is a potent inducer of gene amplification. Science 329: 943– 946.

-Greenwell, P. W., Kronmal, S. L., Porter, S. E., Gassenhuber, J., Obermaier, B., and Petes, T. D. 1995. TEL1, a gene involved in controlling telomere length in s. cerevisiae, is homologous to the human ataxia telangiectasia gene. Cell, 82(5):823–829.

-Gregg AV, McGlynn P, Jaktaji RP, et al. 2002. Direct rescue of stalled DNA replication forks via the combined action of PriA and RecG helicase activities. Mol Cell 9: 241–51.

-Grimwade JE, Torgue JJ, McGarry KC, Rozgaja T, Enloe ST, Leonard AC. 2007. Mutational analysis reveals Escherichia coli oriC interacts with both DnaA-ATP and DnaA-ADP during pre-RC assembly. Mol. Microbiol. 66(2):428–39.

-Grompone G, Ehrlich SD, Michel B. 2003. Replication restart in gyrB Escherichia coli mutants. Mol Microbiol. 48: 845–54.

-Grompone G, Sanchez N, Ehrlich SD, et al. 2004. Requirement forRecFOR-mediated recombination in priA mutant. Mol Microbiol. 52:551–62.

-Grompone G, Seigneur M, Ehrlich SD, et al. 2002. Replication fork reversal in DNA polymerase III mutants of Escherichia coli: a role for the b clamp. Mol Microbiol 44: 1331–9.

-Gruss, A. Michel, B. 2001. The replication-recombination connection: insights from genomics. Curr. Opin. Microbiol. 4, 595–601.

-Guo C, Tang TS, Bienko M, Parker JL, Bielen AB, Sonoda E, Takeda S, Ulrich HD, Dikic I, Friedberg EC. 2006. Ubiquitin-binding motifs in REV1 protein are required for its role in the tolerance of DNA damage. Mol Cell Biol 26:8892–8900.

-Guo, Z., Kumagai, A., Wang, S. X., Dunphy, W. G. 2000. Requirement for Atr in phosphorylation of Chk1 and cell cycle regulation in response to DNA replication blocks and UV-damaged DNA in Xenopus egg extracts. Genes & Development, 14(21), 2745–2756.

-Handa T, Kanke M, Takahashi TS, Nakagawa T, Masukata H. DNA polymerization-independent functions of DNA polymerase epsilon in assembly and progression of the replisome in fission yeast. Mol Biol Cell. 2012; 23:3240–3253.

-Harigaya, Y., Tanaka, H., Yamanaka, S., Tanaka, K., Watanabe, Y., Tsutsumi, C., et al. 2006. Selective elimination of messenger RNA prevents an incidence of untimely meiosis. Nature, 442(7098), 45–50.

-Hartlerode, A. J., Scully, R. 2009. Mechanisms of double-strand break repair in somatic mammalian cells. Biochem J, 423(2), 157–168.

-Hartwell, L. H. & Weinert, T. A. 1989 Checkpoints: controls that ensure the order of cell cycle events. Science 246, 629–634.

-Hashimoto Y, Puddu F, Costanzo V. 2012. RAD51- and MRE11-dependent reassembly of uncoupled CMG helicase complex at collapsed replication forks. Nat Struct Mol Biol 19: 17–24.

-Hayano, M. et al. 2012. Rif1 is a global regulator of timing of replication origin firing in fission yeast. Genes Dev. 26, 137–150.

-Hayase A, Takagi M, Miyazaki T, Oshiumi H, Shinohara M, Shinohara A. 2004. A protein complex containing Mei5 and Sae3 promotes the assembly of the meiosis-specific RecA homolog Dmc1. Cell, 119(7), 927–940.

-Hayashi, M.T. et al. 2009. The heterochromatin protein Swi6/HP1 activates replication origins at the pericentromeric region and silent mating-type locus. Nat. Cell Biol. 11, 357–362.

-Hays, S.L., Firmenich, A.A., Berg, P. 1995. Complex formation in yeast double-strand break repair: participation of Rad51, Rad52, Rad55, and Rad57 proteins. Proc. Natl Acad. Sci. USA, 92, 6925–6929.

-Heichinger C, Penkett CJ, Bahler J , Nurse P. 2006. Genome wide characterization of fission yeast DNA replication origins. EMBO J. 25(21):5171–79.

-Heller R.C., Marians K.J. 2005B. The disposition of nascent strands at stalled replication forks dictates the pathway of replisome loading during restart, Mol. Cell. 17:733–743.

-Heller R.C., Marians K.J. 2006. Replisome assembly and the direct restart of stalled replication forks, Nat. Rev. Mol. Cell Biol. 7:932–943.

-Heller RC, Marians KJ. 2005A. Unwinding of the nascent lagging strand by Rep and PriA enables the direct restart of stalled replication forks. J Biol Chem 280: 34143–51.

-Hellman A., Rahat A., Scherer S. W., Darvasi A., Tsui L.-C., Kerem, B. 2000. Replication delay along FRA7H, a common fragile site on human chromosome 7, leads to chromosomal instability. Molecular and Cellular Biology, vol. 20, no. 12, pp. 4420–4427.

-Hennessy KM, Clark CD, Botstein D. 1990. Subcellular localization of yeast CDC46 varies with the cell cycle. Genes Dev 4: 2252–2263.

-Heyer, W.D., Li, X., Rolfsmeier, M., Zhang, X.P. 2006. Rad54: the Swiss Army knife of homologous recombination? Nucleic Acids Res., 34, 4115–4125.

-Hingorani MM, O'Donnell M. 1998. ATP binding to the Escherichia coli clamp loader powers opening of the ring-shaped clamp of DNA polymerase III holoenzyme. J. Biol. Chem. 273:24550–63.

-Hiraoka, Y., Toda, T., Yanagida, M. 1984. The NDA3 gene of fission yeast encodes beta-tubulin: a cold-sensitive nda3 mutation reversibly blocks spindle formation and chromosome movement in mitosis. Cell, 39(2 Pt 1), 349–358.

-Hodgson, B., Calzada , A. , Labib , K. 2007. Mrc1 and Tof1 regulate DNA replication forks in different ways during normal Sphase . Mol. Biol. Cell 18, 3894–3902.

-Hoege C, Pfander B, Moldovan GL, Pyrowolakis G, Jentsch S. 2002. RAD6-dependent DNA repair is linked to modification of PCNA by ubiquitin and SUMO. Nature 419:135–141.

-Hofmann RM, Pickart CM. 1999. Noncanonical MMS2-encoded ubiquitin-conjugating enzyme functions in assembly of novel polyubiquitin chains for DNA repair. Cell; 96:645–653.

-Hope, J.C. et al. 2007. Mus81–Eme1-dependent and –independent crossovers form in mitotic cells during double-strand break repair in Schizosaccharomyces pombe. Mol. Cell. Biol. 27, 3828–3838.

-Hopfner KP, Karcher A, Shin DS, Craig L, Arthur LM, Car- ney JP, Tainer JA. 2000. Structural biology of Rad50 ATPase: ATP-driven conformational control in DNA double-strand break repair and the ABC-ATPase super- family. Cell 101: 789–800.

-Hu, J., Sun, L., Shen, F., Chen, Y., Hua, Y., Liu, Y., et al. 2012. The intra-S phase checkpoint targets Dna2 to prevent stalled replication forks from reversing. Cell, 149(6), 1221–1232.

-Huen, M. S. Y., Grant, R., Manke, I., Minn, K., Yu, X., Yaffe, M. B., & Chen, J. 2007. RNF8 transduces the DNA-damage signal via histone ubiquitylation and checkpoint protein assembly. Cell, 131(5), 901–914.

-Huertas, P., Cortés-Ledesma, F., Sartori, A. A., Aguilera, A., Jackson, S. P. 2008. CDK targets Sae2 to con- trol DNA-end resection and homologous recombination. Nature 455, 689–692.

-Huertas, P., Jackson, S. P. 2009. Human CtIP mediates cell cycle control of DNA end resection and double strand break repair. J. Biol. Chem. 284, 9558–9565.

-Ilves I., Petojevic T., Pesavento J. J., Botchan M. R. 2010. Activation of the MCM2-7 helicase by association with Cdc45 and GINS proteins. Mol Cell, 37(2), 247–258.

-Ip SC, Rass U, Blanco MG, Flynn HR, Skehel JM, West SC. 2008. Identification of Holliday junction resolvases from humans and yeast. Nature. 456(7220), 357–361.

-Ira, G. et al. 2004 DNA end resection, homologous recombination and DNA damage checkpoint activation require CDK1. Nature. 431, 1011–1017.

-Iraqui I, Chekkal Y, Jmari N, Pietrobon V, Fréon K, Costes A, Lambert SA. 2012. Recovery of arrested replication forks by homologous recombination is error-prone. PLoS Genet.8(10):e1002976.

-Irmisch A1, Ampatzidou E, Mizuno K, O'Connell MJ, Murray JM. 2009. Smc5/6 maintains stalled replication forks in a recombination-competent conformation. EMBO J. 21;28(2):144-55.

-Itakura E, Umeda K, Sekoguchi E, Takata H, Ohsumi M, Matsuura A. 2004. ATR-dependent phosphorylation of ATRIP in response to genotoxic stress. Biochem Biophys Res Commun, 323(4), 1197–1202.

-Ivanov, E. L., Sugawara, N., Fishman-Lobell, J. & Haber, J. E. 1996. Genetic requirements for the single-strand annealing pathway of double-strand break repair in Saccharomyces cerevisiae. Genetics. 142, 693–704.

-Jang SW, Elsasser S, Campbell JL, Kim J. 2001. Identification of Cdc6 protein domains involved in interaction with Mcm2 pro- tein and Cdc4 protein in budding yeast cells. Biochem J 354: 655–661.

-Jeruzalmi D, O'Donnell M, Kuriyan J. 2001. Crystal structure of the processivity clamp loader gamma (gamma) complex of E. coli DNA polymerase III. Cell 106:429–41.

-Johnson RE, Henderson ST, Petes TD, Prakash S, Bankmann M, Prakash L. 1992. Saccharomyces cerevisiae RAD5-encoded DNA repair protein contains DNA helicase and zinc-binding sequence motifs and affects the stability of simple repetitive sequences in the genome. Mol Cell Biol; 12:3807– 3818.

-Johnson, R.D., Symington, L.S. 1995. Functional differences and interactions among the putative RecA homologs Rad51, Rad55, and Rad57. Mol. Cell. Biol., 15, 4843–4850.

-Kai, M., Boddy, M. N., Russell, P., Wang, T. S. F. 2005. Replication checkpoint kinase Cds1 regulates Mus81 to preserve genome integrity during replication stress. Genes & Development, 19(8), 919–932.

-Kai, M., Furuya, K., Paderi, F., Carr, A. M., & Wang, T. S. F. 2007. Rad3-dependent phosphorylation of the checkpoint clamp regulates repair-pathway choice. Nature Cell Biology, 9(6), 691–697.

-Kai, M., Wang, T. S. F. 2003. Checkpoint activation regulates mutagenic translesion synthesis. Genes & Development, 17(1), 64–76.

-Kakarougkas A., Jeggo P. 2014. DNA DSB repair pathway choice: an orchestrated handover mechanism. Br J Radiol, 87(1035), 20130685.

-Kanke, M., Nishimura, K., Kanemaki, M., Kakimoto, T., Takahashi, T. S., Nakagawa, T., Masukata, H. 2011. Auxin-inducible protein depletion system in fission yeast. BMC Cell Biology, 12(1), 8.

-Kannouche PL, Wing J, Lehmann AR. 2004. Interaction of human DNA polymerase η with monoubiquitinated PCNA: a possible mechanism for the polymerase switch in response to DNA dam- age. Mol Cell 14:491–500.

-Katayama T, Ozaki S, Keyamura K, Fujimitsu K. 2010. Regulation of the replication cycle: conserved and diverse regulatory systems for DnaA and oriC. Nat. Rev. Microbiol. 8(3):163–70.

-Katou Y, Kanoh Y, Bando M, Noguchi H, Tanaka H, Ashikari T, Sugimoto K, Shirahige K. 2003. S-phase checkpoint proteins Tof1 and Mrc1 form a stable replication-pausing complex. Nature. 424(6952):1078-83.

-Klar AJ. 2007. Lessons learned from studies of fission yeast mating-type switching and silencing. Annu Rev Genet. 41:213-36.

-Knott, S.R. et al. .2009. Genome-wide replication profiles indicate an expansive role for Rpd3L in regulating replication initiation timing or efficiency, and reveal genomic loci of Rpd3 function in Saccharomyces cerevisiae. Genes Dev. 23, 1077–1090.

-Kobayashi T., Horiuchi T. 1996. A yeast gene product, Fob1 protein, required for both replication fork blocking and recombinational hotspot activities, Genes Cells 1:465–474.

-Kobayashi, T., and T. Horiuchi. 1996. A yeast gene product, Fob1 protein, required for both replication fork blocking and recombinational hotspot activities. Genes Cells 1:465–474.

-Kong D, Coleman TR, DePamphilis ML. 2003. Xenopus origin recognition complex (ORC) initiates DNA replication preferentially at sequences targeted by Schizosaccharomyces pombe ORC. EMBO J. 22(13):3441–50.

-Kowalski D., Eddy MJ. 1989. The DNA unwinding element: a novel cis-acting component that facilitates opening of the Escherichia coli replication origin. EMBO J. 8(13):4335–44.

-Kozak, M. 2002. Pushing the limits of the scanning mechanism for initiation of translation. Gene, 299(1-2), 1–34.

-Kozlov, S. V., Graham, M. E., Peng, C., Chen, P., Robinson, P. J., Lavin, M. F. 2006. Involvement of novel autophosphorylation sites in ATM activation. The EMBO Journal, 25(15), 3504–3514.

-Krejci L, Van Komen S., Li Y., Villemain J., Reddy M.S., Klein H., Ellenberger T., Sung P. 2003. DNA helicase Srs2 disrupts the Rad51 presynaptic filament, Nature 423;305–309.

-Krejci, L., Song, B., Bussen, W., Rothstein, R., Mortensen, U.H., Sung,P. 2002. Interaction with Rad51 is indispensable forrecombination mediator function of Rad52. J. Biol. Chem., 277,40132–40141.

-Krings, G., and D. Bastia. 2004. swi1- and swi3-dependent and independent replication fork arrest at the ribosomal DNA of Schizosaccharomyces pombe. Proc. Natl. Acad. Sci. USA 101:14085–14090.

-Krogh, B.O. and Symington, L.S. 2004. Recombination proteins in yeast. Annu. Rev. Genet. 38, 233–271.

-Kumagai A, Dunphy WG. 2000. Claspin, a novel protein required for the activation of Chk1 during a DNA replication checkpoint response in Xenopus egg extracts. Mol Cell. 6(4):839-49.

-Kumagai A, Shevchenko A, Dunphy WG. 2011. Direct regulation of Treslin by cyclin-dependent kinase is essential for the onset of DNA replication. J Cell Biol, 193:995-1007.

-Kumagai, A., Kim, S.-M., & Dunphy, W. G. 2004. Claspin and the activated form of ATR-ATRIP collaborate in the activation of Chk1. The Journal of Biological Chemistry, 279(48), 49599–49608.

-Kumagai, A., Lee, J., Yoo, H. Y., Dunphy, W. G. 2006. TopBP1 activates the ATR-ATRIP complex. Cell, 124(5), 943–955.

-Kumar, S., Burgers, P. M. 2013. Lagging strand maturation factor Dna2 is a component of the replication checkpoint initiation machinery. Genes & Development, 27(3), 313–321.

-Kurokawa Y, Murayama Y, Haruta-Takahashi N, Urabe I, Iwasaki H. 2008. Reconstitution of DNA strand exchange mediated by Rhp51 recombinase and two mediators. PLoS Biol. 15;6(4):e88.

-Labib K, Diffley JFX, Kearsey SE. 1999. G1-phase and B-type cyclins exclude the DNA-replication factor Mcm4 from the nucleus. Nat Cell Biol 1: 415–422.

-Labib, K., De Piccoli, G. 2011. Surviving chromosome replication: the many roles of the S-phase checkpoint pathway. Philosophical Transactions of the Royal Society of London. Series B, Biological Sciences, 366(1584), 3554–3561.

-Lambert S, Carr AM. 2005.Checkpoint responses to replication fork barriers. Biochimie 87(7):591-602.

-Lambert S, Mizuno K, Blaisonneau J, Martineau S, Chanet R, Fréon K, Murray JM, Carr AM, Baldacci G. 2010. Homologous recombination restarts blocked replication forks at the expense of genome rearrangements by template exchange. Mol Cell. 2010 39(3):346-59.

-Lambert, S., Watson, A., Sheedy, D. M., Martin, B., Carr, A. M. 2005. Gross chromosomal rearrangements and elevated recombination at an inducible site-specific replication fork barrier. Cell, 121(5), 689–702.

-Lammens K, Bemeleit DJ, Mockel C, Clausing E, Schele A, Hartung S, Schiller CB, Lucas M, Angermuller C, Soding J, et al. 2011. The Mre11:Rad50 structure shows an ATP- dependent molecular clamp in DNA double-strand break repair. Cell 145: 54–66.

-Lao JP, Oh SD, Shinohara M, Shinohara A, Hunter N. 2008. Rad52 promotes postinvasion steps of meiotic double-strand-break repair. Mol Cell. 29(4):517-24.

-Larner, J. M., Lee, H., Little, R. D., Dijkwel, P. A., Schildkraut, C. L., Hamlin, J. L. 1999. Radiation down-regulates replication origin activity throughout the S phase in mammalian cells. Nucleic Acids Res. 27, 803-809.

-Larsen NB, Sass E, Suski C, Mankouri HW, Hickson ID. 2014. The Escherichia coli Tus-Ter replication fork barrier causes site-specific DNA replication perturbation in yeast. Nat Commun. 7;5:3574.

-Lavin MF. 2007. ATM and the Mre11 complex combine to recognize and signal DNA double-strand breaks. Oncogene. 10;26(56):7749-58.

-Le Beau M. M., Rassool F. V., Neilly M. E. et al. 1998. Replication of a common fragile site, FRA3B, occurs late in S phase and is delayed further upon induction: implications for the mech- anism of fragile site induction. Human Molecular Genetics, vol. 7, no. 4, pp. 755–761.

-Le Breton, C., Dupaigne, P., Robert, T., Le Cam, E., Gangloff, S., Fabre, F., Veaute, X. 2008. Srs2 removes deadly recombination intermediates independently of its interaction with SUMO-modified PCNA. Nucleic Acids Research, 36(15), 4964–4974.

-Leach CA, Michael WM. 2005. Ubiquitin/SUMO modification of PCNA promotes replication fork progression in Xenopus laevis egg extracts. J Cell Biol 171:947–954.

-Lee C, Hong B, Choi JM, Kim Y, Watanabe S, et al. 2004. Structural basis for inhibition of the replication licensing factor Cdt1 by geminin. Nature 430(7002):913–17.

-Lee, H., Larner, J. M., Hamlin, J. L. 1997. A p53-independent damage-sensing mechanism that functions as a checkpoint at the G1/S transition in Chinese hamster ovary cells. Proc. Natl. Acad. Sci. USA 94, 526-531.

-Lee, S. J., Schwartz, M. F., Duong, J. K., Stern, D. F. 2003. Rad53 phosphorylation site clusters are important for Rad53 regulation and signaling. Molecular and Cellular Biology, 23(17), 6300–6314.

-Lee, Y. D., Wang, J., Stubbe, J. & Elledge, S. J. 2008. Dif1 is a DNA-damage-regulated facilitator of nuclear import for ribonucleotide reductase. Mol. Cell 32, 70 – 80.

-Lees, E. 1995. Cyclin dependent kinase regulation. Current Opinion in Cell Biology, 7(6), 773–780.

-Lehmann AR, Fuchs RP. 2006. Gaps and forks in DNA replication: Rediscovering old models. DNA Repair (Amst) 5: 1495 – 1498.

-Lehmann AR, Niimi A, Ogi T, Brown S, Sabbioneda S, Wing JF, Kannouche PL, Green CM. 2007. Translesion synthesis: Y- family polymerases and the polymerase switch. DNA Repair 6:891–899.

-Lei M., Kawasaki Y., Young M.R., Kihara M., Sugino A., Tye B.K. 1997. Mcm2 is a target of regulation by Cdc7-Dbf4 during the initiation of DNA synthesis, Genes Dev. 11:3365–3374.

-Lengsfeld, B. M., Rattray, A. J., Bhaskara, V., Ghirlando, R., Paull, T. T. 2007. Sae2 is an endonuclease that processes hairpin DNA cooperatively with the Mre11/Rad50/Xrs2 complex. Molcel, 28(4), 638–651.

-Leupold U. 1993. The origin of Schizosaccharomyces pombe genetics. In The Early Days of Yeast Genetics. Edited by Hall MN, Linder P. Cold Spring Harbor: Cold Spring Harbor Laboratory Press; 125-128.

-Lewis, P. J., M. T. Smith, and R. G. Wake. 1989. A protein involved in termination of chromosome replication in Bacillus subtilis binds specifically to the terC site. J. Bacteriol. 171:3564–3567.

-Li, X., Heyer,W.D. 2009. RAD54 controls access to the invading 30-OH end after RAD51-mediated DNA strand invasion in homologous recombination in Saccharomyces cerevisiae. Nucleic Acids Res., 37, 638–646.

-Liang C, Weinreich M, Stillman B. 1995. ORC and Cdc6p interact and determine the frequency of initiation of DNA replication in the genome. Cell 81(5):667–76.

-Liku ME, Nguyen VQ, Rosales AW, Irie K, Li JJ. 2005. CDK phosphorylation of a novel NLS-NES module distributed between two subunits of the Mcm2-7 complex prevents chromosomal rereplication. Mol Biol Cell 16: 5026–5039.

-Lim HS, Kim JS, Park YB, Gwon GH, Cho Y. 2011. Crystal structure of the Mre11 Rad50-ATPgS complex: Under- standing the interplay between Mre11 and Rad50. Genes Dev 25: 1091–1104.

-Limbo O, Chahwan C, Yamada Y, de Bruin RA, Wittenberg C, Russell P. 2007. Ctp1 is a cell-cycleregulated protein that functions with Mre11 complex to control double-strand break repair by homologous recombination. Mol Cell. 28:134–46.

-Limbo, O., Chahwan, C., Yamada, Y., de Bruin, R. A., Wittenberg, C. & Russell, P. 2007. Ctp1 is a cell-cycle- regulated protein that functions with Mre11 complex to control double-strand break repair by homologous recombination. Mol. Cell 28, 134 – 146.

-Lindsay H.D., Griffiths D.J., Edwards R.J., Christensen P.U., Murray J.M., Osman F., et al. 1998. S-phase-specific activation of Cds1 kinase defines a subpathway of the checkpoint response in Schizosaccharomyces pombe, Genes Dev. 12:382–395.

-Lisby M., Barlow J.H., Burgess R.C., Rothstein R. 2004. Choreography of the DNA damage response: spatiotemporal relationships among checkpoint and repair proteins, Cell 118 (2004) 699–713.

-Liu, S., Shiotani, B., Lahiri, M., Maréchal, A., Tse, A., Leung, C. C. Y., et al. 2011. ATR autophosphorylation as a molecular switch for checkpoint activation. Molecular Cell, 43(2), 192–202.

-Llorente B, Smith CE, Symington LS. 2008. Break-induced replication: what is it and what is it for? Cell Cycle. 7(7):859-64.

-Lloyd, J. et al. 2009. A supramodular FHA/BRCT-repeat architecture mediates Nbs1 adaptor function in response to DNA damage. Cell. 139, 100–111.

-Lopes M., Cotta-Ramusino C., Pellicioli A., Liberi G., Plevani P., Muzi-Falconi M., Newlon C.S., Foiani M. 2001. The DNA replication checkpoint response stabilizes stalled replication forks, Nature 412:557–561.

-López de Saro FJ, Georgescu RE, Goodman MF, O'Donnell M. 2003. Competitive processivity-clamp usage by DNA polymerases during DNA replication and repair. EMBO J. 1;22(23):6408-18.

-Lopez-Girona, A., Tanaka, K., Chen, X. B., Baber, B. A., McGowan, C. H., Russell, P. 2001. Serine-345 is required for Rad3-dependent phosphorylation and function of checkpoint kinase Chk1 in fission yeast. Proceedings of the National Academy of Sciences of the United States of America, 98(20), 11289–11294.

-Lopez-Mosqueda, J., Maas, N. L., Jonsson, Z. O., Defazio-Eli, L. G., Wohlschlegel, J., Toczyski, D. P. 2010. Damage-induced phosphorylation of Sld3 is important to block late origin firing. Nature 467, 479-483.

-Lorenz, A., Osman, F., Folkyte, V., Sofueva, S., Whitby, M.C. 2009. Fbh1 Limits Rad51-Dependent Recombination at Blocked Replication Forks. Mol. Cell. Biol. 29, 4742–4756.

-Lucca C., Vanoli F., Cotta-Ramusino C., Pellicioli A., Liberi G., Haber J., Foiani M. 2004. Checkpoint-mediated control of replisome-fork association and signalling in response to replication pausing, Oncogene 23,1206–1213.

-lves I, Petojevic T, Pesavento JJ, Botchan MR. 2010. Activation of the MCM2-7 helicase by association with Cdc45 and GINS proteins. Mol Cell. 37:247-258.

-MacAlpine HK, Gordan R, Powell SK, Hartemink AJ, MacAlpine DM. 2010. Drosophila ORC localizes to open chromatin and marks sites of cohesin complex loading. Genome Res. 20(2):201–11.

-MacDougall, C. A., Byun, T. S., Van, C., Yee, M.-C., Cimprich, K. A. 2007. The structural determinants of checkpoint activation. Genes & Development, 21(8), 898–903.

-Magdalou, I., Lopez, B. S., Pasero, P., Lambert, S. A. E. 2014. The causes of replication stress and their consequences on genome stability and cell fate. Seminars in Cell and Developmental Biology, 30, 154–164.

-Mailand, N., Bekker-Jensen, S., Faustrup, H., Melander, F., Bartek, J., Lukas, C., Lukas, J. 2007. RNF8 ubiquitylates histones at DNA double-strand breaks and promotes assembly of repair proteins. Cell, 131(5), 887–900.

-Maiorano D, Lemaitre JM, Mechali M. 2000. Stepwise regulated chromatin assembly of MCM2-7 proteins. J. Biol. Chem. 275(12):8426–31.

-Majka, J., Binz, S. K., Wold, M. S., Burgers, P. M. J. 2006A. Replication protein A directs loading of the DNA damage checkpoint clamp to 5'-DNA junctions. The Journal of Biological Chemistry, 281(38), 27855–27861.

-Majka, J., Niedziela-Majka, A., & Burgers, P. M. J. 2006B. The checkpoint clamp activates Mec1 kinase during initiation of the DNA damage checkpoint. Molcel, 24(6), 891–901.

-Maki H, Kornberg A. 1985. The polymerase subunit of DNA polymerase III of Escherichia coli. II. Purification of the alpha subunit, devoid of nuclease activities. J Biol Chem. 25;260(24):12987-92.

-Mantiero, D. et al. 2011. Limiting replication initiation factors execute the temporal programme of origin firing in budding yeast. EMBO J. 30, 4805–4814.

-Marians KJ. 1992. Prokaryotic DNA replication. Annu. Rev. Biochem. 61:673-719.

-Maringele, L., Lydall, D. 2002. EXO1-dependent single-stranded DNA at telomeres activates subsets of DNA damage and spindle checkpoint pathways in budding yeast yku70Delta mutants. Genes & Development, 16(15), 1919–1933.

-Marini, V., Krejci, L. 2010. Srs2: the “Odd-Job Man” in DNA repair. DNA Repair, 9(3), 268–275.

-Marszalek J, Kaguni JM. 1994. DnaA protein directs the binding of DnaB protein in initiation of DNA replication in Escherichia coli. J. Biol. Chem. 269(7):4883–90.

-Masai, H., Miyake, T., Arai, K.-I. 1995. hsk1+, a Schizosaccharomyces pombe gene related to Saccharomyces cerevisiae CDC7, is required for chromosomal replication. EMBO J. 14, 3094–3104.

-Masuda Y, Piao J, Kamiya K (2010) DNA replication-coupled PCNA mono-ubiquitination and polymerase switching in a human in vitro system. J Mol Biol 396:487–500.

-Masumoto H, Muramatsu S, Kamimura Y, Araki H. 2002. S-Cdk- dependent phosphorylation of Sld2 essential for chromosomal DNA replication in budding yeast. Nature. 415:651-655.

-Matos J, Blanco MG, Maslen S. et al. 2011. Regulatory control of the resolution of DNA recombination intermediates during meiosis and mitosis. Cell 147:158–172.

-Matsuoka, S., Rotman, G., Ogawa, A., Shiloh, Y., Tamai, K., Elledge, S. J. (2000). Ataxia telangiectasia-mutated phosphorylates Chk2 in vivo and in vitro. Proceedings of the National Academy of Sciences of the United States of America, 97(19), 10389–10394.

-Mazin AV, Alexeev AA, Kowalczykowski SC. 2003. A novel function of Rad54 protein –Stabilization of the Rad51 nucleoprotein filament. J. Biol. Chem. 278:14029–14036.

-Mazin, A.V., Mazina, O.M., Bugreev, D.V., Rossi, M.J. 2010. Rad54, the motor of homologous recombination. DNA Repair), 9, 286–302.

-McGlynn P, Al-Deib AA, Liu J, et al. 1997. The DNA replication protein PriA and the recombination protein RecG bind D-loops. J Mol Biol 270:212–21.

-McHenry CS, Crow W. 1979. DNA polymerase III of Escherichia coli. Purification and identification of subunits. J Biol Chem. 10;254(5):1748-53.

-McIlwraith, M. J. & West, S. C. 2008. DNA repair synthesis facilitates RAD52-mediated second-end capture during DSB repair. Mol. Cell. 29, 510–516.

-McMacken R, Kornberg A. 1978. A multienzyme system for priming the replication of fX174 viral DNA. J Biol. Chem. 253: 3313–9.

-McMacken R, Ueda K, Kornberg A. 1977. Migration of Escherichia coli dnaB protein on the template DNA strand as a mechanism in initiating DNA replication. Proc Natl Acad Sci USA 74: 4190–4.

-Mechali M. 2010. Eukaryotic DNA replication origins: many choices for appropriate answers. Nat. Rev. Mol. Cell Biol. 11(10):728–38.

-Meister P., Taddei A., Vernis L., Poidevin M., Gasser S.M., Baldacci G. 2005. Temporal separation of replication and recombination requires the intra-S checkpoint. J. Cell Biol. 168:537–544.

-Melendy, T., Stillman, B. 1993. An interaction between replication protein A and SV40 T antigen appears essential for primosome assembly during SV40 DNA replication. The Journal of Biological Chemistry, 268(5), 3389–3395.

-Melo, J. A., Cohen, J., Toczyski, D. P. 2001. Two checkpoint complexes are independently recruited to sites of DNA damage in vivo. Genes & Development, 15(21), 2809–2821.

-Merrill BJ, Holm C. 1998. The RAD52 recombinational repair pathway is essential in pol30 (PCNA) mutants that accumulate small single-stranded DNA fragments during DNA synthesis. Genetics. 148(2):611-24.

-Merrill BJ, Holm C. 1999. A requirement for recombinational repair in Saccharomyces cerevisiae is caused by DNA replication defects of mec1 mutants. Genetics. 153(2):595-605.

-Meselson M, Stahl FW. 1958. The replication of DNA in Escherichia coli. Proc Natl Acad Sci USA. 44:671–682.

-Mimitou, E. P., Symington, L. S. 2008. Sae2, Exo1 and Sgs1 collaborate in DNA double-strand break processing. Nature 455, 770 – 774.

-Mitsui, J. et al. 2010. Mechanisms of genomic instabilities underlying two common fragile-site-associated loci, PARK2 and DMD, in germ cell and cancer cell lines. Am. J. Hum. Genet. 87, 75–89.

-Miyabe I, Kunkel TA, Carr AM. 2011. The major roles of DNA polymerases epsilon and delta at the eukaryotic replication fork are evolutionarily conserved. PLoS Genetics 7:e1002407.

-Mizukoshi T, Tanaka T, Arai K, et al. 2003. A critical role of the 3’ terminus of nascent DNA chains in recognition of stalled replication forks. J Biol Chem 278: 42234–9.

-Mizuno, K., Lambert, S., Baldacci, G., Murray, J. M., Carr, A. M. 2009. Nearby inverted repeats fuse to generate acentric and dicentric palindromic chromosomes by a replication template exchange mechanism. Genes & Development, 23(24), 2876–2886.

-Mizuno, K., Miyabe, I., Schalbetter, S. A., Carr, A. M., Murray, J. M. 2013. Recombination-restarted replication makes inverted chromosome fusions at inverted repeats. Nature, 493(7431), 246–249.

-Mochida, S., Esashi, F., Aono, N., Tamai, K., O'Connell, M. J., Yanagida, M. 2004. Regulation of checkpoint kinases through dynamic interaction with Crb2. The EMBO Journal, 23(2), 418–428.

-Moldovan GL, Dejsuphong D, Petalcorin MI, Hofmann K, Takeda S, Boulton SJ, D'Andrea AD. 2012. Inhibition of homologous recombination by the PCNA-interacting protein PARI. Mol Cell 45:75–86.

-Moldovan GL, Pfander B, Jentsch S. 2007. PCNA, the maestro of the replication fork. Cell 129:665–679.

-Morin, I. et al. 2008. Checkpoint-dependent phosphorylation of Exo1 modulates the DNA damage response. EMBO J. 27, 2400–2410.

-Morin, I., Ngo, H.-P., Greenall, A., Zubko, M. K., Mor- rice, N. & Lydall, D. 2008. Checkpoint-dependent phosphorylation of Exo1 modulates the DNA damage response. EMBO J. 27, 2400 – 2410.

-Morrow, D. M., Tagle, D. A., Shiloh, Y., Collins, F. S., & Hieter, P. 1995. TEL1, an S. cerevisiae homolog of the human gene mutated in ataxia telangiectasia, is functionally related to the yeast checkpoint gene MEC1. Cell, 82(5), 831–840.

-Motegi A, Liaw HJ, Lee KY, Roest HP, Mass A, et al. 2008. Lysine 63-linked polyubiquitination of proliferating cell nuclear antigen by HLTF and SHPRH prevents genomic instability from stalled replication forks. Proc Natl Acad Sci USA.

-Moyer SE, Lewis PW, Botchan MR. 2006. Isolation of the Cdc45/ Mcm2-7/GINS (CMG) complex, a candidate for the eukaryotic DNA replication fork helicase. Proc Natl Acad Sci USA. 103:10236-10241.

-Mulcair, M. D., P. M. Schaeffer, A. J. Oakley, H. F. Cross, C. Neylon, T. M. Hill, Dixon N. E. 2006. A molecular mousetrap determines polarity of termination of DNA replication in E. coli. Cell 125:1309–1319.

-Mulugu, S. , Potnis, A. , Shamsuzzaman, S. , Taylor, J. , Alexander, K. , Bastia, D. 2001. Mechanism of termination of DNA replication of Escherichia coli involves helicase contrahelicase interaction . Proc. Natl. Acad. Sci. USA 98, 9569 – 9574.

-Muramatsu S, Hirai K, Tak YS, Kamimura Y, Araki H. 2010. CDK-dependent complex formation between replication proteins Dpb11, Sld2, Pol epsilon, and GINS in budding yeast. Genes Dev. 24:602-612.

-Murray JM, Tavassoli M, al-Harithy R, Sheldrick KS, Lehmann AR, Carr AM, Watts FZ. 1994. Structural and functional conservation of the human homolog of the Schizosaccharomyces pombe rad2 gene, which is required for chromosome segregation and recovery from DNA damage. Mol Cell Biol. 14(7):4878-88.

-Murray M., Carr A. 2008. Smc5/6: a link between DNA repair and unidirectional replication? Nat. Rev. Mol. Cell. Biol. 9:177-182.

-Myung K, Kolodner RD. 2002. Suppression of genome instability by redundant S-phase checkpoint pathways in Saccharomyces cerevisiae. Proc Natl Acad Sci USA, 99:4500-4507.

-Nakajima R, Masukata H. 2002. SpSld3 is required for loading and maintenance of SpCdc45 on chromatin in DNA replication in fission yeast. Mol Biol Cell, 13:1462-1472.

-Naktinis V, Turner J, O'Donnell M. 1996. A molecular switch in a replication machine defined by an internal competition for protein rings. Cell. 12;84(1):137-45.

-Neale, M.J. et al. 2005. Endonucleolytic processing of covalent proteinlinked DNA double-strand breaks. Nature 436, 1053–1057.

-Neylon C, Kralicek AV, Hill TM, Dixon NE. 2005. Replication termination in Escherichia coli: structure and antihelicase activity of the Tus-Ter complex. Microbiol Mol Biol Rev. 69(3):501-26.

-Nezi, L., Musacchio, A. 2009. Sister chromatid tension and the spindle assembly checkpoint. Curr. Opin. Cell Biol. 21, 785–795.

-Nguyen VQ, Co C, Irie K, Li JJ. 2000. Clb/Cdc28 kinases promote nuclear export of the replication initiator proteins Mcm2-7. Curr Biol 10: 195–205.

-Nick McElhinny SA, Gordenin DA, Stith CM, Burgers PMJ, Kunkel TA. 2008. Division of labor at the eukaryotic replication fork. Mol Cell 30:137–144.

-Nimonkar, A.V. et al. 2008. Human exonuclease 1 and BLM helicase interact to resect DNA and initiate DNA repair. Proc. Natl. Acad. Sci. U. S. A. 105, 16906–16911.

-Nishitani H, Lygerou Z, Nishimoto T, Nurse P. 2000. The Cdt1 protein is required to license DNA for replication in fission yeast. Nature 404(6778):625–28.

-Nitani N, Nakamura K, Nakagawa C, Masukata H, Nakagawa T. 2006. Regulation of DNA replication machinery by Mrc1 in fission yeast. Genetics. 174(1):155-65.

-Noguchi E, Noguchi C, Du LL, Russell P. 2003. Swi1 prevents replication fork collapse and controls checkpoint kinase Cds1. Mol Cell Biol. 23(21):7861-74.

-Noguchi E, Noguchi C, McDonald WH, Yates JR 3rd, Russell P. Swi1 and Swi3 are components of a replication fork protection complex in fission yeast. 2004. Mol Cell Biol. 24(19):8342-55.

-Nurse P., Zavitz K.H., Marians K.J. 1991. Inactivation of the Escherichia coli priA DNA replication protein induces the SOS response, J. Bacteriol. 173:6686–6693.

-Nurse, P. 1991, December 5. Cell cycle. Checkpoints and spindles. Nature, pp. 356–358.

-Nurse, P. 1997. Checkpoint pathways come of age. Cell, 91(7), 865–867.

-Nurse, P. 2002. Cyclin dependent kinases and cell cycle control (nobel lecture). Chembiochem: a European Journal of Chemical Biology, 3(7), 596–603.

-O'Connell, M. J., Walworth, N. C., Carr, A. M. 2000. The G2-phase DNA-damage checkpoint. Trends in Cell Biology, 10(7), 296–303.

-O'Donnell, M., Onrust, R., Dean, F. B., Chen, M., Hurwitz, J. 1993. Homology in accessory proteins of replicative polymerases--E. coli to humans. Nucleic Acids Research, 21(1), 1–3.

-Oh SD, Lao JP, Hwang PY, Taylor AF, Smith GR, Hunter N. 2007. BLM ortholog, Sgs1, prevents aberrant crossing-over by suppressing formation of multichromatid joint molecules.Cell. 130(2), 259–272.

-Okazaki R, Okazaki T, Sakabe K, Sugimoto K, Sugino A. 1968. Mechanism of DNA chain growth. I. Possible discontinuity and unusual secondary structure of newly synthesized chains. Proc Natl Acad Sci USA. 59:598–605.

-Osman, F., Dixon, J., Barr, A. R. & Whitby, M. C. 2005. The F-Box DNA helicase Fbh1 prevents Rhp51-dependent recombination without mediator proteins. Mol. Cell. Biol. 25, 8084–8096.

-Ozaki S, Kawakami H, Nakamura K, Fujikawa N, Kagawa W, et al. 2008. A common mechanism for the ATP-DnaA-dependent formation of open complexes at the replication origin. J. Biol. Chem. 283(13):8351–62.

-Ozeri-Galai E., Lebofsky R., Rahat A., Bester A. C., Bensi- mon A., Kerem B. 2011.Failure of origin activation in response to fork stalling leads to chromosomal instability at fragile sites. Molecular Cell, vol. 43, no. 1, pp. 122–131.

-Pacek M, Tutter AV, Kubota Y, Takisawa H, Walter JC. 2006. Localization of MCM2-7, Cdc45, and GINS to the site of DNA unwinding during eukaryotic DNA replication. Mol Cell. 21:581-587.

-Paciotti, V., Clerici, M., Lucchini, G., Longhese, M. P. 2000. The checkpoint protein Ddc2, functionally related to S. pombe Rad26, interacts with Mec1 and is regulated by Mec1-dependent phosphorylation in budding yeast. Genes & Development, 14(16), 2046–2059.

-Paciotti, V., Clerici, M., Scotti, M., Lucchini, G., Longhese, M. P. 2001. Characterization of mec1 kinase-deficient mutants and of new hypomorphic mec1 alleles impairing subsets of the DNA damage response pathway. Molecular and Cellular Biology, 21(12):3913–3925. PMID: 11359899.

-Painter, R. B., Young, B. R. 1980. Radiosensitivity in ataxia-telangiectasia: a new explanation. Proc. Natl Acad. Sci. USA 77, 7315–7317.

-Palakodeti A., Han Y., Jiang Y., Le Beau M. M. 2004. The role of late/slow replication of the FRA16D in common fragile site induction. Genes Chromosomes and Cancer, vol. 39, no. 1, pp. 71–76.

-Palakodeti A., Lucas I., Jiang Y., et al. 2010.Impaired replication dynamics at the FRA3B common fragile site. Human Molecular Genetics, vol. 19, no. 1, pp. 99–110.

-Papouli E, Chen S, Davies AA, Huttner D, Krejci L, Sung P, Ulrich HD. 2005. Crosstalk between SUMO and ubiquitin on PCNA is mediated by recruitment of the helicase Srs2p. Mol Cell 19:123–133.

-Parker JL, Bielen AB, Dikic I, Ulrich HD. 2007. Contributions of ubiquitin and PCNA binding domains to the activity of polymerase η in Saccharomyces cerevisiae. Nucleic Acids Res 35:881– 889.

-Paull, T.T. and Gellert, M. 1998. The 3' to 5' exonuclease activity of Mre 11 facilitates repair of DNA double-strand breaks. Mol. Cell 1, 969–979.

-Pearson, C., Sinden, R. 1996. Alternative structures in duplex DNA formed within the trinucleotide repeats of the myotonic dystrophy and fragile X loci. Biochemistry 35:5041–5053.

-Perkins G, Drury LS, Diffley JFX. 2001. Separate SCF(CDC4) recognition elements target Cdc6 for proteolysis in S phase and mitosis. EMBO J 20: 4836–4845.

-Petrini, J.H. and Stracker, T.H. 2003. The cellular response to DNA double strand breaks: defining the sensors and mediators. Trends Cell Biol. 13, 458–462.

-Petukhova,G., Stratton,S. and Sung,P. 1998. Catalysis of homologous DNA pairing by yeast Rad51 and Rad54 proteins. Nature, 393, 91–94.

-Pfander B, Moldovan GL, Sacher M, Hoege C, Jentsch S. 2005. SUMO-modified PCNA recruits Srs2 to prevent recombination during S phase. Nature 436:428–433.

-Pfander, B., Diffley, J. F. X. 2011. Dpb11 coordinates Mec1 kinase activation with cell cycle-regulated Rad9 recruitment. The EMBO Journal, 30(24), 4897–4907.

-Planta RJ, Gonçalves PM, Mager WH. 1995. Global regulators of ribosome biosynthesis in yeast. Biochem Cell Biol. 73(11-12):825-34.

-Plosky BS, Vidal AE, de Henestrosa AR, McLenigan MP, McDonald JP, Mead S, Woodgate R. 2006. Controlling the subcellular lo- calization of DNA polymerases ι and η via interactions with ubiquitin. EMBO J 25:2847–2855.

-Podust, V. N., Tiwari, N., Ott, R., Fanning, E. 1998. Functional interactions among the subunits of replication factor C potentiate and modulate its ATPase activity. The Journal of Biological Chemistry, 273(21), 12935–12942.

-Prakash S, Johnson RE, Prakash L. 2005. Eukaryotic translesion synthesis DNA polymerases: specificity of structure and function. Annu Rev Biochem; 74:317–353.

-Prelich, G., Tan, C. K., Kostura, M., Mathews, M. B., So, A. G., Downey, K. M., Stillman, B. 1987. Functional identity of proliferating cell nuclear antigen and a DNA polymerase-delta auxiliary protein. Nature, 326(6112), 517–520.

-Puddu, F., Granata, M., Di Nola, L., Balestrini, A., Piergiovanni, G., Lazzaro, F., et al. 2008. Phosphorylation of the budding yeast 9-1-1 complex is required for Dpb11 function in the full activation of the UV-induced DNA damage checkpoint. Molecular and Cellular Biology, 28(15), 4782–4793.

-Pursell ZF, Isoz I, Lundstrom E-B, Johansson E, Kunkel TA. 2007. Yeast DNA polymerase ε participates in leading-strand DNA replication. Science 317:127–130.

-Qu, M., Yang, B., Tao, L., Yates, J. R., Russell, P., Dong, M.-Q., & Du, L.-L. (2012). Phosphorylation-dependent interactions between Crb2 and Chk1 are essential for DNA damage checkpoint. PLoS Genetics, 8(7), e1002817.

-Randell JC, Fan A, Chan C, Francis LI, Heller RC, Galani K, Bell SP. 2010. Mec1 is one of multiple kinases that prime the Mcm2-7 helicase for phosphorylation by Cdc7. Mol Cell. 40:353-363.

-Rass, U., Compton, S. A., Matos, J., Singleton, M. R., Ip, S. C. Y., Blanco, M. G., et al. 2010. Mechanism of Holliday junction resolution by the human GEN1 protein. Genes & Development, 24(14), 1559–1569.

-Remus D, Beuron F, Tolun G, Griffith JD, Morris EP, Diffley JFX. 2009. Concerted loading of Mcm2-7 double hexamers around DNA during DNA replication origin licensing. Cell. 139:719-730.

-Reyes-Lamothe R, Possoz C, Danilova O, Sherratt DJ. 2008. Independent positioning and action of Escherichia coli replisomes in live cells. Cell 133:90–102.

-Rhind, N., Furnari, B., Russell, P. 1997. Cdc2 tyrosine phosphorylation is required for the DNA damage checkpoint in fission yeast. Genes & Development, 11(4), 504–511.

-Rhind, N., Russell, P. 2000. Chk1 and Cds1: linchpins of the DNA damage and replication checkpoint pathways. Journal of Cell Science, 113 (Pt 22), 3889–3896.

-Ried, K. et al. 2000. Common chromosomal fragile site FRA16D sequence: identification of the FOR gene spanning FRA16D and homozygous deletions and translocation breakpoints in cancer cells. Hum. Mol. Genet. 9, 1651–1663.

-Robert T, Dervins D, Fabre F, Gangloff S. 2006. Mrc1 and Srs2 are major actors in the regulation of spontaneous crossover. EMBO J 25:2837–2846.

-Roseaulin, L., Yamada, Y., Tsutsui, Y., Russell, P., Iwasaki, H., Arcangioli, B. 2008. Mus81 is essential for sister chromatid recombination at broken replication forks. The EMBO Journal, 27(9), 1378–1387.

-Sabatinos, S. A., Forsburg, S. L. 2009. Measuring DNA content by flow cytometry in fission yeast. Methods in Molecular Biology (Clifton, N.J.), 521, 449–461.

-Sakofsky, C. J., Ayyar, S., Malkova, A. 2012. Break-Induced Replication and Genome Stability. Biomolecules, 2(4), 483–504.

-Samitt CE, Hansen FG, Miller JF, Schaechter M. 1989. In vivo studies of DnaA binding to the origin of replication of Escherichia coli. EMBO J. 8(3):989–93.

-Sandler SJ, Marians KJ, Zavitz KH, et al. 1999. dnaC mutations suppress defects in DNA replication- and recombination-associated functions in priB and priC double mutants in Escherichia coli K-12. Mol Microbiol 34: 91–101.

-Sandler SJ, Marians KJ. 2000. Role of PriA in replication fork reactivation in Escherichia coli. J Bacteriol. 182(1):9-13.

-Sandler SJ. 2000. Multiple genetic pathways for restarting DNA replication forks in Escherichia coli K-12. Genetics 155: 487–97.

-Santamaria, D., G. de la Cueva, M. L. Martinez-Robles, D. B. Krimer, P. Hernandez, Schvartzman J. B. 1998. DnaB helicase is unable to dissociate RNA-DNA hybrids. Its implication in the polar pausing of replication forks at ColE1 origins. J. Biol. Chem. 273:33386–33396.

-Sartori AA, Lukas C, Coates J, Mistrik M, Fu S, Bartek J, et al. 2007. Human CtIP promotes DNA endresection. Nature. 450:509–14.

-Scheller, J., Schürer, A., Rudolph, C., Hettwer, S., Kramer, W. 2000. MPH1, a yeast gene encoding a DEAH protein, plays a role in protection of the genome from spontaneous and chemically induced damage. Genetics, 155(3), 1069–1081.

-Scholefield G, Errington J, Murray H. 2012. Soj/ParA stalls DNA replication by inhibiting helix forma- tion of the initiator protein DnaA. EMBO J. 31(6):1542–55.

-Schwartz, E. K., Heyer, W.D. 2011. Processing of joint molecule intermediates by structure-selective endonucleases during homologous recombination in eukaryotes. Chromosoma, 120(2), 109–127.

-Schwartz, M. F., Duong, J. K., Sun, Z., Morrow, J. S., Pradhan, D., Stern, D. F. 2002. Rad9 phosphorylation sites couple Rad53 to the Saccharomyces cerevisiae DNA damage checkpoint. Molcel, 9(5), 1055–1065.

-Sclafani RA, Holzen TM. 2007. Cell cycle regulation of DNA replication. Annu Rev Genet 41: 237–280.

-Seong, C., Sehorn,M. G., Plate, I., Shi, I., Song, B., Chi, P., Mortensen, U., Sung, P., Krejci, L. 2008. Molecular anatomy of the recombination mediator function of Saccharomyces cerevisiae Rad52. J. Biol. Chem., 283, 12166–12174.

-Setlow,R.B., Swenson,P.A., Carrier,W.L. 1963. Thymine dimers and inhibition of DNA synthesis by ultraviolet irradiation of cells. Science. 142, 1464–1466.

-Sheu YJ, Stillman B. 2010. The Dbf4-Cdc7 kinase promotes S phase by alleviating an inhibitory activity in Mcm4. Nature. 463:113-117.

-Shimmoto M, Matsumoto S, Odagiri Y, Noguchi E, Russell P, Masai H. 2009. Interactions between Swi1-Swi3, Mrc1 and S phase kinase, Hsk1 may regulate cellular responses to stalled replication forks in fission yeast. Genes Cells. 14(6):669-82.

-Shinohara A, Ogawa H, Ogawa T. 1992. Rad51 protein involved in repair and recombination in S. cerevisiae is a RecA-like protein. Cell. 69:457–470.

-Shinohara, A., Ogawa, H., Ogawa, T. 1992. Rad51 protein involved in repair and recombination in S. cerevisiae is a RecA-like protein. Cell, 69, 457–470.

-Shinohara, A., Ogawa,T. 1998 Stimulation by Rad52 of yeast Rad51-mediated recombination. Nature, 391, 404–407.

-Shirahige, K., Hori, Y., Shiraishi, K., Yamashita, M., Takahashi, K., Obuse, C., Tsurimoto, T., Yoshikawa, H. 1998. Regulation of DNA-replication origins during cell-cycle progression. Nature 395, 618-621.

-Sinden, R. R. 1994. DNA structure and function. Academic Press, Inc., SanDiego, CA.

-Singleton MR, Scaife S, Wigley DB. 2001. Structural analysis of DNA replication fork reversal by RecG. Cell 107: 79–89.

-Smith, M. T., and R. G. Wake. 1992. Definition and polarity of action of DNA replication terminators in Bacillus subtilis. J. Mol. Biol. 227:648–657.

-Snaith H.A., Brown G.W., Forsburg S.L. 2000. Schizosaccharomyces pombe Hsk1p is a potential cds1p target required for genome integrity, Mol. Cell. Biol. 20:7922–7932.

-Sogo J.M., Lopes M., Foiani M. 2002. Fork reversal and ssDNA accumulation at stalled replication forks owing to checkpoint defects. Science 297:599–602.

-Solinger, J.A., Kiianitsa, K., Heyer, W.D. 2002. Rad54, a Swi2/Snf2-like recombinational repair protein, disassembles Rad51:dsDNA filaments. Mol. Cell, 10, 1175–1188.

-Solinger,J.A. and Heyer,W.-D. 2001. Rad54 protein stimulates the postsynaptic phase of Rad51 protein-mediated DNA strand exchange. Proc Natl Acad Sci U S A. 17;98(15):8447-53.

-Song, B., Sung, P. 2000. Functional interactions among yeast Rad51 recombinase, Rad52 mediator, and replication protein A in DNA strand exchange. J. Biol. Chem., 275,15895–15904.

-Soulier, J., Lowndes, N. F. 1999. The BRCT domain of the S. cerevisiae checkpoint protein Rad9 mediates a Rad9-Rad9 interaction after DNA damage. Current Biology : CB, 9(10), 551–554.

-Speck C, Chen Z, Li H, Stillman B. 2005. ATPase-dependent cooperative binding of ORC and Cdc6 to origin DNA. Nat. Struct. Mol. Biol. 12(11):965–71.

-Speck C, Messer W. 2001. Mechanism of origin unwinding: sequential binding of DnaA to double- and single-stranded DNA. EMBO J. 20(6):1469–76.

-Stelter P, Ulrich HD. 2003. Control of spontaneous and damage-induced mutagenesis by SUMO and ubiquitin conjugation. Nature 425:188–191.

-Stevenson, J.B. and Gottschling, D.E. 1999. Telomeric chromatin modulates replication timing near chromosome ends. Genes Dev. 13, 146–151.

-Stewart, G. S., Wang, B., Bignell, C. R., Taylor, A. M. R., Elledge, S. J. 2003. MDC1 is a mediator of the mammalian DNA damage checkpoint. Nature, 421(6926), 961–966.

-Stinchcomb DT, Struhl K, Davis RW. 1979. Isolation and characterisation of a yeast chromosomal replicator. Nature 282(5734):39–43.

-Studwell-Vaughan PS, O'Donnell M. 1993. DNA polymerase III accessory proteins. V. Theta encoded by holE. J Biol Chem. 5;268(16):11785-91.

-Studwell-Vaughan, P. S., O'Donnell, M. 1991. Constitution of the twin polymerase of DNA polymerase III holoenzyme. J Biol Chem, 266(29), 19833–19841.

-Stukenberg PT, Studwell-Vaughan PS, O'Donnell M. 1991. Mechanism of the sliding beta-clamp of DNA polymerase III holoenzyme. J Biol Chem. 15;266(17):11328-34.

-Sugiyama, T., Kantake, N.,Wu, Y. & Kowalczykowski, S. C. 2006. Rad52-mediated DNA annealing after Rad51-mediated DNA strand exchange promotes second ssDNA capture. EMBO J. 25, 5539–5548.

-Sugiyama, T., New, J.H., Kowalczykowski, S.C. 1998. DNAannealing by RAD52 protein is stimulated by specific interaction with the complex of replication protein A and single-stranded DNA. Proc. Natl Acad. Sci. USA, 95, 6049–6054.

-Sun, W., Nandi, S., Osman, F., Ahn, J. S., Jakovleska, J., Lorenz, A., Whitby, M. C. 2008. The FANCM ortholog Fml1 promotes recombination at stalled replication forks and limits crossing over during DNA double-strand break repair. Molecular Cell, 32(1), 118–128.

-Sung, P. 1997. Yeast Rad55 and Rad57 proteins form a heterodimer that functions with replication protein A to promote DNA strand exchange by Rad51 recombinase. Genes Dev., 11, 1111–1121.

-Sung, P., Krejci, L., Van Komen, S., Sehorn, M.G. 2003. Rad51 recombinase and recombination mediators. J. Biol. Chem., 278, 42729–42732.

-Symington LS. 1998. Homologous recombination is required for the viability of rad27 mutants. Nucleic Acids Res. 26(24):5589-95.

-Symington LS. 2002. Role of RAD52 epistasis group genes in homologous recombination and double-strand break repair. Microbiol Mol Biol Rev. 66(4):630-70.

-Symington, L. S. 2014. End resection at double-strand breaks: mechanism and regulation. Cold Spring Harbor Perspectives in Biology, 6(8).

-Symington, L. S., Gautier, J. 2011. Double-strand break end resection and repair pathway choice. Annu. Rev. Genet. 45, 247–271.

-Takahagi M, Iwasaki H, Shinagawa H. 1994. Structural requirements of substrate DNA for binding to and cleavage by RuvC, a Holliday junction resolvase. J Biol Chem 269:15132–15139.

-Takeda T., Ogino K., Matsui E., Cho M.K., Kumagai H., Miyake T., Arai K., Masai H. 1999. A fission yeast gene, him1(+)/dfp1(+), encoding a regulatory subunit for Hsk1 kinase, plays essential roles in S-phase initiation as well as in S-phase checkpoint control and recovery from DNA damage, Mol. Cell. Biol. 19:5535–5547.

-Takeishi, Y., Ohashi, E., Ogawa, K., Masai, H., Obuse, C., & Tsurimoto, T. 2010. Casein kinase 2-dependent phosphorylation of human Rad9 mediates the interaction between human Rad9-Hus1-Rad1 complex and TopBP1. Genes to Cells : Devoted to Molecular & Cellular Mechanisms, 15(7), 761–771.

-Takeuchi, Y., T. Horiuchi, and T. Kobayashi. 2003. Transcription-dependent recombination and the role of fork collision in yeast rDNA. Genes Dev. 17:1497–1506.

-Tan, C. K., Castillo, C., So, A. G., Downey, K. M. 1986. An auxiliary protein for DNA polymerase-delta from fetal calf thymus. The Journal of Biological Chemistry, 261(26), 12310–12316.

-Tanaka K, Russell P. 2001. Mrc1 channels the DNA replication arrest signal to checkpoint kinase Cds1. Nat Cell Biol. 3(11):966-72.

-Tanaka S, Diffley JFX. 2002. Interdependent nuclear accumulation of budding yeast Cdt1 and Mcm2-7 during G1 phase. Nat Cell Biol 4: 198–207.

-Tanaka S, Umemori T, Hirai K, Muramatsu S, Kamimura Y, Araki H. 2007. CDK-dependent phosphorylation of Sld2 and Sld3 initiates DNA replication in budding yeast. Nature. 445:328-332.

-Tanaka T, Taniyama C, Arai K, et al. 2003. ATPase/helicase motif mutants of Escherichia coli PriA protein essential for recombinationdependent DNA replication. Genes Cells 8: 251–61.

-Tanaka T, Umemori T, Endo S, Muramatsu S, Kanemaki M, Kamimura Y, Obuse C, Araki H. 2011. Sld7, an Sld3-associated protein required for efficient chromosomal DNA replication in buddingyeast. EMBO J. 18;30(10):2019-30.

-Tanaka, S. et al. 2011. Origin association of Sld3, Sld7, and Cdc45 proteins is a key step for determination of origin-firing timing. Curr. Biol. 21, 2055–2063.

-Tazumi, A. et al. 2012. Telomere-binding protein Taz1 controls global replication timing through its localization near late replication origins in fission yeast. Genes Dev. 26, 2050–2062.

-Tercero J.A., Diffley J.F. 2001. Regulation of DNA replication fork progression through damaged DNA by the Mec1/Rad53 checkpoint, Nature 412:553–557.

-Tercero JA, Labib K, Diffley JFX. 2000. DNA synthesis at individual replication forks requires the essential initiation factor Cdc45p. EMBO J. 19:2082-2093.

-Tercero, J. A., Diffley, J. F. 2001. Regulation of DNA replication fork progression through damaged DNA by the Mec1/Rad53 checkpoint. Nature 412, 553-557.

-Tercero, J. A., Longhese, M. P., Diffley, J. F. 2003. A central role for DNA replication forks in checkpoint activation and response. Molecular Cell, 11(5):1323–1336.

-Toda, T., Umesono, K., Hirata, A., Yanagida, M. 1983. Cold-sensitive nuclear division arrest mutants of the fission yeast Schizosaccharomyces pombe. J Mol Biol, *168*(2), 251–270.

-Tomimatsu N, Mukherjee B, Hardebeck,MC. et al. 2014. Phosphorylation of EXO1 by CDKs 1 and 2 regulates DNA end resection and repair pathway choice. Nat Commun, 5, 3561.

-Tran, P. T., Erdeniz, N., Symington, L. S., Liskay, R. M. 2004. EXO1-A multi-tasking eukaryotic nuclease. DNA Repair, 3(12), 1549–1559.

-Trinh, T. Q., and R. R. Sinden. 1991. Preferential DNA secondary structure mutagenesis in the lagging strand of replication in E. coli. Nature 352:544–547.

-Tsang, E., Carr, A. M. 2008. Replication fork arrest, recombination and the maintenance of ribosomal DNA stability. DNA Repair, 7(10), 1613–1623.

-Tsang, E., Miyabe, I., Iraqui, I., Zheng, J., Lambert, S. A. E., Carr, A. M. 2014. The extent of error-prone replication-restart by homologous recombination is controlled by Exo1 and checkpoint proteins. Journal of Cell Science.

-Tsubouchi H1, Roeder GS. 2004. The budding yeast mei5 and sae3 proteins act together with dmc1 during meiotic recombination. Genetics. 168(3):1219-30.

-Tsukamoto Y, Mitsuoka C, Terasawa M, Ogawa H, Ogawa T. 2005. Xrs2p regulates Mre11p translocation to the nucle- us and plays a role in telomere elongation and meiotic recombination. Mol Biol Cell 16: 597–608.

-Tsurimoto, T., Stillman, B. 1991. Replication factors required for SV40 DNA replication in vitro. I. DNA structure-specific recognition of a primer-template junction by eukaryotic DNA polymerases and their accessory proteins. The Journal of Biological Chemistry, 266(3), 1950–1960.

-Turner J, Hingorani MM, Kelman Z, O'Donnell M. 1999. The internal workings of a DNA polymerase clamp-loading machine. EMBO J. 18:771–83.

-Ulrich HD, Jentsch S. 2000. Two RING finger proteins mediate cooperation between ubiquitin-conjugating enzymes in DNA repair. EMBO J; 19:3388–3397.

-Ulrich, H. D. 2011. Timing and spacing of ubiquitin-dependent DNA damage bypass. FEBS Letters, 585(18), 2861–2867.

-Ulrich, H. D., Takahashi, T. 2013. Readers of PCNA modifications. Chromosoma, 122(4), 259–274.

-Umesono, K., Toda, T., Hayashi, S., Yanagida, M. 1983. Cell division cycle genes nda2 and nda3 of the fission yeast Schizosaccharomyces pombe control microtubular organization and sensitivity to anti-mitotic benzimidazole compounds. J Mol Biol, 168(2), 271–284.

-Unk I, Hajdu I, Fatyol K, Hurwitz J, Yoon JH, Prakash L, Prakash S, Haracska L. Human HLTF functions as a ubiquitin ligase for proliferating cell nuclear antigen polyubiquitination. Proc Natl Acad Sci USA. 2008; 105:3768–3773.

-Uziel, T., Lerenthal, Y., Moyal, L., Andegeko, Y., Mittelman, L., Shiloh, Y. 2003. Requirement of the MRN complex for ATM activation by DNA damage. The EMBO Journal, 22(20), 5612–5621.

-van Brabant, A.J. et al. 2000. Binding and melting of D-loops by the Bloom syndrome helicase. Biochemistry. 39, 14617–14625.

-van den Bosch, M., Lohman, P.H.M., Pastink A. 2002. DNA double-strand break repair by homologous recombination. Biol Chem, 383(6), 873–892.

-Van Komen,S., Petukhova,G., Sigurdsson,S., Stratton,S. and Sung,P. 2000. Superhelicity-driven homologous DNA pairing by yeast recombination factors Rad51 and Rad54. Mol. Cell. 6, 563–572.

-Veaute X., Jeusset J., Soustelle C., Kowalczykowski S.C., Le Cam E., Fabre F. 2003. The Srs2 helicase prevents recombination by disrupting Rad51 nucleoprotein filaments, Nature 423;309–312.

-Vialard, J. E., Gilbert, C. S., Green, C. M., Lowndes, N. F. 1998. The budding yeast Rad9 checkpoint protein is subjected to Mec1/Tel1-dependent hyperphosphorylation and interacts with Rad53 after DNA damage. The EMBO Journal, 17(19), 5679–5688.

-Vogelauer, M. et al. 2002. Histone acetylation regulates the time of replication origin firing. Mol. Cell 10, 1223–1233.

-Wang G, Klein MG, Tokonzaba E, Zhang Y, Holden LG, Chen XS. 2008. The structure of a DnaB-family replicative helicase and its interactions with primase. Nat. Struct. Mol. Biol. 15(1):94–100.

-Wang L., Darling J., Zhang J.-S., Huang H., Liu W., Smith D. I. 1999. Allele-specific late replication and fragility of the most active common fragile site, FRA3B. Human Molecular Genetics, vol. 8, no. 3, pp. 431–437.

-Watanabe K, Tateishi S, Kawasuji M, Tsurimoto T, Inoue H, Yamaizumi M. 2004. Rad18 guides polη to replication stalling sites through physical interaction and PCNA monoubiquitination. EMBO J 23:3886–3896.

-Watson, A. T., Daigaku, Y., Mohebi, S., Etheridge, T. J., Chahwan, C., Murray, J. M., Carr, A. M. 2013. Optimisation of the Schizosaccharomyces pombe urg1 Expression System. *PloS One*, *8*(12), e83800.

-Watson, A. T., Werler, P., Carr, A. M. 2011. Regulation of gene expression at the fission yeast Schizosaccharomyces pombe urg1 locus. Gene, 484(1-2), 75–85.

-Watt, S., Mata, J., López-Maury, L., Marguerat, S., Burns, G., Bähler, J. 2008. urg1: a uracil-regulatable promoter system for fission yeast with short induction and repression times. PloS One, 3(1), e1428.

-Weinert, T. A., Hartwell, L. H. 1988. The RAD9 gene controls the cell cycle response to DNA damage in Saccharomyces cerevisiae. Science 241, 317 – 322.

-Weinert, T., Kaochar, S., Jones, H., Paek, A., Clark, A. J. 2009. The replication fork's five degrees of freedom, their failure and genome rearrangements. Current Opinion in Cell Biology, 21(6), 778–784.

-Weinreich M., Stillman B. 1999. Cdc7p-Dbf4p kinase binds to chromatin during S phase and is regulated by both the APC and the RAD53 checkpoint pathway, EMBO J. 18:5334–5346.

-Wickner S, Hurwitz J. 1975. Interaction of Escherichia coli dnaB and dnaC(D) gene products in vitro. Proc. Natl. Acad. Sci. USA 72(3):921–25.

-Williams GJ, Williams RS, Williams JS, Moncalian G, Arvai, AS,LimboO, Guenther G, Sildas S, Hammel M, Russell P, et al. 2011. ABC ATPase signature helices in Rad50 link nucleotide state to Mre11 interface for DNA repair. Nat Struct Mol Biol 18: 423–431.

-Wohlschlegel JA, Dwyer BT, Dhar SK, Cvetic C, Walter JC, Dutta A. 2000. Inhibition of eukaryotic DNA replication by geminin binding to Cdt1. Science 290(5500):2309-12.

-Wood A, Garg P, Burgers PM.2007. A ubiquitin-binding motif in the translesion DNA polymerase Rev1 mediates its essential functional interaction with ubiquitinated proliferating cell nuclear antigen in response to DNA damage. J Biol Chem; 282:20256–20263.

-Wood, V., Gwilliam, R., Rajandream, M.-A., Lyne, M., Lyne, R., Stewart, A., et al. 2002. The genome sequence of Schizosaccharomyces pombe. Nature, 415(6874), 871–880.

-Wu L, Hickson ID. 2006. DNA helicases required for homologous recombination and repair of damaged replication forks. Annu Rev Genet. 40:279-306.

-Wu, L., Hickson, I.D. 2003. The Bloom's syndrome helicase suppresses crossing over during homologous recombination. Nature 426, 870–874.

-Wu, X. & Huang, M. 2008. Dif1 controls subcellular localization of ribonucleotide reductase by mediating nuclear import of the R2 subunit. Mol. Cell. Biol. 28, 7156 – 7167.

-Wyatt H, Sarbajna S, Matos J, West SC. 2013. Coordinated Actions of SLX1-SLX4 and MUS81-EME1 for Holliday Junction Resolution in Human Cells. Mol Cell, 52(2), 234–247.

-Xia, Z., Morales, J. C., Dunphy, W. G., Carpenter, P. B. 2001. Negative cell cycle regulation and DNA damage-inducible phosphorylation of the BRCT protein 53BP1. The Journal of Biological Chemistry, 276(4), 2708–2718.

-Xu, L., Marians, K. J. 2003. PriA mediates DNA replication pathway choice at recombination intermediates. Mol. Cell. 11, 817–826.

-Xu, Y.-J., Davenport, M., Kelly, T. J. 2006. Two-stage mechanism for activation of the DNA replication checkpoint kinase Cds1 in fission yeast. Genes & Development, 20(8), 990–1003.

-Yabuuchi H, Yamada Y, Uchida T, Sunathvanichkul T, Nakagawa T, Masukata H. 2006. Ordered assembly of Sld3, GINS and Cdc45 is distinctly regulated by DDK and CDK for activation of replication origins. EMBO J. 25:4663-4674.

-Yamazaki, S. et al. 2012. Rif1 regulates the replication timing domains on the human genome. EMBO J. 31, 3667–3677.

-Yamazaki, S., Hayano, M., Masai, H. 2013. Replication timing regulation of eukaryotic replicons: Rif1 as a global regulator of replication timing. Trends in Genetics : TIG, 29(8), 449–460.

-Yeeles, J. T. P., Poli, J., Marians, K. J., Pasero, P. 2013. Rescuing Stalled or Damaged Replication Forks. Cold Spring Harbor Perspectives in Biology, 5(5), a012815–a012815.

-You, Z. and Bailis, J.M. 2010. DNA damage and decisions: CtIP coordinates DNA repair and cell cycle checkpoints. Trends Cell Biol. 20, 402–409.

-Yue, M., Singh, A., Wang, Z., & Xu, Y.-J. 2011. The phosphorylation network for efficient activation of the DNA replication checkpoint in fission yeast. Journal of Biological Chemistry, 286(26), 22864–22874.

-Zachos, G., Rainey, M. D. and Gillespie, D. A. 2003. Chk1-deficient tumour cells are viable but exhibit multiple checkpoint and survival defects. EMBO J. 22, 713-723.

-Zegerman P, Diffley JFX. 2007. Phosphorylation of Sld2 and Sld3 by cyclin-dependent kinases promotes DNA replication in budding yeast. Nature. 445:281-285.

-Zegerman, P., Diffley, J. F. 2010. Checkpoint-dependent inhibition of DNA replication initiation by Sld3 and Dbf4 phosphorylation. Nature 467, 474-478.

-Zhang, H., Lawrence, C. W.2005. The error-free component of the RAD6/RAD18 DNA damage tolerance pathway of budding yeast employs sister-strand recombination.

Proceedings of the National Academy of Sciences of the United States of America, 102(44), 15954–15959.

-Zhao, H., Tanaka, K., Nogochi, E., Nogochi, C., Russell, P. 2003. Replication checkpoint protein Mrc1 is regulated by Rad3 and Tel1 in fission yeast. Molecular and Cellular Biology, 23(22), 8395–8403.

-Zhao, X., Muller, E. G. & Rothstein, R. 1998. A suppres- sor of two essential checkpoint genes identifies a novel protein that negatively affects dNTP pools. Mol. Cell 2, 329 – 340.

-Zhu, Z. et al. 2008. Sgs1 helicase and two nucleases Dna2 and Exo1 resect DNA double-strand break ends. Cell 134, 981–994.

-Zhuang Z, Johnson RE, Haracska L, Prakash L, Prakash S, Benkovic SJ. 2008. Regulation of polymerase exchange between Poleta and Poldelta by monoubiquitination of PCNA and the movement of DNA polymerase holoenzyme. Proc Natl Acad Sci U S A 105:5361–5366.

-Zou L, Elledge SJ. 2003. Sensing DNA damage through ATRIP recognition of RPA-ssDNA complexes. Science, 300(5625), 1542–1548.

-Zou L., Elledge S.J. 2003. Sensing DNA damage through ATRIP recognition of RPA-ssDNA complexes. 300(5625), 1542–1548.

-Zou, L., Liu, D., Elledge, S. J. 2003. Replication protein A-mediated recruitment and activation of Rad17 complexes. Proceedings of the National Academy of Sciences of the United States of America, 100(24), 13827–13832.

APPENDIX

OPEN ACCESS Freely available online

PLOS ONE

Optimisation of the *Schizosaccharomyces pombe urg1* Expression System

Adam T. Watson, Yasukazu Daigaku, Saed Mohebi, Thomas J. Etheridge, Charly Chahwan, Johanne M. Murray, Antony M. Carr*

Genome Damage and Stability Centre, School of Life Sciences, University of Sussex, Brighton, East Sussex, United Kingdom

Abstract

The ability to study protein function *in vivo* often relies on systems that regulate the presence and absence of the protein of interest. Two limitations for previously described transcriptional control systems that are used to regulate protein expression in fission yeast are: the time taken for inducing conditions to initiate transcription and the ability to achieve very low basal transcription in the "OFF-state". In previous work, we described a Cre recombination-mediated system that allows the rapid and efficient regulation of any gene of interest by the *urg1* promoter, which has a dynamic range of approximately 75-fold and which is induced within 30-60 minutes of uracil addition. In this report we describe easy-to-use and versatile modules that can be exploited to significantly tune down P_{urg1} "OFF-levels" while maintaining an equivalent dynamic range. We also provide plasmids and tools for combining P_{urg1} transcriptional control with the auxin degron tag to help maintain a null-like phenotype. We demonstrate the utility of this system by improved regulation of HO-dependent site-specific DSB formation, by the regulation Rtf1-dependent replication fork arrest and by controlling $Rhp18^{Rad18}$-dependent post replication repair.

Citation: Watson AT, Daigaku Y, Mohebi S, Etheridge TJ, Chahwan C, et al. (2013) Optimisation of the *Schizosaccharomyces pombe urg1* Expression System. PLoS ONE 8(12): e83800. doi:10.1371/journal.pone.0083800

Editor: Marco Muzi-Falconi, Universita' di Milano, Italy

Received October 2, 2013; **Accepted** November 17, 2013; **Published** December 20, 2013

Funding: This work was supported by Medical Research Council (UK) grant G1100074 (www.mrc.ac.uk/) and European Research Council grant 268788-SMI-DDR (www.erc.europa.eu/). The funders had no role in study design, data collection and analysis, decision to publish, or preparation of the manuscript.

Competing Interests: The authors have declared that no competing interests exist.

* E-mail: a.m.carr@sussex.ac.uk

Introduction

The study of protein function *in vivo* is greatly aided by systems that deplete the protein of interest. Whether or not depletion of a protein is biologically significant (causes a phenotype) will depend on the amount of protein required for its function. The amount of cellular protein is the result of multiple levels of regulation, including transcription rate, mRNA stability, translational efficiency and protein turnover. The study of gene function may require control over one or more of these processes.

In the fission yeast *Schizosaccharomyces pombe* transcription rate has traditionally been controlled using modified constitutive or inducible promoters of varying strength. The promoter of the alcohol dehydrogenase ($adh1^+$) gene, it's weak derivative *adh1*-15 and it's much weaker derivative *adh1*-81, are typical examples of a widely used constitutive promoter [1,2,3]. The most widely used inducible promoter used in *S. pombe* is derived from the $nmt1^+$ (no message in thiamine) gene [4]. The *nmt1* promoter has the added advantage of intermediate promoter strengths that are achieved through mutation of the TATA box, generating intermediate (*nmt41*) and low (*nmt81*) strength versions [5].

While these *nmt*-derived promoters offer a choice of transcription levels, they all take 12-16 hours to show induction and 15–21 hours to reach maximum induction levels once thiamine is removed. This is a significant disadvantage considering that the fission yeast cell cycle is completed within 2–3 hours. More recently, Watt et al, (2008) characterised the promoter of the $urg1^+$ gene, where *urg1* transcript levels peak 30 minutes after the addition of uracil [6]. However, attempts to reproduce this ectopically resulted in a significant increase in "OFF-state" transcription, severely limiting the dynamic range and thus its utility. We recently demonstrated that induction kinetics driven by the *urg1* promoter (P_{urg1}), and the dynamic range, are maintained when ectopic open reading frames (ORFs) replace the native *urg1* ORF [7]. To facilitate rapid and simple manipulation of *urg1* locus, a Cre recombinase and lox recombination site-based Recombination-Mediated Cassette Exchange (RMCE) system was developed [7]. This facilitates rapid and efficient exchange of sequences to place any chosen ORF under control of the endogenous P_{urg1} (for schematic, see Figure 1A).

While it is now possible to regulate transcription of any gene at the *urg1* locus in response to uracil addition, several disadvantages remain: first, while the dynamic range of ~75 fold is good, the basal level of proteins regulated by P_{urg1} remain significant. Thus, the minimal repressed ("OFF") level of protein is often too high to visualise a phenotype equivalent to a null mutation. Second, the induced ("ON") level is correspondingly also high, which may cause problems when studying proteins who's endogenous levels are comparatively low. Third, while P_{urg1} transcription resets to basal levels within 30–60 minutes of uracil removal, the protein being studied will decay with kinetics that are determined by the stability of the protein produced. We thus sought mechanisms to further regulate P_{urg1}-dependent transcript levels and to facilitate removal of the induced protein following transcription shut-off.

In *S. pombe*, a mechanism for the selective removal of meiosis-specific mRNAs in mitotic cells has been characterised. The

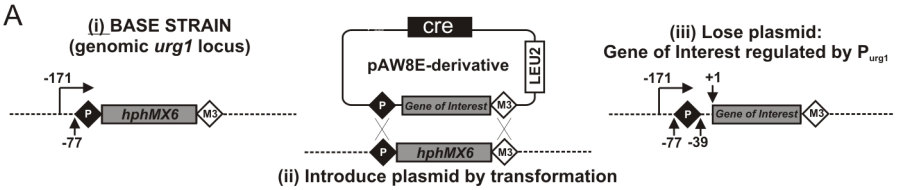

B

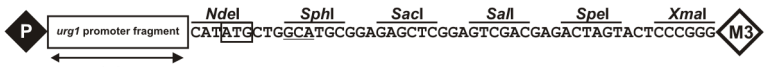

DSR	plasmid name	accession number
NONE	pAW8ENdeI	JF340115

C

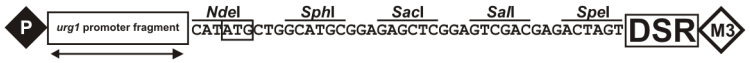

DSR	plasmid name	accession number
3X	pAW8ENdeI-3XDSR	KF361355
4X	pAW8ENdeI-4XDSR	KF361356
6X	pAW8ENdeI-6XDSR	KF361357
8X	pAW8ENdeI-8XDSR	KF361358
spo5	pAW8ENdeI-*spo5*DSR	KF361359

D

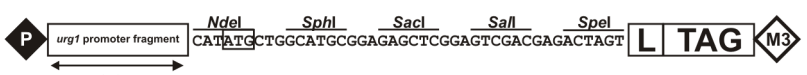

DSR	TAG description	plasmid name	accession number
NONE	yEGFP	pAW8ENdeI-cyEGFP	JF340116
NONE	3XHA	pAW8ENdeI-c3HA	JF340118
NONE	auxin-inducible degron	pAW8ENdeI-cHAIAA17	KF361360

E

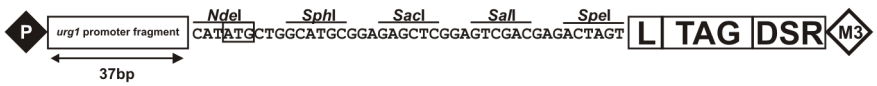

DSR	TAG description	plasmid name	accession number
3X	yEGFP	pAW8ENdeI-cyEGFP3XDSR	KF361361
4X		pAW8ENdeI-cyEGFP4XDSR	KF381191
6X		pAW8ENdeI-cyEGFP6XDSR	KF381192
8X		pAW8ENdeI-cyEGFP8XDSR	KF381193
spo5		pAW8ENdeI-cyEGFP*spo5*DSR	KF381194
3X	3XHA	pAW8ENdeI-c3HA3XDSR	KF381195
4X		pAW8ENdeI-c3HA4XDSR	KF381196
6X		pAW8ENdeI-c3HA6XDSR	KF381197
8X		pAW8ENdeI-c3HA8XDSR	KF381198
spo5		pAW8ENdeI-c3HA*spo5*DSR	KF381199
spo5	auxin-inducible degron	pAW8ENdeI-cHAIAA17*spo5*DSR	KF381200

Figure 1. Principals of RCME and plasmids created. (**A**). Schematic showing the process of RCME (Watson 2008): (i) starting with a base strain in which the *urg1* ORF is replaced by an antibiotic marker (each of *hphMX6*, *natMX6* and *kanMX6* are available) that is flanked by (incompatible) loxP and loxM3 sites, a plasmid (ii) is introduced. This plasmid contains the cloned gene of interest and any tagging sequences positioned between loxP and loxM3 sites. It also expresses Cre recombinase. Site-directed recombination next exchanges the sequences between the plasmid and the chromosome (iii). Successful exchange can easily be identified by loss of the antibiotic marker, typically seen in greater than 50% of cells. Plasmid loss in these colonies is then confirmed by replica plating to verify colonies are leu^{-}. In our experience, all of these are successful integrants. (**B**). Plasmid for expression of untagged sequences (NO DSR) as previously published [7]. Shown is a schematic of the sequence between loxP (P) and loxM3 (M3) for pAW8E*Nde*I. A start codon is formed from an *Nde*I site. (**C**) Equivalent schematic of pAW8E*Nde*I containing various DSR sequences. (**D**) Schematic of plasmid used to express proteins with either a yEGFP tag, a 3xHA tag or an HA combined with an IAA17 degron tag (HAIAA17) (all with NO DSR). L = poly-tyrosine–glycine–serine (TGS) linker: TAG = yEGFP, 3xHA or HAIAA17 protein tag. (**E**) Equivalent schematic of pAW8E*Nde*I C-terminal tagging plasmids that also contain various DSR sequences. HA = human influenza hemagglutinin protein tag, yEGFP = yeast codon optimised green fluorescent protein, HAIAA17 = Degron from Arabidopsis thaliana transcription repressor.
doi:10.1371/journal.pone.0083800.g001

removal involves the YTH-domain containing protein Mmi1 [8] which binds meiosis-specific mRNAs containing Determinant of Selective Removal (DSR) sequences, usually located at the 3' end of the transcript. Mmi1 greatly increases transcript turnover by directing DSR-containing transcripts to nuclear exosomes for degradation [8,9]. By deletion analysis, the DSR elements of *ssm4*,

rec8 and *spo5* mRNAs were identified [8]. Recent studies have recognised a hexanucleotide motif U(U/C)AAAC that is highly enriched in the DSR elements and have shown that tandem repeats of this motif can function as an artificial DSR in heterologous gene systems [10,11].

Recent studies in *S. pombe* indicate that ~1 mRNA copy per cell defines a functional norm for productive gene expression [12]. Since aggregate levels of significantly less than 1 transcript per cell will provide a distribution of 0 or 1 transcripts in most of the cells in the population, this may help explain why it is difficult to obtain "null" phenotypes using transcriptional control alone: individual cells in the population will be producing significant quantities of protein, even when the aggregate transcript level appears very low. Furthermore, even if a transcript is ''shut-off'' completely, the intrinsic stability of the protein expressed will determine how quickly a null phenotype will be established when ''shut-off'' experiments are performed.

Protein levels can be manipulated independently of transcription using various protein degradation systems. These generally involve the fusion of a domain (known as a 'degron') to the target protein to induce degradation. The auxin-inducible degron (AID) system [13] was recently adapted for use in fission yeast [1]. In plants, the hormone auxin bind to the transport inhibitor response 1 (TIR1) F-box protein and promotes binding of the E3 ubiquitin ligase SCF^{TIR1}, an SCF (Skp1, Cullin and F-box) ubiquitin ligase complex, to auxin or IAA (Aux/IAA) transcription repressors [14]. The Aux/IAA proteins are subsequently poly-ubiquitinated by SCF^{TIR1} and degraded by the proteasome. All eukaryotes have multiple subtypes of the SCF ubiquitin ligases, but orthologs of TIR1 and Aux/IAAs are only found in plants. The degradation system described by Nishimura et al. (2009) for budding yeast uses the IAA17 degron from Arabidopsis thaliana. When fused to a protein target, this degron sequence promotes proteasome and ubiquitin-dependent degradation in an auxin-dependent manner if a functional TIR1 F-box protein is also concomitantly expressed. Rapid depletion of a target protein within 30 mins in the presence of auxin was observed, allowing the generation of conditional mutants [13]. The AID system has also been adapted for *S. pombe*, but appears to be somewhat less efficient. However, auxin-dependent conditional mutant phenotypes were obtained for several proteins when the corresponding protein was tagged with IAA17, a TIR1-Skp1 fusion protein was expressed and the system was combined with transcription repression [1].

Here we describe for *S. pombe* a P_{urg1}-based, uracil regulatable protein expression system that exploits control over the combination of transcription rate, mRNA stability and protein-depletion to tightly control target protein expression levels in *S. pombe*. The rapid induction of the $urg1^+$ promoter controls transcription rate, DSR sequences regulate transcript levels via constitutive mRNA degradation and the auxin-inducible protein degradation system controls protein turnover. To facilitate a choice of ''ON'' and ''OFF'' levels we have constructed a range of plasmid vectors that allow researchers to use RMCE to rapidly and efficiently insert their gene of interest at the *urg1* locus in the context of the desired DSR and degron sequences (Figure 1). The plasmids contain a variety of DSR constructs to determine different levels of transcript stability and further allow the cloned ORF to be untagged or tagged with yeast codon-optimised green fluorescent protein yEGFP, the hemagglutinin epitope tag HA as well as the auxin-inducible IAA17 degron.

Results

The Mmi1/DSR mRNA degradation system reduces protein levels expressed from the *urg1* locus

An advantage of the *S. pombe nmt1* (*no message in thiamine*) inducible promoter system is the ability to attenuate promoter activity levels through progressive deletion of the TATAA-box sequence [5]. However, deletion of a potential *urg1* promoter TATAA box sequence identified by 5' RACE [7] did not significantly reduce promoter activity (data not shown). We therefore decided to exploit the recently characterised mechanism that selectively removes meiosis-specific mRNAs from mitotic cells in *S. pombe*. The mechanism involves Mmi1 binding to a target region – the DSR (Determinant of Selective Removal) and guiding the mRNA for degradation via the nuclear exosomes [8,9]. The hexanucleotide motif U(U/C)AAAC is highly enriched in the DSR and tandem repeats of this motif function as an artificial DSR in heterologous gene systems [10,11].

We modified our published *urg1* promoter system [7] to contain either the 157bp DSR element derived from the *S. pombe spo5* gene or various numbers of repeats of the DSR core motif: TTAAAC. To achieve this, we modified the Cre-expression plasmid pAW8E*Nde*I [7] by inserting either the 157bp *spo5*DSR element or between 1 and 8 copies (referred to as 1XDSR through 8XDSR) of the DSR core motif adjacent to the pAW8E*Nde*I multiple cloning site such that, in the corresponding mRNA, it will be 3' of the ORF. To maintain identical motif spacing to that previously characterised [10], the repeat motifs were separated by six base pairs copied randomly from bacteriophage lambda DNA. We next introduced the open reading frame (ORF) of the yeast codon-optimised green fluorescent protein (yEGFP) between the MCS and the DSR sequences. When integrated at the *urg1* locus, these constructs will express GFP as the ATG initiation codon contained within the *Nde*I restriction enzyme site (CAT<u>ATG</u>), present in pAW8E*Nde*I MCS, is in-frame with the yEGFP ORF. These pAW8E*NdeI*-cyEGFP-DSR plasmids were then used to create, via Cre-mediated RMCE, a series of yeast strains where expression of yEGFP was controlled at the *urg1* locus by the $P_{urg1lox}$ (we designate the modified *urg1* promoter, which remains at the *urg1* locus, but contains a loxP recombination site at –37, $P_{urg1lox}$ to distinguish it from the endogenous promoter). The transcripts resulting from the $P_{urg1lox}$ in these cells contain, in their 3' untranslated regions, various forms of the DSR (Figure 2A). A control strain containing no DSR sequences (NO DSR) and another carrying 8 copies of the mutated core motif GTAAAC (8XmDSR) were also constructed. This mutated core motif has been shown to largely ablate DSR activity [10].

To examine how efficiently the DSR/Mmi1 RNA degradation pathway reduced yEGFP protein levels, the amount of yEGFP in extracts prepared from log-phase cells in the absence ($P_{urg1lox}$ OFF) or presence ($P_{urg1lox}$ ON) of uracil were analysed by immunoblotting (Figure 2B). The *$P_{urg1lox}$-yEGFP-NO DSR* cells accumulated high levels of yEGFP protein 120mins after induction (lane 13) but a clear signal was also observable in un-induced *$P_{urg1lox}$-yEGFP-NO DSR* cells when compared to control AW501 ($urg1^+$) cells (lanes 2 and 1 respectively). This demonstrates the rapid induction of the *urg1* system and also the ''leakiness'' of the repressed *urg1* promoter. One and two copies of the DSR core motif (TTAAAC) show no significant reduction of yEGFP protein levels either in un-induced (lanes 4 and 5) or induced cells (lanes 15 and 16). However, increasing the number of core motifs to three (*$P_{urg1lox}$-yEGFP-3XDSR* cells) resulted in an observable reduction in protein levels for both un-induced (lane 6) and induced (lane 17) situations. Further reductions in yEGFP expression levels were observed with

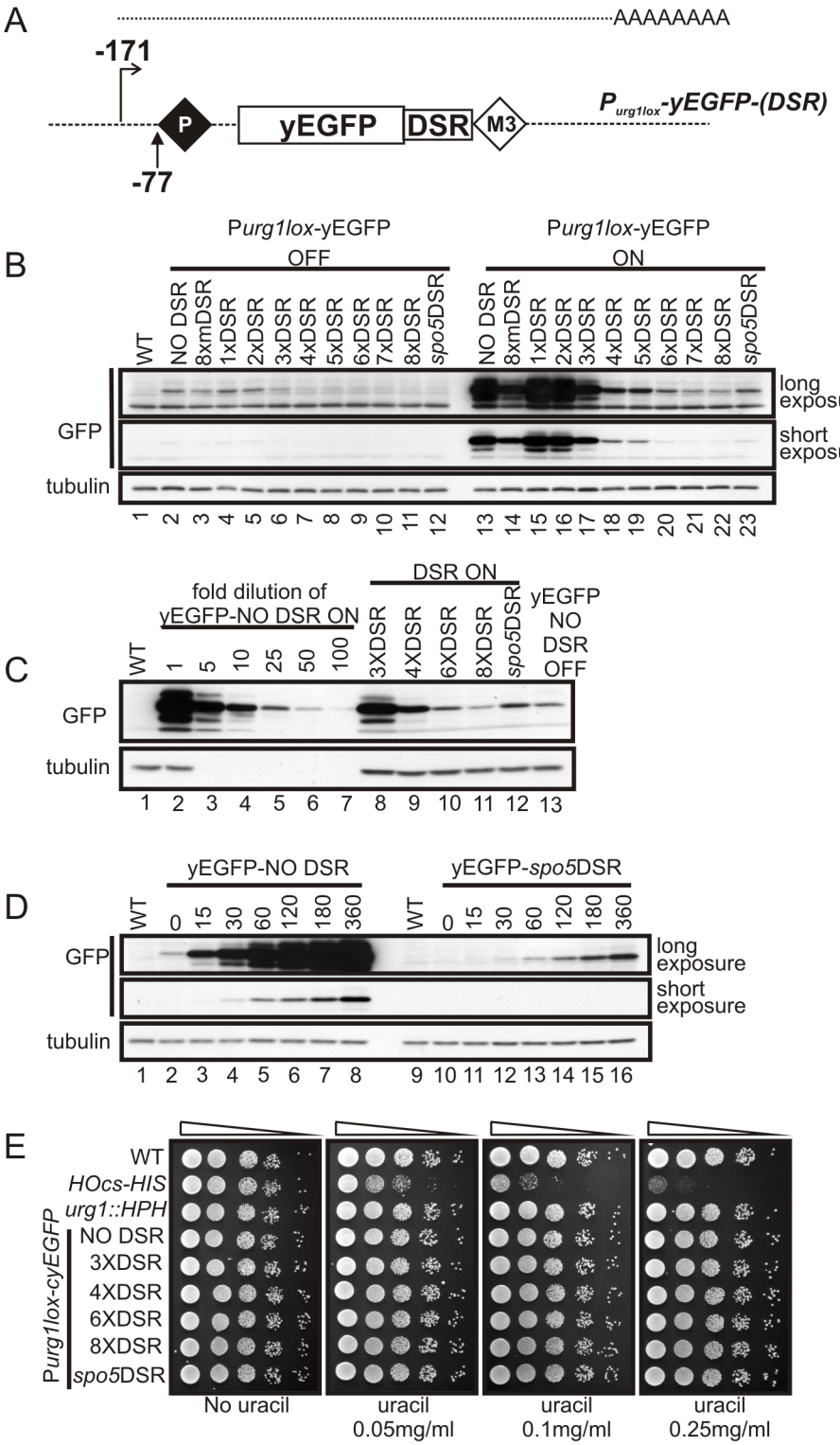

Figure 2. Determinant of Selective Removal (DSR) sequences can reduce protein levels expressed from $P_{urg1lox}$. (**A**). Schematic of the $P_{urg1lox}$ locus following RCME to introduce yEGFP under the control of the *urg1* promoter. The resulting transcript encodes the ORF followed immediately after the stop codon by one of a variety of DSR sequences. These act to target the transcript to the nuclear exosome. (**B**). The strains created with the yEGFP ORF with and without DSR sequences present in the 3′ UTR: AW640 (NO DSR), AW702 (8XmDSR), AW726 (1XDSR), AW728 (2XDSR), AW730 (3XDSR), AW732 (4XDSR), AW694 (5XDSR), AW696 (6XDSR), AW698 (7XDSR), AW700 (8XDSR) and AW638 (*spo5*DSR) (see also Table 1). The strains were cultured in EMM+L to $\sim 5\times10^6$ cells at 30°C (uracil absent - $P_{urg1lox}$ OFF). Uracil was added at 0.25 mg/ml and cells grown for 120 minutes ($P_{urag1lox}$ ON). Total protein extracts from un-induced $P_{urg1lox}$ OFF cells (lanes 2–12) and induced $P_{urg1lox}$ ON cells (lanes 13–23) were separated by SDS PAGE prior to Western blotting using anti-GFP to detect yEGFP (upper panels) and anti-tubulin for a loading control (lower panel). Lane 1 = WT control *urg1*$^+$ strain (AW501). (**C**) Comparison of the induced $P_{urg1lox}$-yEGFP levels in B. Induced cell total protein extracts were used to estimate

the fold-decrease in protein levels after induction. The NO DSR sample (lane 13 panel B) was serially diluted using SDS sample buffer and analysed (lanes 2 to 7) alongside undiluted induced 3XDSR (AW730 - lane 8), 4XDSR (AW732 - lane 9), 6XDSR (AW696 - lane 10), 8XDSR (AW700 - lane 11) and *spo5*DSR (AW638 - lane 12) samples. Lane 13 = undiluted un-induced NO DSR sample (the same as lane 2 panel B). (**D**) The kinetics of yEGFP accumulation is unaffected when using a DSR element. Time-course showing yEGFP protein levels in NO DSR (AW640 - lanes 2 to 8) and *spo5*DSR (AW638 - lanes 10 to 16) cells after addition of uracil at 0.25 mg/ml to induce $P_{urg1lox}$. Analysis of yEGFP levels by western blot as described in B. Samples taken at time-points shown (mins). Lanes 1 and 9 = control *urg1*$^+$ strain (AW501). (**E**) Over-expression of mRNAs containing DSR sequences does not affect cells growth/viability. Strains shown were serially diluted 10-fold in water and spotted on EMM+L plates supplemented with uracil at concentration shown. Pictures were taken after 3 days at 30°C.
doi:10.1371/journal.pone.0083800.g002

increasing number of DSR repeats (lanes 18 to 22) indicating increased RNA processing.

$P_{urg1lox}$-yEGFP-8mXDSR cells, our negative control which harbours eight copies of the mutated (GTAAAC) motif, accumulated significant levels of yEGFP protein (lanes 3 and 14) although there was a modest decrease when compared to the NO DSR control. This implies the mutated motif retains some function. In our positive control cells, *$P_{urg1lox}$-yEGFP-spo5DSR*, the amount of yEGFP was significantly reduced following induction by uracil addition. In the un-induced cell samples the detection limit of our western blot analysis was insufficient to show yEGFP levels for *$P_{urg1lox}$-yEGFP-4XDSR* through *$P_{urg1lox}$-yEGFP-8XDSR* and *$P_{urg1lox}$-yEGFP-spo5DSR* cells (lanes 7 to 12). Thus, for these cells we require a more sensitive method to determine $P_{urg1lox}$ repressed protein levels (see below). Induced *$P_{urg1lox}$-yEGFP-spo5DSR* cells showed similar yEGFP levels to those observed for *$P_{urg1lox}$-yEGFP-6XDSR* cells (lanes 20 and 23). The relationship between the number of core TTAAAC repeats and DSR activity was not, however, linear (Figure 2B). This may reflect the mechanism whereby Mmi1 binds the DSR containing transcript.

To estimate the fold decrease in induced protein levels we used the samples from Figure 2B for further western blot analysis. The induced *$P_{urg1lox}$-yEGFP-NO DSR* sample was serially diluted in SDS-sample buffer 5-, 10-, 25-, 50- and 100-fold (lanes 2 to 7) and immunoblotted along with undiluted induced *$P_{urg1lox}$-yEGFP-3XDSR, -4XDSR, -6XDSR, -8XDSR* and *-spo5DSR* cell samples (lanes 8-12, Figure 2C). Three tandem repeats of the DSR core element reduce levels approximately 5-fold when compared to cells containing no DSR sequences. Cells carrying 4, 6 and 8 core repeat motifs reduce levels further (10-, 25- and 50-fold lower respectively). In *$P_{urg1lox}$-yEGFP-spo5DSR* cells, the level is reduced approximately 25-fold compared to the NO DSR control. Importantly, the yEGFP level in NO DSR repressed cells (lane 13) lies between the induced levels seen for cells containing 8 DSR repeats (lane 11) and the *spo5DSR* (lane 12). Thus, by exploiting the constitutive degradation of transcripts through the introduction of different DSR constructs we can choose "ON" (+ uracil) and "OFF" (- uracil) levels of protein across a significantly better dynamic range when compared to the constitutive *$P_{urg1lox}$* RMCE system.

The rapid induction of the *$P_{urg1lox}$* is the major advantage of the expression system [7]. To establish if this rapid induction is maintained when DSR regulatory sequences are used, we performed an induction time-course and determined yEGFP protein levels by western blotting (Figure 2D). While the *spo5DSR* sequences reduced the total level of yEGFP, the kinetics of yEGFP accumulation in *$P_{urg1lox}$-yEGFP-NO DSR* and *$P_{urg1lox}$-yEGFP-spo5DSR* remained very similar (compare the long exposure for *spo5*DSR with the short exposure for NO DSR). These data demonstrate that DSR/Mmi1 RNA degradation pathway allows only a small percentage of DSR-containing transcripts to be translated prior to removal. Following the addition of uracil and the induction of $P_{urg1lox}$ transcription rate, the increased DSR-containing mRNA levels will result in higher translation efficiency and the kinetics of induction are maintained.

It has been shown that the disruption of *mmi1* severely impairs cell growth [8] and we were concerned that over-expression of mRNAs containing DSR sequences may affect cell growth/viability by titrating the available Mmi1 activity. We therefore performed a spot-test, where cells containing DSRs were spotted onto media containing uracil to induce $P_{urg1lox}$ (Figure 2E). For a positive control, the strain AW507 was used [7]. In this strain (described in more detail in the next section) the expression of HO-endonuclease is under the control of the *urg1* promoter (*$P_{urg1lox}$-HO*) and the cells contain the HO cut site (HOcs) within the *S. pombe his3*$^+$ selectable marker (*HOcs-HIS*). HO-dependent cleavage of *HOcs-HIS* thus prevents cell growth when the media does not contain histidine. As expected, growth in presence of uracil and absence of histidine lead to *$P_{urg1lox}$-HO*, *HOcs-HIS* cell inviability linked to the concentration of uracil in the growth media (Figure 2E). However, all the DSR containing strains tested grew equally as well on plates either with or without uracil.

Taken together these results show core-repeat and the *spo5* DSR elements retain selective removal activity when inserted into the 3' UTR of mRNAs expressed at the *urg1* locus and that the DSR/Mmi1 RNA degradation system successfully reduced yEGFP levels without affecting the speed of induction or cell viability/growth.

The Mmi1/DSR mRNA degradation system attenuates HO expression levels

Because the detection limit of western blot analysis, we were unable to estimate the decrease in "OFF" levels of protein in the various repressed DSR cells (see Figure 2B). We therefore attempted to demonstrate lower $P_{urg1lox}$ OFF protein levels using biological assays. We used the previously described *S. pombe* single-strand annealing (SSA) assay [7]. The SSA strain contains the MATα minimal HO recognition sequence (HOcs) in-frame and within the coding sequence of the *S. pombe his3*$^+$ selectable marker. This construct, flanked by two homologous sequences, is integrated into chromosome 1 (*HOcs-HIS*; [7]). Regulation of the expression level of the HO endonuclease using $P_{urg1lox}$ induces double strand breaks (DSBs) at HOcs. DSB ends then undergo resection that results in single strand DNA (ssDNA) tails. If the chromosome is cut in G1 or both sister chromosomes are cut following replication of the region, homologous recombination (HR) repair is not an option and resection continues until both regions of homology become single stranded. Once this occurs, the homologous ssDNAs anneal, resulting in the repair of the chromosome at the expense of loss of the intervening sequences. These sequences include the HOcs and the *his3*$^+$ selectable marker. SSA rates can thus be measured by calculating the percentage of histidine auxotrophic cells by plating cells prior to and after induction of $P_{urg1lox}$-HO onto histidine containing media and then replica plated onto media lacking histidine. SSA is an efficient repair mechanism, and thus the rate of marker loss reflects the HO expression level.

In *S. pombe*, for >80% of the cell cycle a sister chromatid is present, allowing DSB repair by homologous recombination. When HO is expressed at high levels in *HOcs-HIS* cells, both sister

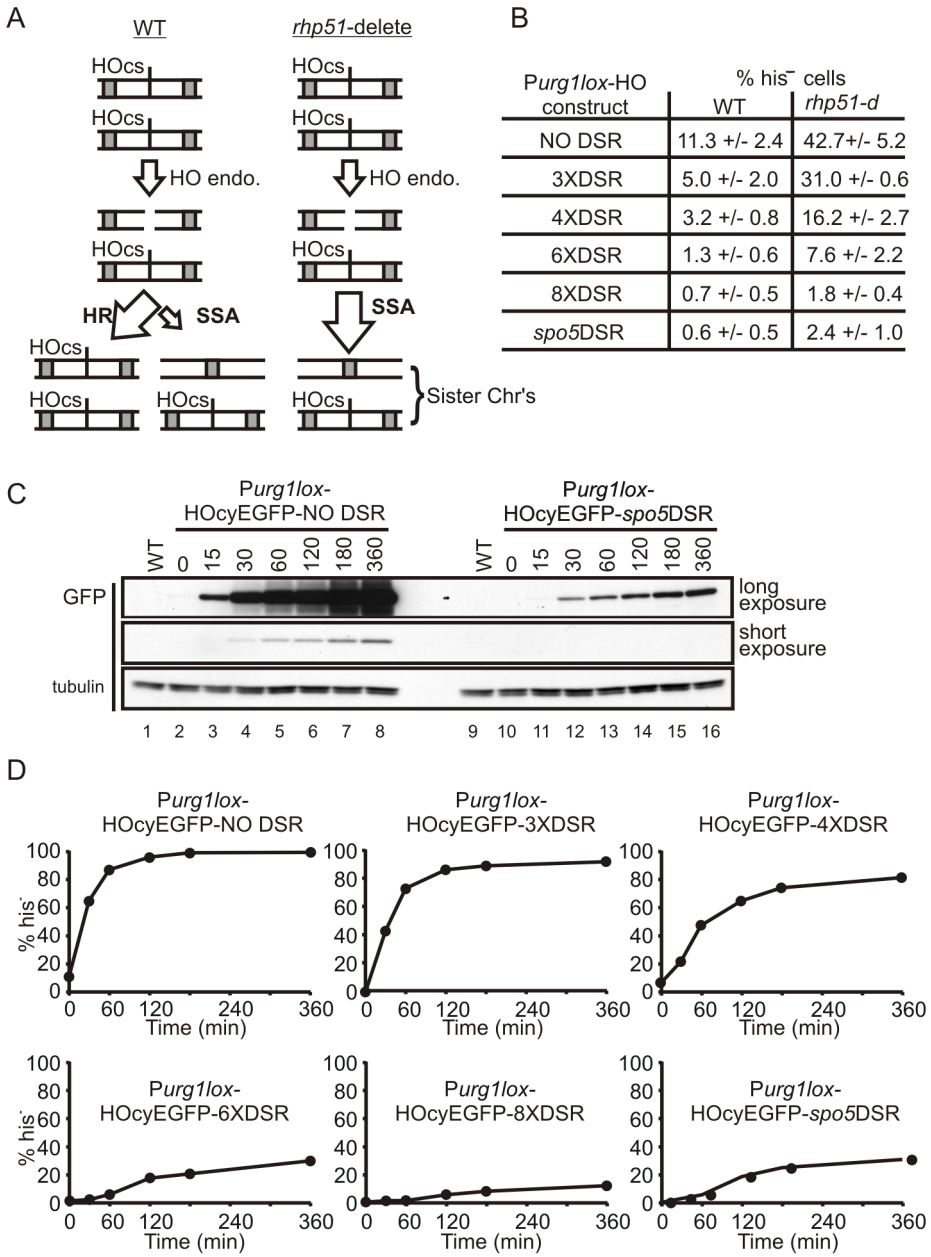

Figure 3. DSR activity reduces both induced and repressed $P_{urg1lox}$ protein levels. (**A**) Schematic illustration outlining the repair of a single HO-induced DSB in a G2 phase *S. pombe* cell. Repair in a normal (WT) cell can occur by either by homologous recombination (HR) or single strand annealing (SSA) (left panel) whereas repair in an HR deficient *rhp51*-delete cell can only occur via SSA (right panel). Grey box = region of homology, HOcs = HO endonuclease cut site. (**B**). Steady-state rate of *his3*$^+$ marker loss in WT HR proficient cells compared to HR deficient *rhp51*-delete cells. The HO endonuclease ORF tagged at the C-terminus with yEGFP was inserted by Cre-mediated cassette exchange into the *urg1* locus in WT cells containing the HOcs-HIS construct to create AW741 (NO DSR), AW743 (3XDSR), AW745 (4XDSR), AW747 (6XDSR), AW749 (8XDSR) and AW751 (*spo5*DSR) and in *rhp51*-delete cells to create AW734 (NO DSR), AW816 (3XDSR), AW818 (4XDSR), AW820 (6XDSR), AW822 (8XDSR) and AW739 (*spo5*DSR). Logarithmically growing cells cultured in EMM+L were plated onto EMM+LH plates and grown at 30°C. Colonies were replica plated onto EMM+L plates and the percentage of histidine auxotrophic (his$^-$) cells calculated. The assay was repeated at least three times and the average numbers are presented as the mean +/− SD. (**C**) The kinetics of HO-cyEGFP protein accumulation is unaffected by DSR activity. Time-course showing accumulation of HO-cyEGFP protein levels following induction of $P_{urg1lox}$. Logarithmically growing AW671 (NO DSR) and AW673 (*spo5*DSR) cells (see Table 1) were induced by the addition of uracil at 0.25mg/ml. HO-cyEGFP protein levels were examined by western blot analysis as described in Figure 2B. Samples taken at time points shown (mins). (**D**) DSR activity slows *his3*+ marker loss in the $P_{urg1lox}$-HO/HOcs-HIS SSA assay. Strains AW741 (NO DSR), AW743 (3XDSR), AW745 (4XDSR), AW747 (6XDSR), AW749 (8XDSR) and AW751 (*spo5*DSR) were grown in EMM+L to mid-log phase and uracil added at 0.25 mg/ml to induce $P_{urg1lox}$. Cells were plated onto EMM+LH plates and grown at 30°C. Colonies were replica plated onto EMM+L plates and the percentage of histidine auxotrophic cells calculated. Samples taken at time-points shown (mins). The assay was repeated twice and numbers shown are the mean. X axis = percentage of histidine auxotrophic cells, Y-axis = time in minutes.
doi:10.1371/journal.pone.0083800.g003

chromatids are likely to be cut in a single cell. However, when HO is expressed at low levels (due to leakiness of the $P_{urg1lox}$ promoter for example) the DSBs that occur are likely to be formed in only one of the two sister chromatids. This gives the cell the opportunity to use HR to repair the DSB. HR repair from the sister chromosome is silent: it restores both the HOcs site and retains the *his3*$^+$ marker (Figure 3A). When the HR pathway is not available for repair, as in the *rad51*-delete strain, a DSBs on a single sister chromatid can only be repaired using SSA. Following sister segregation at mitosis, one daughter cell will be his$^+$ and the other his$^-$. Therefore, the rate of marker loss at low levels of HO expression is expected to be higher in *rhp51*-delete cells when compared to WT cells (Figure 3A) and that rate should be a direct reflection of the number of DSBs introduced.

To test the effectiveness of the DSR/Mmi1 pathway, we subcloned the HO endonuclease ORF to create Cre-expression plasmids *pAW8ENdeI-HO-yEGFP-NO DSR*, *-3XDSR*, *-4XDSR*, *-6XDSR*, *-8XDSR* and *-spo5DSR*. Using an *urg1* base strain containing the *HOcs-HIS* construct (AW467 – Table 1), the HO-cyEGFP fusion ORF with and without DSR sequences was inserted at the *urg1* locus by cassette exchange. From the resulting strains, the steady-state level of histidine auxotrophic (his$^-$) cells in otherwise wild type cells growing logarithmically in the absence of uracil ($P_{urg1lox}$ OFF) was determined (Figure 3B). For $P_{urg1lox}$*-HO-cyEGFP-NO DSR* cells we observed 11.3 (+/– 2.4)% of cells had lost the *his3*$^+$ marker with all strains carrying DSR elements showing significantly lower levels of marker loss. In cells containing 3 copies of the core DSR motif ($P_{urg1lox}$*-HO-cyEGFP-3XDSR*), the rate was reduced to 5.0 (+/– 2.0)% and increasing number of core motifs furthers decreases the percentage of histidine auxotrophic cells. The *HO-cyEGFP-spo5DSR* cells showed a steady state level of marker loss of 0.6 (+/– 0.5)%, similar to that for *HO-cyEGFP-8XDSR* cells.

As discussed above, it is predicted that in HR deficient *rhp51*-delete cells the steady state level of *his3*$^+$ marker loss will increase compared to wild type cells because the alternative DSB repair pathway (HR) has been removed. The HO-cyEGFP Cre-expression plasmids were transformed into an *urg1* base strain containing the HOcs-HIS construct where the *rhp51* gene is also deleted (AW686 – Table 1). Following cassette exchange, the strains were again analysed in the $P_{urg1lox}$ OFF condition to determine the state-state level of histidine auxotrophic cells. For all the *rhp51*-delete strains studied, the rate of marker loss increased relative to the HR proficient WT strains (Figure 3B). The level increased in $P_{urg1lox}$*-HO-cyEGFP-NO DSR*, *rhp51-d* cells to ~ 43% compared to ~ 11% in WT *rhp51*$^+$ cells. As observed for HR-proficient *rhp51*$^+$ cells, marker loss decreased in cells where HO expression was attenuated by DSR regulatory elements with the steady state levels in 8XDSR and spo5DSR cells around 2%.

We next preformed a time course to monitor HO-cyEGFP proteins levels following induction of $P_{urg1lox}$ by uracil addition. The samples were western blotted and probed with anti-GFP antibody (Figure 3C). As was observed for yEGFP protein levels (Figure 2D), following $P_{urg1lox}$ induction the kinetics of HO-cyEGFP protein increase was similar for *HO-cyEGFP-spo5DSR* cells and *HO-cyEGFP-NO DSR* cells, but a significant overall reduction in expressed protein levels was evident when the *spo5DSR* was present (Figure 3C). To investigate the kinetics *his3*$^+$ marker loss following induction of $P_{urg1lox}$, cells containing either NO DSR, the *spo5DSR*, 3xDSR, 4xDSR, 6xDSR or 8xDSR were analysed for marker loss following induction by uracil (Figure 3D). The kinetics of marker loss was clearly influenced by DSR activity and correlated well with yEGFP levels observed in Figure 2. For example, in induced $P_{urg1lox}$*-yEGFP-6xDSR* and $P_{urg1lox}$*-yEGFP-spo5DSR* cells the protein levels were comparable (Figure 2A and 2B) and the levels and profile of *his3*$^+$ marker loss in *HO-cyEGFP-6XDSR* and *HO-cyEGFP-spo5DSR, HOcs-HIS* cells are also similar.

Overall, these data demonstrate that, despite being unable to detect the protein by western blot due to the low levels, the biological activity of the HO endonuclease in the $P_{urg1lox}$ OFF state is decreased by the presence of DSR motifs. This is consistent with protein levels in $P_{urg1lox}$ repressed cells being decreased when the transcript contains DSR elements. The implied "OFF" state protein levels mirror the protein levels observed by western blot analysis when the $P_{urg1lox}$ promoter was induced by uracil addition. Increasing the tandem core DSR repeat number showed increasing DSR activity, presumably reflecting RNA processing. Despite containing 6 DSR repeats, the 157bp *spo5* DSR element exhibits RNA processing activity in the "ON" state similar to that seen for 6 tandem core repeats (Figure 3B) but in the "OFF" state appears equivalent to 8XDSR repeats (see below). This suggests that other factors such as motif spacing may be important for efficient Mmi1 binding and RNA processing.

Efficient regulation of replication fork barrier activity

In *S. pombe*, site-specific replication fork arrest and recombination-dependent fork restart have been studied extensively [15,16,17,18]. The systems used involve the directional fork barrier sequence, *RTS1*, which is dependent for activity on the Myb-domain DNA binding protein Rtf1. To date, replication arrest at *RTS1* has been regulated by transcriptional control of the *rtf1*$^+$ gene via the thiamine repressible promoter, *nmt41*. However, the *nmt41* promoter is slow to induce (12–16 hrs) compared to the cell cycle time of *S. pombe* (2–3 hours). The *urg1* inducible system is quick to induce, with mRNA levels peaking 30 minutes after the addition of uracil [6]. However, previous attempts to regulate Rtf1 protein levels using $P_{urg1lox}$ were unsuccessful because the repressed level of $P_{urg1lox}$ transcription was too high for the system to be biologically off [7]. We therefore tested if the addition of the *spo5*DSR regulatory element was sufficient reduce Rtf1 "OFF" levels in $P_{urg1lox}$ repressed cells.

The study of template exchange following fork restart has involved a system in which two inverted copies of *ura4*$^+$ gene are flanked by *RTS1* sequences [17,18]. This is referred to as the *RuiuR* construct (Figure 4A). We chose this system for testing the effectiveness of the *spo5* DSR element. The *RuiuR* construct was crossed into *urg1* base strain (AW469) to create YSM077 (Table 1). Using plasmid pAW8E*NdeI-rtf1-spo5*DSR (see materials and methods) we created YSM098 (*urg1::*$P_{urg1lox}$*-rtf1-spo5DSR, RuiuR*) by Cre-mediated cassette exchange. Rtf1 activity in these cells can be monitored by detection of replication intermediates (RIs) arising from stalled replication forks using native two-dimensional gel electrophoresis (2DGE). Passive replication of the *RuiuR* locus (Rtf1 absent) is predicted to result in a Y-arc being detected (Figure 4B, left panel cartoon). However, upon site-specific fork arrest (Figure 4B, right panel cartoon), the intensity of the Y-arc is predicted to be reduced and an intense spot is predicted on the Y-arc, corresponding to the position of arrested forks.

In the complete absence of Rtf1 (*rtf1* deleted: *rtf1*D), replication this region is replicated passively (Figure 4C). When Rtf1 is under control of $P_{urg1lox}$ in association with the s*po5*DSR and repressed (Figure 4C; t = 0), the Y-arc is clearly visible with a faint spot corresponding to a low level of replication fork stalling. This is presumably because, as seen for the regulation HO using DSR sequences, the DSR/Mmi1 pathway of mRNA degradation is not 100% efficient. 180 minutes after the addition of uracil (Rtf1 induced), the Y-arc is no longer visible and an intense spot arising from fork arrest is seen (Figure 1C; t = 180). These data show that

Table 1. *S. pombe* strains used in this study.

Strains created via Cre-lox recombination mediated cassette exchange during this study		
***urg1* base strain employed**	**RCME plasmid used**	**Genotype of strain created**
h-, urg1::RMCE$_{hphMX6}$, leu1-32 (AW459) (Watson et al 2011)	pAW8E*Nde*I-cyEGFP	*h-, urg1::Purg1lox-cyEGFP, leu1-32 (AW640)*
	pAW8E*Nde*I-cyEGFP-1xDSR	*h-, urg1::Purg1lox-cyEGFP-1xDSR, leu1-32 (AW726)*
	pAW8E*Nde*I-cyEGFP-2xDSR	*h-, urg1::Purg1lox-cyEGFP-2xDSR, leu1-32 (AW728)*
	pAW8E*Nde*I-cyEGFP-3xDSR	*h-, urg1::Purg1lox-cyEGFP-3xDSR, leu1-32 (AW730)*
	pAW8E*Nde*I-cyEGFP-4xDSR	*h-, urg1::Purg1lox-cyEGFP-4xDSR, leu1-32 (AW732)*
	pAW8E*Nde*I-cyEGFP-5xDSR	*h-, urg1::Purg1lox-cyEGFP-5xDSR, leu1-32 (AW694)*
	pAW8E*Nde*I-cyEGFP-6xDSR	*h-, urg1::Purg1lox-cyEGFP-6xDSR, leu1-32 (AW696)*
	pAW8E*Nde*I-cyEGFP-7xDSR	*h-, urg1::Purg1lox-cyEGFP-7xDSR, leu1-32 (AW698)*
	pAW8E*Nde*I-cyEGFP-8xDSR	*h-, urg1::Purg1lox-cyEGFP-8xDSR, leu1-32 (AW700)*
	pAW8E*Nde*I-cyEGFP-8mxDSR	*h-, urg1::Purg1lox-cyEGFP-8mxDSR, leu1-32 (AW702)*
	pAW8E*Nde*I-cyEGFP-*spo5*DSR	*h-, urg1::Purg1lox-yEGFP-spo5DSR, leu1-32 (AW638)*
	pAW8E*Nde*I-HO-cyEGFP	*h-, urg1::Purg1lox-HO-cyEGFP, leu1-32 (AW671)*
	pAW8E*Nde*I-HO-cyEGFP-spo5DSR	*h-, urg1::Purg1lox-HO-cyEGFP-spo5DSR, leu1-32 (AW673)*
h-, urg1::RMCE$_{hphMX6}$, LEU-HOcs-his3+-λ-EU2, leu1-32, his3-D1 (AW467 Watson et al 2011)	pAW8E*Nde*I-HO-cyEGFP	*h-, urg1::Purg1lox-HO-cyEGFP, LEU-HOcs-his3+-λ-EU2, leu1-32, his3D1 (AW741)*
	pAW8E*Nde*I-HO-cyEGFP-3XDSR	*h-, urg1::Purg1lox-HO-cyEGFP-3XDSR, LEU-HOcs-his3+-λ-EU2, leu1-32, his3D1 (AW743)*
	pAW8E*Nde*I-HO-cyEGFP-4XDSR	*h-, urg1::Purg1lox-HO-cyEGFP-4XDSR, LEU-HOcs-his3+-λ-EU2, leu1-32, his3D1 (AW745)*
	pAW8E*Nde*I-HO-cyEGFP-6XDSR	*h-, urg1::Purg1lox-HO-cyEGFP-6XDSR, LEU-HOcs-his3+-λ-EU2, leu1-32, his3D1 (AW747)*
	pAW8E*Nde*I-HO-cyEGFP-8XDSR	*h-, urg1::Purg1lox-HO-cyEGFP-8XDSR, LEU-HOcs-his3+-λ-EU2, leu1-32, his3D1 (AW749)*
	pAW8E*Nde*I-HO-cyEGFP-*spo5*DSR	*h-, urg1::Purg1lox-HO-cyEGFP-spo5DSR, LEU-HOcs-his3+-λ-EU2, leu1-32, his3D1 (AW751)*
h- smt0, urg1::RMCE$_{hphMX6}$, LEU-HOcs-his3+-λ-EU2, rhp51::kanMX6 leu1-32, his3-D1 (AW686)	pAW8E*Nde*I-HO-cyEGFP	*h- smt0, urg1::Purg1lox-HOcyEGFP, LEU-HOcs-his3+-λ-EU2, rhp51::kanMX6, leu1-32, his3D1 (AW734)*
	pAW8E*Nde*I-HO-cyEGFP-3XDSR	*h- smt0, urg1::Purg1lox-HOcyEGFP-3XDSR, LEU-HOcs-his3+-λ-EU2 rhp51::kanMX6, leu1-32, his3D1 (AW816)*
	pAW8E*Nde*I-HO-cyEGFP-4XDSR	*h- smt0, urg1::Purg1lox-HOcyEGFP-4XDSR, LEU-HOcs-his3+-λ-EU2,rhp51::kanMX6, leu1-32, his3D1 (AW818)*
	pAW8E*Nde*I-HO-cyEGFP-6XDSR	*h- smt0, urg1::Purg1lox-HOcyEGFP-6XDSR, LEU-HOcs-his3+-λ-EU2,rhp51::kanMX6, leu1-32, his3D1 (AW820)*
	pAW8E*Nde*I-HO-cyEGFP-8XDSR	*h- smt0, urg1::Purg1lox-HOcyEGFP-8XDSR, LEU-HOcs-his3+-λ-EU2, rhp51::kanMX6, leu1-32, his3D1 (AW822)*
	pAW8E*Nde*I-HO-cyEGFP-*spo5*DSR	*h- smt0, urg1::Purg1lox-HOcyEGFP-spo5DSR, LEU-HOcs-his3+-λ-EU2, rhp51::kanMX6, leu1-32, his3D1 (AW739)*
h- smt0, urg1::RMCE$_{hphMX6}$, RuiuR, rtf1::natMX6, leu1-32, nda3-KM311 (YSM077)	pAW8E*Nde*I-rtf1-*spo5*DSR	*h- smt0, urg1::Purg1lox-rtf1-spo5DSR, RuiuR, rtf1::natMX6, leu1-32, nda3-KM311 (YSM098)*
h+ urg1::RMCE$_{kanMX6}$, leu1-32, ade6::ade6+-P$_{adh15}$-skp1-AtTIR1-2NLS-9myc (AW617)	pAW8E*Nde*I-*rhp18-HAIAA17*	*h+ urg1:: Purg1lox-rhp18-HAIAA17, leu1-32 ade6::ade6+-P$_{adh15}$-skp1-atTIR1-2NLS-9myc, rhp18::kanMX6* (YDP210)*
	pAW8E*Nde*I-*rhp18-HAIAA17-spo5*DSR	*h+ urg1:: Purg1lox-rhp18-HAIAA17-spo5DSR, leu1-32 ade6::ade6+-P$_{adh15}$-skp1-atTIR1-2NLS-9myc, rhp18::kanMX6* (YDP231)*
Other *S. pombe* strains used in the study		
	Strain number and source	Genotype
	AW501 (Watson et al 2011)	*h-, leu1-32*
	JMM1015 (lab stock)	*h- smt0, rhp51::kanMX6, ade6-704, leu1-32, ura4-D18*
	AW507 (Watson et al 2011)	*h-, urg1::Purg1lox-HO, LEU-HOcs-his3+-λ-EU2, his3-D1, leu1-32*
	AW598 (lab stock)	*h+, urg1::RMCE$_{kanMX6}$, ade6-704, his3-D1, leu1-32*

Table 1. Cont.

Strains created via Cre-lox recombination mediated cassette exchange during this study		
***urg1* base strain employed**	**RCME plasmid used**	**Genotype of strain created**
	YDP273 (this study)	*h+, urg1::RMCE$_{kanMX6}$, leu1-32, ade6::ade6+-P$_{adh15}$-skp1-AtTIR1-2NLS-9myc, rhp18::natMX6*
	HM2468 (Kanke et al., 2011)	*h-, ade6::ade6+-P$_{adh15}$-skp1-AtTIR1-2NLS-9myc*

* = following cassette exchange, *rhp18* ORF deleted with kanMX6 selectable marker using standard homologous recombination techniques
doi:10.1371/journal.pone.0083800.t001

the degradation of the *rtf1-spo5DSR* mRNA reduces the cellular concentrations of Rtf1 protein sufficiently to allow use of the rapidly inducible $P_{urg1lox}$ system to study blocked replication forks by 2DGE. Importantly, this will allow the study of synchronised cells cultures to further elucidate the mechanisms of recombination-dependent fork restart in *S. pombe*.

Production of a null rhp18 phenotype by the addition of an auxin-inducible protein depletion system

The above experiments demonstrate that the addition of DSR sequences to destabilise the transcripts produced by the basal level of uninduced $P_{urg1lox}$ provides a level of attenuation of the "OFF" level of protein function that is sufficient to allow the manipulation of a cellular function that is sensitive to low levels of protein. However, additional control of the protein stability would offer two additional advantages: first, it would allow even greater control of "OFF" level function and second, it would allow more rapid removal of residual protein upon "shut off" of P_{urg1} transcription, which would add to the versatility of the system. To establish a test system to validate the utility of combining the auxin degron (Figure 5A) with our $P_{urg1lox}$ DSR system, we turned to a well characterised DNA repair function; Rhp18-dependent post replication repair (PRR). Rhp18 is the homolog of *S. cerevisiae* Rad18. The *S. pombe* $Rhp18^{Rad18}$ ubiquitin ligase is essential for PRR, allowing cells to progress through and survive S-phase in the presence of replication blocking lesions [19]. *rhp18^{rad18}* delete mutants are hypersensitive to DNA-damaging agents [20], allowing us to test for a null allele phenotype. Together with Rhp6 (*S. cerevisiae* Rad6 homologue), $Rhp18^{Rad18}$ mono-ubiquitylates the sliding clamp protein proliferating cell nuclear antigen (PCNA; Pcn1 in *S. pombe*) in S phase and in response to DNA lesions [19,21].

Using RMCE, we created strains where the *rhp18^{rad18}* ORF, tagged at the C-terminus with the IAA17 degron, was inserted at the *urg1* locus either with or without the *spo5*DSR element. Plasmids pAW8E*NdeI-rhp18IAA17* and pAW8E*NdeI-rhp18IAA17-spoDSR* (see materials and methods) and the *urg1* base strain YDP273 were used to create strains YDP210 (*P$_{urg1lox}$-rhp18-cIAA17*) and YDP231 (*P$_{urg1lox}$-rhp18-cIAA17-spo5DSR*) respectively (Table 1). Base strain YDP273 also contains the *P$_{adh15}$-skp1-AtTIR1* fusion necessary for the efficient poly-ubiquitination of the IAA17 degron tag (Kanke et al 2011). Strains YDP210 (*rhp18^{rad18}-delete, P$_{urg1lox}$-rhp18-cIAA17-spo5DSR*,), AW617 (*rhp18^{rad18+}*) and YDP273 (*rhp18^{rad18}*-delete) were serially diluted and spotted onto YEA media (control) and YEA media containing the UV memetic 4-Nitro-Quinoline-1-Oxide (4NQO) (Figure 5B). To regulate $Rhp18^{Rad18}$ induction, uracil was added or omitted from the growth media. To regulate $Rhp18^{Rad18}$ stability, the synthetic plant auxin NAA was either added or omitted. Following growth at 30°C, a null *rhp18^{rad18}* phenotype was only observed in *rhp18-cIAA17-spo5DSR* cells where $P_{urg1lox}$ expression is repressed (uracil absent) and auxin-dependent Rhp18-IAA7 degradation induced (NAA present) (Figure 5B bottom middle panel). The *rhp18-cIAA17-spo5DSR* cells were only partially sensitive to 4NQO in the absence of NAA (Figure 5B bottom left panel) demonstrating that transcription repression and RNA processing alone are insufficient to obtain the desired phenotype. These results demonstrate that

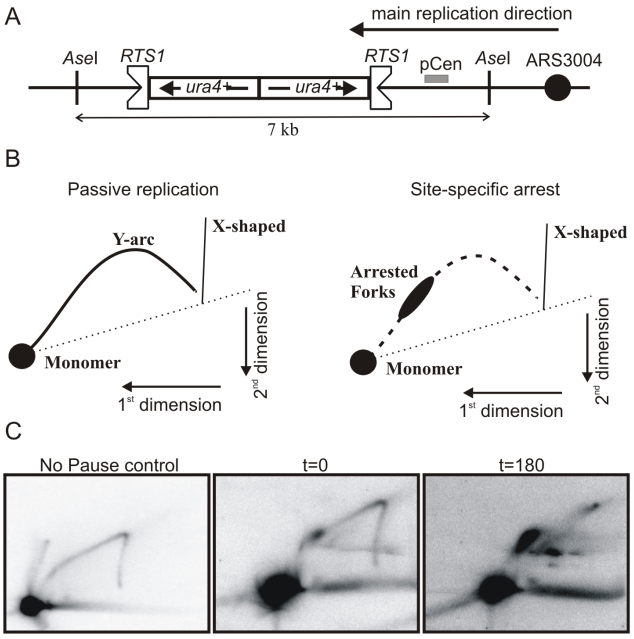

Figure 4. Use of the *S. pombe spo5* gene DSR element allows for tighter regulation of Rtf1 expression in an RTS1-dependent replication fork stall system. (A) Schematic illustration of inverted *ura4* repeat double RTS1 (*RuiuR*) construct. *RTS1* is a polar replication fork barrier. The triangular indent indicates the surface that prevents fork progression. (B) Cartoon representation of the expected replication intermediates (RIs) at the *RuiuR* locus as analysed by two-dimensional gel electrophoresis (2DGE). Left panel: RIs expected when the *Ase*I fragment indicated is replicated passively (no fork arrest at the *RTS1* barrier). Right panel - RIs expected in *RuiuR* cells upon fork arrest. (C) Left panel: control cells with no pause, demonstrating the position of the Y-arc. Middle and right panels: The *rtf1* ORF was inserted at the *urg1* locus in rtf1Δ cells by Cre-mediated cassette exchange to create YSM098 (see Table 1). The strain was grown in EMM+LA at 30°C (asynchronous culture) and Rtf1 protein induced by the addition of uracil at 0.25 mg/ml. Samples taken at time-points shown. Chromosomal DNA was digested by *Ase*I, and RIs were analysed by 2DGE.
doi:10.1371/journal.pone.0083800.g004

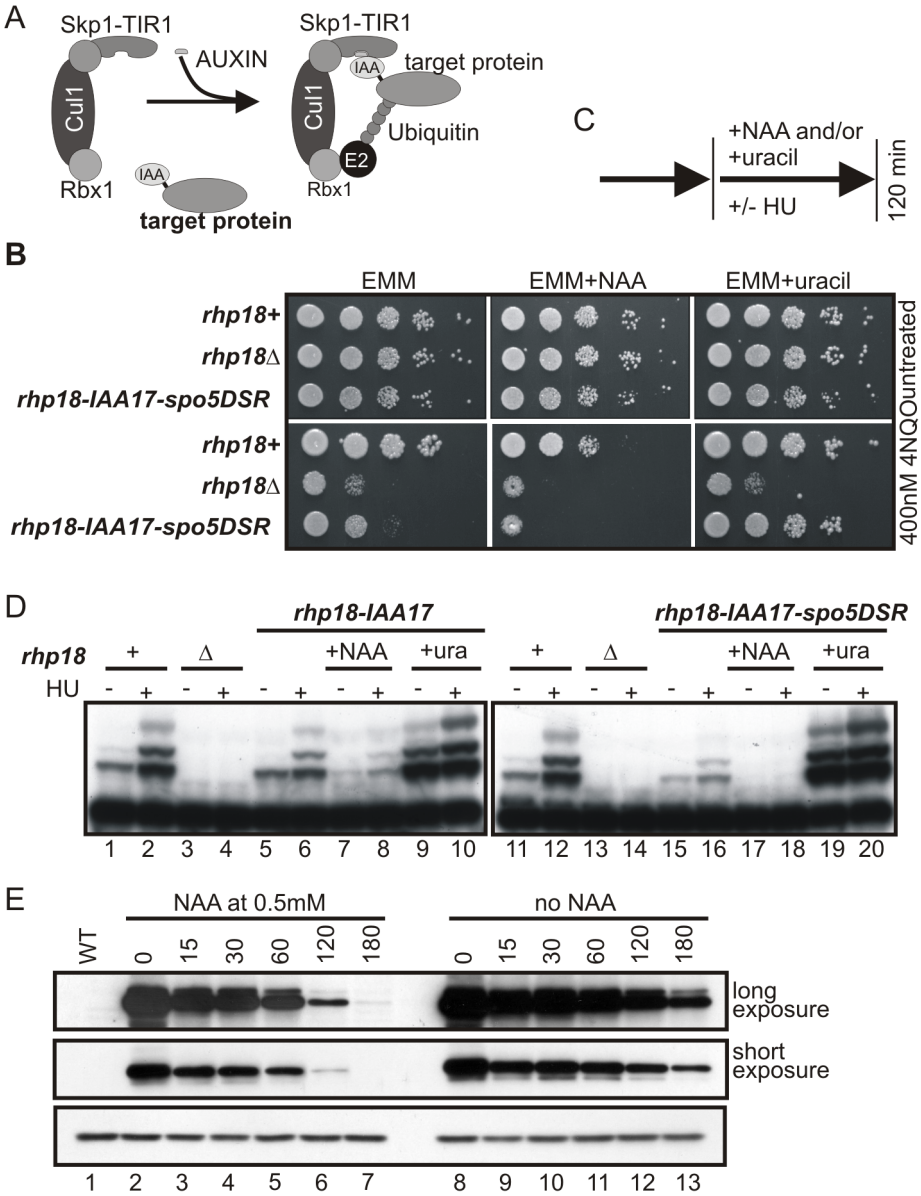

Figure 5. Use of an auxin-inducible degron allows for the generation of a conditional *rhp18* mutant strain. (**A**) Cartoon of the IAA17 degron system: addition of auxin allows binding of the TIR adaptor (fused to Skp1) to the IAA17 tag (IAA), which is fused to the target protein. This induces ubquitination and proteasome degradation. (**B**) Strains AW617 (*rhp18*$^{+}$), YDP273 (*rhp18*Δ) and YDP231 (*rhp18*Δ, $P_{urg1lox}$-*rhp18-HAIAA17-spo5DSR*) were serially diluted 10-fold in water and spotted on EMM+L plates supplemented as shown with uracil at 0.25 mg/ml, NAA at 0.5 mM and/or 4NQO at 400 nM. Time of incubation at 30°C: Top panels 3 days, bottom panels 5 days. (**C**) Schematic of experimental procedure used in D. HU = hydroxyurea, NAA = 1-naphthaleneacetic acid. (**D**) Ubiquitination of PCNA is abolished in $P_{urg1lox}$-*rhp18-HAIAA7-spo5DSR* cells in the presence of NAA. Logarithmically growing AW617 (*rhp18*$^{+}$), YDP273 (*rhp18*-delete), YDP210 (*rhp18*-delete, $P_{urg1lox}$-*rhp18-HAIAA17*) and YDP231 (*rhp18*-delete, $P_{urg1lox}$-*rhp18-HAIAA17-spo5DSR*) cells cultured in EMM+L at 30°C untreated (−) or treated with 10 mM HU (+) and grown for a 120 minutes or grown for 120 minutes in the presence of NAA at 0.5 mM or uracil at 0.25 mg/ml. Total protein extracts were separated by SDS PAGE prior to Western blotting using anti-PCNA antibody. (**E**). The auxin degron promotes protein degradation upon "shut-off". $P_{urg1/lox}$. YDP210 (*rhp18*-delete, $P_{urg1lox}$-*rhp18-HAIAA17*) cells were grown in EMM+L and $P_{urg1lox}$ induced by the addition of uracil at 0.25 mg/ml. After 3 h induction, cells were pelleted by centrifugation, washed twice in EMM+L and re-suspended in EMM+L. Samples taken at time-points shown (mins). Total protein extracts were separated by SDS PAGE prior to Western blotting revealed protein levels using anti-HA to detect Rhp18-HAIAA17 (upper panels) and anti-tubulin to detect tubulin as a loading control (lower panel). WT represents control strain AW501 (*h*$^{-}$, *leu1-32*).
doi:10.1371/journal.pone.0083800.g005

protein destabilisation can add a further level of control when proteins are regulated via transcription from $P_{urg1lox}$.

Rhp18^{Rad18} is required for the ubiquitination of Pcn1 (*S. pombe* PCNA homolog), which occurs during S-phase and accumulates in cells treated with hydroxyurea [19]. Thus, the levels of Ub-Pcn1 in growing and hydroxyurea-treated cells provides a biochemical readout of Rhp18^{Rad18} activity. To compare the utility of the auxin degron, the regulation by DSR motifs and the combination of the two together we thus explored the levels of Ub-Pcn1 in a variety of strains and conditions. Cells in which Rhp18^{Rad18}-IAA17 is regulated by $P_{urg1lox}$ either with or without an associated *spo5*DSR element were grown to mid-log phase and either treated,

or not, with 10 mM hydroxyurea. Where appropriate, 0.25 mg/ml of uracil was added to induce $Rhp18^{Rad18}$-IAA17 and 0.5 mM NAA was added to induce $Rhp18^{Rad18}$-IAA17 instability (for a schematic of experimental design, see Figure 5C). After 120 minutes incubation at 30°C, cell extracts were prepared and analysed by western blot using an α-PCNA antibody (Figure 4D). As expected, in the control *rhp18^{rad18+}* cells (*rhp18+*), higher molecular weight Ub-Pcn1 species were observed in both logarithmically growing cells and, at higher levels, hydroxyurea arrested cells (Figure 5D, lanes 1 and 2; 11 and 12). These modifications were absent in the *rhp18^{rad18}*-deleted control (*rhp18Δ*) strain (Figure 5D, lanes 3 and 4; 13 and 14).

In both untreated and hydroxyurea-treated *rhp18^{rad18}-cIAA17* (YPD210) and *rhp18^{rad18}-cIAA17-spo5DSR* (YDP231) cells, the levels of Ub-Pcn1 decreased in the repressed conditions (uracil absent) when compared to *rhp18^{rad18+}* (Figure 5D, lanes 5 and 6; 15 and 16). However, significant residual signal remained, even in the DSR-containing construct. Thus, while repressed $P_{urg1lox}$ transcript levels appear lower that of the endogenous *rhp18^{rad18}* locus and this is further reduced by the presence of the *spo5*DSR, biological function is not completely ablated. When cells were concomitantly treated with the synthetic auxin, NAA, modification levels were further decreased in both strains. Importantly, Ub-Pcn1 was undetectable in both untreated and HU-treated *rhp18-cIAA17-spo5DSR* cells (Figure 5D, lanes 17 and 18), while residual levels of modifications remained in *rhp18-cIAA17* cells (Figure 5D, lanes 7 and 8). Over-expression of *$P_{urg1lox}$-rhp18-IAA17* (presence of uracil, absence of auxin) results in higher levels of PCNA ubiquitilation when compared to control *rhp18^{rad18+}* cells (Figure 5D, lanes 9 and 10; 19 and 20).

To establish if, upon shut-off of $P_{urg1lox}$-dependent transcription, auxin addition resulted in more rapid removal of CIAA17-tagged protein, we grew cells in the presence of uracil for 3 hours before transferring them to fresh media without uracil, either supplemented, or not, with auxin (Figure 5E). Loss of the GFP signal was more rapid in the presence of auxin. Taken together, these results show that control over transcription rate, RNA turnover and protein depletion may all be required to obtain a null allele phenotype.

Influence of arginine and urea

During the course of our experiments, we have noticed that the level of $P_{urg1lox}$-dependent transcription was significantly reduced in cells grown in EMM media containing arginine. Subsequent experiments demonstrated that, uniquely amongst the commonly used amino acid supplements, arginine significantly suppress the "ON" level (uracil present) of $P_{urg1lox}$-dependent GFP expression (Figure 6A, lane 14). Importantly, the "OFF" level (uracil absent) was also reduced when compared to cells pre-cultured in the absence of arginine (Figure 6A, lane 6 versus lane 2) (see also figure 6C, lane 11 versus lane 2). A similar reduction was seen with the presence of adenine in this experiment, but unlike that seen with arginine, this was not always reproducible. To further improve the $P_{urg1lox}$ system, we thus investigated the potential use of arginine for reducing "OFF" level transcription. We first tested if, biologically, the presence of arginine could increase the sensitivity observed when *rhp18* is under the control of $P_{urg1lox}$ and is suppressed by the absence of uracil (Figure 6B). Indeed, when grown in the absence of uracil (no induction) and the presence of arginine (inhibition), the phenotype of *rhp18-d*, *$P_{urg1lox}$-rhp18-spo5DSR* cells was closer to that seen for the *rhp18* null mutant. We next investigated the kinetics of induction for $P_{urg1lox}$ in cells pre-cultured in arginine-containing medium and transferred into fresh arginine-free medium and induced immediately by addition of uracil (Figure 6D). To our surprise, the kinetics of induction was improved, with higher levels of yEGFP present at the earlier time points when compared to cells pre-cultured without arginine. Levels of yEGFP were comparable 3 hours post induction (Figure 6C). The use of arginine in the pre-culture can therefore markedly increase the dynamic range of the $P_{urg1lox}$ promoter system and increase the speed of induction.

A novel uracil catabolic pathway has recently been described in the budding yeast *Saccharomyces kluyveri*. This pathway is dependent on a pair of genes, *URC1* and *URC4*, that are highly conserved in many bacteria and fungi [22]. The *S. kluyveri URC1* and *URC4* genes are the orthologs of the *S. pombe urg1$^+$* and *urg3$^+$*, respectively. In *S. kluyveri*, Urc1, together with Urc4 and a set of other enzymes, breaks down uracil into urea and 3-hydroxypropionic acid [22]. When considering that the early commitment step of a metabolic pathway is usually subject to feedback inhibition by the final product of that pathway [23] and the fact that arginine can be broken down into urea by arginase when nitrogen is limiting [24], it is conceivable that Urc1/Urg1 expression or activity might be subject to negative regulation by urea. As *S. pombe* can use urea as a sole nitrogen source, we explored if replacing the ammonium in the EMM growth media with urea would have a similar effect on expression levels as was observed for arginine. Compared to cells grown in ammonim-containing media, there was no significant decrease of the "ON" level of GFP when urea was used as the sole nitrogen source (Figure 6A, lane 15), indeed the level was higher (lane 15 versus lane 2). The equivalent "OFF" level was also higher (Figure 6A, lane 7). Furthermore, no reduction in the "ON" level of $P_{urg1lox}$-dependent GFP expression was seen in ammonium-EMM media supplemented with lower concentrations of urea (0.5 mM and 25 uM) (Figure 6A lanes 16 and 17). As seen in Figure 6B, the addition of 25 uM urea also had no effect on the sensitivity of *$P_{urg1lox}$-rhp18* cells to 4NQO. Despite these observations, an initial inhibition of yEGFP induction was evident when cells were grown in the presence of 10 mM urea before being transferred into fresh urea-free medium (with ammonium as a nitrogen source) and induced by addition of uracil (Figure 6D). Thus, while urea does directly or indirectly have an effect on *urg1* promoter activity, a simple model of substrate inhibition does not explain the complexity of P_{urg1} regulation.

Discussion

For *S. pombe*, the control of gene expression has remained a problem for many years because a rapidly and easily inducible transcriptional regulation system, i.e. one equivalent to the P_{GAL} system of *S. cerevisiae*, has not been available. A number of regulatable expression systems have been established characterised, and each has advantages and disadvantages. The *nmt1* promoter has most commonly been used to manipulate protein levels, and thus gene function, because it presents several distinct advantages: first, it is functional when integrated at different sites in the genome; second, it has a good dynamic range (~75 fold in our hands); third, through the use of TATA-box mutations several different strengths of promoter are available. Importantly, these maintain the dynamic range between "ON" and "OFF" states. However, the *nmt1* promoter has one major disadvantage: it takes between 12 and 16 hours to induce and induction is not particularly synchronous. This has limited its utility for the many experiments that require rapid and synchronous induction to study, for example, the cell cycle specificity of a proteins function.

The recently described *urg1$^+$* promoter [6], which is induced by the addition of uracil to the media, offers the most plausible alternative to P_{nmt1} since it has a similar dynamic range (~1:75)

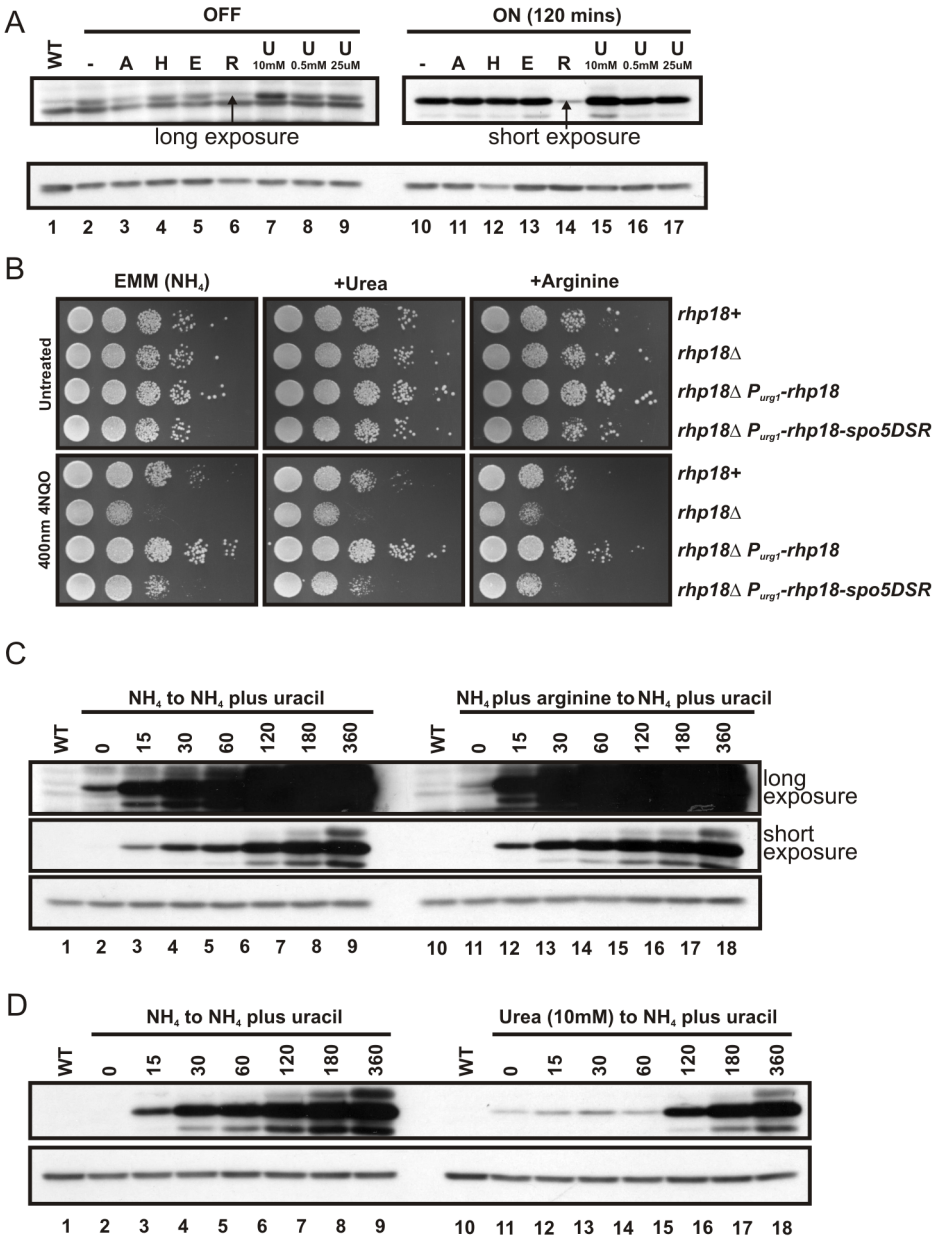

Figure 6. The effect of arginine and urea on $P_{urg1lox}$ expression levels. (**A**) Arginine reduces both $P_{urg1lox}$ induced and repressed protein levels. AW640 (*$P_{urg1lox}$-cyEGFP*) cells were grown in EMM+L or EMM+L supplemented with adenine (A), histidine (H), arginine (R), EMM media where NH_4Cl was substituted for 22 mM glutamic acid (E), EMM media where NH_4Cl was substituted for urea at 10 mM (U 10 mM) or EMM media supplemented with urea at 0.5 mM (U 0.5 mM) or 25 μM (U 25 μM). Cells were induced by the addition of uracil at 0.25 mg/ml and cells grown for 2h. A long exposure of the $P_{urg1lox}$ OFF and a short exposure of the $P_{urg1lox}$ ON are shown. Arrows mark band of interest. (**B**). Strains AW617 (*rhp18*$^{+}$), YDP273 (*rhp18*Δ), YDP210 (*rhp18*Δ, *$P_{urg1lox}$-rhp18*) and YDP231 (*rhp18*Δ, *$P_{urg1lox}$-rhp18-spo5DSR*) were serially diluted 10-fold in water and spotted on EMM+L plates or supplemented as shown with urea at 25 uM or arginine at 100 μg/ml, with or without 4NQO at 400 nM. Time of incubation at 30°C was 3 days. (**C**). The induction kinetics of $P_{urg1lox}$ is improved when cells are pre-cultured in EMM supplemented with arginine. AW640 (*$P_{urg1lox}$-cyEGFP*) cells were pre-cultured in EMM+L or EMM+L supplemented with arginine at 100 μg/ml ($P_{urg1lox}$ OFF). Cells were pelleted by centrifugation, washed twice in EMM+L and re-suspended in EMM+L containing uracil at 0.25 mg/ml ($P_{urg1lox}$ ON). Samples taken at time-points shown (mins). (**D**). The induction kinetics of $P_{urg1lox}$ is significantly delayed when cells are pre-cultured in the presence of urea. AW640 (*$P_{urg1lox}$-cyEGFP*) cells were pre-cultured in EMM+L or EMM+L where the nitrogen source is 10 mM urea ($P_{urg1lox}$ OFF). Cells were pelleted by centrifugation, washed twice in EMM+L and re-suspended in EMM+L containing uracil at 0.25 mg/ml ($P_{urg1lox}$ ON). Samples taken at time points shown (mins). For (A), (C) and (D), total protein extracts were separated by SDS PAGE prior to Western blotting using anti-GFP to detect yEGFP (upper panels) and anti-tubulin to detect tubulin as a loading control (lower panel). WT represents control strain AW501 (*h*$^{-}$, *leu1-32*).
doi:10.1371/journal.pone.0083800.g006

and is induced within 30 minutes by a simple media manipulation: the addition of uracil, which does not otherwise significantly alter cell physiology. However, P_{urg1} does suffer from a number of disadvantages: first it does not work well outside of its normal locus; second, its basal level of transcription is relatively high; and third, it is induced during meiosis. In previous work [7] we

described a system that overcame the first of these disadvantages. We established a Recombination Mediated Cassette Exchange system that allowed the rapid and simple replacement of the *urg1* ORF with any sequence of interest. In this report, we have overcome the second of these disadvantages by providing two additional levels of regulation: one at the level of RNA stability and the second at the level of protein stability.

While we do not provide any analysis of how the P_{urg1} promoter functions, we note two things that may be informative: First, the locus is part of a widely conserved operon that has been shown to carry out a novel uracil catabolic cascade in response to nitrogen availability. In addition to the $urg1^+$ and $urg3^+$ genes, this operon also includes genes that are predicted to encode for a uracil transporter, uracil phosphoribosyltransferases, and perhaps most importantly, a putative transcription factor, which belongs to the Zinc finger family of transcription factors [22]. The conserved genomic organization of this bouquet of genes in a wide diversity of fungi and bacteria suggests that the transcriptional regulation of $urg1^+$ expression is likely to be complex. This may be one reason why it has not been possible to transfer the dynamic range of the $P_{urg1lox}$ promoter available at the native locus to a plasmid-based system. Second, we observed that arginine, when supplemented into the growth media, represses uracil-dependent induction by $P_{urg1/lox}$. In particular, arginine suppresses the "OFF" state transcription – i.e. reducing the "leakiness" of the promoter and improves the induction kinetics. Our analysis shows that, serendipitously, this provide an additional opportunity, when combined with our DSR sequences and/or cIAA17 degron tag, to tightly regulate processes that are particularly sensitive to very low protein levels.

While the use of the modified P_{urg1} system we describe here will not solve all the problems associated with gene regulation in *S. pombe*, we have demonstrated, both here and in our own unpublished data, that the system is both versatile, robust, easy to use and applicable to a range of biological questions. Most importantly, we have succeeded in regulating protein functions which are sensitive to low levels of protein in cells and have exploited the system to study induced conditions in a cell cycle-dependent manner. For our own purposes we chose to regulate HO-dependent site-specific DSB formation, Rtf1-dependent replication fork arrest and $Rhp18^{Rad18}$-dependent post replication repair. However, other functions can also be regulated by application of this modified $P_{urg1lox}$ system. The availability of the generic "base strain" required for RMCE and the convenience of a range of plasmids compatible with the Cre-mediated site specific recombination on which RMCE is based, mean that any sequence can be simply and easily cloned into an appropriate RMCE plasmid and targeted directly to the *urg1* locus via a simple transformation and selection procedure at an efficiency that is routinely greater than 50% of cells. Once integrated, the sequence (usually an ORF) will be under transcriptional control such that it can be regulated simply by the addition of uracil. Based on which RMCE vector the sequence of interest is cloned into, both the "ON" and "OFF" state transcript levels can be attenuated by the desired amount due to the inclusion of one or more DSR elements in the non-translated region of the resulting transcript. Similarly, protein stability can be regulated by inclusion of a protein tag derived from the Arabidopsis IAA17 degron, which is regulated by the addition of auxin. Here we have shown that both these systems function and that they can be combined to generate genuine conditional null allele phenotypes. Finally, the vercitility of the $P_{urg1lox}$ system can be further enhanced by the simple addition of arginine in pre-induction cultures.

Materials and Methods

Strains and growth conditions

Strains used in this work are listed in Table 1 and all strains grown at 30°C. The media composition was as described [25]. The nitrogen source used in Edinburgh Minimal Media was either 5 g/litre NH_4Cl (94 mM), 3.75 g/litre L-glutamic acid (22 mM) or 0.6 g/litre urea (10 mM). In the text, EMM refers to nitrogen source used as NH_4Cl unless stated otherwise. For selection of G418, hygromycin (HPH) and nourseothricin (NAT) resistant cells, G418 disulsuphate (Melford), hygromycin B (Melford) and nourseothricin-dihydrogen sulphate (Melford) were added to YEA plates at a final concentration of 200 μg/ml, 200 μg/ml and 100 μg/ml respectively. Synthetic plant auxin 1-Naphthaleneacetic acid (NAA) (Sigma) powder was dissolved in a small volume of 0.1N NaOH and then diluted with double distilled water to the required concentration (0.5 M). EMM media was supplemented with leucine (L), adenine (A), arginine (R) and histidine (H) at 100 μg/ml as required. Yeast transformations were performed using a lithium acetate method [26]. Cell pre-cultures for $P_{urg1lox}$ induction assays were not grown to stationary phase before sub-culturing. *E. coli* strain DH5α was used for all cloning procedures.

Construction of DSR plasmids for cassette exchange at the *urg1* locus

Complimentary oligonucleotides containing 1 to 8 repeats of the DSR core element (TTAAAC) (1xDSR to 8xDSR) and 8 repeats of the mutated core element (GTAAAC) (8mxDSR) were synthesised (P1 to P18 - Table 2). The core motifs were separated by 6 nucleotides of randomly selected bacteriophage lambda DNA sequence. After annealing complimentary oligonucleotides, the resulting DNA duplex was flanked by overhangs compatible with *Bgl*II and *Xma*I restriction enzymes. The annealed oligonucleotides were ligated into *Bgl*II/*Xma*I restricted pAW8E*Nde*I-CTAP [7], replacing the CTAP tag to create pAW8E*Nde*I-L-1xDSR through to pAW8E*Nde*I-L-8xDSR and pAW8E*Nde*I-L-8mxDSR. The yeast codon optimised yEGFP ORF from pAW8E*Nde*I-cyEGFP (Watson et al 2011) was sub-cloned as a *Bgl*II fragment into the DSR plasmids to create pAW8E*Nde*I-cyEGFP-1xDSR through to pAW8E*Nde*I-cyEGFP-8xDSR and pAW8E*Nde*I-cyEGFP-8mx DSR. The 3HA sequence (encoding 3 copies of the hemagglutinin epitope tag) from pAW8E*Nde*I-c3HA (Watson et al., 2011) was sub-cloned as a *Bgl*II fragment into pAW8E*Nde*I-L-3xDSR, pAW8E*Nde*I-L-4xDSR, pAW8E*Nde*I-L-6xDSR and pAW8E*Nde*I-L-8xDSR to create pAW8E*Nde*I-c3HA-3xDSR, pAW8E*Nde*I-c3 HA-4xDSR, pAW8E*Nde*I-c3HA-6xDSR and pAW8E*Nde*I-c3HA-8xDSR respectively.

The 157bp DSR element of the *S. pombe spo5* gene as identified by Harigaya et al. (2006) was amplified using the KOD HotStart DNA polymerase system (Novagen - used for all subsequent PCR reactions) from total genomic DNA using primers P19 and P20 (Table 2). The product was cloned into *Xma*I restricted pAW8E*Nde*I-cyEGFP to create pAW8E*Nde*I-cyEGFP-*spo5*DSR. The 3HA sequence from pAW8E*Nde*I-c3HA was sub-cloned into pAW8E*Nde*I-cyEGFP-*spo5*DSR as *Bgl*II fragment to create pAW8E*Nde*I-c3HA-*spo5*DSR.

The IAA17 degron tag sequence was amplified from the plasmid template pMK43 [13] using primers P21 and P22 and the resulting fragment was cloned into the *Bgl*II site of pAW8E*Nde*I-cyEGFP and pAW8E*Nde*I-cyEGFP-*spo5*DSR, replacing the yEGFP sequence, to create pAW8E*Nde*I-cIAA17 and pAW8E*Nde*I-cIAA17-*spo5*DSR respectively. A single copy of the HA hemagglutinin epitope tag was inserted between the MCS and the poly-TGS linker by annealing complimentary oligonucleotides P23 and P24

Table 2. Primers used in this study.

NAME	SEQUENCE (5′ TO 3′)
P1	GATCTTTAAACC
P2	CCGGGGTTTAAA
P3	GATCTTTAAACTCCGTATTAAACC
P4	CCGGGGTTTAATACGGAGTTTAAA
P5	GATCTTTAAACTCCGTATTAAACCCATTCTTAAACC
P6	CCGGGGTTTAAGAATGGGTTTAATACGGAGTTTAAA
P7	GATCTTTAAACTCCGTATTAAACCCATTCTTAAACAGAACTTTAAACC
P8	CCGGGGTTTAAAGTTCTGTTTAAGAATGGGTTTAATACGGAGTTTAAA
P9	GATCTTTAAACTCCGTATTAAACCCATTCTTAAACAGAACTTTAAACGGCAGGTTAAACC
P10	CCGGGGTTTAACCTGCCGTTTAAAGTTCTGTTTAAGAATGGGTTTAATACGGAGTTTAAA
P11	GATCTTTAAACTCCGTATTAAACCCATTCTTAAACAGAACTTTAAACGGCAGGTTAAACGTAATGTTAAACC
P12	CCGGGGTTTAACATTACGTTTAACCTGCCGTTTAAAGTTCTGTTTAAGAATGGGTTTAATACGGAGTTTAAA
P13	GATCTTTAAACTCCGTATTAAACCCATTCTTAAACAGAACTTTAAACGGCAGGTTAAACGTAATGTTAAACAGGTGCTTAAACC
P14	CCGGGGTTTAAGCACCTGTTTAACATTACGTTTAACCTGCCGTTTAAAGTTCTGTTTAAGAATGGGTTTAATACGGAGTTTAAA
P15	GATCTTTAAACTCCGTATTAAACCCATTCTTAAACAGAACTTTAAACGGCAGGTTAAACGTAATGTTAAACAGGTGCTTAAACTTTATGTTAAACC
P16	CCGGGGTTTAACATAAAGTTTAAGCACCTGTTTAACATTACGTTTAACCTGCCGTTTAAAGTTCTGTTTAAGAATGGGTTTAATACGGAGTTTAAA
P17	GATCTGTAAACTCCGTAGTAAACCCATTCGTAAACAGAACTGTAAACGGCAGGGTAAACGTAATGGTAAACAGGTGCGTAAACTTTATGGTAAACC
P18	CCGGGGTTTACCATAAAGTTTACGCACCTGTTTACCATTACGTTTACCCTGCCGTTTACAGTTCTGTTTACGAATGGGTTTACTACGGAGTTTACA
P19	AAAACCCGGGACTACGCCATATCATGCCCA
P20	AAAACCCGGGGCTTTGTCTAACAGGTTTTATGTTGGTTTAAGT
P21	AAAAAGATCTATGATGGGCAGTGTCGAGCT
P22	AAAACCCGGGTCAAGCTCTGCTCTTGCACTTCTC
P23	CTAGTGGTTATCCTTATGATGTTCCTGATTATGCTT
P24	CTAGAAGCATAATCAGGAACATCATAAGGATAACCA
P25	CCCCATATGCAAGGAAAAAACAATTTAAGTTGCAGA
P26	CCCACTAGTGCATAAATCATCGGCGTTAGAAAAAGC
P27	GCGAGAGACCTTCTTATTAAAACCAAAAGACTTCC
P28	ATAAGAAGGTCTCTCGCAGCCACA
P29	AAAACATATGCAAGGAAAAAACAATTTAAGTTGCAGACC
P30	AAAAAGATCTCTAGCATAAATCATCGGCGTTAGAAAAAGC
P31	TTTAAATCAAATCTTCCATGCG
P32	GATGCCAGACCGTAATGACAAAA

doi:10.1371/journal.pone.0083800.t002

and cloning the resulting DNA duplex into *Spe*I restricted pAW8E*Nde*I-cIAA17 and pAW8E*Nde*I-cIAA17-*spo5*DSR to create pAW8E*Nde*I-cHAIAA17 and pAW8E*Nde*I-cHAIAA17-*spo5*DSR respectively.

To create non-tagging Cre-expression DSR plasmids, the sequence located between the loxP and loxM3 sites of pAW8E*Nde*I (Figure 1) was replaced with a construct containing the 37bp *urg1* promoter fragment, an MCS of *Nde*I-*Sph*I-*Sac*I-*Sal*I-*Spe*I and the required DSR sequence. Constructs were synthesised (Genscript) and sub-cloned into *Nhe*I/*Xma*I restricted pAW8E*Nde*I to create pAW8E*Nde*I-3xDSR, pAW8E*Nde*I-4xDSR, pAW8E*Nde*I-6xDSR, pAW8E*Nde*I-8xDSR and pAW8E*Nde*I-*spo5*DSR.

Plasmids created are listed in Figure 1 including Genbank accession numbers for each. Plasmids are available from Addgene.

DSR plasmid inserts

The *S. pombe rtf1* ORF was amplified from total genomic DNA using primers P25 and P26 and cloned into pAW8E*Nde*I-cyEGFP as an *Nde*I/*Spe*I fragment to generate pAW8E*Nde*I-*rtf1*-cyEGFP. The *Bgl*II restriction enzyme site was removed from the *rtf1* ORF of pAW8E*Nde*I-*rtf1*-cyEGFP using the QuikChange Site-Directed Mutagenesis Kit (Stratagene) and the primers P27 and P28. The mutated *rft1* ORF was amplified using P29 and P30 and cloned into pAW8E*Nde*I-cyEGFP*spo5*DSR as an *Nde*I/BglII fragment, removing cyEGFP tag, to generate pAW8E*Nde*I-*rtf1*-*spo5*DSR. The *rtf1* plasmid insert was confirmed by sequencing.

The HO endonuclease ORF was sub-cloned from pAWE*Nde*I-HO-cyEGFP [7] as an *Nde*I/*Spe*I fragment into pAW8E*Nde*I-cy EGFP-DSR plasmids to create pAWE*Nde*I-HO-cyEGFP, pAWE *Nde*I-HO-cyEGFP-3xDSR, pAWE*Nde*I-HO-cyEGFP-4xDSR, pA WE*Nde*I-HO-cyEGFP-6xDSR, pAWE*Nde*I-HO-cyEGFP-8xDSR, and pAWE*Nde*I-HO-cyEGFP-*spo5*DSR.

S. pombe strain construction

All $P_{urg1lox}$ strains were generated using Cre-mediated cassette exchange. See Table 1 for a list of strains created, plus the base

strain and pAW8E*Nde*I Cre-expression plasmid used for each. Other strains used in this study are also listed in Table 1. To create *urg1* base strain AW686, strains AW469 and JMM1015 were crossed (Table 1). The *urg1* base strain AW617 was generated by crossing HM2468 with AW598 (Table 1). The *rhp18*^{rad18} gene locus in AW617 was deleted using the *natMX6* selectable marker to create strain YDP273 (Table 1).

Cassette exchange

Cassette exchange was performed essentially as described [7]. The procedure was adapted for the introduction of HO-endonuclease gene sequences into HR deficient *rhp51*-delete *urg1* base strains containing the HOcs single strand annealing (SSA) system. After transformation of the Cre-expression plasmids containing the HO gene into the *rhp51*-delete *urg1* base strain AW686 (Table 1), cells were plated directly onto EMM plates supplemented with 15 μM thiamine (EMM+T - P_{nmt1} OFF). Following incubation at 30°C for 4–5days, transformants were re-streaked onto fresh EMM+T plates. Transformants were grown in 50 mls liquid EMM media supplemented with leucine but with thiamine omitted (EMM+L) overnight to approximately 1×10^6 cells/ml and 500 cells plated onto EMM+L plates and grown at 30°C until colonies appear. Colonies were replica plated onto YEA plates supplemented with hygromycin at 200 μg/ml. Following incubation overnight at 30°C, colonies sensitive to hygromycin were re-streaked onto EMM+L plate and replica plated onto EMM plates to confirm loss of the plasmid. The leucine auxotrophic colonies were used for subsequent experiments.

SSA assay growth conditions and genetic colony assay

Logarithmically growing cells grown at 30°C in EMM+L were pelleted and re-suspended in pre-warmed EMM+LH ($P_{urg1lox}$ OFF) or EMM+LH supplemented with uracil at 0.25 mg/ml ($P_{urg1lox}$ *ON*) and incubation continued at 30°C. At the indicated time points 500 cells were plated on EMM+LH agar and grown at 30°C until colonies appeared. The resulting colonies were replica plated onto EMM+L agar, grown at 30°C and the percentage of histidine auxotrophic colonies calculated.

Preparation of total cell extract and Western blot analysis

Preparation of cell extracts for SDS-PAGE and Western blotting was performed as previously described [7]. Mouse monoclonal anti-GFP antibody (Roche) was diluted 1:5,000, rabbit anti-PCNA antibody (Gift: A. Lehmann) was diluted 1:2,000 and mouse monoclonal anti-HA (Santa Cruz Biotechnology) diluted 1:2,500. As a loading control, mouse monoclonal anti-tubulin antibody (diluted 1:10,000; Sigma) was used.

2D gel electrophoresis

Cells were grown in EMM media supplemented with adenine and leucine (EMM+AL) at 30°C to a density of approximately 1×10^7 cells/ml and 1.25×10^9 cells harvested by centrifugation. $P_{urg1lox}$-*rtf1* expression was induced by the addition of uracil at 0.25 mg/ml ($P_{urg1lox}$ *ON*). Chromosomal DNA was extracted using standard procedures, embedded in agarose plugs and digested using 30 units of A*se*I. Digested chromosomal DNA was analysed by 2D gels [27], using 0.35% and 0.9% agarose for the first and second dimensions, respectively. Replication intermediates were visualized using pCen (centromere proximal to the *ura4* gene) as a probe. Probe pCen template DNA was amplified from total genomic *S. pombe* DNA using primers P31 and P32. Autoradiography was performed using a storage phosphor screen/Storm PhosphorImager system.

Acknowledgments

We would like to thank all members of the Carr and Murray labs for discussion and suggestions.

Author Contributions

Conceived and designed the experiments: AMC ATW JMM YD CC. Performed the experiments: ATW YD TJE SM. Analyzed the data: AMC ATW JMM. Wrote the paper: ATW AMC.

References

1. Kanke M, Nishimura K, Kanemaki M, Kakimoto T, Takahashi TS, et al. (2011) Auxin-inducible protein depletion system in fission yeast. BMC cell biology 12: 8.
2. Yokobayashi S, Watanabe Y (2005) The kinetochore protein Moa1 enables cohesion-mediated monopolar attachment at meiosis I. Cell 123: 803–817.
3. Yamagishi Y, Sakuno T, Shimura M, Watanabe Y (2008) Heterochromatin links to centromeric protection by recruiting shugoshin. Nature 455: 251–255.
4. Maundrell K (1990) nmt1 of fission yeast. A highly transcribed gene completely repressed by thiamine. The Journal of biological chemistry 265: 10857–10864.
5. Basi G, Schmid E, Maundrell K (1993) TATA box mutations in the Schizosaccharomyces pombe nmt1 promoter affect transcription efficiency but not the transcription start point or thiamine repressibility. Gene 123: 131–136.
6. Watt S, Mata J, Lopez-Maury L, Marguerat S, Burns G, et al. (2008) urg1: a uracil-regulatable promoter system for fission yeast with short induction and repression times. PloS one 3: e1428.
7. Watson AT, Werler P, Carr AM (2011) Regulation of gene expression at the fission yeast Schizosaccharomyces pombe urg1 locus. Gene 484: 75–85.
8. Harigaya Y, Tanaka H, Yamanaka S, Tanaka K, Watanabe Y, et al. (2006) Selective elimination of messenger RNA prevents an incidence of untimely meiosis. Nature 442: 45–50.
9. Yamanaka S, Yamashita A, Harigaya Y, Iwata R, Yamamoto M (2010) Importance of polyadenylation in the selective elimination of meiotic mRNAs in growing S. pombe cells. The EMBO journal 29: 2173–2181.
10. Chen HM, Futcher B, Leatherwood J (2011) The fission yeast RNA binding protein Mmi1 regulates meiotic genes by controlling intron specific splicing and polyadenylation coupled RNA turnover. PloS one 6: e26804.
11. Yamashita A, Shichino Y, Tanaka H, Hiriart E, Touat-Todeschini L, et al. (2012) Hexanucleotide motifs mediate recruitment of the RNA elimination machinery to silent meiotic genes. Open biology 2: 120014.
12. Marguerat S, Schmidt A, Codlin S, Chen W, Aebersold R, et al. (2012) Quantitative analysis of fission yeast transcriptomes and proteomes in proliferating and quiescent cells. Cell 151: 671–683.
13. Nishimura K, Fukagawa T, Takisawa H, Kakimoto T, Kanemaki M (2009) An auxin-based degron system for the rapid depletion of proteins in nonplant cells. Nature methods 6: 917–922.
14. Chapman EJ, Estelle M (2009) Mechanism of auxin-regulated gene expression in plants. Annual review of genetics 43: 265–285.
15. Lambert S, Watson A, Sheedy DM, Martin B, Carr AM (2005) Gross chromosomal rearrangements and elevated recombination at an inducible site-specific replication fork barrier. Cell 121: 689–702.
16. Lambert S, Mizuno K, Blaisonneau J, Martineau S, Chanet R, et al. (2010) Homologous recombination restarts blocked replication forks at the expense of genome rearrangements by template exchange. Molecular cell 39: 346–359.
17. Mizuno K, Lambert S, Baldacci G, Murray JM, Carr AM (2009) Nearby inverted repeats fuse to generate acentric and dicentric palindromic chromosomes by a replication template exchange mechanism. Genes & development 23: 2876–2886.
18. Mizuno K, Miyabe I, Schalbetter SA, Carr AM, Murray JM (2013) Recombination-restarted replication makes inverted chromosome fusions at inverted repeats. Nature 493: 246–249.
19. Frampton J, Irmisch A, Green CM, Neiss A, Trickey M, et al. (2006) Postreplication repair and PCNA modification in Schizosaccharomyces pombe. Molecular biology of the cell 17: 2976–2985.
20. Verkade HM, Teli T, Laursen LV, Murray JM, O'Connell MJ (2001) A homologue of the Rad18 postreplication repair gene is required for DNA damage responses throughout the fission yeast cell cycle. Molecular genetics and genomics : MGG 265: 993–1003.
21. Maga G, Hubscher U (2003) Proliferating cell nuclear antigen (PCNA): a dancer with many partners. Journal of cell science 116: 3051–3060.
22. Andersen G, Bjornberg O, Polakova S, Pynyaha Y, Rasmussen A, et al. (2008) A second pathway to degrade pyrimidine nucleic acid precursors in eukaryotes. Journal of molecular biology 380: 656–666.
23. Savageau MA (1975) Optimal design of feedback control by inhibition: dynamic considerations. Journal of molecular evolution 5: 199–222.

24. Van Huffel C, Dubois E, Messenguy F (1994) Cloning and sequencing of Schizosaccharomyces pombe car1 gene encoding arginase. Expression of the arginine anabolic and catabolic genes in response to arginine and related metabolites. Yeast 10: 923–933.
25. Moreno S, Klar A, Nurse P (1991) Molecular genetic analysis of fission yeast Schizosaccharomyces pombe. Methods in enzymology 194: 795–823.
26. Bahler J, Wu JQ, Longtine MS, Shah NG, McKenzie A 3rd, et al. (1998) Heterologous modules for efficient and versatile PCR-based gene targeting in Schizosaccharomyces pombe. Yeast 14: 943–951.
27. Brewer BJ, Lockshon D, Fangman WL (1992) The arrest of replication forks in the rDNA of yeast occurs independently of transcription. Cell 71: 267–276.